Characterising Complement Behaviour and Inhibition in Normothermic Machine Perfusion for Renal Transplantation



John Fallon

Linacre College

University of Oxford

A thesis submitted for the degree of

Doctor of Philosophy

Hilary 2027

Characterising Complement Behaviour and Inhibition in Normothermic Machine Perfusion for Renal Transplantation

John Fallon

Linacre College

University of Oxford

A thesis submitted for the degree of

Doctor of Philosophy

Hilary 2027

Abstract

Kidney transplantation is the optimal treatment for end-stage renal failure, but outcomes remain limited by ischaemia-reperfusion injury, delayed graft function, and the restricted ability to assess or treat organs before implantation. Normothermic machine perfusion (NMP) has emerged as a promising preservation strategy that may support organ assessment, prolong preservation, and provide a platform for ex vivo therapeutic delivery. Complement is a major mediator of transplant injury, yet its behaviour during renal NMP and its suitability as a graft-directed therapeutic target remain incompletely understood.

This thesis characterises complement activation during renal NMP and evaluates targeted complement inhibition in human ex vivo kidney perfusion models. In the NKP1 clinical trial cohort, perfusate analysis demonstrated measurable complement proteins and activation products across the cascade. Early complement profiles associated with donor characteristics, donor risk, functional delayed graft function, and time to recovery of graft function, suggesting that complement during NMP is both biologically relevant and potentially informative as a biomarker of graft quality.

A human ex vivo model of NMP followed by plasma-based normothermic reperfusion was then established to reproduce early transplant-like complement activation in declined kidneys. Within this model, C2 inhibition with argx-117 achieved effective target depletion but did not consistently suppress terminal pathway activation. In contrast, the membrane-localising CR1-derived inhibitor mirococept, delivered during NMP, was associated with attenuation of early reperfusion C3d and C5b-9 formation.

Overall, this thesis demonstrates that complement is active during renal NMP and supports NMP as a platform for biomarker development and graft-directed complement therapy.

Acknowledgments

I would like to sincerely thank all those who have helped me and educated me over the course of my DPhil. Firstly, to my supervisors, Professor James Hunter, my primary supervisor, who has been hugely supportive throughout, got me involved in so many things to help my career, taught me a lot, as well as enjoying a few pints. Professor Ploeg for his casual wisdom and valued perspective on all things transplant. Professor Friend one of the original authorities on NMP and has been of a huge help, I am particularly grateful for the time he took to help to attain my Kidney Research UK PhD training fellowship, and all the trips to Wisconsin and Philadelphia have been both of great value professionally as well as highly enjoyable.

To my friends and colleagues from the perfusion trenches. First and foremost, Richard Dumbill, who took me under his wing and with whom I learned the nuts and bolts of kidney perfusion, but also everything about how to navigate Oxford and the DPhil sphere. Alex Sagar and Mo Elzawahry, who were an important source of not only perfusion help, but general support and friendship along the way.

Finally, to the wider lab group in general, it was a pleasure to be a part of and a great environment to attempt serious perfusion research.

Abstract

Kidney transplantation is the optimal treatment for end-stage renal failure, but outcomes remain limited by ischaemia-reperfusion injury, delayed graft function, and the restricted ability to assess or treat organs before implantation. Normothermic machine perfusion (NMP) has emerged as a promising preservation strategy that may support organ assessment, prolong preservation, and provide a platform for ex vivo therapeutic delivery. Complement is a major mediator of transplant injury, yet its behaviour during renal NMP and its suitability as a graft-directed therapeutic target remain incompletely understood.

This thesis characterises complement activation during renal NMP and to evaluates targeted complement inhibition in human ex vivo kidney perfusion models. In the NKP1 clinical trial cohort, perfusate analysis demonstrated measurable complement proteins and activation products across the cascade. Early complement profiles associated with donor characteristics, donor risk, functional delayed graft function, and time to recovery of graft function, suggesting that complement during NMP is both biologically relevant and potentially informative as a biomarker of graft quality.

A human ex vivo model of NMP followed by plasma-based normothermic reperfusion was then established to reproduce early transplant-like complement activation in declined kidneys. Within this model, C2 inhibition with argx-117 achieved effective target depletion but did not consistently suppress terminal pathway activation. In contrast, the membrane-localising CR1-derived inhibitor mirococept, delivered during NMP, was associated with attenuation of early reperfusion C3d and C5b-9 formation.

Overall, this thesis demonstrates that complement is active during renal NMP and supports NMP as a platform for biomarker development and graft-directed complement therapy.

Contents

List of Figures & Tables

List of Abbreviations

1 Background & Introduction

1.1 Background

1.1.1 Renal Transplantation & Normothermic Machine Perfusion

1.1.2 Current Paradigms in Renal NMP

1.1.2.1 The Pioneering Experience

1.1.2.2 Robust Pig Transplant Modelling

1.1.2.3 Utilisation of An Approved Device

1.1.2.4 Prolonged Clinical NMP

1.1.2.5 More Recent Adopters

1.1.2.6 Conclusion

1.1.3 NMP as a Model for Transplantation of Human Kidneys

1.2 Complement & The Transplant Kidney

1.2.1 Complement & Organ Donation

1.2.2 Complement & Preservation

1.2.3 Complement & Implantation

1.2.4 Complement & the Transplant Candidate

1.3 Complement Inhibition in Transplantation

1.3.1 C1 Esterase Inhibitors

1.3.2 CR1 Regulation

1.3.3 C5 Cleavage

1.3.4 C5a-C5aR Axis

1.3.5 C3 Blockade

1.3.6 Early Lectin Pathway Components

1.3.7 Alternative Pathway Components

1.4 Concluding Remarks

2 Common Methods

2.1 Perfusion Methodology

2.1.1 XVIVO Device and Circuit

2.1.2 OrganOx Device and Circuit

2.1.3 Normothermic Reperfusion Model

2.1.4 Human Research Organs: Kidney Back table and Cannulation

2.1.5 Research Blood Preparation

2.1.6 NMP Perfusate

2.1.7 Normothermic Reperfusion Perfusate

2.1.8 Generic Sampling

2.2 Perfusate Analysis

2.2.1 Biochemistry

2.2.2 Perfusate Injury Biomarkers

2.2.3 Perfusate Complement

2.3 Tissue Analysis

2.3.1 Formalin-Fixed Tissue Processing

2.3.2 Immunohistochemistry Staining

2.3.3 Immunohistochemistry Trained Model Quantification

2.3.3.1 Manual Definition of Analysis Compartments

2.3.3.2 Nuclear Detection and Nucleus-only DAB Feature Extraction

2.3.3.3 Training and Application of a Supervised Object Classifier

2.3.3.4 Outcome Metric and Export

2.3.3.5 Quality Control

2.3.4 Immunohistochemistry Automated Pipeline Analysis

2.3.5 CellDive Multiplex Immunofluorescence

2.3.6 CellDive Analysis Pipeline

2.3.7 Frozen Tissue Processing

2.3.8 Bicinchoninic Acid Assay

2.3.9 Western Blotting

2.3.10 Native Gel Blotting

3 Characterising Complement in Prolonged Clinical Normothermic Perfusion for Renal Transplantation

3.1 Introduction

3.1.1 NKP1 Clinical Trial

3.1.2 Evidence of Renal Complement Production

3.1.3 Complement During NMP

3.1.4 Selected Complement Measures

3.1.5 Time to Creatinine-50 (TCr50)

3.2 Aims and Objectives

3.3 Methods

3.3.1 NKP1 Trial Methodology

3.3.2 Perfusate Complement Analysis

3.3.3 Wieslab Complement System Screen

3.3.4 Data Handling and Statistical Analysis

3.3.5 Tissue Multiplex Immunofluorescence

3.4 Results

3.4.1 Perfusate Complement Proteins

3.4.1.1 Complement Protein Dynamics

3.4.1.2 Wieslab Assays

3.4.1.3 Complement and Donor Factors

3.4.1.4 Complement Proteins and functional DGF

3.4.1.5 Stratification by TCr50, UKDRI and Cox Regression

3.4.2 Tissue Multiplex Immunofluorescence

3.4.2.1 Relative Expression Pre- and Post-perfusion

3.4.2.2 Relative Expression by Outcome

3.5 Discussion

3.5.1 Evidence of Complement Activation During NMP

3.5.2 Functional Pathway Potential and Perfusate Complement Biology

3.5.3 Activation and Consumption Across the Pathways

3.5.4 Circuit Artefact versus Organ Biology

3.5.5 Early Complement Profiles as a Signal from Donor and Retrieval Biology

3.5.6 Complement Signals Predict Recovery and Add to UKDRI

3.5.7 Complement as Marker versus Mediator

3.5.8 Tissue Proteins: Separating Donor Priming & Reperfusion Biology

3.5.9 Limitations, Implications & Next Steps

4 Assessing C2 inhibition in NMP and Normothermic Reperfusion

4.1 Introduction

4.1.1 Argx-117 Mechanism of Binding & Safety

4.1.2 C2-Inhibition in a Rat Transplant Model

4.1.3 Current Phase II Trial Design for DGF in Renal Transplantation

4.1.4 Modelling with Human Kidneys Ex-Vivo

4.2 Aims & Objectives

4.3 Methods

4.3.1 Model Development

4.3.2 Blood Only Perfusions

4.3.3 Single Kidney Perfusions

4.3.4 Paired Perfusions

4.3.5 Sample Analysis & Data Handling

4.3.5.1 Perfusate Biochemistry

4.3.5.2 Perfusate Injury Biomarkers

4.3.5.3 Perfusate Complement Proteins & Activity

4.3.5.4 Wieslab Functional Complement Assay

4.3.5.5 Tissue Complement: Western Blotting & Native Gel Electrophoresis

4.3.5.6 Tissue Multiplex Immunofluorescence (CellDIVE)

4.3.5.7 Tissue Complement Immunohistochemistry (QuPath)

4.4 Results

4.4.1 Model Development Perfusions

4.4.2 Blood Only Perfusions

4.4.3 Single Kidney Perfusions

4.4.3.1 Flow and Blood Gas Parameters

4.4.3.2 Perfusate Injury Biomarkers

4.4.3.3 C2 Blockade and Complement Activation Products

4.4.3.4 Tissue C5b-9 Immunohistochemistry

4.4.4 Paired Kidney Perfusions

4.4.4.1 Perfusion Parameters

4.4.4.2 Perfusate Biochemistry

4.4.4.3 Perfusate Injury Biomarkers

4.4.4.4 Perfusate Complement Proteins & Activity

4.4.4.5 Wieslab Assay

4.4.4.6 Tissue Complement on Western Blotting & Native Gel Electrophoresis

4.4.4.7 Tissue Multiplex IF

4.5 Discussion

4.5.1 Model Development and Blood Only Perfusions

4.5.2 Single Kidney Perfusions and Dose Assessment

4.5.3 Paired Kidney Perfusions

4.5.4 Model Limitations and Observations

4.5.5 Concluding Remarks

4.5.6 Further Work

5 Assessing C3b inhibition in NMP and Normothermic Reperfusion

5.1 Introduction

5.1.1 Mirococept, Mechanism & Pre-clinical Development

5.1.2 EMPIRIKAL, Porcine Dose Finding & EMPIRIKAL-2

5.1.3 Mirococept and NMP Delivery

5.2 Aims & Objectives

5.3 Methods

5.3.1 Kidney allocation and Perfusions

5.3.2 Perfusate Analysis

5.3.3 Tissue Analysis

5.3.3.1 Western Blotting and Native Gel Electrophoresis

5.3.3.2 C5b-9 IHC and Quantification

5.4 Results

5.4.1 Dose Assessment Perfusions

5.4.1.1 Perfusion Parameters and Blood Gas Analysis

5.4.1.2 Perfusate C5b-9 Formation

5.4.1.3 Tissue Complement on Western Blotting & Native Gel Electrophoresis

5.4.2 Paired Perfusions

5.4.2.1 Perfusion Parameters and Blood Gas Analysis

5.4.2.2 Perfusate Injury Biomarkers

5.4.2.3 Perfusate Complement Proteins

5.4.2.4 Tissue Complement on Western Blotting & Native Gel Electrophoresis

5.4.2.5 C5b-9 IHC

5.5 Discussion

5.5.1 Dose Finding Perfusions

5.5.2 Paired Perfusions

5.5.3 The Model & Its Limitations

5.5.4 Overall Conclusion & Translational Implications

6 Concluding Remarks

6.1 Thesis Objectives

6.2 Summary of Key Points

6.3 Outstanding Basic Scientific Questions

6.4 Future Clinical and Pre-Clinical Directions

List of Figures & Tables

List of Figures

Figure 1.1 Schematic overview of renal ischaemia–reperfusion injury during kidney transplantation.
Figure 1.2 Schematic overview of the complement cascade and its major effector pathways.

Figure 2.1 Schematic overview of the modified XVIVO circuit.
Figure 2.2 Schematic overview of the OrganOx circuit.

Figure 3.1 Paired comparison of perfusate complement biomarkers across the NKP1 cohort.
Figure 3.2 Association between perfusion duration and change in perfusate complement biomarkers across the NKP1 cohort.
Figure 3.3 Paired comparison of functional complement activity measured by Wieslab assay in a subset of NKP1 kidneys.
Figure 3.4 Paired comparison of functional complement activity measured by Wieslab assay in a subset of NKP1 kidneys stratified by perfusate complement activity group.
Figure 3.5 Donor factor associations with early and end-perfusion complement biomarkers in the NKP1 cohort.
Figure 3.6 Association between perfusate complement biomarkers and delayed graft function in the NKP1 cohort.
Figure 3.7 Probability of functioning graft in the NKP1 cohort stratified by perfusate complement biomarker groups and donor risk
Figure 3.8 Paired comparison of tissue immunofluorescence marker positivity in pre-NMP and post-recipient reperfusion biopsies.
Figure 3.9 Associations between tissue complement immunofluorescence markers, functional delayed graft function, donor risk, and perfusion duration.

Figure 4.1 Schematic overview of the complement cascade showing the site and mechanism of action of Argx-117.
Figure 4.2 Macroscopic clot formation and coagulation profile in NMP pilot perfusions.
Figure 4.3 Complement behaviour during blood-only perfusions.
Figure 4.4 Physiological and blood gas parameters during isolated kidney perfusions performed for Argx-117 dose refinement.
Figure 4.5 Perfusate injury biomarker concentrations during isolated kidney perfusions performed for Argx-117 dose refinement.
Figure 4.6 Perfusate C2 and sC5b-9 profiles during isolated kidney perfusions performed for Argx-117 dose refinement.
Figure 4.7 Tissue C5b-9 immunohistochemistry in biopsies from isolated kidney perfusions performed for Argx-117 dose refinement.

Figure 4.8 Renal artery flow and urine production during paired perfusions with Argx-117.
Figure 4.9 Perfusate biochemical and blood gas parameters during paired perfusions with Argx-117.
Figure 4.10 Paired comparison of renal function during paired perfusions with Argx-117.
Figure 4.11 Perfusate injury biomarkers in paired perfusions with Argx-117.
Figure 4.12 Perfusate C2 concentrations during paired perfusions with Argx-117.
Figure 4.13 Perfusate C3a concentrations during paired perfusions with Argx-117.
Figure 4.14 Perfusate C4d concentrations during paired perfusions with Argx-117.
Figure 4.15 Perfusate sC5b-9 concentrations during paired perfusions with Argx-117.
Figure 4.16 Perfusate sC5b-9 terminal complex concentrations during paired perfusions with Argx-117, measured using an alternative antibody and assay.
Figure 4.17 Perfusate C3bBbP concentrations during paired perfusions with Argx-117.
Figure 4.18 Functional classical and lectin pathway activity measured by Wieslab assay during paired perfusions with Argx-117.
Figure 4.19 Western blot analysis of complement proteins in paired perfusions with Argx-117.
Figure 4.20 Western blot analysis of tissue complement across all perfused kidneys grouped by experimental timepoint.
Figure 4.21 Tissue C4d deposition on multiplex immunofluorescence across the perfusion model.

Figure 5.1 Schematic overview of the complement cascade and mechanism of action of mirococept.
Figure 5.2 Schematic overview of the mirococept dosing protocols across all perfused kidneys.
Figure 5.3 Renal artery flow and urine output during mirococept dose refinement perfusions.
Figure 5.4 Perfusate C5b-9 concentrations during mirococept dose refinement perfusions.
Figure 5.5 Perfusate C5b-9 concentrations during mirococept dose refinement perfusions compared with unpaired controls.
Figure 5.6 Change in tissue C3d/C3dg deposition over NMP and NR during mirococept dose refinement.
Figure 5.7 Tissue C3d/C3dg and C5b-9 levels in biopsies from mirococept dose refinement perfusions.
Figure 5.8 Tissue C5b-9 levels at baseline, end of NMP, and end of NR in mirococept-treated kidneys compared with unpaired controls.
Figure 5.9 Renal artery flow and urine output during paired mirococept perfusions.
Figure 5.10 Perfusate and urine biochemistry during paired mirococept perfusions.
Figure 5.11 Creatinine clearance and fractional excretion of sodium during paired

mirococept perfusions.
Figure 5.12 Perfusate injury biomarker concentrations during paired mirococept perfusions.
Figure 5.13 Perfusate C3d concentrations during paired mirococept perfusions.
Figure 5.14 Perfusate C5b-9 concentrations during paired mirococept perfusions.
Figure 5.15 Tissue complement deposition in biopsies from paired mirococept perfusions.
Figure 5.16 Tissue C5b-9 deposition in paired kidneys over the course of perfusion and reperfusion in paired mirococept perfusions.
Figure 5.17 Baseline tissue biopsies demonstrating consistency between pairs.
Figure 5.18 End of NR tissue biopsies demonstrating consistency between pairs.
Figure 5.19 C5b-9 staining in thrombosed positive control kidney.

List of Tables

Table 4.1 Donor and graft characteristics for kidneys included in the Argx-117 single kidney perfusion series.
Table 4.2 Donor and kidney characteristics for the paired perfusions with Argx-117.

Table 5.1 Published use of mirococept (APT070) across animal models, xenotransplant settings, human islet studies, healthy volunteer trials, and kidney transplantation.
Table 5.2 Donor and kidney characteristics for mirococept dose refinement perfusions.
Table 5.3 Donor and graft characteristics for kidneys included in the paired mirococept perfusions.

List of Abbreviations

aHUS ..... atypical haemolytic uraemic syndrome

ABOi ..... ABO incompatible

AKI ..... acute kidney injury

AMR ..... antibody-mediated rejection

AP ..... alternative pathway

ARC ..... assessment and reconditioning centre

ATN ..... acute tubular necrosis

AUC ..... area under the curve

BCA ..... bicinchoninic acid

CIT ..... cold ischaemia time

CP ..... classical pathway

CR1 ..... complement receptor 1

CR2 ..... complement receptor 2

CR3 ..... complement receptor 3

CR4 ..... complement receptor 4

DAB ..... 3,3'-diaminobenzidine

DAF ..... decay-accelerating factor

DAMP ..... damage-associated molecular pattern

DBD ..... donation after brain death

DCD ..... donation after circulatory death

DGF ..... delayed graft function

DNA ..... deoxyribonucleic acid

List of Abbreviations

eGFR..... estimated glomerular filtration rate

ELISA ..... enzyme-linked immunosorbent assay

ePTFE ..... expanded polytetrafluoroethylene

FFP ..... fresh frozen plasma

FB ..... factor B

FD ..... factor D

FH ..... factor H

FI ..... factor I

GN ..... glomerulonephritis

GST ..... glutathione S-transferase

GST-Pi ..... glutathione S-transferase pi

HLA ..... human leukocyte antigen

HMP..... hypothermic machine perfusion

IF ..... immunofluorescence

IgG ..... immunoglobulin G

IgM ..... immunoglobulin M

IHC ..... immunohistochemistry

IL-18 ..... interleukin-18

IRI ..... ischaemia-reperfusion injury

L-FABP ..... liver-type fatty acid-binding protein

LDH ..... lactate dehydrogenase

LP ..... lectin pathway

List of Abbreviations

MAC ..... membrane attack complex

MASP ..... mannose-binding lectin-associated serine protease

MBL ..... mannose-binding lectin

MCP ..... membrane cofactor protein

NGAL ..... neutrophil gelatinase-associated lipocalin

NKP1 ..... Normothermic Kidney Perfusion 1

NMP..... normothermic machine perfusion

NR ..... normothermic reperfusion

PCR ..... polymerase chain reaction

pO_2 ..... partial pressure of oxygen

pCO_2 ..... partial pressure of carbon dioxide

PK/PD ..... pharmacokinetics/pharmacodynamics

PRBC ..... packed red blood cells

PTFE ..... polytetrafluoroethylene

PVC ..... polyvinyl chloride

QUOD ..... Quality in Organ Donation

RCT..... randomised controlled trial

RNA ..... ribonucleic acid

ROS ..... reactive oxygen species

sC5b-9..... soluble terminal complement complex

SCS..... static cold storage

SST ..... serum separator tube

TCr50 ..... time to creatinine-50

List of Abbreviations

TLR ..... Toll-like receptor

UKDRI ..... United Kingdom Donor Risk Index

UW ..... University of Wisconsin solution

WIT ..... warm ischaemia time

1

Background & Introduction

Contents

1.1 Background

1.1.1 Renal Transplantation & Normothermic Machine Perfusion

1.1.2 Current Paradigms in Renal NMP

1.1.2.1 The Pioneering Experience

1.1.2.2 Robust Pig Transplant Modelling

1.1.2.3 Utilisation of An Approved Device

1.1.2.4 Prolonged Clinical NMP

1.1.2.5 More Recent Adopters

1.1.2.6 Conclusion

1.1.3 NMP as a Model for Transplantation of Human Kidneys

1.2 Complement & The Transplant Kidney

1.2.1 Complement & Organ Donation

1.2.2 Complement & Preservation

1.2.3 Complement & Implantation

1.2.4 Complement & the Transplant Candidate

1.3 Complement Inhibition in Transplantation

1.3.1 C1 Esterase Inhibitors

1.3.2 CR1 Regulation

1.3.3 C5 Cleavage

1.3.4 C5a-C5aR Axis

1.3.5 C3 Blockade

1.3.6 Early Lectin Pathway Components

1.3.7 Alternative Pathway Components

1.4 Concluding Remarks

1.1 Background

1.1.1 Renal Transplantation & Normothermic Machine Perfusion

Kidney transplantation is the treatment of choice for end-stage renal failure, improving both quality and quantity of life[1]. It has been a monumental development in modern medicine for end-stage organ failure, along with developments in immunosuppressive medications this has resulted in excellent long-term outcomes, particularly for liver and kidney transplantation, leading to an increase in transplant numbers and broadening of indications. As a result, waiting lists have increased and we find ourselves in a situation where we are limited by organ supply which does not meet current demand. This has meant over recent years in many countries the boundaries of what organs are considered 'transplantable' have continued to be pushed, by increased use of organs from donors after circulatory death (DCD), older ages, increasing co-morbidity or those with acute kidney injury[2,3]. With an increased number of marginal organs in the donor pool, utilisation of these organs is an issue, with discard rates of 10-15% for kidneys after retrieval[4]. Most of these declined organs are considered marginal, but it is likely that many of them would perform adequately for the right patient. However, which of them to select is challenging without clearer predictability of how they will perform or without improvement to the organ prior to implantation they will continue to go unused.

A central challenge in transplantation is ischaemia reperfusion injury (IRI) which occurs after re-oxygenation following hypoxia, when the kidney is reperfused with the recipients' blood during the transplant. This causes endothelial damage, which has multiple sequelae; complement activation leading to cell wall rupture, opsonisation of antibodies and attraction of neutrophils and macrophages; and activation of platelets and the clotting cascade all together resulting in tubular damage, endothelial stress and acute inflammation (Fig 1.1). Clinically, this can translate to delayed graft function (DGF), where kidneys do not begin to function immediately, longer hospital stays and poor long-term function[5-8].

Static cold storage (SCS) has been the prevailing preservation method since transplantation began. At retrieval organs are cold flushed with preservation solution, submerged and placed on ice at 0-4°C till implantation. It remained the status quo

because it was cheap, easy and achieved reliable results, but outcomes worsen with longer storage durations, especially in more marginal organs[9]. Hypothermic machine preservation (HMP) is a preservation method that uses a device to pump preservation solution through the vasculature of an organ at 4-10°C prior to implantation. This technology provides a more thorough flush of the microvascular system, clearance of metabolic waste and toxins and offers the option to deliver substrates, nutrients or oxygen during preservation. Despite being pioneered in clinical transplantation in 1968[10], HMP laid dormant due to technological limitations and has only been popularised over the last few decades. Various novel devices have been approved in Europe and the USA for clinical use, and HMP has been very broadly adopted in deceased donor renal transplant. It is superior to SCS, primarily through a reduction in DGF and improvement in graft survival. The most significant benefit is in DCD kidneys, but there is benefit in the DBD setting, particularly with extended criteria donor[11-14].

As technology has advanced further normothermic machine perfusion (NMP) has become more feasible. NMP is a complex organ preservation method which involves perfusing donor organs with a warmed, oxygenated solution, known as a perfusate, to supply the tissue with adequate oxygenation and substrate to support the organ ex vivo in as near a physiological state as possible[15].

NMP, as a pseudo-physiological method of preservation may offer some benefits over the hypothermic methods, static cold storage (SCS) or HMP which are the clinical standard. A key concept in NMP is to reduce IRI which occurs following transplant due to re-oxygenation of ischaemic tissue. This causes oxidative stress and complement activation leading to delayed graft function, acute rejection and leads to fibrosis and reduced function.

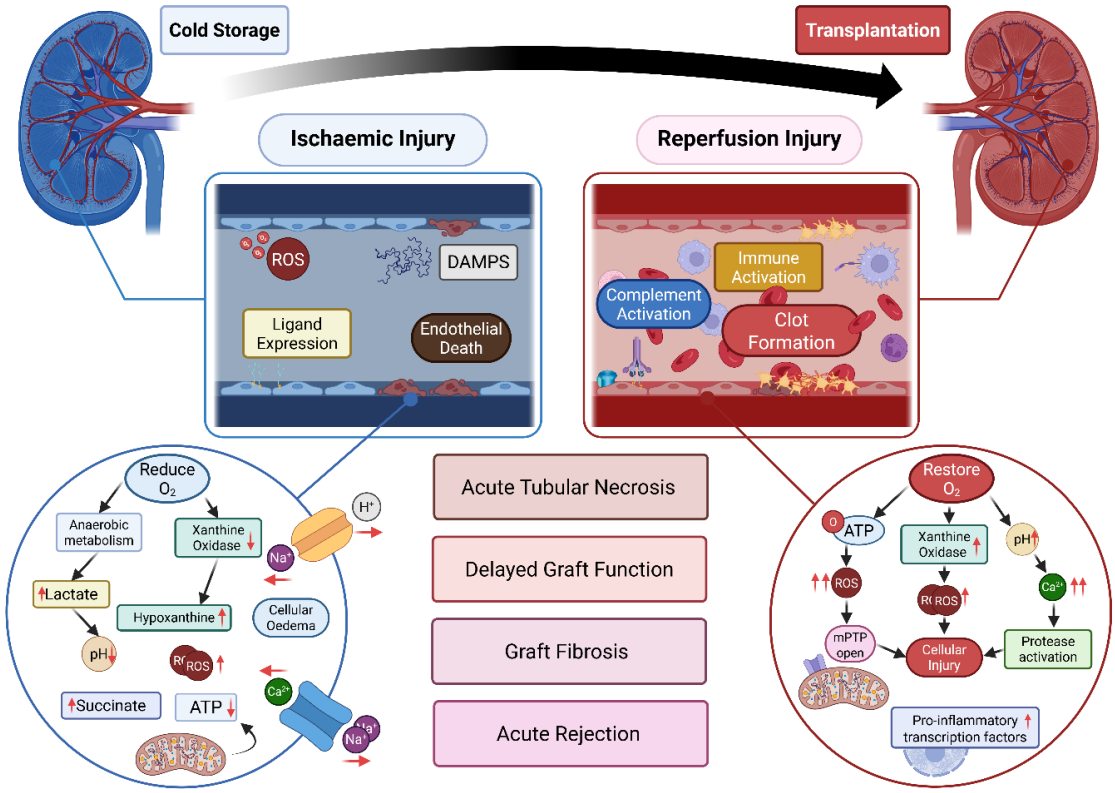


Figure 1.1 ***Schematic overview of renal IRI during kidney transplantation.*** *The transition from cold storage to transplantation and the key mechanisms contributing to renal IRI. During the ischaemic phase, interruption of oxygen delivery suppresses aerobic metabolism, resulting in ATP depletion, a shift towards anaerobic metabolism, lactate accumulation, intracellular acidosis, hypoxanthine accumulation, and failure of ion homeostasis with sodium and calcium dysregulation. These changes promote cellular oedema, mitochondrial dysfunction, ROS generation, endothelial activation, ligand expression, DAMP release, and endothelial and tubular injury. On reperfusion, restoration of oxygen delivery triggers a second wave of injury characterised by rapid ROS generation, mitochondrial permeability transition, calcium-mediated protease activation, complement activation, immune activation, and clot formation within the microvasculature. Together, these result in the sequalae of renal IRI, ATN, DGF, graft fibrosis, and acute rejection.*

The benefits of NMP are potentially wider than simply mitigation of IRI, and the areas which have been considered or are possible uses of the technology are resuscitation, preservation, organ assessment, organ repair and delivery of bespoke therapies[16]. Resuscitation and preservation are the areas that have been explored so far, the paradigms from the key research groups are discussed below.

Assessment has been of interest from the outset with NMP, initially with perfusion parameters, and latterly biomarkers. The number of kidneys that have undergone NMP, particularly those with longer duration NMP and subsequent transplant is limited, so correlation with outcome is in its infancy. This is a continuation of concepts taken from HMP research. Following evidence of the success of HMP over SCS for kidney transplantation huge numbers of kidneys have been transplanted following HMP and thus provide outcome data that can be linked with potential biomarkers. In a systematic

review and meta-analysis of 29 human studies there was sufficient data to scrutinise the most commonly occurring: GST, LDH, lactate, FABP, IL-18 and NGAL, which are mainly taken from acute kidney injury (AKI) research. GST (total and isoforms) is the most studied and the most promising with regards association with DGF, but with only moderate discrimination (typical AUC 0.61–0.70) and assay/isoform heterogeneity that limits thresholds and external validity to some extent. LDH often tracks with DGF especially in DCD datasets but is nonspecific and its independent predictive power is weak. Lactate performs inconsistently and rarely survives adjustment. Signals exist for H-/L-FABP, IL-18, and lipid peroxidation products in select analyses. NGAL, while a notable in AKI, is inconsistent in the context of HMP and transplantation[17]. More recently, extracellular histone H3 emerged as an independent predictor of DGF and 1-year graft survival in a large cohort[18]. HMP biomarkers may complement pump parameters, but none have sufficient accuracy for routine decision-making, at least without evidence from further large, prospective, standardised studies. However, the existing evidence does provide a basis for investigating these HMP markers in the context of NMP. While in HMP metabolic rate is low and cellular production of these proteins should be minimal (Indeed, it is more likely these are biomarkers indicative of the injury sustained prior to HMP and flushed out during storage), in NMP the cells are metabolically active and it is reasonable to assume that this may improve the predictive power of the measure. Over the course of a perfusion the pre-existing injury can manifest as IRI on the device and the biomarkers may give a more granular picture of post-transplant function.

Repair and therapy delivery go hand in hand, but in its current form NMP does not appear to be a treatment in and of itself, more likely a mechanism of delivery for therapy. It may be that it is a preferable storage modality than SCS or HMP, with warm preservation being less deleterious than cold preservation time. This would mean that the concept of repair centres in which organs are held on NMP would enable delivery of therapeutics which target various areas within transplant injury or early recipient factors. The theoretical breadth of what could be targeted is of course wide, but two areas that would clearly be of interest is modulating IRI and immune reactivity upon implant[16]. Regarding modulation of IRI, areas that have been and continue to be

explored include: the mitochondrial permeability transition, NRF2 cytoprotective axis, endothelial NO synthase pathway, endothelial barrier integrity, glycocalyx protection, DAMP/TLR signalling, extracellular DNA, coagulation-fibrosis balance and complement activation. Regarding early allo-immunity, co-stimulation blockade, endothelial activation, cytokine axis, chemokine trafficking, regulatory immune cells, gene transfer of regulatory proteins and again complement modulation[19-21]. For both IRI and immune reactivity it is multifactorial and ultimately targeting multiple pathways together that will likely be the most effective, while renal NMP as a preservation platform is at a relatively early stage of development, before long it will be a mainstream preservation modality.

1.1.2 Current Paradigms in Renal NMP

Due to its infancy, renal NMP is a fast-moving space, with perspectives on it varying dramatically between research groups across the world. In reality, there are a limited number of groups that have published work in which kidneys have been transplanted following NMP. The groups with the most experience are Cambridge, Oxford, Toronto and Rotterdam, but smaller case series from Sydney[22], Essen[23], Barcelona[24] and Glasgow[25] have also been published. There is variability in how these groups have performed NMP, the perfusate composition, the device, device settings and the duration have all been different, and sufficiently different such that any particular intervention is highly unlikely to produce consistent outcomes.

1.1.2.1 The Pioneering Experience

The Cambridge group, led by Professor Michael Nicholson are the pioneers, and world-leaders with the largest experience, performing the first-in-human NMP transplant in 2011[26]. Their paradigm from that moment which culminated in a large multi-centre RCT published in 2023 was 1-hour of end-ischaemic resuscitative NMP, with the aim of lowering DGF rates, particularly in DCD kidneys[27]. Their earlier clinical work had promising results with lower rates of DGF, but this did not translate into the same effect in the RCT, where there was no difference between NMP and SCS. As with any complex

intervention, taking it from a controlled setting done within the confines of one research group, by a select group of very experienced people and expanding it to a multi-centre RCT setting is challenging, the reduction in tight control resulted in 55 protocol deviations, for example. While the trial was a landmark achievement in kidney perfusion it had limitations, some of which hampered the possibility of detecting the efficacy of NMP that they had demonstrated with their earlier work. The primary endpoint was DGF, but recruitment included patients who were pre-dialysis, with a disproportionate number in the control arm, and in whom the primary endpoint could not be assessed. Due to the body of pre-clinical work, the trial was designed with a limit of 1-hour end-ischaemic NMP, and this resulted in a second duration of cold storage (median 130 minutes) possibly reversing or limiting the benefit of the resuscitative NMP.

Regardless, it achieved an important outcome, a large number of NMP transplants were carried out in a multi-centre setup without inferior outcomes to SCS, which is a vital safety outcome. It is precedent for NMP as a preservation strategy which could be performed elsewhere, and given this proven safety of 1-hour, this opens the door to perfusions of longer duration. Another important consideration is that there are possible interventions or kidney directed drug delivery strategies that could be achieved within short duration NMP. An example is provided by their own work using glycosidase to convert blood group A kidneys to blood group O. In this study the enzyme was delivered during NMP and by the second hour of perfusion the A-antigen had reduced to below 20% of its starting value[28].

From a technical standpoint the Cambridge group (and the others involved in the trial) used a device that was assembled at the time of NMP, consisting of commercially-available cardiopulmonary bypass components. The circuit was made up of a controllable Medtronic bio-pump 560, membrane oxygenator connected to carbogen (95% oxygen, 5% carbon dioxide), PVC tubing, a TX50P flow probe, a heat exchanger, and a temperature probe, with the kidneys perfused at a set pressure of 75 mmHg. The perfusate consisted of one unit of packed red cells (O positive or O negative), diluted in Ringer's lactate supplemented with mannitol, heparin, sodium bicarbonate, dexamethasone, parenteral nutrition solution, multivitamins, and prostacyclin. The absence of colloid resulted in a lower than physiological oncotic pressure. The urine

was not recirculated, and the excreted volume was replaced by Ringers' solution. As with all clinical perfusion, the cannulation is an important consideration, the method used was a patch clamp or direct cannulation tied into the vessel, the latter of course sacrifices the vessel patch. In this trial 8.2% of those assigned to NMP could not undergo NMP due to anatomical constraints, also, for the most part the vein was not cannulated as this was optional in the protocol to allow for short renal veins or complex anatomy and then was an open system design.

1.1.2.2 Robust Pig Transplant Modelling

Another pioneer in this area has been Markus Selzner and his research group in Toronto: they focused far more extensively on pre-clinical porcine transplant modelling of their methods with longer NMP durations, prior to undertaking a human clinical trial[29]. Their first publication documenting the large animal model was published in 2015, with their first human work published in 2022. The porcine work taken collectively had looked at different durations of NMP combined with different durations of SCS, finding in essence that the greater proportion of the preservation time done with NMP the lower the peak post-operative creatinine. The clinical trial consisted of 13 transplants from DCD & DBD donors following 1-3 hours of NMP (median 171 minutes) after prior storage on HMP, compared to historical matched control 2:1 on HMP alone. The outcome was that their protocol was safe and feasible, but unsurprisingly given the small cohort no significant differences in DGF or function at 1, 6 or 12 months were detected[30].

Similar to the system developed at Cambridge, this device was custom-built using existing cardiopulmonary bypass components and incorporated the same fundamental elements (S3 heart–lung device, Medtronic Biomedicus console, Revolution centrifugal pump, Dideco Kids D100 oxygenator, venous reservoir, PVC tubing and a ParaTherm heat exchanger). Neither of the Toronto or Cambridge systems were portable and thus were inherently designed as an end-ischaemic intervention. Their perfusate however was different, containing packed red cells with 175mL Ringer's lactate, 200mL STEEN solution, 27mL double reserve-osmosis water, 1000 IU heparin, and sodium bicarbonate and calcium to achieve a physiological pH and calcium concentration, with urine volume replaced with Ringer's lactate. The inclusion of the proprietary lung perfusion solution, STEEN is an important inclusion, given it contains both albumin and

dextran providing a normal oncotic pressure. This creates a more physiological state for the kidney perfusion and is theoretically more amenable to longer durations. It is important to note that major alterations in the perfusate such as this have ramifications in interpreting parameters on the machine, which should not be treated as interchangeable across protocols. Logically, those with higher oncotic pressures will have a lower urine production, or those with higher viscosity a lower blood flow (for example). In Toronto, both artery and vein were cannulated, the artery was approached in the same way, using patch clamps or end cannulation with a tie fixation, thereby forming a closed system.

1.1.2.3 Utilisation of An Approved Device

The group at Erasmus MC, followed the Cambridge paradigm (directly referencing some of their early methodology), published in 2021 they had performed 11 transplants following 2 hours NMP after HMP, in a mix of DCD and DBD kidneys. Their perfusate was essentially the same as Cambridge, but with Ringer's lactate replaced with Stereofundin solution (a balanced crystalloid more like plasma electrolyte concentrations), as before, in this cohort there was no improvement with the use of NMP compared to the 8 contralateral controls and 53 historic controls[31]. However, there was an important feature of this trial, it used the CE marked Kidney Assist machine (at the time Organ Assist Products B.V., now XVIVO B.V.) granted a CE mark for up to 6 hours of perfusion at 37 degrees, the utilisation of a CE marked device brings the possibility of standardisation and technical reliability across multi-centre work.

1.1.2.4 Prolonged Clinical NMP

Our group in Oxford, has a shorter history with the development of a clinical NMP protocol, but a significant one nonetheless. Across a series of porcine and subsequent human kidneys declined for transplant both a device, perfusate and protocol were developed which culminated in the 2025 publication[32]. 36 patients received transplants from DBD and DCD donors following up to 24 hours (median 5.8 hours, 2.2-23.4 hours) of end-ischaemic NMP following SCS, these were matched to historic controls. The perfusate takes forward the concept of more physiological oncotic pressure from the Toronto group and consisted of: 1-unit PRBC, 100 mL 20% human albumin, 100 mL

0.45% saline, meropenem 125 mg, caspofungin 12.5 mg, fondaparinux 2.5 mg, verapamil 2.5 mg, 10% $CaCl_2$ 1.8–2 mL with an infusion of insulin in 5% glucose at 1 mL/h. The device was a purpose-built prototype from OrganOx Ltd, which is an automated perfusion device akin to the company's liver device, consisting of centrifugal pump, hollow-fibre oxygenator, heat exchanger, heated water column, soft-shell reservoir, inline blood-gas sensor (automated O_2/air control for paO_2/pCO_2), pressure control (set to 75 mmHg), three syringe drivers for infusions and a display for perfusion parameters which is continuously logged. The sterile pre-packaged disposable set comes as a single unit from OrganOx and is fitted to the device in a straightforward fashion at the time of use. The cannulation method was devised in such a way as to preserve the full length of the vein and the patch of the artery. For arterial cannulation, a hooded ePTFE graft was used such that an ultra-wide anastomosis could be made to the patch around the main renal artery or including nearby accessory vessels such that the suture line was beyond the margin of the patch that will be utilised for implantation. Should accessory vessels be present that are not within this patch, they can be reconstructed onto the main renal artery at this point or if they are positioned such that within the recipient there will be two or more arterial anastomoses they can be anastomosed to the PTFE graft along its length in an end to side fashion with or without a patch. For the vein, a venous cannula was placed with a snugger and a 5-0 stay sutures at the margins then tied to the body of the cannula to keep it from slipping, all right veins received a stapled venous extension. For management of perfusate electrolytes and circuit volume the 'urine' was recirculated in the protocol, which was the first time this had been done clinically, and aided in prolonged perfusion management. As with the smaller clinical studies from the other groups this was a safety and feasibility study and not designed to show functional superiority, either in DGF or longer-term function. Within the NMP cohort biomarkers relating to outcome were found with associations of GST-Pi delta, L-FABP, IL-18 (with respect to early function) and GST-Pi delta (with respect to with 12-month eGFR (R=0.54, p=0.001)). This Oxford trial was an important step for several reasons, firstly it safely extended the perfusion duration to 24 hours, far beyond what had been done clinically, to durations that are more meaningful logistically or for more prolonged therapeutic intervention. Logistically, within the trial (although not specified within the protocol) the use of the

NMP device safely shifted the peak time of recipient reperfusion from 10pm to 11am, with equivalent outcomes despite the longer overall preservation time (median 15.74 hours vs 8.88 hours). The second important logistic issue was the cannulation method: while surgically more involved, the use of the sutured PTFE graft meant that no anatomy was prohibitive, and the vessels remained in optimum condition for reimplantation. Thirdly, it was performed on an automated portable prototype with accompanying manufactured sterile disposable set which was a great step forward from the custom-built devices.

1.1.2.5 More Recent Adopters

The most recent important development is a 2025 publication from the Sydney group. They performed a paired study from 18 DCD donors, in which one kidney was allocated to SCS and the other to 1-3 hours of end-ischaemic NMP on the XVIVO kidney assist, with red cell-based perfusate, using gelofusine as the oncotic component[22]. The cannulation method was as with Cambridge, Toronto and Erasmus, which in one case caused NMP to end prematurely due to leakage. Potentially importantly, there was no significant second CIT with a median of 14 minutes. The important finding reported in this work is an efficacy signal with respect to DGF, 23.5% in the NMP cohort and 64.7% in the contralateral kidney from the SCS cohort (P=0.04), there was no difference in eGFR up to 1 year. It is worth noting the SCS only group had a slightly longer CIT 9 hours vs 6 hours, so how much of the effect was replacement of cold storage time with warm and how much was due to the intervention of NMP in and of itself is unclear.

1.1.2.6 Conclusion

The collective impression from the work of these groups is that renal NMP is likely to play a pivotal role in the preservation of kidneys for transplantation. Professor Nicholson and Dr Hosgood pioneered the concept with the first-in-human transplant, subsequent promising early clinical results and the completed a large multi-centre randomised trial. Rotterdam performed work similar to the Cambridge group, but brought into play a CE marked device, an important step towards broadening use and standardisation. Toronto's extensive porcine work has contributed hard evidence that

warm preservation is less damaging than cold preservation and then into clinical NMP with extended NMP times using a more physiological perfusate with oncotic pressure. Oxford, using an automated portable perfusion device, safely extended preservation times substantially to clinically meaningful durations, the benefits of which might translate to logistic advantages, improved assessment or therapeutic intervention. Then finally Sydney performed a paired trial design of NMP showing an efficacy signal in improved short-term function.

This advances the case for renal NMP in two important respects. First, to be used in a wider program setting as part of a hub and spoke system in which selected organs are placed on NMP for assessment or logistic benefit and transferred to an implanting centre for daytime transplantation. Second, to start a programme of testing a range of therapeutic interventions on kidneys in pilot trials. There has been global interest in complement modulation in the context of kidney transplantation for many years, and there are potential therapeutic complement-based interventions that might be suited to NMP delivery.

1.1.3 NMP as a Model for Transplantation of Human Kidneys

When considering any investigation into characterising a biological process in the context of transplantation or assessing an intervention, whether that be NMP itself or therapeutics delivered during NMP, there is a choice as to how to best model that prior to embarking on a human clinical case. When considering complement biology, species matters. Despite being an evolutionarily ancient part of mammalian immunity porcine and human complement systems are not interchangeable: many core proteins (C3, C5, factor H/I, properdin) and regulators (CD46/MCP, CD55/DAF, CD59) differ in sequence and function, and cross-species regulation is poorly conserved (i.e. human regulators do not effectively control porcine convertases and vice versa)[33-35]. This leads to exaggerated xeno-triggering on pig endothelium (anti-Gal/Neu5Gc driven classical/lectin activation) seen in early xenotransplantation, which is absent in human-to-human settings[36,37]. Crucially, several lead therapeutics are species specific, a classic example being the C3 inhibitors from the compstatin family which are primate-

specific[38] or anti-C5 antibodies like eculizumab which have no affinity for porcine C5[39,40], so efficacy, dose, and PK/PD in pigs are unreliable surrogates. Because renal tubular and endothelial complement expression and regulation during NMP are human-specific, and drug targets and epitopes differ, trying to investigate and test interventions in porcine kidneys is limiting, and an ex vivo human model is needed.

There has not been an extensive number of publications using ex vivo reperfusion modelling with human kidneys but taken with porcine studies there is a reasonable body of work using NMP with whole blood or whole blood like perfusates to mimic transplantation. For porcine work there is of course the available option of transplantation, which is the gold standard in an animal setting, an ex vivo model can still have some advantages. In a reperfusion model, experimental conditions can be very tightly controlled, and a higher degree of scrutiny and sampling can take place on a circuit. With declined human organs it is of course the only option, and we must be aware of its limitations. Ex situ perfusion of declined organs is reliably limited to 24-48 hours, meaning the model is only useful for scrutinising the very early post-transplant period[41]. The kidney is in isolation and therefore lacking in the physiological interplay between different systems, such as the reticuloendothelial system for the management of free haemoglobin. The circuit is composed of artificial surfaces, notably a hollowfibre oxygenator which depending on the type of biology being scrutinised could have confounding effects.

The ex vivo kidney perfusion model has clear potential for studying early IRI and complement biology, having already been adapted to reproduce a model for an ABO-incompatible transplant environment and ABMR from donor specific antibodies (DSAs to donor HLA), achieved by modifying a standard NMP circuit to permit complement activation through restoration of key plasma proteins[42]. The circuit was primed with packed red cells and supplemented with clinically unused FFP as the source of complement and coagulation factors, while heparin was deliberately minimised to preserve thrombo-inflammatory readouts without circuit thrombosis. The investigators found that after an initial stabilisation phase, introducing antibody triggers generated reproducible rejection phenotypes. For their HLA-incompatible setting, the complement-fixing anti-HLA class I monoclonal antibody W6/32 (with low-titre FFP)

caused rapid haemodynamic collapse with multifocal linear glomerular capillary C4d and microvascular/macroscopic thrombosis, consistent with early classical-pathway activation. In their ABO-incompatible setting, high-titre anti-A/anti-B FFP produced a marked fall in flow and peritubular microthrombi even without detectable C4d, indicating that the complement/thrombotic signature varies with the initiating antibody stimulus. These models demonstrate that one can create a strong platform to interrogate complement activation and inhibition in a controlled, transplant-relevant system.

1.2 Complement & the Transplant Kidney

The complement system itself is evolutionarily ancient; at a basic level, it is a proteolytic surveillance network that predates adaptive immunity. There are complement-like systems present across invertebrates and early vertebrates, particularly lectin- and alternative-pathway–like recognition and amplification systems, which are detectable well beyond mammals[43]. Among invertebrates, the horseshoe crab with evolutionary lineage back roughly 450 million years, have a system akin to a very basic complement-type innate response. In jawless vertebrates such as hagfish, divergent at a similar time, complement components spanning lectin/alternative mechanisms are present in the absence of immunoglobulin-based adaptive immunity[44].

In humans, the complement system comprises >50 soluble and membrane-associated proteins, with pattern-recognition molecules, zymogens, convertase components, receptors and regulators which are encoded across the genome and operating as a continuously poised system[45]. Basal activation is counterbalanced by layered regulation on host surfaces and in plasma, such that a rapid, focused inflammatory response can be unleashed when activation signals are generated, but with most of the collateral self-injury inhibited.

Activation proceeds through the three main pathways, classical, lectin and alternative which differ in their initiating triggers, but converge on a common pathway, with the formation of C3 convertases, cleavage of C3, amplification, and then C5 cleavage and C6-9 activation resulting in terminal membrane attack complex (MAC or C5b-9) formation. The classical pathway is typically initiated when C1q binds immune complexes, either IgM or IgG, or altered-self structures and pentraxins. Then the associated proteases C1r/C1s cleave C4 and C2 to generate the classical/lectin C3 convertase (C4bC2a). The lectin pathway is initiated by pattern-recognition molecules, MBL, ficolins and collectins which bind carbohydrate motifs on microbes or stressed cells, this activates MASP proteases that similarly cleave C4 and C2 to form the same C3 convertase. The alternative pathway is constitutively engaged via C3 hydrolysis and becomes a powerful amplification loop when C3b is deposited on permissive surfaces, recruiting factor B and factor D to assemble the alternative C3 convertase (C3bBb),

stabilised by properdin. Regardless of entry route, progressive C3 activation drives opsonin deposition and inflammatory signalling, while addition of C3b to convertases permits C5 cleavage and assembly of C5b-9 as MAC or as soluble terminal complement complex in fluid phase (sC5b-9)[46].

Crucially, complement activation is not only direct cell lysis. Its other biologically relevant outputs in transplantation are often opsonisation, anaphylatoxin-driven inflammation, and sublytic MAC signalling, all under tight regulatory control. Opsonins, principally C3 fragments (C3b, iC3b, C3d/C3dg) are deposited on surfaces and engage complement receptors (CR1/CR3/CR4/CR2), shaping phagocytosis, immune complex handling, antigen retention, and B-cell co-stimulation[47,48]. Anaphylatoxins, C3a and C5a, signal through their receptors, C3aR, C5aR1 and C5aR2 to recruit and activate leukocytes, amplify cytokine production, and promote endothelial activation[49]. These effects are particularly relevant in IRI and early microvascular inflammation. C5b-9 can be directly cytolytic on vulnerable cells, but often in nucleated cells acts sublytically to trigger intracellular signalling, inflammasome activation, and pro-inflammatory gene programs. Complement regulators exist in both fluid-phase, in the form of factor H, factor I, C4BP and C1 inhibitor, and membrane-bound, with CD46/MCP, CD55/DAF and CD59 being crucial[50]. These regulators set the threshold for activation and determine whether complement remains contained or becomes injurious on renal endothelial and tubular surfaces (Fig 1.2).

The kidney is not a passive recipient of liver-derived complement proteins, with multiple renal cell types able to synthesise complement, and tubular epithelium in particular is a major intrarenal source of complement components[51]. This local production matters in transplantation because donor-derived complement can contribute to injury and shape rejection biology, complementing the effects of circulating recipient complement. Alongside extracellular complement, a further layer of intracellular complement signalling, sometimes termed the complosome, has been implicated in maintaining cellular homeostasis and may influence how renal endothelial and epithelial cells respond to stress[52].

Complement biology and nephrology are deeply intertwined, with the kidney being both a frequent target of complement-mediated injury and an active participant in

complement biology[53]. In native kidney disease, dysregulated complement is central to a spectrum of conditions that progress to kidney failure. Atypical haemolytic uraemic syndrome (aHUS) is a prototypical example, where defective regulation at the endothelial surface results in excessive alternative pathway (AP) amplification, culminating in thrombotic microangiopathy and acute kidney injury with high relapse risk, including after transplantation[54]. C3 glomerulopathy (C3G) similarly reflects AP-dominant dysregulation, commonly through acquired drivers such as C3 nephritic factor stabilising AP C3 convertase or genetic variants affecting AP control. The pathological hallmark is predominant glomerular C3 fragment deposition with inflammation and progressive loss of function and can also recur after transplantation when the systemic dysregulation persists[55]. In lupus nephritis, immune complexes initiate classical pathway (CP) activity, generating C4d/C3 fragments and inflammatory recruitment[56]. Related patterns are seen across other immune-complex glomerulonephritides, such as some forms of membranoproliferative GN or C2 deficiency causing lupus-like nephritis, where complement activation products both mark disease activity and contribute to effector injury[57].

In transplantation, this means that some patients may arrive on the waiting list because of complement driven kidney failure, and their post-transplant risk is shaped by that disease process. However, there is further involvement for complement in transplantation due to the unique stages the transplant kidney goes through. Donor physiology and death, procurement and cold storage, machine perfusion strategies, implantation with reperfusion, and then the long tail of alloimmune and non-alloimmune injury. Across all these phases, complement acts as a cause or an amplifier of sterile inflammation and a mechanistic bridge between injury and adaptive immunity, in part why early graft dysfunction and ischaemic burden translate into later immunogenicity and inferior graft survival[53].

This is why complement can be engaged early, locally and persistently in the transplant kidney, even when systemic markers only partially capture the tissue-level biology, and why further understanding its biology and manipulating with targeted therapeutics is an important avenue of research.

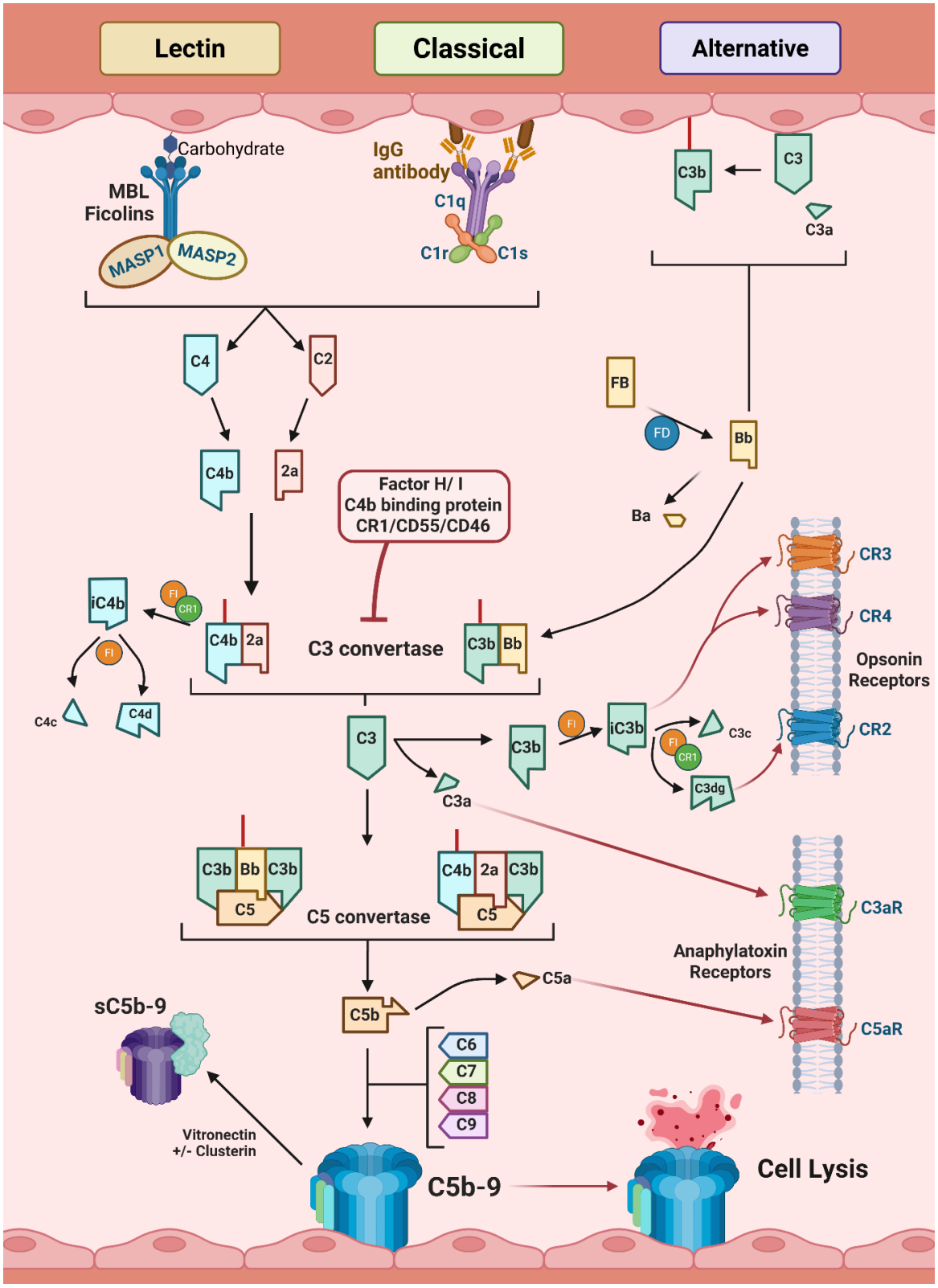


Figure 1.2 ***Schematic overview of the complement cascade and its major effector pathways.*** *An overview of activation via the lectin, classical and alternative pathways and their convergence on C3 and C5 cleavage. The LP is initiated by pattern-recognition molecules such as MBL and ficolins binding carbohydrate structures, with downstream activation of MASP1 and MASP2. The classical pathway is triggered by antibody-mediated activation of the C1 complex. Both pathways generate the classical/lectin C3 convertase, C4b2a. The alternative pathway is initiated by spontaneous C3 hydrolysation and amplification through FB and FD, generating the alternative pathway*

C3 convertase, C3bBb. Endogenous inhibitory regulators of C3 convertase include FH, C4BP, CR1, CD55 and CD46. The C3 convertases cleave C3 to C3a and C3b, promoting both anaphylatoxin signalling and opsonisation. Surface-bound C3b is further processed by FI to generate breakdown products including iC3b and C3dg/C3d. These fragments interact with complement receptors including CR1, CR2, CR3 and CR4, mediating opsonisation and immune cell responses. Addition of C3b to the C3 convertases forms the C5 convertases, which cleave C5 into C5a and C5b. C5a acts through C3aR and C5aR to mediate inflammatory signalling, while C5b initiates assembly of the terminal pathway with C6, C7, C8 and C9 to form C5b-9. Terminal pathway activation results in either membrane insertion of C5b-9, causing cell injury and lysis, or formation of soluble sC5b-9 in the presence of regulatory proteins such as vitronectin and clusterin.

This thesis will aim to expand on what is known by scrutinising complement proteins during kidney NMP and through controlled ex vivo modelling, in a hope to better understand when and where complement is activated, how this relates to measurable injury and function, and how pathway-specific inhibition may modulate those processes. However, some of the mechanistic groundwork has already been laid across distinct phases of the transplant journey, which are outlined below.

1.2.1 Complement & Organ Donation

There is some evidence that complement activation begins upstream of procurement, particularly in deceased donation. Compared with living donation, where physiology is stable and ischaemic times are minimised, the deceased donors experience profound systemic effects that prime organs for inflammatory injury. For DCD organs the process of death and subsequent warm ischaemia is added to the donor's premorbid and peri-mortem inflammatory state. For DBD organs, the brain death itself appears to be an early trigger of systemic and intrarenal complement activity, with its classical catecholamine storm, haemodynamic instability, hormonal dysregulation and a surge of inflammatory signalling affecting the endothelium and microcirculation.

Using the QUOD biobank, Knijff and colleagues analysed plasma samples at various points of brain death management, immediately after brain-death declaration, at the end of donor management, and just before cross-clamp/retrieval, as well as pre-implantation donor kidney biopsies[58]. They observed that circulating complement activation products were significantly elevated in DBD donors compared with the living donor controls. They found elevated levels of C4d, Bb, C3c, and C5b-9, and importantly that this activation was already present early after brain death and remained elevated through management. The study was of clinical importance because higher systemic

complement activation at retrieval showed associations with poorer short-term outcomes. Higher Bb was linked to DGF, and higher C4d trended toward higher DGF and lower early eGFR. At the tissue level, donor biopsies demonstrated local complement deposition of C4d, C3d and C5b-9, and semiquantitative compartmental scoring highlighted the vascular pole as a notable site of terminal pathway signal, with greater C3d and C5b-9 staining in kidneys that subsequently developed DGF. When donors were stratified by short, medium, and long brain-death duration, upstream activation products, C4d and Bb, tended to decline over time in those with prolonged brain death, consistent with rapid early activation followed by consumption and stabilisation over the course of brain death management. This study only contains DBD donors but is nonetheless important as it adds to a small existing body of clinical evidence. An older, but larger cohort included a small number of DCD donors (n=33) within it, with plasma samples taken immediately prior to withdrawal of life sustaining treatment. DCD donors as with DBD had elevated circulating of C5b-9, C4d and Bb, which they found to be associated with acute rejection, mainly vascular type Banff II/III, but not with DGF or graft survival[59]. A smaller more recent cohort had slightly contradictory findings with lower C4b being mildly associated with acute rejection in the first year, though the key message of the paper was comparing DBD and DCD with healthy controls. They found that DCD donors had higher C3, but lower C2, C4b and Factor D compared with DBD, but both donor types had all markers raised relative to healthy controls[60].

While there is limited evidence, collectively the current published literature does support that complement activation is not merely a reperfusion phenomenon, it is already active in the donor and may prime the graft's microvasculature for subsequent IRI, rejection and early dysfunction.

1.2.2 Complement & Preservation

The preservation time is of course not a passive time window, with many deleterious effects ongoing, as demonstrated by the direct relationship with longer CIT and poor outcome[61]. One of the important effects is the priming for later complement activation[62]: during cold storage, ischaemia drives metabolic stress and anaerobic metabolism with progressive acidosis, and these conditions can directly favour alternative pathway activation. Acidic microenvironments interfere with normal

complement regulation and lower the threshold for amplification, while anaerobic metabolism generates nucleophiles such as ammonia that can initiate alternative pathway convertase formation via C3 modification[63]. These biochemical shifts provide a basis for early complement engagement during preservation, before the graft ever encounters recipient reperfusion.

Ischaemia also remodels the renal endothelial and parenchymal cell phenotype in ways that make the graft surface more permissive to subsequent complement attack. A key protective feature of healthy endothelium is its antithrombotic and anti-complement glycocalyx layer, rich in proteoglycans that help localise inhibitory regulators. During ischaemia, endothelial heparanase and metalloproteinases are upregulated, promoting glycocalyx cleavage and breakdown. This shedding leads to loss of surface-associated inhibitors of complement and coagulation, including factors such as C4b-binding protein, factor H, and C1 inhibitor, making the endothelial surface less protected and more prone to uncontrolled activation[64]. In parallel, endothelial activation driven by cytokines and by insertion of sublytic C5b-9 shifts the vasculature toward a pro-adhesive, pro-coagulatory and pro-inflammatory phenotype, with complement serving as both a trigger and an amplifier of the sterile inflammation[65].

A further layer of initiation arises from pattern recognition. Hypoxic injury to the endothelium exposes damage-associated molecular patterns (DAMPs) on tubular and endothelial surfaces that are recognised by complement pattern-recognition molecules, C1q for the CP and the LP proteins such as MBL, collectins and ficolins[66]. Natural IgM binding to altered-self epitopes provides an additional route to engage upstream activation, and once C3b is deposited, the AP amplification loop propagates[67].

Therefore, it is plausible that ischaemia duration is a driver of these preservation-phase signals. Longer CIT accentuates endothelial stress, glycocalyx degradation, loss of regulatory protection and DAMP exposure, all of which lower the threshold for complement activation and amplify effector generation when perfusion is initiated or when the kidney is rewarmed. Mouse transplant models have previously demonstrated longer CIT is associated with greater subsequent intragraft complement, with higher C3 mRNA expression after reperfusion[68]. Human pre-reperfusion biopsy studies similarly

demonstrate increased renal C3 gene expression in deceased donors compared with living donors, and this increased local C3 expression has been associated with inferior short-term graft function after transplantation[59,69].

As machine preservation expands, with HMP being standard of care in many countries, there is data emerging on preservation-phase complement biology. Proteomic analysis of DBD kidneys preserved with $HMPO_2$ by van Leeuwen et al.[70] analysed perfusate early after starting HMP and again at the end of perfusion, comparing kidneys with good and suboptimal one-year outcomes. Interestingly, kidneys with good outcomes showed higher abundance of several classical-pathway–associated proteins, including C1 complex components and the regulator C4b-binding protein alpha chain, whereas suboptimal outcomes were more characterised by signatures consistent with structural injury later in perfusion. The authors interpreted these findings as supporting the concept that perfusate wash-out reflects tissue-resident proteins and the local regulatory environment at the glycocalyx, and that complement-related signals can already discriminate organ quality during preservation.

Machine perfusion has expanded preservation into a therapeutic and diagnostic platform. NMP creates a physiological environment where this injury can manifest, and an accessible circuit for serial sampling of complement activation products, functional complement activity, and injury biomarkers. This is conceptually attractive for complement modulation because it occurs before the complete inflammatory biology of implantation in the recipient, and because local delivery to the graft may limit the risks associated with systemic complement suppression. The prospect of preventing complement activation from becoming established on renal surfaces or blunting downstream effector formation before implantation has made complement inhibitors prior to implantation an attractive prospect.

1.2.3 Complement & Implantation

Implantation and reperfusion represent the most consequential moment for complement-mediated injury, when the ischaemia-conditioned kidney is abruptly re-exposed to oxygenated blood and recipient plasma with its abundance of complement

proteins. Reperfusion initially amplifies injury through oxidative stress, endothelial activation, microvascular dysfunction and innate immune recruitment[71].

Complement is engaged early in this setting because IRI exposes and generates triggers for the complement system, altered-self surfaces, cellular debris, and injured endothelium. Ischaemia and reperfusion stress renal endothelial and tubular epithelial cells, disrupt the endothelial glycocalyx, and reduce the functional protection normally conferred by surface-bound complement regulators[64]. At the same time, DAMP exposure on hypoxic tubules and activated endothelium provides ligands for complement pattern-recognition molecules, facilitating classical/lectin initiation with rapid downstream amplification, particularly once C3b deposition allows the alternative pathway to act as a potent amplification loop[53].

Once activated, complement contributes to renal IRI not just direct C5b-9 mediated lysis. C3 activation deposits opsonic fragments on injured renal surfaces and debris, while the anaphylatoxins C3a and C5a amplify inflammation by recruiting and activating innate immune cells and increasing endothelial activation, adhesion molecule expression, and microvascular inflammatory tone[72]. These effects promote leukocyte margination and interstitial infiltration, linking intravascular complement activation to parenchymal damage. In parallel, terminal pathway activation generates C5b-9, which in nucleated renal endothelial and tubular cells often acts at sublytic levels as a signalling stimulus that augments cellular activation and inflammatory programmes, thereby reinforcing the injury cycle established at reperfusion[73].

A recurring observation in the transplant literature is that deceased-donor kidneys, but not living-donor kidneys, can release substantial quantities of terminal complement products, such as sC5b-9, around reperfusion, consistent with the concept that greater ischaemic burden and pre-existing donor inflammation translate into more intense complement effector generation at implantation[74]. While reperfusion is an unavoidable aspect of receiving a transplant, intervention could be undertaken during donation, preservation or systemically in the recipient to dampen the complement response when it occurs.

1.2.4 Complement & the Transplant Candidate

Complement also affects the transplant landscape before implantation through the biology of the transplant candidate. As discussed, many candidates reach transplantation because of complement-mediated kidney diseases, such as aHUS or C3 glomerulopathy, making complement simultaneously a cause of native kidney failure and a determinant of post-transplant risk.

There are also considerations in the dialysis dependant recipient, dialysis itself adds an important layer to implantation because it repeatedly exposes the potential recipient's blood to artificial surfaces, promoting complement activation and potentially altering the balance of activators and regulators before transplantation. Haemodialysis membranes can trigger complement, classically described via alternative pathway biomaterial-induced activation which produces anaphylatoxins (C3a/C5a) and C5b-9 during sessions[75,76]. Beyond triggering activation, there is evidence that key soluble complement inhibitors can be lost by adsorption to dialysis membranes, including factor H and clusterin, so dialysis can both activate complement and reduce inhibitory capacity[77,78]. Repeated complement activation during dialysis contributes to systemic inflammation and endotheliopathy, which could lower the threshold for exaggerated inflammatory responses at transplantation and potentially increasing the risk of early graft dysfunction[79].

Finally, in sensitised candidates and in ABO/HLA incompatibility, complement is central to antibody-mediated rejection. Donor-specific and natural antibodies can fix complement on the graft endothelium, producing microvascular inflammation and tissue injury via complement and subsequent immune recruitment[80,81]. During implantation and reperfusion, a highly stressed graft endothelium is suddenly exposed to recipient plasma containing complement proteins, activation fragments, and variable inhibitory reserve. A recipient with repeated dialysis-associated complement activation and potential depletion of regulators may therefore have increased early microvascular inflammation through C3a/C5a signalling and terminal pathway activity at a moment when the graft's glycocalyx and surface regulators are already compromised by ischaemia.

While complement is a vital part of human immunity, the abnormal nature of transplantation, from brain death and organ retrieval to dialysis for the recipients, cause complement dysregulation across the process. For this reason, complement is the focus of much research and the development of complement modulating drugs, some of which could be potentially beneficial in transplantation.

1.3 Complement Inhibition in Transplantation

Given the extent of the number of proteins involved in the complement cascade as discussed above, there are a wide range of potential drug targets for inhibition or upregulation to modulate and limit complement activation in a variety of disease settings.

1.3.1 C1 Esterase Inhibitors

C1 esterase inhibitors are plasma-derived C1-INH, the endogenous regulator which is a fluid-phase serine protease that inhibits C1r/C1s and MASP1/2, thereby inhibiting the CP and LP. There are 3 commercially made drug therapies, berinert and cinryze which are plasma-derived and ruconest which is recombinant. The drugs are approved for the treatment of hereditary angioedema (HAE), but are possibly the most exciting of the transplantation trials, principally used in a kidney context for DGF and ABMR.

A recipient delivered phase I/II trial with 70 high-risk DCD recipients randomised and received 2 doses of 50U/kg at induction and 24 hours post-op of berinert is the largest experience. The primary endpoint of dialysis in week 1 was not different with C1 inhibition, but dialysis burden was lower over subsequent weeks, and 1 year eGFR was significantly higher compared with placebo. In the 3-year follow-up study the improved eGFR persisted within the cohort who received C1-INH[82,83].

A further trial delivered berinert during cold flush has shown promise for direct renal delivery. 40 deceased donor kidneys randomised for back-table flush with 500U of C1-INH with the hope of reducing DGF rate, which did not change, but at 6 months, and 30 months the eGFR was higher in C1-INH group. Their presented biopsies showed good intragraft localisation of C1-INH and a reduction in C4d staining[84].

In the context of ABMR, a phase I/II placebo-controlled trial in 20 highly sensitised recipients receiving desensitisation demonstrated C1-INH (20 IU/kg intra-op then twice weekly for 7 doses) was safe, achieved expected pharmacodynamic effects (higher C1-INH levels and increased circulating C3/C4), and showed a numerically lower ABMR, but was inadequately powered for clinical endpoints[85].

For established acute ABMR, a multicentre double-blind pilot tested C1-INH as add-on to plasmapheresis/IVIg in 18 patients aiming to demonstrate significant improvement on clinically relevant transplant glomerulopathy on 6-month biopsy. While there was no significant difference in biopsy scoring, there were signals to renal functional improvement and numerically less transplant glomerulopathy on 6-month biopsies in treated recipients, alongside the important observation that plasmapheresis substantially reduces endogenous functional C1-INH. Suggesting the therapy is providing replacement as well as inhibition rationale in this setting[86].

These suggest C1-level inhibition is feasible and appears safe in the peri-transplant period, with potentially improved longer-term graft function rather than a binary reduction in early DGF. The initial experience suggesting these effects are still present from cold flush delivered inhibitor is interesting, presumably acting primarily on the already bound C1r/s and MASP complexes bound during death, retrieval and storage, rather than dynamically acting on reperfusion, given it is a fluid-phase inhibitor. Nonetheless the strategy appears to influence local CP/LP suppression while minimising systemic complement impairment. If this effect can be demonstrated in a larger multi-centre setting it could be a valuable adjunct to the kidney back-table.

1.3.2 CR1 Regulation

Complement receptor 1 (CR1/CD35) is an endogenous regulator that accelerates decay of C3/C5 convertases and acts as a cofactor for factor I–mediated inactivation of C3b/C4b. Therapeutics built from CR1, of which there are a few iterations, provide broad proximal regulation across all pathways. Soluble CR1 (TP-10, recombinant sCR1) is a fluid-phase convertase inhibitor originally explored for IRI settings of cardiopulmonary bypass and lung transplantation. In a randomised, double-blind, placebo-controlled multicentre trial in lung transplantation, 59 recipients were randomised, with the intervention cohort receiving a single pre-reperfusion systemic dose of TP-10. TP-10 achieved high complement inhibition during the first 24 hours, measured by a dramatic difference in CH_{50} (total haemolytic complement) and C3a levels, which returned to normal by 72 hours. This resulted in a significant different in their primary endpoint of extubation within 24 hours, 50% vs 19%[87]. This 20-year-old trial is one of the clearest peri-reperfusion complement-inhibition proof-of-concept

trials in transplantation, with simple clear mechanistic data supporting a clinically meaningful outcome.

In kidney transplantation, CR1-based strategies have focused on graft-targeted inhibition. This is in the form of mirococept (APT070), a CR1-derived regulator engineered to localise to membranes. It is designed to bind ischemia-exposed surfaces and locally suppress complement convertase activity, conceptually aiming to reduce systemic immunosuppression while protecting the graft microvasculature. The method of delivery is the same as the success seen in C1-INH, however unlike C1-INH, this molecule is membrane bound it has the potential for being effective on complement binding and activation injury prior to but also including reperfusion. While the concept is solid, early clinical trial was ineffective, due to dosing insufficiency[88]. With the dose refined in animal modelling, a phase IIa RCT is underway which could be as exciting as another simple kidney directed intervention, which could also be delivered in other preservation modalities as will be explored later in this thesis[89].

1.3.3 C5 Cleavage

C5 cleavage is a central step in the cascade that generates the potent anaphylatoxin C5a and initiates terminal pathway assembly via C5b, culminating in C5b-9 formation. Clinically used anti-C5 monoclonals, notably eculizumab and the longer-acting ravulizumab, are fluid-phase inhibitors that bind C5, preventing activation, thereby blocking both C5a and C5b-9 production. Although originally developed for PNH and aHUS, there is a strong transplant rationale where terminal pathway effector injury is central, particularly complement-fixing DSAs causing microvascular injury in ABMR, and in IRI and the subsequent DGF setting.

ABMR prevention has the highest quality trials, a phase 2, multicentre, open-label RCT in sensitised living-donor kidney recipients undergoing pre-transplant desensitisation (102 randomised, 51 allocated to eculizumab post-transplant). The primary endpoint was a week-9 composite of biopsy-proven acute ABMR (Banff 2007 grade II/III), graft loss, death, or loss to follow-up, but there was no significant difference between eculizumab and standard care (9.8% vs 13.7%)[90]. Similar results were found in an open-label, single-arm, multicentre international phase 2 study in sensitised deceased-donor

kidney recipients with preformed DSA, designed to prevent acute ABMR early post-transplant. Here, the trial used the same composite within the first 9 weeks, which was significantly lower than what was expected for standard care in preformed DSA (8.8% vs 40%), but this was not a randomised comparator group[91].

Two trials have been conducted using eculizumab focusing on DGF and early function. An adult trial containing 27 recipients, 16 receiving eculizumab systemically prior to reperfusion show no difference in DGF, which was its primary endpoint (44% vs 45%), and early creatinine reduction and graft function through 180 days were similar[92]. A single-centre prospective randomised trial in 57 paediatric kidney transplant recipients, where half received a single pre-transplant eculizumab dose in a steroid-free regimen. The children who received eculizumab had better early graft function and less chronic injury on protocol biopsies, but noted an unacceptably high number of early graft losses among non-vaccinated eculizumab-treated children during flu-like infections, highlighting the potential dangers of systemic terminal pathway blockade in immunosuppressed recipients[93].

Despite the potential risks, there remains interest in systemic complement blockade. A long acting C5 inhibitor, ravulizumab is currently in a phase 3, double-blind, randomized, placebo-controlled multicentre trial (AWAKE; NCT06830798) in adults receiving a deceased-donor kidney from ECDs. The intervention is a single IV dose administered from 24 hours to 30 minutes before transplantation. The primary endpoint is to reduce DGF severity as measured by time to freedom from dialysis. The intervention may be risky, but the endpoint shifts from binary DGF to a more granular measure of DGF burden, which captures early function and is a step forward.

The interest is based on pre-clinical animal models large-animal kidney models, where C5 blockade has repeatedly shown biologic effect on inflammation and microvascular injury. In a porcine kidney preservation model (18 hours SCS followed by 4 hours NMP reperfusion model), kidneys randomised to C5 inhibition showed that NMP-associated inflammatory response was attenuated compared with controls[94]. In pig-to-primate renal xenotransplantation, anti-C5 strategies (including tesidolumab) have been used to reduce early antibody-mediated graft injury and improve short-term survival, and in pig-to-human decedent kidney xenotransplantation, eculizumab has been associated with

reduced thrombotic microangiopathy, collectively reinforcing a role for terminal complement in early microvascular injury from complement activation even when the precise triggers differ from allotransplantation[95].

Overall, C5 inhibition in kidney transplantation has the clearest mechanistic fit and is most mature in high-risk ABMR whereas adult DGF prevention with eculizumab has not shown efficacy in pilot RCTs. The direction of travel appears to be towards longer-acting C5 blockade with endpoints that better capture DGF severity, but still within the concept of recipient delivery rather than organ or donor.

1.3.4 C5a-C5aR Axis

Blocking the C5a–C5aR axis aims to suppress the chemotactic and leukocyte-activating arm of complement while potentially preserving C5b-9-mediated antimicrobial defence. The clinically established agents are avacopan, an oral C5aR1 antagonist developed and approved for ANCA-associated vasculitis[96], and vilobelimab, an IV anti-C5a antibody trialled in sepsis[97].

Within transplantation the field has not moved beyond mouse and rat studies. In a mouse allotransplant model with short-term recipient treatment with a C5aR antagonist there was an improvement in renal allograft survival and reduced apoptosis and inflammatory infiltration[98]. In another mouse transplant model, it has been added during SCS which reportedly improved early graft survival from a low baseline of 29% in a syngeneic model to 57%[99]. For a rat renal IRI model IV C5aR antagonism reduced tissue TNF-α, vascular leakage and haematuria and preserved creatinine clearance better than control[100].

While interesting the translation to large animal models and human studies has not yet been made, with possible reticence over difficulty in finding efficacy in more prominent central blockade and that a limited focused approach such as this may only have a small signal hard to discern in human trials.

1.3.5 C3 blockade

C3 is a central protein, the convergence and amplification hub for all pathways. Inhibiting C3 prevents opsonisation, anaphylatoxin generation (C3a, and indirectly C5a),

and C5b-9 formation. Clinically, the compstatin-family has established that systemic proximal blockade is feasible, with pegcetacoplan, a fluid-phase C3/C3b inhibitor approved for PNH, providing proof-of-concept that sustained C3 inhibition can be delivered systemically, albeit with the expected requirement for rigorous infection prevention and monitoring[101].

In transplantation, the published work has gone as far as large-animal preclinical work. In a sensitised non-human primate kidney allograft model, with DSA and immunologic memory enriched for complement-fixing antibody injury, recipients received transient peri-transplant Cp40 around the time of transplantation. This strategy significantly prolonged renal allograft survival and mitigated ABMR-associated tissue injury compared with controls, supporting the concept that proximal blockade can attenuate C5b-9 injury and modify the inflammatory milieu in sensitised transplantation[102]. The same Cp40 demonstrated reduction in complement activity in a xenoreactive study of wild-type pig hearts perfused with human blood[5].

Clinical transplant studies with dedicated C3 inhibitors will be emerging, a phase 3, randomised, placebo-controlled, multicentre trial of pegcetacoplan for DGF prevention is registered (NCT07020832), yet to start recruitment. It will be a trial of adults receiving a high risk deceased-donor kidneys, explicitly designed around DGF risk, aligning C3 blockade with an IRI-heavy clinical setting. This follows on from the NOBLE trial, a phase 2 prospective multicentre open-label randomised controlled trial evaluated pegcetacoplan 1080 mg twice weekly subcutaneous infusion plus standard-of-care vs standard-of-care alone in recurrent C3 glomerulopathy (C3G) or immune complex MPGN following transplant. The primary endpoint was reduction in C3c staining on renal biopsy at week 12, and pegcetacoplan produced marked reductions in biopsy C3 deposition in a substantial proportion of treated participants, with accompanying improvements in complement activation markers and improved proteinuria trends[103]. Given the mechanistic response, and level of blockade achieved, a translation into DGF could be effective, albeit with careful monitoring of infective complications.

1.3.6 Early Lectin Pathway Components

The lectin pathway is initiated by pattern recognition molecules (MBL, ficolins, CL-11) and propagated by MASP proteases (especially MASP-2), which then cleaves C2 and C4 producing C3 convertase and joining the common terminal pathway. This area of the cascade has not been much explored in organ transplantation. The most advanced therapeutic is narsoplimab, a monoclonal antibody targeting MASP-2 which has been used in haematopoietic stem cell transplant-associated thrombotic microangiopathy (TA-TMA), where lectin pathway activation contributes to endothelial injury[104]. A small cohort was given weekly IV narsoplimab for TA-TMA with a mortality rate exceeding 50%, in those that responded to treatment (61%) mortality decreased to 6%[105], which correlates with similar improved survival in another more recent trial including children as well as adults[106]. This has not translated into transplant research, with only mouse renal IRI studies thus far, in which MASP-2 inhibition protects against ischaemic AKI[107].

C2 inhibition has had limited publications thus far, but demonstrated promise in a rat kidney transplant model, showing a significant improvement in renal recovery rate following transplant[108]. A modified human version, empasiprubart has been taken forward into a phase 2 human clinical trial currently recruiting, following a phase 1 safety study in healthy volunteers[109]. The trial aims to assess addition of systemic C2 blockade delivered to the recipient prior to transplant improves 6-month eGFR. This compound will be explored in ex vivo modelling in this thesis.

CL-11 has not had any translation to large animal or human trials, with the evidence remaining in rodent transplant and IRI models. CL-11 being an endothelial stress ligand, that in its absence with genetically deficient mice, renal injury is reduced, with improved function and less post-injury fibrosis in syngeneic transplant[110]. CL-11 can be competitively blocked with L-fucose, which has been tested only in a mouse IRI model thus far and appears protective[66].

1.3.7 Alternative Pathway Components

The AP is both a constitutive system ticking-over and the dominant amplification loop for complement activation. AP-targeted therapy aims to suppress amplification while preserving classical/lectin antimicrobial functions. It can be suppressed by acting on

either factor B or factor D, though there has not been extensive research in the area. An oral factor B inhibitor, iptacopan, has been produced for AP-driven native-kidney glomerular diseases such as IgA nephropathy and C3G[111], but it has been tested in a small number of cases for recurrent C3G in allografts, with early clinical improvement and graft stability reported[112,113]. Transplant specific studies remain in mice, where allotransplants into factor B deficient mice, they have reduced IRI, reduced allo-reactive T-cell response and prolonged allograft survival[114]. In a mouse renal IRI model using anti-factor B monoclonal antibody has also been demonstrated to be protective[115]. It has also been given to rats prior to inducing brain death, and attenuated brain-death related renal injury[116].

There is also an oral factor D inhibitor, danicopan, again used in the context of native-kidney glomerular diseases, tested in C3G[117], but has not been studied in renal IRI or a transplant settings as yet.

1.4 Concluding Remarks

Transplantation has transformed outcomes for patients with end-stage kidney failure, but its success has created a situation where demand outweighs supply, and too many retrieved kidneys, especially higher-risk DCD, older, co-morbid, or AKI donors, are still declined. Improving utilisation therefore depends on two linked advances: better confidence in organ quality, and credible means to modify risk before implantation. The questions for NMP are now can we preserve longer, assess robustly, and intervene safely?

Renal NMP is now a more stable, scalable platform. Early paradigms established safety and feasibility, but heterogeneity in devices, perfusates, cannulation strategies, and cold–warm times make interpretation across studies inappropriate. With the most recent prolonged NMP experience, automated perfusion on purpose-built systems showed that extended NMP is technically achievable and clinically deliverable with similar outcomes to standard care and offering logistical benefit. This is important as the potential value of NMP is not restricted to preservation, it is the potential creation of a therapeutic and diagnostic window.

Within that window, complement is a compelling biological process to interrogate and modulate. Across donation, preservation, and implantation, complement plausibly acts as a mechanistic bridge between ischaemic burden and early graft dysfunction, and through inflammatory amplification and immune priming, between early injury and later outcomes. Complement activation is not confined to the moment of reperfusion, it can be initiated in the donor, shaped during preservation, and then accelerated at implantation. Complement biology during kidney NMP remains poorly characterised, it is unclear when and where activation occurs in typical red-cell–based circuits, whether measured perfusate fragments reflect true intrarenal biology versus washout from donor biology, and how reliably complement can be assessed during perfusion as potential biomarkers.

Therapeutically, the breadth of the cascade provides many points of intervention, with encouraging progress for some strategies, particularly C1-level inhibition, where longer-term functional outcomes may improve even when binary DGF does not. Other

approaches remain earlier in the transplant pipeline or raise practical trade-offs between efficacy and infectious risk. There are two important conclusions, first, complement inhibition can be delivered peri-transplant with demonstrable pharmacodynamic effects. Second, the most attractive strategies for broad implementation may be those that achieve strong local graft protection while minimising systemic complement impairment.

The logical next steps, and the central rationale for this thesis, robust NMP systems make it realistic to test complement-focused interventions in controlled, transplant-relevant human models and, ultimately, in carefully designed clinical pilots. NMP offers a window into the organ biology prior to transplant while the organ is metabolically active. This could allow us to define the kinetics and compartmentalisation of complement activation, relate this to outcome, and then assess whether inhibition can be effectively delivered and an effect on the organ assessed.

2

Common Methods

Contents

2.1 Perfusion Methodology

2.1.1 XVIVO Device and Circuit

2.1.2 OrganOx Device and Circuit

2.1.3 Normothermic Reperfusion Model

2.1.4 Human Research Organs: Kidney Back table and Cannulation

2.1.5 Research Blood Preparation

2.1.6 NMP Perfusate

2.1.7 Normothermic Reperfusion Perfusate

2.1.8 Generic Sampling

2.2 Perfusate Analysis

2.2.1 Biochemistry

2.2.2 Perfusate Injury Biomarkers

2.2.3 Perfusate Complement

2.3 Tissue Analysis

2.3.1 Formalin-Fixed Tissue Processing

2.3.2 Immunohistochemistry Staining

2.3.3 Immunohistochemistry Trained Model Quantification

2.3.3.1 Manual Definition of Analysis Compartments

2.3.3.2 Nuclear Detection and Nucleus-only DAB Feature Extraction

2.3.3.3 Training and Application of a Supervised Object Classifier

2.3.3.4 Outcome Metric and Export

2.3.3.5 Quality Control

2.3.4 Immunohistochemistry Automated Pipeline Analysis

2.3.5 CellDive Multiplex Immunofluorescence

2.3.6 CellDive Analysis Pipeline

2.3.7 Frozen Tissue Processing

2.3.8 Bicinchoninic Acid Assay

2.3.9 Western Blotting

2.3.10 Native Gel Blotting

2.1 Perfusion Methodology

2.1.1 XVIVO Device and Circuit

The XVIVO Kidney Assist™ is a CE-marked device for kidney perfusion from 12–37°C, approved for NMP up to 6 hours. The device base unit consisted of two modules, one a water heater unit which pumped heated water and the other the sensor and control unit. The sensor unit had two temperature sensors, arterial and venous return, a pressure sensor, and an ultrasonic flow sensor; the centrifugal pump driver was also on this unit. The user could control the target perfusate temperature and perfusion pressure, the heater unit heated the water circuit to achieve the desired temperature, and the pump speed adjusted to deliver the set perfusion pressure.

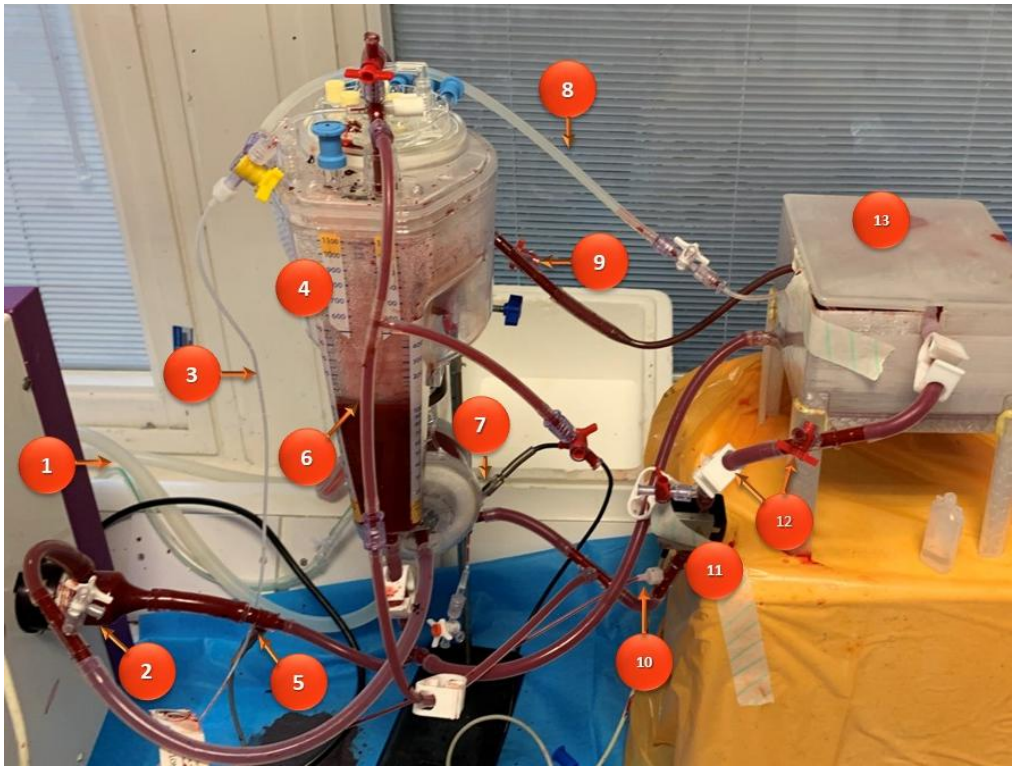


Figure 2.1 ***A Schematic overview of the modified XVIVO circuit.*** *1) tubing from XVIVO heater unit and tubing from external gas supply for the hollow fibre oxygenator, 2) the centrifugal pump on the XVIVO unit, 3) infusion line, 4) hard shell reservoir and hollow fibre oxygenator (Terumo CAPIOX FX), 5) venous temperature sensor, 6) bypass line, 7) arterial temperature sensor, 8) urine line, 9) venous three-way tap for flushing, 10) arterial pressure line, 11) arterial flow probe, 12) Robert's clamp and arterial three-way tap for in-situ flushing, 13) organ chamber.*

The device was intended to be used with an XVIVO sterile disposable set which was designed as an open system for the organ to be submerged in the perfusate with venous effluent flowing freely into the bowl. In order to make the perfusion paradigm as similar to the NKP1 clinical trial and to minimise haemolysis, a custom closed-circuit design

was used. The custom circuit consisted of a Terumo CAPIOX FX Series oxygenator with hardshell reservoir, centrifugal pump, and organ chamber connected with silicone tubing including an A-V shunt. The artery and vein were cannulated with Roberts clamps and a ¼ inch connector with two-way tap such that the kidney could be isolated and flushed without entraining air into the system or needing to disconnect the kidney from the circuit. The ureter was cannulated for periodic volume measurements and sampling but was otherwise left freely to drain into the organ chamber, which drained back into the circuit.

The XVIVO machine design allowed the user to set the temperature and perfusion pressure, which were set to 37°C and 75 mmHg as per the perfusion parameters used on the OrganOx prototype for the NKP1 trial.

2.1.2 OrganOx Device & Circuit

The prototype kidney perfusion device, named Metra-K (K100), was constructed by OrganOx Ltd.; this came as a retained base unit onto which an OrganOx Metra-K disposable set could be placed. The base unit components were a centrifugal pump driver, a pressure sensor input, urine flow sensor, ultrasonic flow sensor in the arterial line, a heater unit, and a gas supply system, which could mix oxygen from a concentrator and room air according to measured partial pressures. The latter two were controlled by measurements from the integrated inbuilt Terumo CDI-500H blood in-line blood gas analyser, the temperature sensor communicating with the device heater unit and the pH, pCO2, and pO2 sensors regulating the behaviour of the gas supply system. The device had a front-mounted touchscreen for the user to interact with the device graphical user interface, allowing control to some degree and monitoring of the perfusion. All measured metrics, including arterial flow, urine flow, pH, pCO2, pO2, potassium, and sodium levels, were stored on the device and could be downloaded via USB.

The manufactured disposable set was sterile and contained a softshell reservoir, centrifugal blood pump, hollow-fibre oxygenator, blood gas sensor situated on an A-V shunt, urine flow sensor, pressure sensor on the arterial inflow, organ container, infusion connection points, and associated silicone tubing.

The set was designed as a closed perfusion circuit; the artery and vein were cannulated, which created a closed circuit and minimised the perfusate-to-air interface, with the logic being to reduce haemolysis. The ureter was cannulated and the urine recirculated back into the reservoir, with a view to trying to maintain electrolyte haemostasis and avoid physiologically inappropriate replacement with stock solutions.

OrganOx had designed the prototype with a high level of automation to minimise user error. The centrifugal pump speed was regulated based on the pressure sensor to achieve the predetermined set point of 75 mmHg, which was hard coded on this version of the software such that the user could not alter it. The heater unit responded to the temperature sensor in the Terumo CDI-500H analyser to reach a perfusate temperature of 37°C, again pre-set. The inflow gas mixture delivered by the supply system was a mix of concentrated oxygen and room air depending on the partial pressures sensed by the CDI-500H device. There were also three infusion lines which could deliver anything of the user's choice, but at a set 1 mL/hr, which could not be altered.

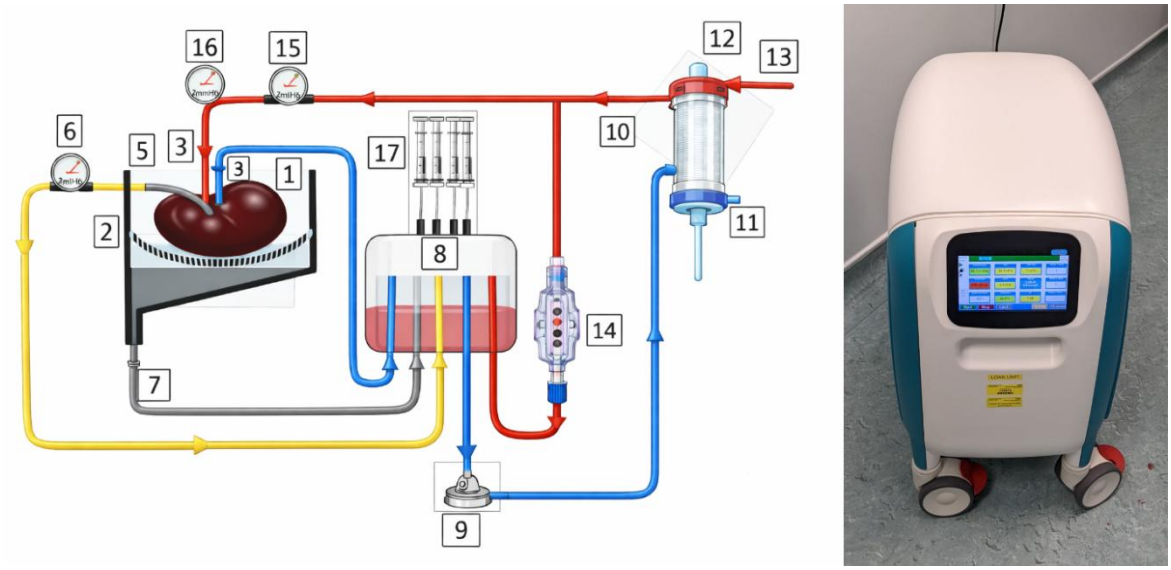


Figure 2.2 ***A Schematic overview of the OrganOx circuit.*** *Left: 1) kidney, 2) organ chamber, 3) arterial line, 4) venous line, 5) urine line, 6) urine flow sensor, 7) organ chamber drain (passively recirculated to reservoir), 8) soft shell reservoir, 9) centrifugal blood pump, 10) hollow-fibre oxygenator, 11) heated water column, 12) integrated assembly for gas and heat exchange, 13) gas supply (from air/O2 concentrator), 14) shunt sensor (Terumo unit, providing in-line pH, pCO2, pO2, and temperature measurement), 15) flow sensor;, 16) pressure sensor, 17) syringe drivers (for infusions run during perfusion). Right: Image of device with front facing GUI display and cover over disposable set inside.*

To facilitate the flushing of the kidney and circuit for the transition from NMP to NR while maintaining an air-free system, the cannulation required modification from intended use as per the NKP1 clinical trial. On both the arterial and venous cannulae there was

an extra ¼ inch straight connector with a two-way tap attached and a Robert's clamp proximal to them such that the kidney could be isolated from the device and a cold flush could be run through the kidney without entraining air into the system.

2.1.3 Normothermic Reperfusion Model

For clinical translation and interrogation of the complement activity human kidneys are required, as such a model must be used to mimic transplantation following NMP. The model of normothermic reperfusion (NR) used in this thesis was a plasma based perfusate with fresh frozen plasma (FFP) and packed red cells. FFP is a readily available, easy to store and contains the full spectrum of complement proteins needed as substrate for activation and to scrutinise the cascade's behaviour ex-situ.

The model started with 6 hours of NMP following arrival of the donor organ on SCS, at which point the perfusion was paused and the kidney flushed with cold Plasma-Lyte in situ, the inflow was connected via giving set to a two-way tap on a straight connector, with a Robert's clamp placed on the machine side, and the venous outflow connected to 1/8 inch silicone tubing via a two-way tap on a straight connector with a Robert's clamp again on the machine side allowing the effluent to be drained into a collection bowl, allowing the kidney to flush in isolation. While the 500ml of Plasma-Lyte was directly flushing the kidney, the set was drained and flushed through with 2L of 0.9% normal saline, once clear and the set was empty, it was re-primed with the NR perfusate: the pump was then started and run via the A-V shunt in the circuit. The kidney flush was disconnected and the kidney unclamped and brought back into circulation, the process took 12-16 minutes, to replicate a second warm ischaemic time closely analogous to the anastomosis duration.

2.1.4 Human Research Organs: Kidney Back table & Cannulation

Human kidneys deemed unsuitable for transplantation after organ retrieval are offered out for research nationally, researchers with registered studies submit their interest for use in a study, and they are allocated on where that study is ranked by a national committee on importance for allocation. When kidneys appropriate for this project were available, a bid was made for them under study approved by the London Research Ethics Committee (21/PR/1546), sponsored by the University of Oxford. When allocated

to this study, transport would be arrange for the organs to be transported to the NHS BT laboratory in Oxford, where the perfusions were conducted.

Standard kidney back table was performed as per clinical standard. It was important that the bench work was meticulous, as the lack of any platelets or clotting factors in the NMP phase, and the anticoagulation used in the NR phase, meant that any bleeding would be difficult to stop. Whilst perfusate lost in this way was passively recirculated into the reservoir and small losses were tolerable, larger volume losses could threatened the volume status of the machine if pooling occurs, particularly if the circulating volume was low due to smaller blood units. It was also desirable to take all possible steps to minimise haemolysis; large volumes of perfusate running over the floor of the organ chamber and down into the reservoir were likely to contribute to this, especially with red cells that have not been utilised for transfusion due to expiration or improper storage, which were more liable to lyse[118,119].

The organs were not being implanted, so vessel length and post-perfusion integrity for anastomosis were not factors that needed to be considered here. This meant that cannulation did not need to be as atruamatic as it was in the NKP1 clinical trial. Vessel damage or length were not an issue in the research setting; short barbed cannulae could be placed in vessels as short as 5 mm, and multiple cannulae could be used for multiple vessels if needed. The vein was cannulated with a 20–22 Fr right-angled wire-wound venous cannula and secured with a 0-silk tie to keep the tip of the cannula at the correct depth; there was no circumstance in which this was not possible.

For arterial connection, there was more variation. Most commonly there was a single artery into which a reducing to ¼ inch straight tubing connector (Qosina No.11480) could be inserted and secured with 2-0 silk. If proximal intimal dissection had occurred, it was possible to cut the artery back to reach good quality intima and place the connector at this point. In the event of multiple arteries, they could be individually cannulated with reducing connectors or, if small polar arteries, with male to 1/16- or 1/32-inch connectors and then linked with y-connectors or straight connectors with a Luer port.

Prior to connection, a 5 mm punch biopsy was taken from the upper pole, packed with a small piece of fat, and closed with 4-0 or 5-0 prolene. If a QUOD or retrieval biopsy had been taken, then this was closed in the same fashion. The kidneys were weighed and then flushed with Plasma-Lyte to clear the high potassium UW.

When the kidney and device were both ready, the cannulated kidneys could be connected. The cannulated kidney was then positioned in such a fashion as to allow the connecting tubing to be positioned around the edge of the organ chamber. The cannulae were then primed, excluding all air from the arterial line with a 60 mL syringe containing Plasma-Lyte, with a blunt-tipped needle. The arterial and venous connections were made, and perfusion started. The ureter was cannulated once perfusion was established and either connected to the circuit in the case of the OrganOx circuit or allowed to drain on the XVIVO. An acorn-tipped small vessel cannula, two Luer-type connectors, and a length of silicone, purchased separately as a biliary T-tube, could be used. Any bleeding could be assessed, and further ties placed as required, before closing the organ chamber.

2.1.5 Research Blood Preparation

Packed red blood cells for research were acquired from the John Radcliffe Hospital blood bank after they had not been utilised for transfusion as a result of expiry, non-usage, or incorrect storage. Two units of group matched and rhesus compatible red cells were required per kidney for NMP and subsequent reperfusion. Each unit was washed, in which the blood bag was filled to maximum capacity with 0.9% normal saline, spun at 4°C for 20 minutes under 2200 g, and the supernatant containing the free haemoglobin and potassium was siphoned off. The process was repeated a second time to minimise remaining potassium and free haemoglobin; the red cells were then resuspended with 60 mL of Plasma-Lyte. The washing was done immediately prior to the perfusions to avoid the need for resuspension in SAGM and further storage.

2.1.6 NMP Perfusate

The NMP perfusate used was principally based on NKP1 clinical trial, with some minor tweaks. I added 1 unit of washed packed red cells to 100mL of 20% human albumin solution and 100mL Plasma-Lyte added to the reservoir, and the machine then set to

priming mode to start reaching temperature. While reaching temperature, the following were added: 125mg meropenem, 2.5mg verapamil and 5000 units of heparin. Once nearing 37°C, an 50mL of additional crystalloid was added (mix of 0.45% and 0.9% saline, titrated to sodium concentration measured using a blood gas analyser), 1.8-2mL 10% calcium chloride (titrated to blood gas results to reach normal ionized calcium of 1.16-1.31 mmol/L), and sodium bicarbonate as required to titrate start pH to 7.1 to the reservoir prior to the start of perfusion.

In the case of the OrganOx device there were three infusion pumps which held 30 mL syringes running at 1 mL/hr and were set up at the start of perfusion: one syringe containing 1 unit of insulin in 30 mL 5% glucose solution, one with just 5% glucose, and the other containing 0.45% saline. The 0.45% saline channel could be swapped for a vasodilator infusion, GTN or epoprostenol sodium, if required, although none of the paired perfusions required this supplementation.

In the case of the XVIVO device and external infusion was set-up for the 1 unit of insulin in 30mL 5% glucose solution, and if required a second infusion for vasodilator (again, no kidneys required this)

The variations from the NKP1 clinical trial protocol were, first, the use of Plasma-Lyte which was chosen to restore the potassium after blood washing and ease of titrating calcium. Second, the exclusion of anti-fungal medication which I considered to be redundant in 6 hours NMP or NR for a non-clinical perfusion. Third, the use of heparin instead of fondaparinux, done as the NR phase requires more powerful anticoagulation due to its plasma base, for ease heparin used in both phases. Finally, the washing of the blood, which was not done in the clinical trial as the red cells were clinical issue blood, deemed thereby to be of sufficient quality for inclusion in perfusate, whereas non-utilised blood with improper storage or expiration required washing.

2.1.7 Normothermic Reperfusion perfusate

The NR perfusate was a plasma-based NMP perfusate, using FFP from the blood bank which had expired or had been inappropriately stored. For paired perfusions, it was obviously important that the plasma was the same for each kidney, the minimum volume of a unit of FFP was 240 mL, so the perfusate began with 1 unit of washed red

cells added to 120 mL of plasma. Following this, the construction of the perfusate was the same as that of the NMP perfusate with the addition of magnesium for normal complement physiology. Due to the use of 120 mL of plasma, there was a volume of only 30 mL available for titrating sodium and normalising haematocrit; this was generally not an issue as plasma had a physiological electrolyte composition, although extra calcium was required due to the citrate in the FFP.

The infusion set-up for the NMP phase could be continued as all would have been sufficient to last the duration of the overall 12 hours of perfusion.

2.1.8 Generic Sampling

All biopsies were obtained using a 5 mm punch and were subsequently split vertically, with half placed in formalin and the other half freshly frozen in liquid nitrogen. Biopsies were obtained before NMP, at the end of NMP, and at the end of NR.

Perfusate was taken at various timepoints in both serum separator tubes (SST) and ethylenediaminetetraacetic acid (EDTA) tubes, which underwent centrifugation. The supernatant was assessed on the blood gas analyser for free haemoglobin and aliquoted into 1 mL cryovials and immediately stored in liquid nitrogen to minimise ongoing biological processes. Urine was also collected and aliquoted into 1 mL cryovials and placed in liquid nitrogen.

Baseline samples of the FFP used for the NR and the donor plasma with the kidney were also aliquoted into 1 mL cryovials and placed in liquid nitrogen. At the end of the perfusions all samples were transferred to a -80°C freezer for longer-term storage.

2.2 Perfusate Analysis

2.2.1 Biochemistry

The radiometer ABL90 blood gas analyser was used throughout the perfusions for: pH, pCO_2, pO_2, sO_2, glucose, lactate, calcium, chloride, potassium, sodium and haemoglobin. Perfusate and urine samples were also sent to John Radcliffe hospital clinical biochemistry lab for: albumin, bicarbonate, urea, calcium, creatinine, potassium, sodium, magnesium, phosphate and LDH, analysed on Abbot Diagnostics Architect c16000 as per analysis for routine clinical samples.

2.2.2 Perfusate Injury Biomarkers

Perfusate markers IL-18 (R&D, DL180), KIM-1 (R&D, DSKM100), NGAL (R&D, DLCN20) and GST-Pi (Abcam, ab277423) were assayed using ELISA kits, performed in accordance with the manufacturer's instructions. An optimisation experiment was conducted for all species evaluating possible dilutions with standard spikes, calculating percentage recovery. For the assay, all samples were assayed in duplicate, simultaneously, on a single plate for each experimental cohort of kidneys, with the layout designed to eliminate any potential for sequencing effects.

2.2.3 Perfusate Complement

The following perfusate complement proteins were assessed with commercially available kits: C1s (Thermo, EH57RB), C2 (Abcam, ab254501), C3 (Elab Sciences, H6054), C3a (Elab Sciences, H0818), C3d (Hycult, HK3017), C4d (Enzo Life Sciences, ASB-OKCD01390, Factor B (Abcam, ab137973), Fragment Ba (Abcam, ab315062), Collectin-11 (Abcam, ab288579) and C5b-9 (BD Biosciences, 558315). Again, as per the injury biomarkers, all were performed as per the manufactures' instructions, they were all optimised and ran in duplicate.

2.3 Tissue Analysis

2.3.1 Formalin Fixed Tissue Processing

After at least 72 hours of formalin fixation, the punch biopsies could be transferred into appropriately labelled cassettes and stored in formalin. When a batch was ready, cassettes underwent routine dehydration, clearing, and paraffin infiltration on an automated tissue processor using a standard histopathology programme validated in our laboratory and used for Quality in Organ Donation programme (QUOD) tissue sample processing. Reagent quality, change frequency, and processor performance were monitored by the QUOD technicians.

Following processing, tissues were oriented and embedded in histology-grade paraffin in metal moulds to preserve diagnostic planes. Blocks were cooled on a temperature-controlled surface before trimming and microtomy.

2.3.2 Immunohistochemistry Staining

Formalin-fixed, paraffin-embedded tissue sections were deparaffinised in xylene and rehydrated through different grades of ethanol to distilled water, followed by PBS equilibration. Antigen retrieval was performed for 30 min with 0.1% Proteinase XXIV in PBS. Endogenous peroxidase activity was quenched for 30 min using PBS containing 0.01% sodium azide and 0.3% hydrogen peroxide. After washing, sections were blocked in PBS with 1% BSA for 1 h at room temperature.

Slides were incubated overnight at room temperature with a mouse monoclonal anti-human C5b-9 antibody (clone aE11, Hycult HM2167, 2 µg/mL in PBS/1% BSA) alongside an isotype control (mouse IgG2a, Dako X0943). Following PBS washes, sections were incubated sequentially for 30 min each with goat anti-mouse HRP (1:200, Dako P0447) and rabbit anti-goat HRP (1:200, Dako P0449), with PBS washes between steps.

Signal was visualised using NovaRED chromogen (Vector Labs SK-4800) for 15 min in the dark. Slides were counterstained with Mayer's haematoxylin, blued under running tap water, dehydrated, and mounted with Entellan (Merck). Staining produced characteristic glomerular and vascular C5b-9 deposition patterns consistent with complement activation.

Whole-slide scanning in brightfield was performed on the PhenoImager HT (Akoya Biosciences, 2.1.0 software). Resolution: 40x (0.25 µm/pixel).

2.3.3 Immunohistochemistry Trained Model Quantification

Brightfield whole-slide images of immunohistochemistry as TIFF files (haematoxylin counterstain with 3,3'-diaminobenzidine (DAB) chromogen) were analysed using QuPath (version 6.0). DAB staining results from the oxidative reaction with the horseradish peroxidase (HRP) bound to the target antibodies, marking the target protein with characteristic brown staining. Images were imported into a QuPath project and set to Brightfield (H-DAB). Stain separation was performed using colour deconvolution to obtain haematoxylin and DAB components; stain vectors were estimated in representative regions and verified to ensure appropriate separation of nuclear counterstain from chromogen signal prior to downstream detection and measurement.

2.3.3.1 Manual Definition of Analysis Compartments

To restrict analysis to the relevant cellular and structural compartment, regions of interest (ROIs) were defined manually using QuPath's annotation tools. Boundaries were traced around the cellular field of interest, with deliberate exclusion of artefact (tissue folds, tearing, edge effects, precipitate), and areas of poor section quality. All subsequent detection and quantification were performed only within these manually defined annotations.

2.3.3.2 Nuclear Detection & Nucleus-only DAB Feature Extraction

Within each annotated ROI, nuclei were detected using QuPath's in-built cell and nucleus detection workflow, using the haematoxylin signal to identify nuclear objects. Detection parameters (including requested pixel size, smoothing/background subtraction, detection threshold and minimum/maximum nuclear area constraints) were applied consistently across the dataset. For each detected nucleus, QuPath generated morphological and intensity/optical density measurements. DAB positivity was assessed nucleus-only, using nuclear DAB optical density measurements, rather than cytoplasmic or whole-cell measurements.

2.3.3.3 Training & Application of a Supervised Object Classifier

A supervised object classifier was manually trained to classify detected nucleated cells as DAB-positive or DAB-negative. Training data were generated by manually assigning classes to detected nuclei within representative ROIs spanning the full range of staining intensity and background. QuPath's Train object classifier function was then used to learn a classification rule based on the measured nuclear features, including nuclear DAB optical density. Training was performed iteratively: predictions were reviewed visually, additional training examples were added to capture borderline/weak staining, and the classifier retrained until performance was satisfactory across representative regions. The final classifier was then applied uniformly to all detected nuclei within all annotated ROIs across the dataset.

2.3.3.4 Outcome Metric & Export

For each manual annotation, QuPath summary measurements were generated and exported. The primary outcome was the percentage of DAB-positive nuclei within each manually defined boundary, calculated as:

% DAB-positive nuclei = (number of nuclei classified Positive ÷ total nuclei detected) × 100

Annotation-level outputs were exported for downstream statistical analysis and figure generation.

2.3.3.5 Quality Control

To make sure results could be compared fairly between slides, the image analysis approach was standardised before the full batch was processed. For each staining batch, the stain separation settings used for colour deconvolution were checked on representative areas to confirm that haematoxylin and DAB were being separated properly and that background signal was not being incorrectly captured. These settings were only changed when there was obvious evidence of poor separation. Manual tissue annotations were also reviewed to ensure that the correct tissue compartment had been included consistently, while artefact, edge effects, and non-specific background were excluded.

Nuclear detection settings were then kept the same for all slides so that cell identification was performed in a consistent way across the dataset. Detection overlays were visually inspected in representative regions to confirm that nuclei were being segmented accurately and that the settings were not systematically over-calling or missing cells. For the object classifier, the training set was designed to include a range of examples, including clearly positive nuclei, weak or borderline staining, and negative or background nuclei. Classifier performance was then checked in separate regions that had not been used for training, to identify any recurring errors in classification.

Once the stain separation, annotations, nuclear detection, and classifier performance were considered satisfactory, the final analysis settings were fixed and applied unchanged to the entire slide set. The resulting outputs were then reviewed for obvious

outliers or unexpected results that might indicate staining problems, scanning artefacts, or analysis failure before the final data were exported.

2.3.4 Immunohistochemistry Automated Pipeline Analysis

Brightfield IHC whole-slide images (.qptiff) were quantified using a custom Python analysis pipeline designed to prioritise tissue detection first, then stain measurement, with extensive quality control at each stage. Slides were opened at a reduced-resolution pyramid level chosen to keep image size manageable for analysis while preserving sufficient detail, aiming for a maximum image dimension of approximately 4500 pixels and a minimum dimension of at least 1200 pixels. Images were read using OpenSlide where possible, with tifffile used as a fallback when needed. File names were cleaned to generate consistent slide identifiers, and all outputs, including summary CSV files, quality-control panels, and histograms, were saved into a dedicated results folder.

For each slide, the first task was to identify the tissue area and separate it from the clean white slide background. This was done by applying thresholding approaches in different colour spaces, specifically using HSV value and CIE-LAB lightness, with Otsu-based thresholds to distinguish darker tissue-containing regions from bright empty background. The initial mask then underwent several morphological clean up steps, including removal of very small objects, binary closing, filling of small holes, and retention of the largest connected tissue regions, so that the final mask more accurately represented a continuous tissue section. To minimise measurement bias from edge artefact, this tissue mask could then be slightly eroded by a fixed number of pixels before quantification, creating a more conservative “core” tissue region.

Where tissue coverage was low or the initial mask appeared fragmented, an additional rescue procedure was used. In these cases, obvious background pixels were first estimated on the basis of being very bright and weakly saturated. The script then looked for extra evidence of tissue using several complementary image features, including haematoxylin channel intensity from HED deconvolution, chromatic information from the LAB a/b channels, and saturation from HSV. Thresholds for these features were defined relative to background signal using mean plus a multiple of the standard deviation, allowing the algorithm to recover tissue regions that might otherwise have

been missed. This rescued mask then underwent the same cleanup steps as the standard mask. For every slide, QC images were saved showing the final tissue mask boundary overlaid on the original image, together with the measured proportion of the slide classified as tissue. All tissue masks were manually reviewed with slide image to ensure tissue captured correctly.

After tissue identification, the chromogenic DAB signal was quantified using HED stain deconvolution, with the DAB channel taken as the main measure of positive staining. To make positivity thresholds comparable across the whole batch, a single global DAB threshold was derived from pooled background pixels from all slides rather than setting an independent threshold for each image. For each slide, the median DAB intensity in background pixels was subtracted from the DAB image to correct for baseline background staining, with negative values clipped to zero. Background-subtracted background pixels from all slides were then combined, and a very high percentile of this pooled distribution, by default the 99.9th percentile, was selected and multiplied by a small safety factor to define the baseline positivity threshold. This was intended to set the positivity cut-off just above the upper range of background signal. To test how sensitive the results were to threshold selection, the analysis was repeated using a series of threshold variants around this baseline, including thresholds that were slightly lower and slightly higher.

Within the final measurement region, either the eroded tissue core where possible or the full tissue mask where erosion was not appropriate, pixels were classified as DAB-positive if their background-corrected DAB signal met or exceeded the applied threshold. The main outcome measure was the fraction of tissue area that was DAB-positive, calculated as the number of positive pixels divided by the total number of tissue pixels. Additional summary measures of staining intensity were also recorded, including mean DAB intensity within positive pixels and mean or median DAB signal across the tissue region as a whole. Alongside these biological outputs, the pipeline also stored processing metadata such as which image reader was used, the pyramid level analysed, image dimensions, tissue coverage, threshold settings, and whether the standard or rescue tissue-mask method had been used.

To support transparency and troubleshooting, multiple QC outputs were generated for every slide and every threshold condition. These included panels showing the original RGB image, the final tissue mask, and the DAB-positive regions overlaid in red, allowing visual review of whether the measured positive signal matched the expected staining pattern. In addition, histograms of tissue DAB values were produced for each threshold setting, using a log-scaled y-axis and marking the applied threshold directly on the distribution. This allowed visual confirmation that the chosen threshold sat in a sensible position relative to the range of DAB intensities present in the tissue.

2.3.5 CellDive Multiplex Immunofluorescence

Multiplex immunofluorescence was performed on formalin-fixed, paraffin-embedded (FFPE) tissue sections using the Cell DIVE™ platform (Leica Microsystems, 2500HS), which enables iterative cycles of antibody staining, imaging, and fluorophore inactivation on a single slide. Following deparaffinisation and a two-step heat-induced antigen retrieval protocol, slides were permeabilised with 0.05% Tween-20 in PBS for 5 minutes and blocked with 1% bovine serum albumin (BSA), 1% normal goat serum, and 1% normal donkey serum in 0.05% Tween-20 for 30 minutes at room temperature.

Slides were initially stained with DAPI and imaged across all fluorescence channels to capture tissue-specific autofluorescence. In the first staining round, slides were incubated with up to three antibodies. All subsequent rounds employed directly conjugated primary antibodies targeting up to three markers per cycle, with DAPI included in each round. Antibody incubations were carried out overnight at 4 °C in a humidified chamber, followed by three washes in PBS, DAPI counterstaining, and mounting with aqueous antifade medium. The investigational antibodies were: C5b-9 (Bioss, BS-2673R), C4d (Bio-Rad, MCA5766GA, clone TDM16), PAI-1 (Proteintech, 13801-1-AP), Fibrin (Merck Millipore, MABS2155, clone 59D8), ICAM-1/CD54 (R&D Systems, AF720), and Integrin β3/CD61 (Proteintech, 18309-1-AP).

Whole-slide images were acquired using a motorised widefield fluorescence microscope equipped with a 20×/0.75 numerical aperture objective. Fluorescence signals were sequentially captured in the DAPI (~460 nm), FITC (~520 nm), Cy3 (~570 nm), and Cy5 (~670 nm) channels. Exposure times were optimised using single-

stained control tissues and held constant across all samples and cycles to ensure quantitative consistency.

Between staining cycles, fluorophores were inactivated by three sequential 15-minute incubations in freshly prepared alkaline hydrogen peroxide solution (3% H_2O_2 in 100 mM $NaHCO_3$, pH 11.2) at room temperature, protected from light. This was followed by treatment with VectaPlex Antibody Removal Kit (Vector Laboratories, VRK-1000), with two 5-minute PBS washes after each step. Slides were then re-imaged across all fluorescence channels to confirm signal clearance and acquire updated autofluorescence profiles, before being re-cover slipped for the next staining round.

This stain–image–bleach/antibody removal sequence was repeated until the entire antibody panel was completed. All image stacks from successive cycles were computationally registered using nuclear DAPI signals to ensure precise alignment.

2.3.6 CellDive Analysis Pipeline

Quantification of CellDIVE immunofluorescence markers was performed on OME-TIFF whole-slide images using a custom Python pipeline developed to produce robust and comparable measures of marker positivity across slides, despite variation in background fluorescence and staining intensity The pipeline was executed in a Windows 11 environment via Anaconda Prompt on a workstation with an NVIDIA GeForce RTX 4050 GPU, although the analysis itself was primarily driven by the Python software environment rather than requiring GPU-specific acceleration. For each OME-TIFF region, QuPath was first used to export downsampled binary masks defining two key regions which was done manually for each slide: the tissue region of interest (tissue mask) and a representative non-tissue background region (background mask). These masks served different purposes in the analysis. The tissue mask defined the area within which positivity was measured, ensuring that calculations were restricted to relevant tissue. The background mask provided a reference region for estimating slide-specific background signal, which was then used to inform threshold setting.

The analysis script also extracted metadata from the OME-XML file, including channel names and physical pixel sizes where available. Because channel naming was not always fully consistent between images, the script used a canonicalisation and alias-

matching approach so that markers could still be identified reliably despite minor naming differences, for example recognising equivalent labels such as PAI1 and PAI_1, ICAM1 and I-CAM, or TCC and C5b-9. Images were analysed at a downsample matched to the exported masks, typically ds4 or ds8, using OME pyramid levels where available so that lower-resolution image data could be loaded directly without having to read the full-resolution slide. Where necessary, masks were resized by nearest-neighbour interpolation to ensure exact alignment with the analysed image dimensions. Tissue area was then calculated from the number of positive pixels in the tissue mask and converted into mm^2 using the physical pixel size metadata together with the applied down sample factor.

Marker positivity was defined on a per-pixel basis within the tissue mask using an adaptive, marker-specific thresholding strategy referred to as the “marker_profile” approach. This was used because quantitative analysis of CellDIVE immunofluorescence is particularly challenging. Many markers show highly polarised intensity distributions, in which most pixels are dim but a small number are extremely bright. In addition, background autofluorescence and non-specific signal can vary substantially between slides, and different markers may show very different spatial patterns, such as sparse punctate staining, endothelial-restricted staining, or more diffuse parenchymal upregulation. Because of this, a single global threshold applied across all slides would be unreliable: on some slides it might incorrectly classify background as positive, while on others it might miss genuine low-level signal.

To address this, thresholds were defined using both background-derived and tissue-derived information. First, a background-anchored threshold was calculated from the upper tail of the slide’s measured background intensity distribution, typically using a very high quantile. This ensured that background noise was unlikely to be called positive. Second, a robust tissue-based threshold was calculated using the tissue median intensity plus a multiple of the tissue intensity spread, estimated using the median absolute deviation and converted into a robust standard deviation-like measure. The final threshold depended on the biological pattern expected for the marker.

For markers expected to show sparse staining, such as C4d, CD41, fibrin, and C5b-9 in this analysis, the final threshold was set as the higher of the background-based threshold and the tissue-based threshold. This was done to prevent weak or noisy signal from being classified as true positivity. An additional safeguard was then applied: if the resulting threshold still classified too large a proportion of tissue pixels as positive, suggesting over-calling caused by broad low-level haze, the algorithm gradually increased the tissue threshold parameter until the proportion of positive tissue pixels fell below a predefined marker-specific cap, or until a maximum value was reached. This acted as a practical guardrail against diffuse non-specific signal being mistaken for true staining.

For markers expected to show more diffuse but biologically plausible upregulation, such as ICAM-1 and PAI-1, a different hybrid rule was used. In these cases, the threshold combined a high tissue quantile with an additional robust dispersion term, while still being constrained not to fall below the background-anchored threshold. In this way, the thresholding strategy could be adapted to the expected staining behaviour of each marker while maintaining consistency and resistance to background-related artefact. The final threshold value and its associated parameters, including the final multiplier used, the estimated robust dispersion, and whether the positivity cap had been reached, were retained in the output to preserve auditability and allow later review of how each threshold had been derived.

Once thresholds had been established, marker positivity metrics were calculated within the tissue mask. These included the total number of positive pixels in tissue, the percentage of tissue area classified as positive, and the mean intensity of the positive pixels. Together, these measures provided information both on the extent of staining and on the intensity of signal within the positive compartment.

To provide an approximate normalisation for differences in cellularity or tissue sampling between slides, the pipeline also generated a nuclei count from the downsampled DAPI channel within the tissue mask. This was done using a simplified segmentation approach intended to provide a rapid surrogate rather than precise nuclear segmentation. The DAPI image was smoothed with a Gaussian filter, thresholded using Otsu’s method within tissue pixels, and then cleaned using morphological opening and

removal of small objects below a minimum size appropriate for the downsample level. Connected-component labelling was then used to count the resulting nuclear objects. This count was recorded as the nuclei number and used to derive an additional normalisation measure, defined as marker-positive pixels per nucleus, which served as a crude density-adjusted estimate of staining burden.

In addition to the quantitative outputs, the pipeline generated several QC outputs for each slide and marker to support rapid visual review and troubleshooting. Histograms were produced showing both tissue and background intensity distributions on the same scale, with the selected threshold marked on the plot. To keep these histograms interpretable, axis limits were clipped at high quantiles so that very bright outliers did not compress the main intensity distribution. Spatial QC tiles were also generated by sampling random locations within tissue and displaying the marker channel in grayscale with tissue and background mask contours overlaid. Where enabled, pixels above threshold within tissue were highlighted so that it could be visually confirmed that positive calls corresponded to biologically plausible staining patterns rather than edge artefact or background fluorescence. A separate mask QC image was also saved for each slide, showing tissue and background regions and reporting the corresponding pixel counts together with the nuclei count.

Taken together, this pipeline was designed to provide a reproducible and transparent framework for quantifying CellDIVE markers in the presence of slide-to-slide variability in fluorescence background and staining intensity. By combining adaptive thresholding with retained threshold metadata and extensive per-slide QC outputs, the approach aimed to improve robustness while allowing the validity of positivity calls to be reviewed directly.

2.3.7 Frozen Tissue Processing

All frozen tissue was processed in a non-reducing method in order to preserve intact C5b-9. Frozen tissue was weighed and placed into Precellys tubes containing 100–200 µL cold 1% Triton X-100 lysis buffer, volume depending on tissue weight. The tissue was lysed in a Precellys homogenizer until complete disruption of the sample (1 or 2 cycles of 30 seconds at 6000 rpm) and placed on ice. The Precellys tubes were then

centrifuged at maximum speed, 15 min, 4 °C to pellet debris. Transfer supernatant to a fresh pre-cooled tube.

2.3.8 Bicinchoninic Acid Assay

Total protein concentration was determined using the Pierce™ Bicinchoninic Acid (BCA) Protein Assay Kit (Thermo Fisher) according to the manufacturer's instructions. Briefly, standards were prepared from bovine serum albumin (BSA) to generate a calibration curve (0–2000 µg/mL). Working reagent (reagent A : reagent B, 50 : 1) was added to each standard and sample in a 96-well microplate. Plates were mixed gently, covered, and incubated at 37 °C for 30 min. After cooling to room temperature, absorbance was measured at 560 nm using a microplate reader. Protein concentrations were calculated from the BSA standard curve.

2.3.9 Western Blotting

Protein expression was analysed by Western blotting. Tissue lysates were prepared from homogenised samples quantified by BCA assay as above, and 20 µg of protein per lane was mixed 1:1 with 2× Laemmli sample buffer containing 2-mercaptoethanol. Samples were vortexed, heated at 60 °C for 10 min, and briefly centrifuged before loading. Proteins were separated on Criterion XT SDS-PAGE gels using 1× MOPS running buffer at 80 V for 20 min followed by 150 V for 1 h.

Following electrophoresis, proteins were transferred onto PVDF membranes using 1× Towbin transfer buffer (25 mM Tris, 192 mM glycine, 20% methanol, pH 8.3) at 80 V for 1 h at 4 °C. Membranes were washed with TBS-Tween (0.1%) and blocked in 5% (w/v) non-fat milk in TBST for 1 h at 4 °C. Primary antibodies were applied overnight at 4 °C in 5% milk/TBST (C3d Hycult, HM2198, 1:1000 & β-actin 1:1000)

After washing, membranes were incubated for 1 h at room temperature with fluorescently labelled secondary antibodies (IRDye 680RD or 800CW, 1:5,000) in 5% milk/TBST with 0.01% SDS, protected from light. Blots were then washed in TBST, rinsed in TBS, and imaged on an infrared fluorescence scanner. Protein band intensity was quantified using manufacturer-recommended software, normalised to β-actin, and expressed relative to internal control lanes.

2.3.10 Native Gel Blotting

Intact C5b-9 was analysed under non-reducing, non-denaturing conditions using a native gel electrophoresis approach. Tissue samples were homogenised and protein quantification done as above.

Samples were resolved on 3–8% Tris-acetate polyacrylamide gels under native conditions at 80–120 V, with electrophoresis performed in a cold room or on ice to preserve high-molecular-weight complexes. Proteins were transferred onto 0.45 µm PVDF membranes using NuPAGE Tris-acetate transfer buffer at low voltage (20–30 V) for 2–3 h. Membranes were confirmed for protein transfer with Ponceau S staining, then blocked in 5% BSA in TBST (0.05% Tween-20) for 1 h at room temperature.

Blots were incubated overnight at 4 °C with anti-C5b-9 primary antibody (Hycult, HM2167, 1:1000), washed extensively in TBST, and probed with IRDye-conjugated secondary antibodies (Abcam, ab184092) for 1 h at room temperature. After final washes, membranes were scanned on a LI-COR infrared imaging system (600/800 nm channels) using optimised focus and intensity settings to visualise high-molecular-weight MAC complexes.

3

Characterising Complement in Prolonged Clinical Normothermic Perfusion for Renal Transplantation

Contents

3.1 Introduction

3.1.1 NKP1 Clinical Trial

3.1.2 Evidence of Renal Complement Production

3.1.3 Complement During NMP

3.1.4 Selected Complement Measures

3.1.5 Time to Creatinine-50 (TCr50)

3.2 Aims and Objectives

3.3 Methods

3.3.1 NKP1 Trial Methodology

3.3.2 Perfusate Complement Analysis

3.3.3 Wieslab Complement System Screen

3.3.4 Data Handling and Statistical Analysis

3.3.5 Tissue Multiplex Immunofluorescence

3.4 Results

3.4.1 Perfusate Complement Proteins

3.4.1.1 Complement Protein Dynamics

3.4.1.2 Wieslab Assays

3.4.1.3 Complement and Donor Factors

3.4.1.4 Complement Proteins and functional DGF

3.4.1.5 Stratification by TCr50, UKDRI and Cox Regression

3.4.2 Tissue Multiplex Immunofluorescence

3.4.2.1 Relative Expression Pre- and Post-perfusion

3.4.2.2 Relative Expression by Outcome

3.5 Discussion

3.5.1 Evidence of Complement Activation During NMP

3.5.2 Functional Pathway Potential and Perfusate Complement Biology

3.5.3 Activation and Consumption Across the Pathways

3.5.4 Circuit Artefact versus Organ Biology

3.5.5 Early Complement Profiles as a Signal from Donor and Retrieval Biology

3.5.6 Complement Signals Predict Recovery and Add to UKDRI

3.5.7 Complement as Marker versus Mediator

3.5.8 Tissue Proteins: Separating Donor Priming & Reperfusion Biology

3.5.9 Limitations, Implications & Next Steps

3.1 Introduction

3.1.1 NKP1 Clinical Trial

Normothermic Kidney Perfusion 1 (NKP1) trial was hoping to address a practical and biological bottleneck in deceased-donor kidney transplantation, although normothermic machine perfusion (NMP) can maintain a kidney in a functioning state ex-situ at 37 °C, most clinical implementations before NKP1 were short duration, most commonly of 1 hour, and essentially in-theatre, limiting NMP's usefulness for wider logistics, detailed graft assessment, or delivery of ex-situ therapies. The Oxford group therefore set out to determine whether prolonged renal NMP (up to 24 h) could be delivered safely and reproducibly before transplantation, and whether extending the duration would unlock the broader promise of NMP as a preservation modality in and of itself, as an assessment tool for marginal kidneys, and as a platform for pre-implant graft optimisation and treatment[32].

The trial was also motivated by what had been published to date. Early clinical NMP reports suggested feasibility for short end-ischaemic perfusions and hinted at the possibility of assessment/reconditioning, but the only published randomised controlled trial comparing 1 h end-ischaemic NMP after SCS versus SCS alone did not demonstrate clinical benefit[27], raising the possibility that duration was insufficient or that NMP alone is not inherently therapeutic. In parallel, pre-clinical work (including porcine auto-transplant models) suggested that replacing a larger proportion of cold preservation with normothermia may produce a larger effect[29], but it was unclear whether these findings would translate to a human transplant setting particularly in the context of more marginal organs. Against this background, NKP1 was a phase 1 safety/feasibility study of longer-duration NMP.

Overall, the central finding was that prolonged renal NMP prior to transplantation was safe and feasible. 30-day graft survival was 100% and patient survival comparable to controls, with no adverse events attributed to the intervention, despite substantially longer total preservation times in the NMP cohort (median 15.7 h vs 8.9 h in controls). Rates of DGF were similar (36% vs 38%), and longer-term graft function was likewise comparable (12-month eGFR 46 vs 50 mL/min/1.73 m^2 ,no significant difference),

consistent with a phase 1 study not powered to demonstrate efficacy and with earlier short-duration RCT experience. Importantly, NKP1 demonstrated the operational advantages of longer NMP, facilitating safer scheduling and shifting reperfusion towards daytime implantation. Several perfusate injury markers measured ex-situ correlated strongly with early outcomes (fDGF, defined as failure of serum creatinine to fall by at least 10% per day for the first 3 days) and even 12-month graft function (notably the association between GST-Pi delta during perfusion and 12-month eGFR). The take-home message is that prolonged NMP can be delivered clinically without compromising outcomes, and that its most immediate translational value may be as an organ assessment platform, with the future work of value to be assessing replacing more of the cold ischaemic interval, by taking NMP closer to retrieval, and combine NMP with targeted ex-situ therapies in adequately powered studies.

3.1.2 Evidence of Renal Complement Production

Due to the comparatively limited number of renal transplants performed after NMP globally, particularly those with durations greater than 2 hours, there is very limited published evidence on complement proteins in this setting, and none with a relationship to clinical outcome[120].

While the liver is the main source of complement production in humans, it is known the kidney is a major extra-hepatic source of complement. For the core activation components C2, C3, C4 and C5 there is evidence of renal production in human kidneys[53].

Evidence for intrarenal C3 production in humans is particularly strong. Cell culture has demonstrated that proximal tubular epithelial cells (PTECs)[121], podocytes[122] and glomerular resident cells[123] can synthesise and secrete it, which has been supported by mRNA expression in renal biopsies[124]. The canonical human evidence exploits a common polymorphism in C3, C3 R102G, resulting in two allotypes, C3 fast (C3F), and C3 slow (C3S), named for how they migrate on electrophoresis. A cohort of mismatched donor and recipient pairs with differing C3 allotypes were utilised and following transplant assessment of circulating complement and biopsy assessment have

demonstrated clearly there is in vivo renal production[125]. The transplant kidney appears to account for around 5% of circulating C3, but this increases to around 16% during episodes of rejection, and that the donor-recipient combination has a significant influence on outcome[126,127].

For C2 and C4 evidence is limited to cell culture, but there is clear evidence that human PTECs can synthesise and secrete C2 and C4, particularly in response to IFN-γ[128], along with biopsy evidence of gene expression in human kidney tissue[129]. Of the core proteins, C5 is probably the least produced, with the least evidence, with only recent transcriptomic data for tubulointerstitial C5 expression in the context of disease states, rather than stable production, particularly in poor outcome lupus nephritis[130], diabetic nephropathy[131,132], chronic ABMR. In cell culture upregulation of gene expression from Shiga toxin stimulation has not been mirrored in actual protein synthesis, so the amount of C5 the kidney is able to produce is likely small[133].

For the key classical pathway components, C1q, r and s there is evidence for expression and to some extent production in human kidneys. For C1q, it can easily be found on IHC, but expression in human kidney tissue is consistently mapped to kidney resident macrophage populations rather than tubular epithelium[134], with increased expression in rejection[135], thus its presence on IHC could represent a combination of local synthesis and deposition from plasma sources. For C1s and r there is evidence of tubular epithelial synthesis, again with amplification in diseased states, such as lupus[136], and both play a role in fibrosis[137]. In the context of IRI, both C1s and C1r also demonstrate increased expression, with rising amounts as CIT increases[69].

For pattern recognition molecules of the lectin pathway, collectin-10 and -11 are the key proteins, which recognise an abnormal pattern of L-fucose and d-mannose on damaged epithelial surfaces. PTECs in cell culture show the ability to synthesise the proteins, with an increase in production and binding in the setting of ischaemic stress[66,138].

In the alternative pathway, there is evidence for all key components and regulators. Again, cell culture models with human PTECs demonstrate ability to synthesise Factor B (CFB) and Factor H (CFH), particularly in response to inflammatory signals[128,139,140] and that these are important local regulators for renal health[141]. For CFB, biopsy data

supports this with expression found in tissue from kidneys in various diseased states, but with only limited foci in healthy kidneys[142]. For Factor F (CFD), there is biopsy and cell culture model evidence of endothelial production and that its dysregulation is pathological in conditions like malignant nephrosclerosis, such that it plays an important role in localised renal complement activation[143].

The complement regulators are vital and local expression and production play a key role in managing activation and thus are expressed in healthy renal tissue as part of this process. Membrane cofactor protein or CD46 (MCP) is a vital regulator present on most human cells, as the name would suggest it is a membrane protein which, along with Factor I constitutively inactivates C3b and C4b to keep the balance of the cascade and preventing self-damage. Protectin or CD59 is another membrane bound regulator, widely expressed on erythrocytes, leukocytes and vascular endothelium, and is an inhibitor of C5b-9 formation, specifically the pore formation by binding C8/9 and preventing lysis. Both CD46 and CD59 have high and broad renal transcription signals, but the synthesised proteins appear in different compartments on IHC. CD46 appears to be most prominent in collecting ducts and distal tubules, while CD59 is present in vascular endothelium[144,145]. Complement receptor 1 (CR1) or CD35 is another key membrane bound glycoprotein located principally on human erythrocytes, neutrophils and B cells, it binds C3b and C4b to disrupt C3 and C5 convertases, and when on the blood cells, these complexes are transported to the liver and spleen for destruction. In the kidney it is expressed and synthesised, but it is isolated to the podocyte[146] and IHC shows its staining only within glomeruli[144,145].

There is broad evidence that multiple renal cell types can express complement genes and, in some settings, secrete complement proteins; however, expression varies substantially with health, injury, and inflammatory signalling. It is worth noting that much of the evidence derives from cell culture modelling, which may not fully represent the behaviour of the whole organ in various states. A classically transplantable kidney within the donor is at reasonable baseline health, this healthy kidney is then exposed to IRI in the recipient producing inflammatory signal. NMP is an unusual middle ground, in which the kidney is going to be manifesting this IRI response, but in the absence of

plasma. The response of the kidney and whether complement activation occurs has not been well characterised at present.

3.1.3 Complement During NMP

The only published work on human kidney NMP and complement is Jager et al, from the Dutch PROPER trial consortium[120]. Samples from preclinical porcine work on NMP and then 10 human kidneys which underwent 6 hours of NMP with albumin and packed red cell based perfusate but were not subsequently transplanted. The porcine kidneys in the study were perfused for 4 hours with leuko-depleted autologous whole blood. The analysis of the human kidneys reported perfusate levels of C3 and C3d and immunofluorescence of C3d after the 6 hours on NMP. They found that C3 levels stayed relatively static over the course of perfusion and that C3d levels increased over the course of the 6 hours, which they expressed as an increasing C3d/C3 ratio. C3d levels increased from 0 to around 500ng/mL in the first hour and then to around 1000ng/mL by hour 6, with C3 levels remaining static after the first hour with a median around 1500ng/mL, but with significant variation between kidneys, with 3 donor kidneys around 10000ng/mL. When they assessed by donor type the increase in C3d ratio is greatest in DBD, with this distinction also being true on IF with a significantly higher intensity per area of renal cortex of C3d in DBD kidneys after 6 hours of NMP. The only other analysis on the human kidneys in the manuscript was the increasing perfusate IL-6 and IL-8 over the duration of NMP.

While their porcine series had significant methodological differences due to the perfusate used, it is still relevant in the context of this thesis as it is a model simulating reperfusion, only without preceding clinical NMP. Over the 4-hour perfusion there was progressive accumulation of C3a (0 to 10000ng/mL) and C5b-9 (0 to 100 AU/mL) although the variation in C5b-9 levels varied between kidneys with some ending at 300AU/mL and others around 50AU/mL, but the formation seemed to be progressive from samples taken around 15 minutes then to hour 2 and on to hour 4. The same progression was seen in C3a with the steepest gradient hour 2 to hour 4. The investigators found those kidneys with higher C5b-9 levels had lower creatinine clearance. They refer to, but don't provide data for a kidney-free circuit producing activation, but much lower levels than with the kidney in circuit.

Jager et al concluded that: (i) the formation of perfusate C5b-9 and C3a is evidence of complement activation in the autologous blood porcine perfusions ; (ii) that higher levels of C5b-9 are associated with lower CrCl due to level of injury; (iii) for the human kidneys there is also complement activation during NMP, as evidenced by C3d formation, and that this is most prominent in DBD kidneys. They hypothesised that complement activation during NMP could be helpful by "using up" the graft's complement capacity before recipient reperfusion and by aiding clearance of debris and necrotic cells. However, it may also be harmful by increasing inflammatory cytokines and impairing renal function. In this study, rising perfusate C5b-9 was associated with lower creatinine clearance and greater histological injury, suggesting adverse effects during NMP. Because these were declined kidneys not transplanted, it remains unclear whether complement activation during NMP is ultimately beneficial or detrimental in recipients.

This is a useful starting point, with some good aspects to take forward regarding the present work. Firstly, their whole blood perfusions produced complement activation within the perfusate, and levels seemed to correlate with CrCl ex-vivo, meaning a reperfusion model with plasma is likely to provide a good platform for ex-vivo complement cascade activity, while the circuit itself may not be a large confounder in the level of activation. Secondly, in human kidneys undergoing NMP, C3 and C3d were detectable, and with possible evidence that there was activation taking place. Overall, it was limited in analysis and if they had performed a broader investigation into complement protein profile across all three pathways as well as terminal complement, even with negative findings these would have been hugely informative in a more holistic picture.

Outside of this work, complement NMP information is very sparse with no human data, but with one other piece of work from the same group being of interest. They expanded on the previous porcine work, using the same whole blood NMP, this time in the context of a C5 inhibitor[94]. Pairs of porcine kidneys were cold stored for 18 hours, after which they received 4 hours of whole blood NMP (reperfusion) with one receiving the C5 inhibitor, Zilucoplan (UCB Pharma, Belgium). Zilucoplan is a macrocyclic peptide which binds C5, this prevents its cleavage into and thus its binding to C6 and ongoing C5b-9

formation. Its current license is for treating acetylcholine receptor (AChR)-positive generalized myasthenia gravis. They found the inhibitor resulted in only a significantly lower level of perfusate C5b-9 at 4 hours, 5 CAU/mL vs 8 CAU/mL, but overall the activation curves and speed of formation did look different with significant early formation in the untreated group. There were also significantly lower levels of C3a in the tissue in the inhibited group, but perfusate levels and activation curves were similar. Again, some of the complement readouts were left unreported, tissue C5b-9, or any other perfusate markers across the pathways, C3d, C4d, Factor B or Ba or any lectin pathway triggers. However, this again demonstrates that the NMP model can produce complement activation curves, and they demonstrated a relatively clean signal in perfusate C5b-9 with the C5 inhibitor binding C5 and reducing C5b-9 formation, while upstream pathways are unaffected with equivalent C3a formation.

Human kidneys declined for transplant assessed in the Jager study, and subsequently for the NKP1 cases the source of complement proteins differs from that of the whole blood models. The complement proteins can and will be flushed out of the kidney in the small volumes of residual blood present even after back-table flush, in the pRBCs themselves used for the perfusate there could be a small volume of residual plasma containing proteins, there could be membrane bound complement proteins from the donor which come free due to the sheer stress during NMP and there could be kidney derived synthesis and release.

3.1.4 Selected Complement Measures

While a complete panel of perfusate and tissue complement proteins across time points would provide a completely holistic picture this would be over 50 proteins to assess at different time points, which is not feasible in this exploratory analysis of an area with very little currently published literature. The following selection was made for perfusate analysis: C1s, CL-11, C2, C3, C3d, Factor B, Fragment Ba, C5b-9, and C4d and C5b-9 in the tissue. C1s was selected as classical pathway triggers molecule. CL-11 for the lectin pathway PRMs, given its known production in kidneys. C2 and a classical and lectin shared convertase component. C3 and C3d for C3 convertase activity levels. Factor B and its fragment Ba for alternative pathway activity and C5b-9 for the terminal pathway and its significance to cell damage. Within the tissue C4d, as

the typical marker of classical and lectin activity, taken pre- and post-NMP to establish donor deposition from NMP and C5b-9 for terminal components relates to tissue damage. While not exhaustive the panel should cover all three pathways and interpreted together should give a more detailed picture of what has been done previously.

3.1.5 TCR 50

Given that time to creatinine-50 (TCr50) is not widely used, a brief overview of its inception and validation is provided. It was introduced as a creatinine-kinetics endpoint intended to quantify the speed of early graft functional recovery after kidney transplantation. Rather than classifying recovery using a binary DGF definition, such as requiring dialysis in the first week or not, the approach treats plasma creatinine as a time-series signal that reflects the gradual restoration of filtration. The aim was to derive a continuous measure that captures the spectrum from rapid recovery to slow graft function and is less dependent on centre-specific dialysis practice. Its inception and validation comes from a Danish research group in Aarhus presented across their three key publications involving TCr50[147-149].

Methodologically, the original Krogstrup et al paper assembled serial plasma creatinine measurements for each recipient across the early post-transplant period up to around 30 days, with explicit consideration of dialysis episodes, and then fit a simple parametric recovery curve for everyone[147]. Several plausible curve shapes were evaluated, exponential, logistic, and linear decline, acknowledging that creatinine trajectories can differ between patients and that relying on any single raw day-to-day change can be noisy. From the fitted trajectory, TCr50 was defined as the model-estimated timepoint at which plasma creatinine had fallen by 50% from an early baseline, the half-life of functional recovery derived from all available early measurements rather than one pair of samples.

The clinical rationale is that a curve-based time-to-event metric has practical advantages in trials and cohort studies. Firstly, it is continuous and preserves all the creatinine information rather than the binary DGF. Secondly it still only relies on routinely collected creatinine data, and finally, is more robust to short-term variability

than single-timepoint endpoints. In the initial study they correlated it in a single centre cohort of 100 recipients, demonstrating TCr50 correlated inversely with 1-year eGFR (reported as n = 96, r = −0.369, β = −0.112, p = 0.0002), even when adjusted for donor and recipient characteristics. They also showed that longer TCr50 tracked with greater healthcare utilisation in the form of hospital days, ultrasounds, biopsies, supporting clinical validity as a recovery metric.

It was then validated by its use as a trial end-point in the multicentre CONTEXT randomised trial, which implemented prospectively as the primary outcome for the intervention of remote ischaemic preconditioning, aimed at accelerating early graft recovery[148]. In brief, the study enrolled 225 adult deceased-donor kidney recipients across four transplant centres (Denmark, Sweden, Netherlands) in a blinded, randomised (1:1) sham-controlled design. Methodologically, the key point is how they operationalised recovery: the primary endpoint was the estimated time to TCr50, calculated using serial plasma creatinine measurements collected for up to 30 days post-transplant, or 30 days after the last post-transplant dialysis session, preventing dialysis from biasing the creatinine trajectory. The intervention didn't demonstrate benefit, but TCr50 was a usable and interpretable endpoint under trial conditions. They could compare the groups and it produced an intuitive read-out, median TCr50 was 122 hours (95% CI 98–151) in the RIC arm versus 112 hours (95% CI 91–139) in the sham arm (p=0.58). In parallel, the conventional binary endpoint, dialysis within the first week, also showed no difference (33% vs 35%, p=0.71). So, this paper doesn't validate the prognostic link to 1-year function, but it does validate TCr50 as a feasible primary endpoint for multicentre interventional trials targeting early graft recovery.

However, they went on to perform a 1-year follow-up study to the CONTEXT, in the trial cohort, TCr50 correlated significantly with both measured GFR and multiple eGFR estimates at 12 months, with correlations in the r =−0.30 to −0.39, all p<0.0001, meaning slower early creatinine recovery associated with worse 1-year function[149]. Validating the initial cohort findings in a prospective RCT. They also report that the binary DGF did not show a significant correlation with 12-month eGFR, supporting the idea that TCr50 can be a more sensitive summary of early graft dysfunction's longer-

term relevance. It has since been used in biomarkers studies by the same group, investigating the association of biomarkers with measures of longer-term outcome[150,151].

TCr50 is of use here as it allows modelling on a continuous variable, which is inherently more descriptive than DGF, but given its relationship to 1-year function it can give stronger inference to any biological associations here with complement markers, and as such is a logical additional outcome measure to use.

3.2 Aims & Objectives

This chapter aimed to characterise complement biology during prolonged clinical kidney normothermic machine perfusion in the NKP1 trial. The intention was first to confirm the presence of complement proteins and activation products in perfusate, then to examine their behaviour over the course of perfusion to determine whether this was consistent with ongoing activation and/or consumption across the classical, lectin, alternative, and terminal pathways. A further aim was to assess whether perfusate complement profiles related to donor characteristics, graft injury, and post-transplant outcomes, particularly functional delayed graft function and time to creatinine 50% fall. Finally, tissue multiplex immunofluorescence was used to assess intrarenal complement deposition and related injury signals before perfusion and after recipient reperfusion, to help place the perfusate findings in a graft-level biological context.

Objectives:

- To detect and quantify selected complement proteins and activation products in NKP1 perfusate.
- To describe changes in these proteins during the course of prolonged NMP.
- To assess residual functional pathway activity in perfusate using the Wieslab assay.
- To examine associations between perfusate complement markers and donor factors, including donor type, age, sex, and UKDRI.
- To determine whether perfusate complement markers were associated with early transplant outcomes, particularly functional DGF.
- To evaluate whether complement marker profiles have a relationship to TCr50.
- To assess whether complement information added prognostic value beyond UKDRI alone.
- To compare tissue, complement and injury-marker expression between pre-NMP and post-reperfusion biopsies.

- To explore whether tissue findings related to donor risk or clinical outcome.
- To assess perfusate and tissue findings to consider whether complement during NMP acts as a marker of injury, a mediator of injury, or both.

3.3 Methods

3.3.1 NKP1 Trial Methodology

NKP1 was a single-centre, phase 1, non-randomised, historically controlled trial conducted at the Oxford Transplant Centre (ISRCTN13292277), evaluating the safety and feasibility of prolonged NMP prior to transplantation. The study was approved by the Greater Manchester South Research Ethics Committee (20/NW/0442) and the MHRA (CI/2021/0034/GB), sponsored by the University of Oxford, and supported by OrganOx Ltd, Oxford Clinical Trials Research Unit (OCTRU), and Surgical Intervention Trials Unit (SITU).

The trial comprised three sequential 12-patient stages with maximum permitted NMP durations of 6, 12, and 24 hours, respectively, with independent data monitoring and staged safety reviews. Eligible kidneys were retrieved from DBD or DCD donors aged >16 years, meeting national transplant criteria, and with cold ischaemia time ≤12 h (DCD) or ≤18 h (DBD). Adult recipients on the Oxford waiting list provided informed consent in advance.

The control group consisted of matched historical transplants (2:1 ratio) performed between 2016 and 2021, matched by donor type, induction immunosuppression, donor risk index, and cold ischaemia time.

Similar to the research perfusion methodology described in chapter 2, the OrganOx Metra-K prototype perfusion device-maintained kidneys at 37 °C using a pressure-controlled circuit (initially 90 mmHg, later 75 mmHg) with automated oxygen and CO_2 regulation. The perfusate contained packed red cells, 20% human albumin, verapamil, antibiotics, antifungal, heparinoid, calcium, glucose–insulin, and further vasodilators as required, with urine recirculation in all cases.

Biopsies were taken preperfusion and post-reperfusion in the recipient for histological assessment of acute tubular injury and chronic changes, and scored by an independent blinded pathologist. Perfusate, urine, and blood samples were collected at baseline, 2 hours, and end-of-perfusion, and daily in recipients for 4 days post-transplant. Samples

were centrifuged, aliquoted, and stored at −80 °C for biochemical and biomarker analysis.

Primary outcome was 30-day graft survival. Secondary endpoints included 3- and 12-month graft and patient survival, early graft function, delayed graft function, and adverse events. Exploratory analyses assessed perfusion performance, injury biomarkers (NGAL, KIM-1, L-FABP, GST, LDH, AST, IL-18, cfDNA), and correlations between ex-situ physiology and post-transplant outcomes.

3.3.2 Perfusate Analysis

The following complement fragments were assessed: C1s, C2, C3, C3d, CL-11, Factor B, Fragment Ba, C5b-9 as per the common methods in chapter 2.

In addition to the common methods on complement protein analysis, a Wieslab assay was performed on a selection of samples that had either high or low levels of C5b-9 and C3d. In brief, perfusate was prepared per kit guidance and stored −80 °C to avoid in vitro activation. Samples were thawed on ice, mixed, and diluted pathway-specifically: CP and MBL/lectin 1:101 in their respective diluents; AP 1:18 in AP diluent. Duplicate 100 µL aliquots of blanks, kit negative and positive controls, and diluted samples were added to microplate wells pre-coated with pathway-specific activators (IgM for CP, mannan for MBL, LPS for AP) and incubated 60 minutes at 37 °C. After three washes, wells received alkaline-phosphatase–conjugated anti-C5b-9 neoepitope antibody for 30 min at room temperature, were washed, then developed with pNPP substrate for 30 min at room temperature. Absorbance was read at 405 nm. For each pathway, % activity was calculated as (OD_sample − OD_NC) / (OD_PC − OD_NC) × 100; runs were accepted when PC > 1.0 and NC < 0.2 per IFU.

3.3.3 Data Handling

Relating complement proteins to trial outcomes was an exploratory post-hoc analysis and as such the statistical methods involved in considering associations have reflected that. All data processing and statistical analysis was conducted in RStudio (Version - 2026.01.0+392). For analysis of the complement proteins and possible relationship to outcomes, two complementary non-parametric approaches were used. For binary

predictors (sex, donor type), Wilcoxon rank-sum tests were used, with rank-biserial correlation used as an interpretable effect-size measure. For continuous predictors (donor DRI, donor age, perfusion duration), Spearman rank correlations were used to estimate associations, reporting Spearman's ρ and p-values. Because associations were screened across multiple timepoints, Hour-1, End, and their delta, multiplicity was addressed using Benjamini–Hochberg false discovery rate (BH/FDR) correction across the full association screen, with q value for significance maintained across multiple comparisons.

Time to recovery of graft function was assessed using TCr50, analysed as a time-to-event outcome with the event defined as achieving TCr50 and follow-up time defined by the number of days required to do so. The TCr50 curves were estimated using the Kaplan–Meier survival function, S(t), plots were expressed as cumulative incidence of recovery, defined as 1−S(t). This transformation represents the proportion of recipients who have achieved functional recovery by each timepoint, i.e. those who have a functioning graft. For each stratified curve, the association between strata and recovery timing was assessed using the log-rank test, comparing Kaplan–Meier curves across all levels of the grouping factor. The log-rank statistic was converted to a p-value using the chi-square distribution with degrees of freedom equal to the number of strata minus one. The log-rank test was chosen because it is the standard non-parametric approach for comparing survival curves across groups and makes minimal distributional assumptions, providing a direct global test aligned to the visual separation of the plotted step curves.

To evaluate whether perfusate complement markers contain prognostic information beyond baseline donor risk, UKDRI-based and complement-based strata were constructed using simple, distribution-free rules based on within-cohort medians. UKDRI was operationalised into a high and low group split around the median. For the complement markers these were principally grouped in combinations of two and then a larger 4-marker composite; Hour-1 Ba with Hour-1 C3, Hour-1 C5b-9 with Hour-1 C3d, and end-perfusion C5b-9 with end-perfusion C3d. Each marker was dichotomised at its cohort median. For the grouping based in two markers each kidney was then assigned to one of three ordinal strata based on the number of markers above the median: "High"

if both markers were above median, “Intermediate” if exactly one marker was above median, and “Low” if neither marker was above median. This method of ordinal grouping produces a risk grouping without assuming linearity, normality, or requiring parametric transformations.

The four-marker composite was made from early markers (Hour-1) to determine if this improved prediction. The included markers were Hour-1 Ba, Hour-1 C3, Hour-1 C5b-9, and Hour-1 C3d. Again, dichotomised around the median and grouped into “High” if 3 or 4 markers were above the median, “Intermediate” if exactly two were above, and “Low” if 0 or 1 were above. The composite of early markers could be of use, given this could be taken early in perfusion, but by combining into non-specific groups there is a reduction of dependence on any single assay, reflects potential multi-pathway activation early after reperfusion which can vary between organs.

The UKDRI is a robust tool and provides an important guide in predicting outcome and as such assessing where any biomarker fits within or separate from this is important. To approach these two things have been done, the first is to look at complement markers in the context of high UKDRI organs, so additional analyses repeated the complement stratifications within the subgroup of kidneys with above-median UKDRI within the NKP1 cohort, as the cohort contained most UKDRI 2-3 kidneys. This design directly addresses whether early complement activation can stratify recovery even within a clinically high-risk donor profile, though is severely limited by the reduced sample size and the number of events within the low complement group as a result.

The second approach to formally test whether complement information improved prognostic modelling beyond UKDRI was a Cox proportional hazards. A baseline model included UKDRI alone, and an extended model included UKDRI plus complement information. Model comparison focused on three complementary metrics.

Likelihood ratio test (LRT) comparing models to evaluate whether inclusion of the complement term significantly improved model fit beyond UKDRI alone. Akaike Information Criterion (AIC) to quantify relative model quality while penalising additional parameters i.e. inclusion of more complement biomarkers, lower AIC was interpreted as improved fit accounting for complexity. Harrell’s concordance index (C-index) to

summarise discrimination, interpreted as the probability that the model assigns a higher predicted hazard (slower recovery) to the individual who in fact recovers later, for a randomly selected comparable pair. This combination of outputs was used to distinguish statistical evidence of improved fit (LRT), practical improvement in parsimonious modelling (AIC), and clinically interpretable discrimination (C-index), rather than relying on any single summary alone.

The proportional hazards assumption underpinning Cox modelling was evaluated using Schoenfeld residual testing for each fitted model, with both term-specific and global tests reported. Where evidence of non-proportional hazards was observed (significant Schoenfeld test), the corresponding Cox model was interpreted cautiously as it suggests time-varying covariate effects and potentially unstable hazard ratio interpretation across the recovery period. Overall, this is a complex analysis on a small number of cases, but the only suitable method for attempting to assess benefit beyond UKDRI alone, it is intended to assess signal not as a deployable model, this could only be done if validated in a larger independent cohort.

3.3.4 Tissue Multiplex Immunofluorescence

All multiplex IF was done on the CellDive platform and analysed in the same mixed analysis pipeline of manually defined tissue and background masks with automated pixel intensity and marker specific thresholding as per the detail given in chapter 2 (common methods).

3.4 Results

3.4.1 Perfusate Complement Proteins

3.4.1.1 Complement Protein Dynamics

To characterise within-perfusion complement dynamics for a selection of markers, Hour-1 and End perfusate concentrations were compared within each case using paired Wilcoxon signed-rank tests. There was evidence of progressive complement activation or endothelial/cellular release over the course of perfusion, with significant increases in classical pathway protease C1s and terminal complement complex C5b-9, alongside smaller but significant rises in CL-11 and C3d. In contrast, C2 and Factor B fell over time, consistent with consumption, while C3 and Ba did not change significantly.

C1s increased from 360 ng/mL (285–509) at Hour-1 to 563 ng/mL (536–671) at End ($p<0.00001$). Similarly, C5b-9 rose from 379 ng/mL (159–544) to 1,004 ng/mL (550–1,340) ($p<0.00001$). More modest but significant increases were also observed for CL-11, increasing from 32.02 ng/mL (25.33–42.59) to 34.47 ng/mL (29.24–44.02) ($p=0.0014$), and for C3d, rising from 5.79 µg/mL (3.47–9.67) to 6.48 µg/mL (4.66–11.06) ($p=0.018$).

Conversely, C2 fell from 0.853 µg/mL (0.646–0.999) at Hour-1 to 0.661 µg/mL (0.498–0.758) at End ($p=0.00015$), and Factor B decreased from 9,101 ng/mL (7,389–10,889) to 8,593 ng/mL (6,731–9,738) ($p=0.0046$). In contrast, there was no evidence for a consistent cohort-level change in C3 (Hour-1 5,068 ng/mL (4,303–6,340) vs End 5,603 ng/mL(4,387–7,953), $p=0.517$) or Ba (Hour-1 90 ng/mL (49–162) vs End 70 ng/mL (35–128), $p=0.258$) (Fig 3.1).

To assess whether the magnitude of within-perfusion change (delta = End − Hour-1) varied with perfusion duration, simple linear regressions were fitted for each delta biomarker against perfusion duration. Across analytes, relationships were generally weak, reflected by low R^2 values, indicating that perfusion duration explained only a modest proportion of variance in changes in complement markers. Two analytes showed statistically supported negative relationships with duration, Ba and C2,

implying that longer perfusions were associated with greater decline or greater apparent consumption. Change in C3 showed a borderline negative association.

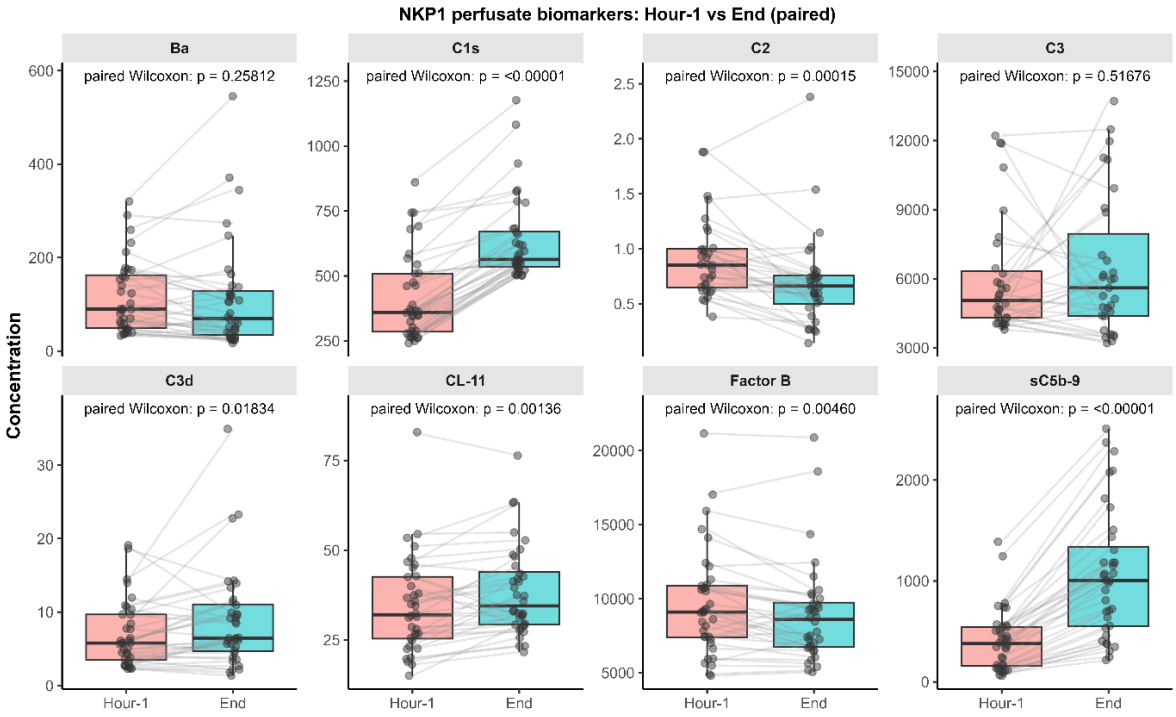


Figure 3.1 ***Paired comparison of perfusate complement biomarkers across NKP1 cohort****. Markers Ba, C1s, C2, C3, C3d, collectin-11 (CL-11), Factor B, and soluble C5b-9 (sC5b-9 were assessed between Hour 1 and end perfusion in the NKP1 cohort. Boxplots show biomarker concentrations at Hour 1 and at the end of perfusion, with individual kidneys linked by grey lines to illustrate within-kidney paired changes over time. Boxes represent the median and interquartile range, with whiskers indicating the spread of the data and overlaid points showing individual observations. Across the perfusion period, C1s, C3d, CL-11, and sC5b-9 increased significantly, while C2 and Factor B decreased significantly between Hour 1 and end perfusion. Ba, C3, and intact C3 showed no statistically significant change over time.).*

For Ba, the regression slope was −4.676 (p = 0.045, R^2 = 0.113). For C2, the slope was −0.025 (p = 0.02253, R^2 = 0.162). C3 showed a similar direction but did not meet statistical significance (slope = −239.063, p = 0.059, R^2 = 0.117).

No clear evidence of association of the amount of change with perfusion duration was observed for C1s (slope = 4.623, p = 0.152, R^2 = 0.059), C5b-9 (slope = −11.650, p = 0.408, R^2 = 0.020), C3d (slope = −0.152, p = 0.419, R^2 = 0.019), CL-11 (slope = −0.345, p = 0.193, R^2 = 0.049), Factor B (slope = −46.711, p = 0.382, R^2 = 0.023), despite significant changes between the start and end of the perfusions (Fig 3.2).

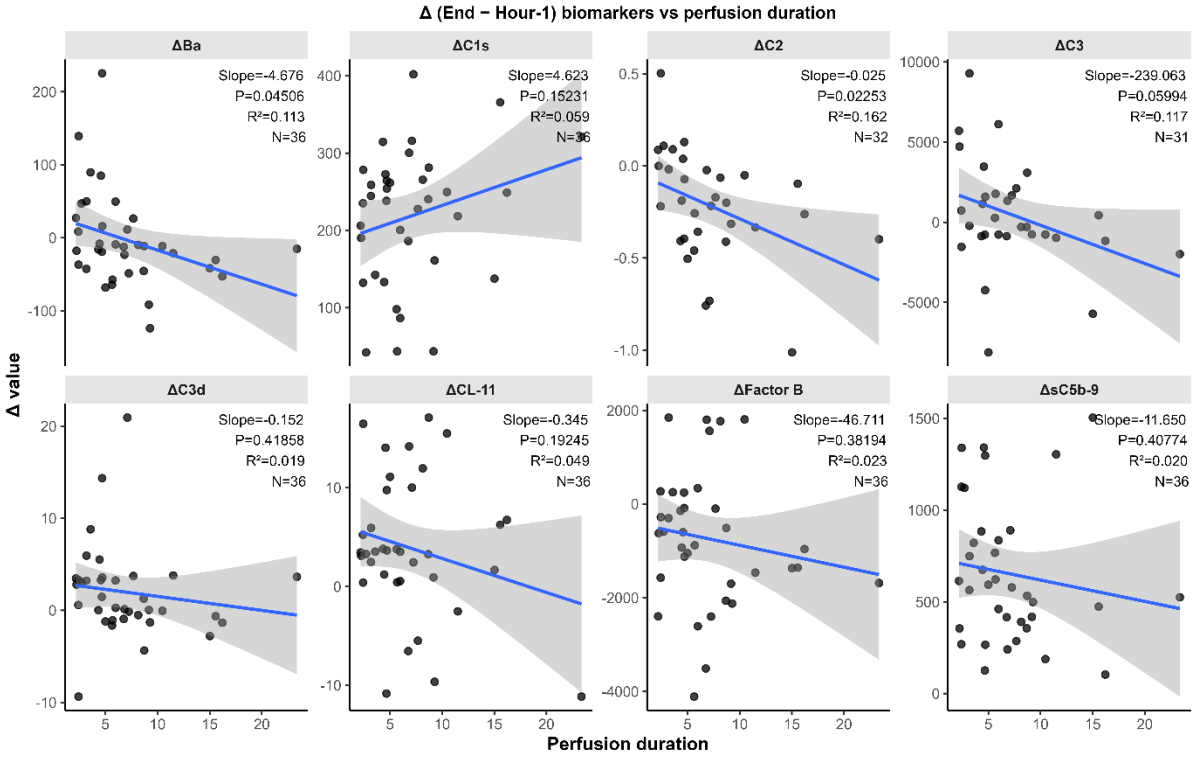


Figure 3.2 ***Association between perfusion duration and change in perfusate complement biomarkers across the NKP1 cohort****. For each biomarker, the change in concentration between end perfusion and Hour 1 (Δ = End − Hour 1) is plotted against total perfusion duration. Each point represents an individual kidney. Blue lines indicate fitted linear regression slopes with grey shaded 95% confidence intervals. The slope, p value, coefficient of determination (R^2), and number of observations included in each analysis are shown within each panel. Longer perfusion duration was significantly associated with a greater fall in Ba and C2 over time, while the association with intact C3 showed a similar negative trend that did not reach conventional statistical significance. No significant relationship was identified between perfusion duration and change in C1s, C3d, CL-11, Factor B, or sC5b-9. Biomarkers displayed are Ba, C1s, C2, C3, C3d, collectin-11 (CL-11), Factor B, and soluble C5b-9 (sC5b-9).*

3.4.1.2 Wieslab Assays

Functional complement pathway activity was assessed in a subset of NKP1 perfusate samples using the Wieslab® Complement System Screen, which quantifies the capacity of a sample to generate plate-bound C5b-9 following pathway-specific stimulation (IgM for classical, mannan for lectin/MBL, LPS for alternative), reported as % of the kit positive control, where the positive control is defined as 100% of normal pathway activity. In healthy blood-donor sera, the manufacturer's reference ranges are approximately 69–129% for CP, 0–125% for LP, and 30–113% AP, with medians of ~100%, 56%, and 73% respectively. In contrast, NKP1 perfusate showed profoundly depressed functional activity across all pathways at both timepoints, with values predominantly <5%.

Functional complement pathway potential activity was assessed in a subset of 13 NKP1 cases (n=6 high complement grouping and n=7 low complement grouping), perfusate samples comparing Hour-1 and End of perfusion. Across all cases, pathway activity was markedly depressed relative to what would be expected for normal serum and showed no evidence of systematic change over perfusion. Classical pathway activity was low at both timepoints (median 1.373% at Hour-1 vs 1.212% at End, p=0.295). Lectin/MBL pathway activity was near-zero (median 0.000% at Hour-1 vs 0.081% at End, p=0.541). Alternative pathway activity was essentially absent (median 0.000% at Hour-1 vs 0.000% at End, p=0.590) (Fig 3.3).

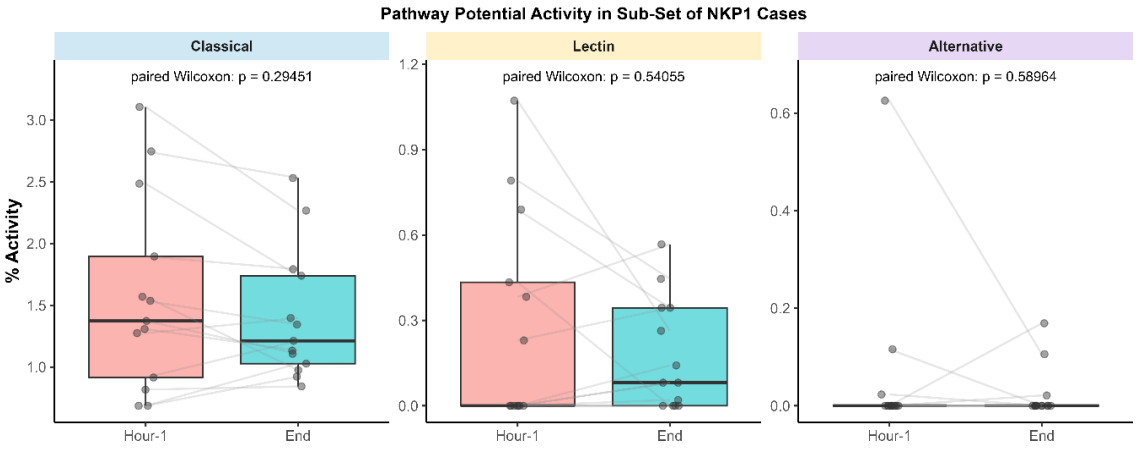


Figure 3.3 ***Paired comparison of functional complement activity measured by Wieslab assay in a subset of NKP1 kidneys****. Boxplots show potential activity of the classical, lectin, and alternative pathways at Hour 1 and end perfusion, expressed as percentage activity. Individual kidneys are linked by grey lines to illustrate within-kidney paired changes over time. Boxes represent the median and interquartile range, with whiskers indicating the spread of the data and overlaid points showing individual observations. Across this subset, there was no statistically significant change in functional activity of the classical, lectin, or alternative pathways between Hour 1 and end perfusion. Alternative pathway activity remained minimal at both timepoints, while classical and lectin pathway activity were low but detectable and showed inter-sample variability without consistent directional change.*

Stratification into “High” and “Low” complement-activity phenotypes gave similar results. In the High group (n = 6), classical activity remained low (median 1.455% to 1.371%, p=0.675) and lectin activity remained low (median 0.306% to 0.213%, p=0.787). In the Low group (n = 7), classical activity remained depressed (median 1.308% to 1.028%, p=0.353) and lectin activity remained near-zero (median 0.000% to 0.081%, p=0.787) (Fig 3.4). Overall, Wieslab demonstrated very limited residual functional capacity in the perfusate to generate stimulated C5b-9 via classical, lectin or alternative pathways, with no detectable paired change from Hour-1 to End in this subset.

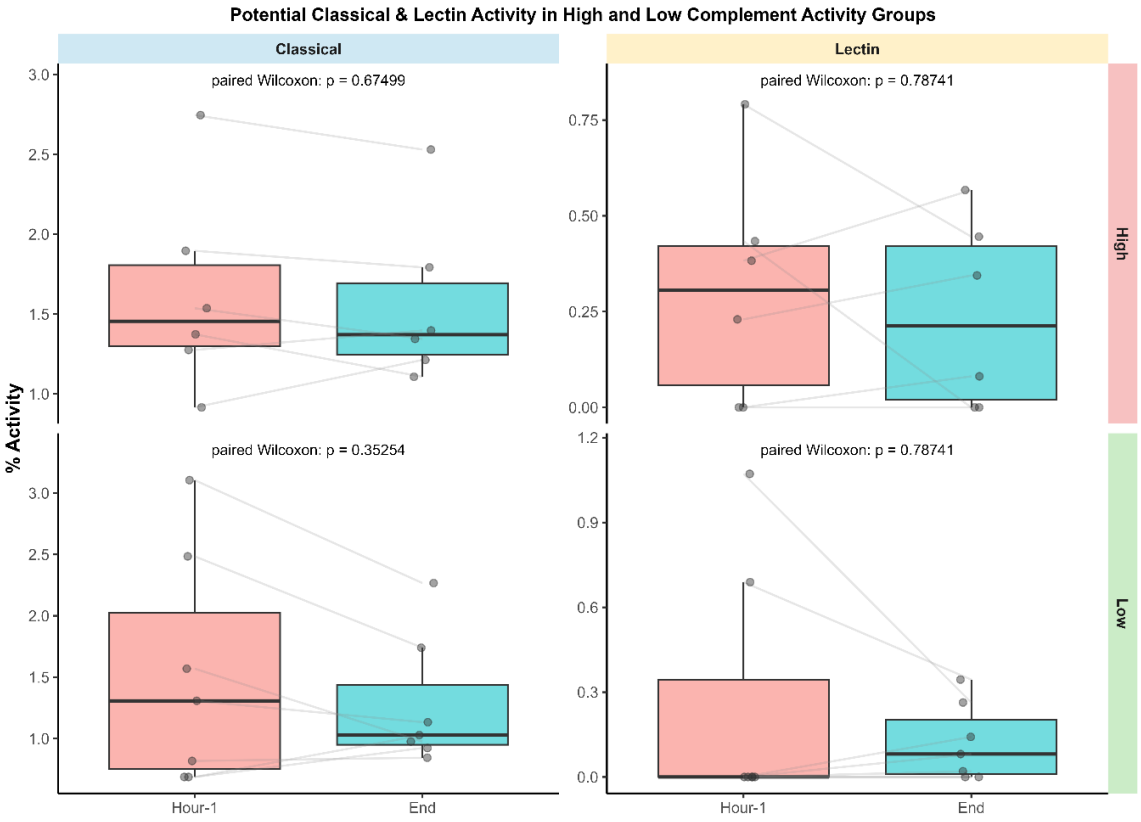


Figure 3.4 ***Paired comparison of functional complement activity measured by Wieslab assay in a subset of NKP1 kidneys stratified by perfusate complement activity group.*** *Kidneys were divided into high and low perfusate complement groups, and potential activity of the classical and lectin pathways was assessed at Hour 1 and end perfusion, expressed as percentage activity. Boxplots show the median and interquartile range, with whiskers indicating the spread of the data and overlaid points representing individual kidneys; grey lines connect paired measurements within the same kidney. Within both the high and low perfusate complement groups, there was no statistically significant change in classical or lectin pathway activity between Hour 1 and end perfusion. Classical pathway activity remained low but detectable in both groups, while lectin pathway activity was generally lower and more variable, particularly in the low complement group.*

3.4.1.3 Complement & Donor Factors

Recipient, operative and post-operative events contribute to early transplant outcome, but in reality, the donor factors, retrieval factors, and the kidney itself exert most of the effect on what happens in the days, weeks and arguably years following implantation. Therefore, if complement signals around the time of death and donation or during NMP are signals that relate to early function, then it is logical that donor factors play a role in these also. To explore basic donor characteristics associated with early complement activity in the NKP1 perfusion cohort, donor type (DBD vs DCD), donor age and donor sex were first examined descriptively, because these can be confounding in the signal possibly seen in complement proteins. UKDRI is a more complex holistic measure which will be dealt with separately in detail.

Due to the small cohort in the trial, there were naturally demographic discrepancies, though none are statistically significant discrepancies by Wilcoxon rank-sum or Fisher's exact test, some are noteworthy. The donors had a median age of 56.5 (46-67 IQR) and a UKDRI of 1.35 (0.89-1.72). Donor type comprised 20/36 DBD (55.6%) and 16/36 DCD (44.4%), while donor sex comprised 13/36 female (36.1%) and 23/36 male (63.9%). Sex distribution differed numerically by donor type: within DBD, donors were 9/20 female (45%) and 11/20 male (55%), whereas within DCD, donors were 4/16 female (25%) and 12/16 male (75%) (p=0.308) (Fig 3.5 A). This imbalance, particularly the predominance of male donors among DCD means that apparent donor-type associations with complement measures could be influenced by sex or donor type with one confounding the other. Therefore, sex associations were tested within donor-type strata, for other donor factors there was no evidence sex discrepancy. For grouping by sex, the ages and UKDRI were not different, male donors were 55.0 (46.0–67.5) and female 59.0 (51.0–63.0) (p=0.974) and for UKDRI male donors were 1.36 (0.99–1.73) and female 1.34 (0.90–1.59) (p-0.974).

As discussed in methodology, the statistical approach was used to scrutinise significant associations such that criteria for association were stringent. For the most part there were no significant associations, C5b-9, C3d and Ba were the only complement proteins which had any significant association across the donor factors. This was a broad exploratory post-hoc analysis which included 130 predictor-outcome tests included in the FDR correction and none of the effects remained significant after correction. None the less the association should be considered for possible plausible biological background.

Early C5b-9 levels highlight the sex-donor type interplay, where levels were elevated in male donors, but stratified by donor sex this was only true in the DBD cohort. Male donors had 410.63 ng/mL vs 116.96 ng/mL in female donors (p=0.012). In the DCD, 491.81 ng/mL vs 339.14 ng/mL (p=0.379), but with only 4 female DCD donor (Fig 3.5 B). However, when looking at donor type, levels were higher in DCD (491.8 ng/mL) compared to DBD (282.5 ng/mL) (p=0.034) (Fig 3.5 D).

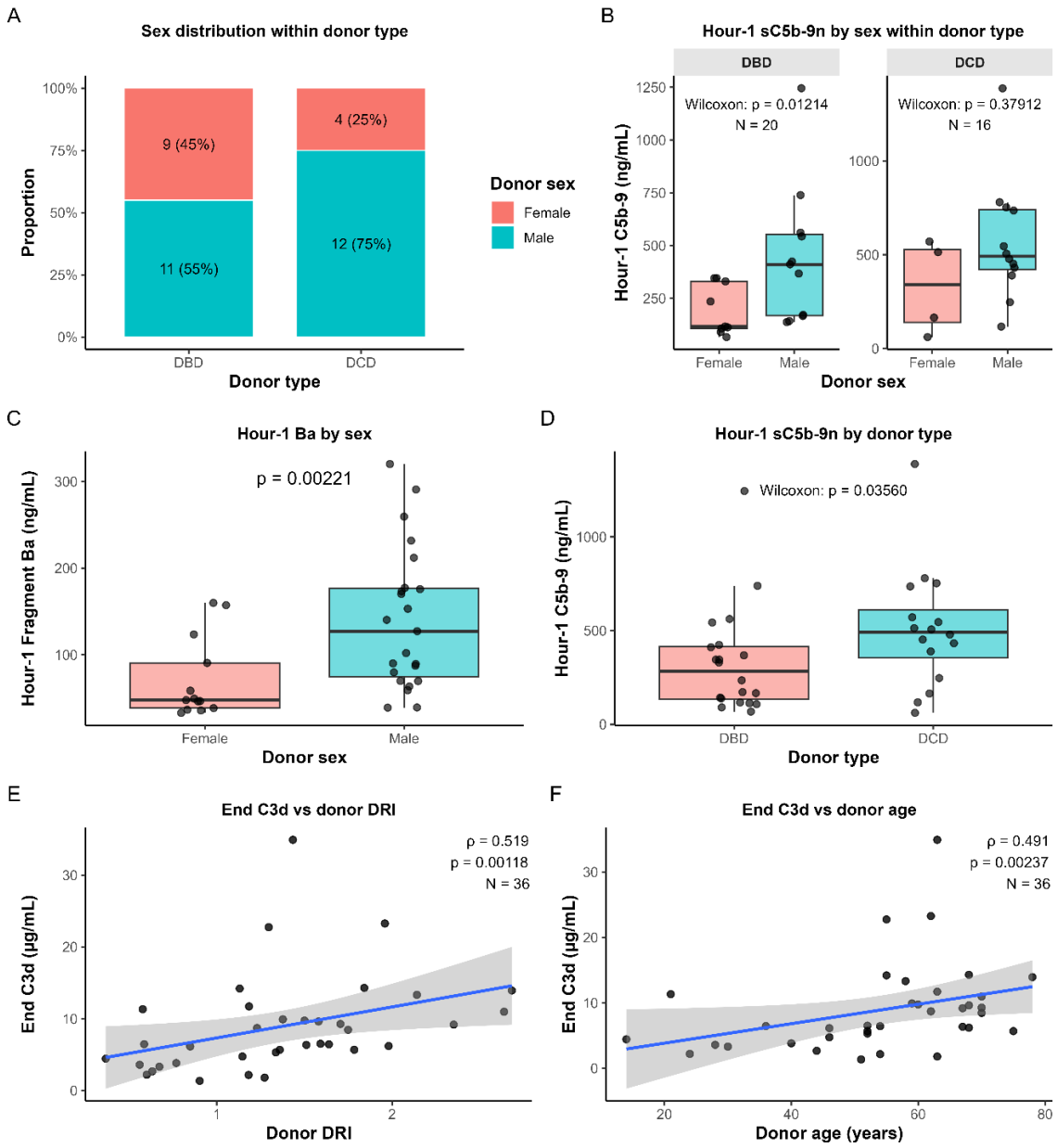


Figure 3.5 ***Donor factor associations with early and end-perfusion complement biomarkers in the NKP1 cohort.*** ***(A)*** *sex distribution within donor type strata, demonstrating a greater proportion of male donors in the DCD group than in the DBD group.* ***(B)*** *Hour-1 sC5b-9 concentrations stratified by donor sex within donor type, showing significantly higher early terminal pathway activation in male versus female DBD kidneys, with no significant sex difference within the DCD subgroup.* ***(C)*** *Hour-1 Ba concentrations by donor sex, demonstrating higher alternative pathway activation fragment levels in male donors overall.* ***(D)*** *Hour-1 sC5b-9 concentrations by donor type, showing higher early terminal complement activation in DCD compared with DBD kidneys.* ***(E)*** *Correlation between end-perfusion C3d concentration and donor DRI, demonstrating a positive association between increasing donor risk and greater complement activation by the end of perfusion.* ***(F)*** *Correlation between end-perfusion C3d concentration and donor age, likewise, showing higher end-perfusion C3d levels with increasing donor age.*

Fragment Ba was the only other complement protein to relate to sex or donor type, with male donors having higher early Ba levels of 127.3 ng/mL vs female with 47.6 ng/mL (p=0.002) (Fig 3.3 C).

The clearest continuous variable signals are seen in end perfusate levels of C3d. Higher UKDRI correlates with a higher ending C3d levels (p = 0.001) (Fig 3.3 E), as does increasing donor age (p = 0.002) (Fig 3.3 F), which is logical as donor age makes up a large part of UKDRI. There were no other uncorrected significant associations.

3.4.1.4 Complement Proteins & Their Relationship with DGF

To assess whether perfusate complement markers were associated with functional delayed graft function (fDGF), biomarkers were compared between recipients who did and did not develop fDGF using two-sided Wilcoxon rank-sum tests, presented as median (IQR). Because multiple complement markers at multiple time points were tested against the same binary outcome, Benjamini–Hochberg false discovery rate, FDR correction was applied as before. There remained some significant associations, the end C5b-9 and early C3 levels withstanding for multiple corrections.

Functional DGF was balanced in the cohort with 18 experiencing it, and 18 not. Across several markers, the fDGF group showed higher measured complement marker concentrations at Hour-1 and/or end perfusion. Two strongest signals were end-perfusate C5b-9 and Hour-1 C3. End C5b-9 was higher in fDGF (median 938.50 (669.25–1160.25) ng/mL) compared with no fDGF (628.50 (525.50–688.25) ng/mL, p=0.002, q=0.050). Similarly, Hour-1 C3 was higher in fDGF (6885.26 (5560.30–11903.63) ng/mL) versus no fDGF (4544.68 (4126.95–5202.18) ng/mL; p=0.004, q=0.050).

Other complement proteins showed nominal evidence of higher values in fDGF, but without surviving FDR correction. Hour-1 Ba was higher in fDGF (133.78 (87.85–172.53) ng/mL) vs no fDGF (58.76 (38.99–115.28) ng/mL, p=0.016, q=0.112), and Hour-1 C5b-9 was higher in fDGF (483.04 (282.19–694.45) ng/mL) vs no fDGF (282.50 (116.96–409.67) ng/mL; p=0.020, q=0.112). End C3d was also higher in fDGF (8.94 (6.44–12.73) µg/mL) compared with no fDGF (5.02 (2.83–9.62) µg/mL, p=0.022, q = 0.112), with concordant increases for end Ba (111.23 (54.07–157.60) vs 48.85 (26.47–101.59) ng/mL, p=0.028, q=0.112) and Hour-1 C3d (7.72 (4.71–10.18) vs 4.68 (2.64–5.81) µg/mL, p=0.039,

q=0.112). The Change in C5b-9 was also greater in fDGF (603.91 (480.26–1253.80) vs 490.22 (266.76–730.77) ng/mL; p=0.040, q=0.112) (Fig 3.6).

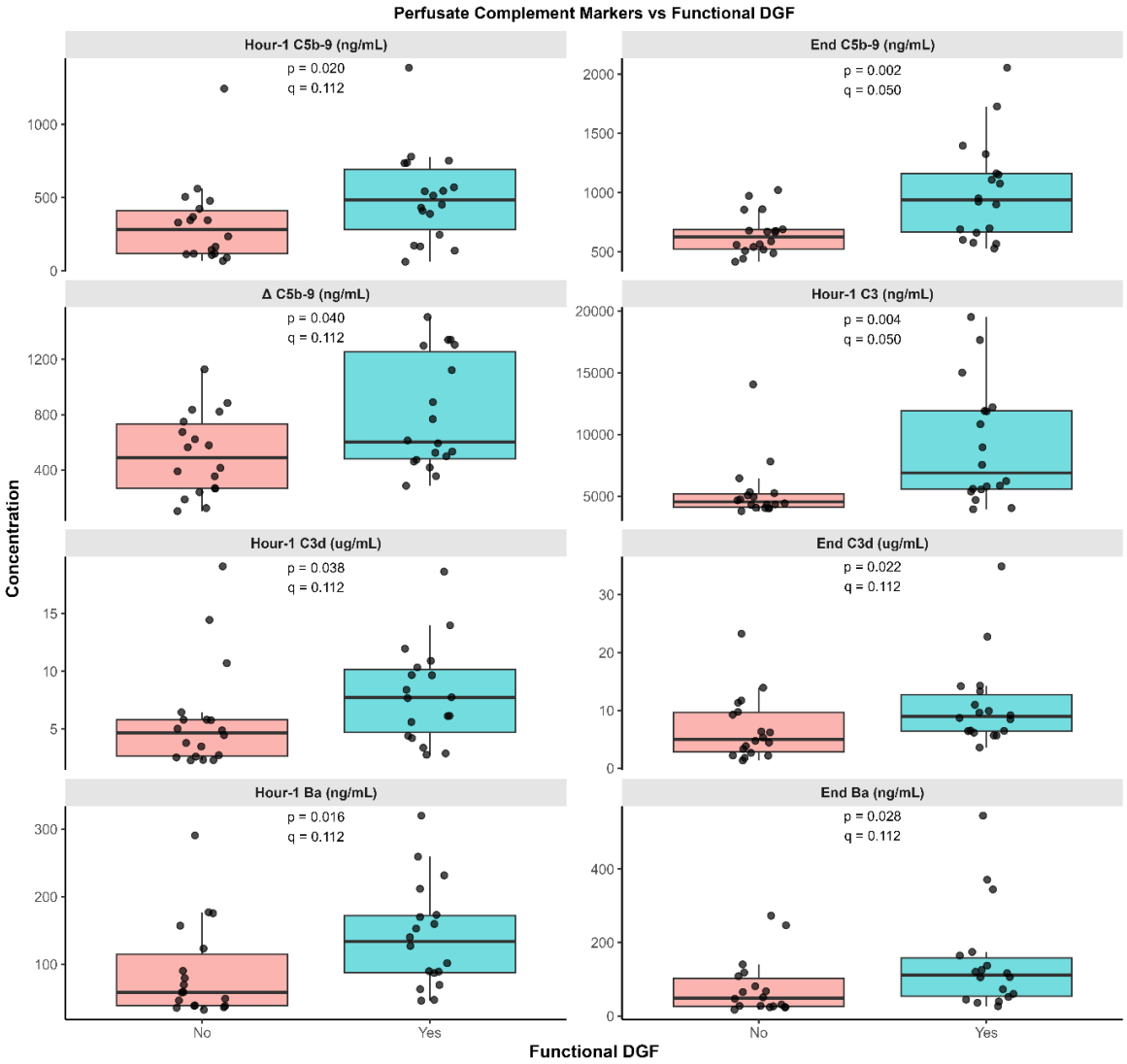


Figure 3.6 ***Association between perfusate complement biomarkers and DGF in the NKP1 cohort****. Boxplots compare kidneys with and without functional DGF according to Hour-1, end-perfusion complement biomarker concentrations. Biomarkers shown include sC5b-9, C3, C3d, and Ba. Boxes represent the median and interquartile range, whiskers indicate the spread of the data, and overlaid points represent individual kidneys. Kidneys that developed functional DGF exhibited higher early and end-perfusion terminal complement activation, with significantly greater Hour-1 and end-perfusion sC5b-9 concentrations, as well as a larger increase in sC5b-9 over the perfusion period. Functional DGF was also associated with higher intact C3 concentrations at Hour 1, together with higher C3d and Ba concentrations at both Hour 1 and end perfusion, consistent with greater upstream complement activation and downstream breakdown product generation in kidneys with poorer early graft function.*

3.4.1.5 Stratification by TCr50, UKDRI & Cox Regression

To stratify the potential added information from complement markers into something less binary than fDGF and a surrogate which possibly relates to longer term outcome, time to creatinine 50 (TCR) has been used. The key question being whether perfusate complement activation markers predict time to recovery of graft function, and whether they provide information that is distinct from, and incremental to the UKDRI. The aim, therefore, is not only to show separation of event curves by complement strata, but to formally evaluate whether adding complement information improves prognostic modelling on top of UKDRI. Significant end and hour-1 markers were grouped and then dichotomised at the medians and combined into three ordinal levels, high, intermediate and low complement activity groups.

The early and late markers were grouped together as they likely represent different mechanisms and given the timing would be hypothetically used differently as prognostic additives. For two-marker combinations; Hour-1 Ba with Hour-1 C3, Hour-1 C5b-9 with Hour-1 C3d, and end-perfusion C5b-9 with end-perfusion C3d. A kidney perfusion was classified into ‘high’ if both markers were above the median, ‘intermediate’ if exactly one was above the median, and ‘low’ if neither was above the median. A four-marker Hour-1 composite was additionally constructed using Ba, C3, C5b-9 and C3d, the number of markers above their median (0–4) determined grouping, ‘high’ (≥3), ‘intermediate’ (=2) and ‘low’ (0–1). To test whether complement information retained discriminatory value among high donor-risk organs, the same complement stratifications were repeated within the subset of kidneys with UKDRI above the median.

Incremental prognostic value beyond UKDRI was formally tested using a Cox proportional hazards model. A baseline model included UKDRI alone, and this was compared with models additionally including either the continuous four-marker score or the three-level composite group. Model comparisons were performed using likelihood ratio tests, with additional reporting of Akaike Information Criterion (AIC; lower indicates improved fit with penalisation for added parameters) and Harrell’s concordance index (C-index; discrimination).

Across the analysable cohort (N = 36; events = 34), UKDRI alone was strongly associated with the tempo of recovery (median split log-rank p = 0.00148), with low-UKDRI kidneys reaching TCr50 much earlier (with the majority of events occurring in the first post-transplant week) and high-UKDRI kidneys recovering more slowly with events spread across approximately weeks 2–4 (Fig 3.7).

Complement phenotypes also separated recovery trajectories when markers were combined into ordinal strata using median thresholds. Separation was evident for end-perfusion markers (end C5b-9 + end C3d; log-rank p = 0.01094), where the “Low” stratum reached TCr50 earliest and the “High” stratum showed delayed recovery. Separation was more pronounced for Hour-1 phenotypes, particularly Hour-1 Ba + Hour-1 C3 (log-rank p < 0.00001), with early divergence over the first few days post-transplant. Hour-1 C5b-9 + Hour-1 C3d also separated trajectories (log-rank p = 0.01909). A four-marker Hour-1 composite (Ba, C3, C5b-9, C3d) provided the strongest overall separation among the Hour-1 approaches (log-rank p = 0.00001), with the “Low” composite group reaching TCr50 earliest and the “High” composite group delayed, consistent with an early multi-pathway activation phenotype tracking slower functional recovery.

Incremental prognostic value beyond UKDRI was assessed using Cox proportional hazards modelling. Adding the continuous four-marker score to a UKDRI-only model improved apparent fit (AIC 188.42 to 180.11; ΔAIC 8.31) and discrimination (C-index 0.6407 to 0.7040), with evidence for incremental information by likelihood ratio test (LR χ^2 = 10.31 on 1 df; p = 0.00132). Representing the composite as a three-level factor (Low/Intermediate/High) further improved fit (AIC 174.90; ΔAIC 13.53 vs UKDRI alone; LR χ^2 = 17.53 on 2 df; p = 0.000156), supporting added prognostic signal when complement status is treated as an ordinal phenotype rather than a linear score. In keeping with this, the grouped composite appeared to contribute more information than the continuous score in this dataset, reflected by the larger AIC reduction and stronger likelihood ratio test signal for the categorical specification.

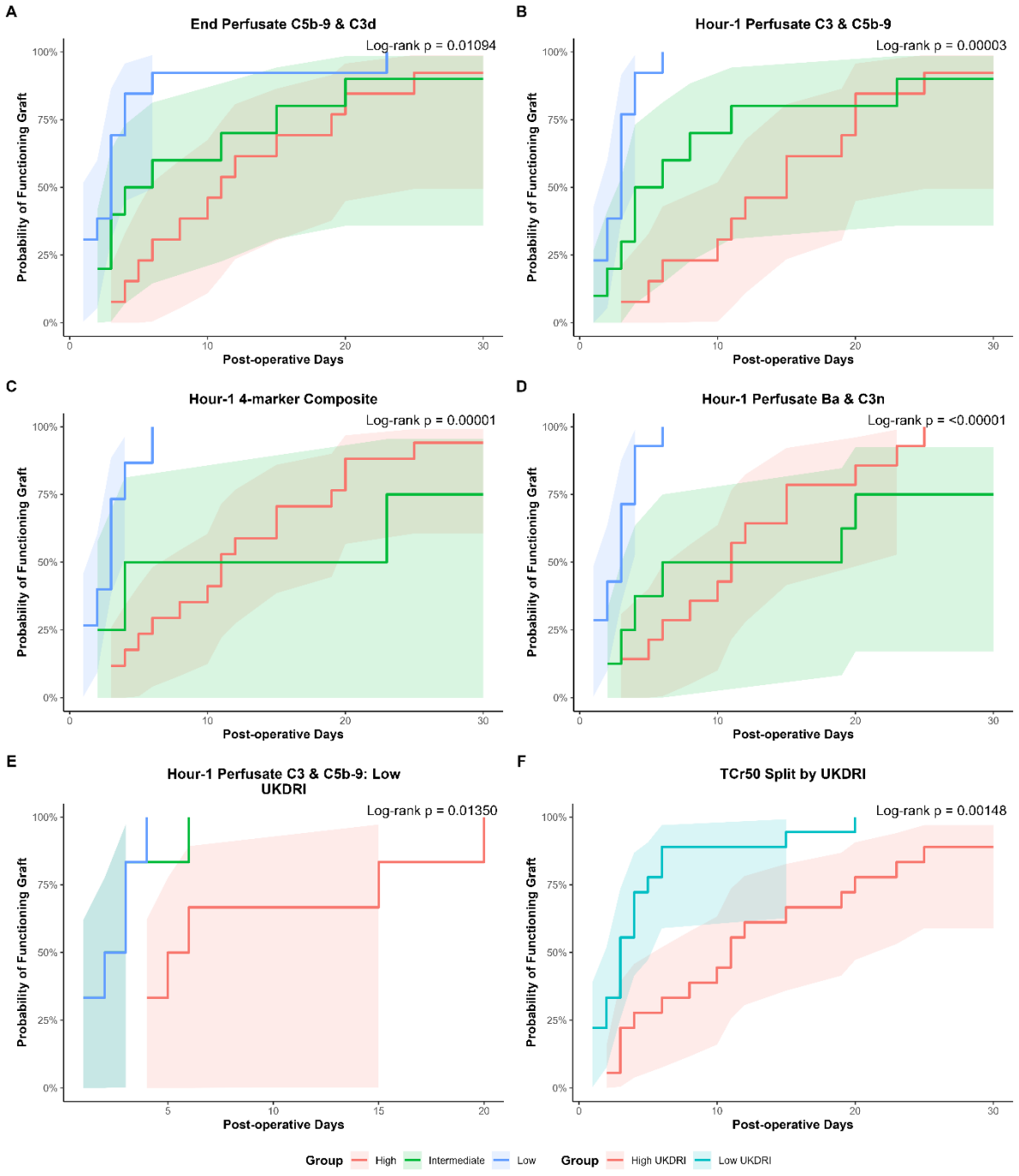


Figure 3.7 ***Probability of functioning graft in the NKP1 cohort stratified by perfusate complement biomarker groups and donor risk.*** *Kaplan–Meier–style plots show the probability of a functioning graft over the first 30 post-operative days after transplantation according to biomarker-defined strata and donor risk. (A) End-perfusion stratification by combined C5b-9 and C3d levels demonstrated significant separation of curves, with higher complement activity associated with a lower probability of functioning graft. (B) Hour-1 stratification by combined C3 and C5b-9 levels similarly separated outcome curves, with the highest biomarker group showing the lowest probability of functioning graft. (C) A Hour-1 4-marker composite score incorporating C3, C5b-9, Ba, and C3n also discriminated graft function over time. (D) Hour-1 stratification by combined Ba and C3n levels showed clear separation, again with worse graft function in the highest complement activity group. (E) In the low-UKDRI subgroup, Hour-1 C3 and C5b-9 retained discriminatory value, identifying kidneys with differing probabilities of functioning graft despite lower donor risk. (F) Stratification by TCr50 split according to UKDRI demonstrated significant separation, with low-UKDRI kidneys showing a higher probability of functioning graft than high-UKDRI kidneys. Shaded areas represent confidence intervals. Log-rank p values are shown on each panel.*

Proportional hazards assumptions were evaluated with Schoenfeld residual testing. The UKDRI-only model showed no evidence of non-proportional hazards (global p = 0.31294). In contrast, the UKDRI + continuous score model showed evidence of non-proportional hazards (global p = 0.00817), suggesting the score's effect may be time-dependent (e.g., concentrated early). The UKDRI + categorical composite model showed no evidence of non-proportional hazards (global p = 0.92325), supporting the categorical specification as the more robust representation in this dataset. Practically, if a clinically usable multivariable model is desired without obvious proportional hazards concerns, the UKDRI + categorical composite grouping is the safer of the two approaches here, whereas the continuous score model should be interpreted more cautiously given evidence for time-varying effects.

Finally, within the high-UKDRI subgroup (above-median UKDRI), complement stratification still identified meaningful heterogeneity in recovery. The hour-1 composite separated recovery curves (log-rank p = 0.03365), although interpretation is limited by sparse numbers in at least one stratum (Fig 3.5). In addition, restricting to high-UKDRI kidneys, the Hour-1 Ba + C3 strata continued to separate outcomes (log-rank p = 0.01308). This effect is also true in low-UKDRI kidneys, with low risk kidneys stratified by hour-1 C3 and C5b-9 also separates prolonged DGF, from primary function and short duration DGF (log-rank p = 0.0135), supporting the biological inference that even among kidneys already high-risk by donor factors, an early complement activation profile still distinguishes those with faster versus slower functional recovery.

Collectively, these analyses suggest that donor risk captured by UKDRI is strongly associated with the tempo of early graft functional recovery, but early perfusate complement activation (especially Hour-1 Ba/C3 and the 4-marker composite) further stratifies outcomes, including within the high-UKDRI subgroup. In multivariable Cox modelling, adding the Hour-1 composite significantly improves model fit over UKDRI alone (ΔAIC up to 13.53; LR $p=1.6\times10^{-4}$), supporting the concept that an early complement activation profile contains prognostic information beyond baseline donor factors. The proportional hazards diagnostics suggest that the composite's effect may vary over time when expressed as a linear score, whereas a categorical

low/intermediate/high representation appears more consistent with proportional hazards in the dataset.

3.4.2 Tissue Multiplex Immunofluorescence

3.4.2.1 Tissue Expression Pre-NMP & Post Recipient Reperfusion

Multiplex immunofluorescence (IF) tissue positivity was compared within kidneys between the pre-NMP biopsy and the post-recipient reperfusion biopsy using paired Wilcoxon signed-rank tests (Fig 3.8). Across markers, several showed clear within-kidney shifts between the biopsy time points, consistent with substantial biological change between baseline tissue state and early post-implant reperfusion following prolonged NMP.

C5b-9 increased 10-fold, from 0.017% (0.007–0.025) pre-NMP to 0.119% (0.014–0.629) post-reperfusion ($p=0.011$), indicating greater terminal complement deposition after implantation. ICAM-1 also increased slightly, from 0.727% (0.507–1.346) to 1.011% (0.544–2.278) ($p=0.016$), consistent with enhanced endothelial activation in the post-reperfusion biopsy.

In contrast, platelet and fibrin-associated staining decreased post-reperfusion. CD41 fell around 6-fold, from 0.220% (0.160–0.427) to 0.034% (0.011–0.086) ($p=0.007$), and fibrin fell by a similar amount, from 0.961% (0.567–1.486) to 0.184% (0.114–0.355) ($p=0.0107$), with the very small amounts of debris present pre-NMP being cleared by the post-reperfusion biopsy.

C4d did not show significant change over time from 0.047% (0.020–0.246) pre vs 0.098% (0.039–0.198) post, $p=0.355$, and PAI-1 similarly showed no consistent paired shift either, 0.778% (0.518–1.842) pre vs 1.100% (0.369–1.927) post, $p=0.927$). Collectively, the dominant paired signals were increased post-reperfusion terminal complement deposition and ICAM-1 expression, alongside reduced CD41 and fibrin.

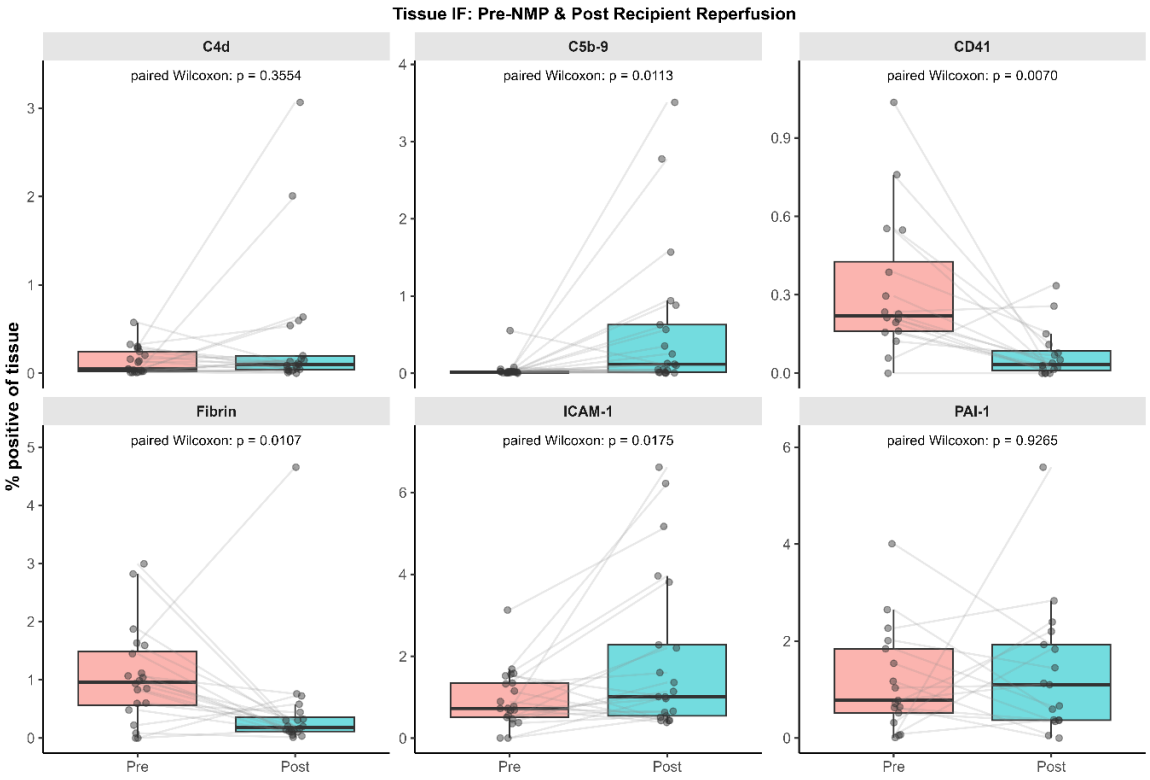


Figure 3.8 ***Paired comparison of tissue immunofluorescence marker positivity in pre-NMP and post-recipient reperfusion biopsies.*** *Boxplots show the percentage of tissue positive for each marker in matched biopsies taken before NMP and after recipient reperfusion, the markers: C4d, C5b-9, CD41, fibrin, ICAM-1, and PAI-1. Individual kidneys are linked by grey lines to illustrate within-kidney paired changes across the transplant process. Boxes represent the median and interquartile range, with whiskers indicating the spread of the data and overlaid points showing individual observations. Terminal complement deposition, endothelial activation, and thrombo-inflammatory injury changed across the paired biopsies. C5b-9 positivity increased significantly after reperfusion, consistent with enhanced terminal pathway deposition in the post-transplant setting. ICAM-1 also increased significantly, indicating greater endothelial activation after reperfusion. In contrast, CD41 and fibrin positivity were significantly lower in post-reperfusion biopsies than in pre-NMP tissue, while C4d and PAI-1 showed no statistically significant paired change.*

3.4.2.2 Tissue Expression & Outcomes

To explore whether tissue IF complement deposition related to early functional outcome, marker positivity was compared between kidneys that did and did not develop functional DGF using Wilcoxon rank-sum tests (Fig 3.9). In this tissue subset, there was no clear evidence that either C4d or C5b-9 tissue positivity at either timepoint was associated with DGF status, although there were trends in the expected direction for some pre-NMP measures.

Pre-NMP C4d tissue positivity was higher in DGF (0.148%, 0.045–0.260) than in those without (0.037%, 0.010–0.135)), but this did not meet conventional significance (p=0.068). Post-reperfusion C4d showed no separation by outcome (p = 0.900). For

terminal complement, pre-NMP C5b-9 was numerically higher in DGF (0.018% (0.012–0.027), n = 12) versus no DGF (0.012% (0.006–0.022)), but again without statistical support (p = 0.105). Post-reperfusion C5b-9 similarly did not differ materially by DGF, 0.113% (0.025–0.361) vs 0.043% (0.000–0.568) p=0.403. Overall, outcome associations were weak, suggesting that any relationship between tissue deposition and DGF is likely modest, if at all present and requires larger sample sizes.

However, there was a biologically interesting signal with pre-NMP C4d positivity correlated positively with UKDRI (p = 0.014), indicating that higher donor risk was associated with greater baseline C4d tissue deposition prior to NMP. Finally, post-reperfusion C5b-9 showed no evidence of correlation with perfusion duration (p=0.7094), suggesting that longer duration NMP was not associated with greater early tissue deposition upon reperfusion (Fig 3.9). There was no association between pre-NMP or post reperfusion C4d or C5b-9 and donor type. Pre-NMP C4d was similar in DBD versus DCD (0.047% (0.019–0.226) vs 0.132% (0.044–0.157), p=0.854), and post-reperfusion C4d likewise showed no separation (0.091% (0.039–0.637) vs 0.134% (0.066–0.432), p=0.867). For terminal complement, pre-NMP C5b-9 was equivalent by donor type (0.013% (0.007–0.025) vs 0.016% (0.011–0.021), p=0.979), while post-reperfusion C5b-9 was numerically higher in DCD (0.127% (0.070–0.941)) than DBD (0.036% (0.006–0.354)) but did not reach statistical significance (p=0.132).

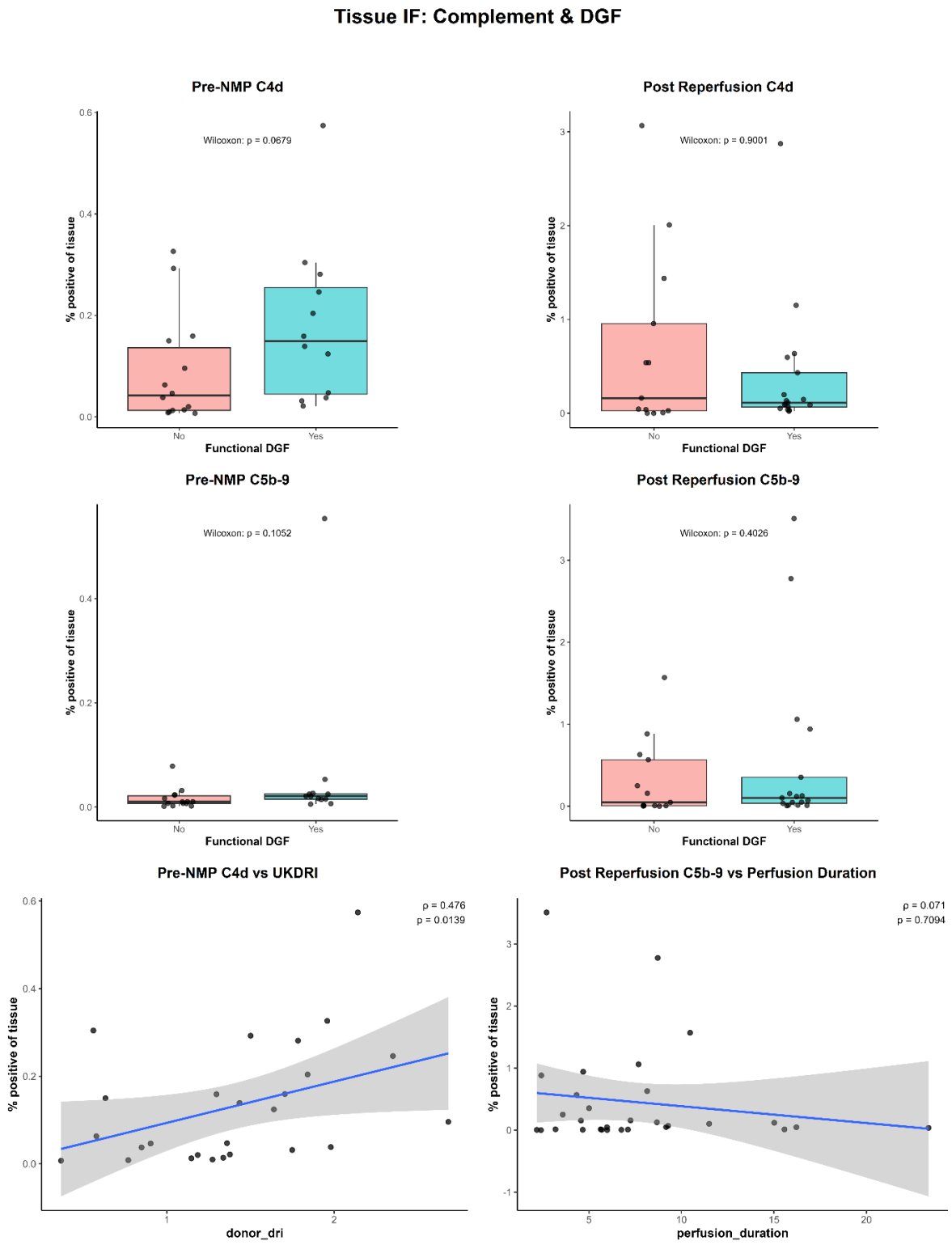


Figure 3.9 ***Associations between tissue complement immunofluorescence markers, functional DGF, donor risk, and perfusion duration.*** *Boxplots compare the percentage of tissue positive for C4d and C5b-9 in pre-NMP and post-recipient reperfusion biopsies according to functional DGF status. Pre-NMP C4d showed a numerically higher tissue positivity in kidneys that subsequently developed functional DGF though not statistically significant, whereas no association with DGF was evident for post-reperfusion C4d, pre-NMP C5b-9, or post-reperfusion C5b-9. Pre-NMP C4d positivity was positively associated with UKDRI, suggesting greater baseline complement deposition in higher-risk donor kidneys. By contrast, post-reperfusion C5b-9 positivity was not associated with perfusion duration.*

3.5 Discussion

3.5.1 Evidence of Complement Activation During NMP

There is compelling evidence that complement activation is a genuine and measurable feature of clinical kidney NMP in the NKP1 cohort. The most direct evidence comes from the dynamics over the perfusions of activation footprints and terminal pathway products. Within individual kidneys, C3d rises significantly from Hour-1 to end perfusion, and C5b-9 shows a large and highly consistent increase. A progressive increase in C3d is difficult to explain without ongoing C3 activation and processing of C3b through to stable degradation products. Some of the C5b-9 accumulation in the perfusate could be from pre-formed products during death and donation and then release following cell lysis as the IRI manifests on the device, however the magnitude and consistency of C5b-9 accumulation support formation of the terminal pathway during perfusion. These patterns would suggest that the NMP setting is likely both revealing background complement levels from pre-NMP but is also a source of continued complement activity over time.

The paired data over the course of the perfusion across the various markers shows a mixed direction, some rise, others fall and some are stable, this strengthens the findings because the accumulations in terminal complement are likely not artefactual from a haemoconcentration effect over the course of perfusion. This makes the behaviour of the various components more consistent with normal biology, activation, consumption, washout and replenishment occurring simultaneously, rather than a technical confounder

3.5.2 Functional Pathway Potential & Perfusate Complement Biology

The Wieslab functional pathway screen adds an orthogonal perspective to the ELISA-based activation readouts by asking a different biological question, whether the perfusate at that time retains the capacity to generate new C5b-9 under standardised pathway-specific stimulation. For the perfusate the pathway potential was profoundly depressed across classical, lectin/MBL and alternative pathways, at both Hour-1 and end-perfusion and showing no consistent paired change. This appears discordant with the ELISA evidence of rising activation footprints; however, these findings are

mechanistically coherent if activation products accumulate despite near-complete loss of freely activatable pathway capacity in the fluid phase. The intact components are depleted, inactivated, diluted, or partitioned away from the free perfusate while stable split products persist, particularly C5b-9, and rise. Complement activation generally, and likely during NMP, is for the most part surface-localised, occurring at the kidney injury interface, microvascular endothelium and tubular epithelium, and likely some on the circuit surfaces. Complement is inherently surface focused: C3b and C4b become covalently attached to nearby targets, convertases assemble on surfaces, and C5b-9 is fundamentally a membrane endpoint, with soluble C5b-9 representing released/solubilised terminal complex. Under this model, key pathway components and activation complexes may be exhausted at sites of injury and/or adsorbed to surfaces, leaving the free perfusate relatively incapable of generating additional stimulated C5b-9 in the Wieslab format, even while the perfusate contains the footprints of what has already occurred.

Finally, Wieslab is validated for serum and the NKP1 samples are perfusate (PRBC/albumin-based with variable haemolysis potential), so the results are representing pathway potential activity in this perfusate rather than absolute systemic complement function as it would be in patient serum, assessing if the required spectrum of complement proteins is present. Nonetheless, the consistent low or near-zero values support the conclusion that this NMP perfusate does not contain a robust, freely activatable complement system, and therefore that observed increases in ELISA markers most likely reflect graft-associated activation and release rather than a serum-like complement system circulating in the perfusate released from the kidney.

3.5.3 Activation & Consumption Across the Pathways

To add to the findings of stable split or terminal product accumulation there is evidence of consumption of products because of activation. The decline in C2 and factor B over time is compatible with utilisation of convertase components, CP/LP and AP substrate pools respectively, though it must be stated that adsorption to circuit surfaces and proteolysis cannot be excluded. In contrast, total C3 does not show a consistent cohort-level decline, which is not necessarily evidence against activation. In an injured

donor kidney undergoing NMP, total C3 concentration represents a balance between multiple competing processes rather than a simple readout of consumption alone.

Specifically, even in the presence of ongoing complement activation, total C3 may be maintained by replenishment through washout of residual donor plasma proteins trapped within the graft microvasculature and interstitium, given that it is one of the most abundant mammalian proteins, or similarly release or leakage from injured vascular and renal cellular compartments as permeability increases during reperfusion. There is also the likely possibility of local renal production given that there is the strongest evidence in humans of C3 production. Intrarenal C3 synthesis is established in tubular and glomerular cell compartments and is inducible by inflammatory cues; therefore, during NMP in which the kidney is metabolically active, it is biologically plausible that C3 availability is maintained despite parallel consumption. Within the NMP kidney we must consider both the substrate proteins (C3, C2, factor B) and the activation footprints and fragments, such as C3d, Ba, and C5b-9.

The alternative pathway signal is best interpreted in light of kinetics and fragment stability. Factor B is declining during perfusion consistent with utilisation and consumption of the AP substrate pool, while Ba does not show a consistent cohort-level rise from Hour-1 to end. This pattern does not necessarily limit AP involvement but could be consistent with a model in which AP amplification is highest early, producing Ba earlier and then due its less than 2-hour half-life its accumulation is attenuated. In contrast, total factor B, with a half-life of 30-70 hours, represents a large and relatively stable pool in which net consumption is easier to detect than transient fragment generation.

This kinetic interpretation is supported by the linked clinical outcome, Hour-1 Ba significantly correlates with fDGF and contributes substantially to the early composite profile that best stratifies within TCr50. Together, the results give that heterogeneous early AP amplification is one component of an adverse complement profile, even if cohort-level paired changes in Ba are not statistically significant.

One further minor biological consideration is that the NKP1 NMP perfusate does not feature magnesium supplementation, this could plausibly dampen AP amplification in-

circuit, given the Mg^{2+} dependence of AP convertase assembly. However, this is unlikely to fully explain the uniformly low Wieslab pathway potential across all pathways, where ionic conditions are largely governed by the diluents provided in the assay.

The perfusate markers support CP/LP involvement, the decline in C2 is compatible with engagement of CP/LP convertase machinery, while the presence and modest rise of CL-11 provide a mechanistic link to lectin recognition of stressed renal epithelium. The increase in C1s, while points to CP involvement it requires cautious interpretation. The antibody used quantifies total C1s, including inactive/complexed/inactivated forms, rather than uniquely measuring enzymatically active C1s at the point of sampling, but this is needed for a perfusate marker, given that active C1s for the most part will be bound to C1q and the surface of injury. This means our rising C1s may reflect a combination of sources washout of donor-derived protein, increased vascular leak/cellular release during reperfusion, and accumulation of C1s that has participated in activation and is now present in inactive forms within the perfusate such as bound to C1-INH or released C1q-r-s complexes.

3.5.4 Circuit Artefact vs Organ Biology

A recurring question in extracorporeal perfusion studies is whether complement activation reflects circuit-driven artefact, which is something addressed experimentally later in this thesis. Within the NKP1 data there are several aspects that go against complement being purely circuit driven. First, there is clear organ-to-organ heterogeneity rather than uniformity. Second, complement markers correlate with clinically meaningful endpoints (fDGF, TCr50) and with donor risk features such as end C3d and C5b-9 associating with age/UKDRI, supporting the interpretation that complement behaviour is tracking graft quality and IRI severity rather than representing a fixed background signal. While circuit contributions cannot be excluded, the association with outcomes provides a strong argument that the measured complement phenotypes are biologically meaningful at the graft level.

3.5.5 Early Complement Profiles as a Signal from Donor & Retrieval Biology

A clinically and mechanistically important inference is that early perfusate complement measurements may predominantly reflect donor biology and the effects of retrieval

surgery, rather than being generated de novo. The Hour-1 phenotype occurs at a time when the organ's biology is still dominated by events around donor death and donation: agonal physiology, inflammatory surges, warm and cold ischaemia, and early reperfusion stress. Complement proteins and activation products measured early may therefore derive from residual donor blood and interstitial compartments being washed into the perfusate after connection, together with kidney-resident complement production that may already have been induced by IRI signalling.

This concept would suggest early complement markers function as an integrated readout of how much innate immune activation has already occurred in the kidney before implantation. This conceptual model aligns closely with the strong prognostic performance of the multiple Hour-1 marker model in the NKP1 cohort, such that the early complement profile can be interpreted as biomarkers of donor and retrieval injury burden and pre-existing complement priming, which then manifest as DGF after transplantation.

3.5.6 Complement Signals Predict Recovery & Adds to UKDRI

The potentially useful translational conclusion is that complement behaviour during NMP is not merely descriptive; it relates to clinically meaningful outcomes. End-perfusion C5b-9 is higher in recipients who develop functional DGF and remains robust after multiple testing correction, consistent with terminal pathway activation tracking early dysfunction. In parallel, Hour-1 C3 is higher in fDGF and also survives correction; while total C3 is not itself an activation fragment, in this setting it can reasonably be interpreted as a marker of substrate availability and/or release of donor complement pool, potentially enabling stronger downstream activation or reflecting greater baseline inflammatory priming.

Beyond binary outcomes, utilising TCr50 analysis shows that complement phenotypes stratify recovery trajectories. Median-split UKDRI separates curves strongly, which as one would expect highlights donor risk index remains a dominant determinant of recovery tempo. However, combining with complement markers, particularly early profiles such as Hour-1 Ba & Hour-1 C3 and the four-marker Hour-1 composite (Ba, C3, C3d, C5b-9) produces pronounced separation of recovery curves and retain

discriminatory value even among above-median UKDRI kidneys. In addition to this multivariable Cox modelling further supports incremental prognostic information, adding the Hour-1 composite improves model fit and discrimination beyond UKDRI alone, and modelling the composite as the ordinal groups of high, intermediate and low appears the most robust with respect to proportional hazards than a purely linear score. Taken together, these results support the conclusion that an early complement activation profiles captures organ-level information about acute IRI and the innate immune state that is partly distinct from and additive to the conventional donor risk index.

3.5.7 Perfusate Complement as Marker vs Mediator

The data would suggest that complement during NMP is both a marker and a mediator, with these roles plausibly dominating at different phases of perfusion. Early in NMP, complement measures likely behave predominantly as biomarkers, reflecting donor physiology and death, then with retrieval induced injury. This provides pre-existing inflammatory priming, and immediate washout of intrarenal and residual intravascular complement proteins and fragments into the circuit. This early phase where they behave as markers explains why early composite signatures are strongly prognostic and why early complement phenotypes can stratify recovery even within high-UKDRI kidneys as well as aligning closely with UKDRI.

As perfusion continues, the progressive accumulation of activation footprints and terminal pathway products, particularly the substantial rise in C5b-9 and the increase in C3d supports the concept that complement is not only being revealed but is likely continuing to be generated within the ex-situ environment. At this later stage, complement becomes increasingly plausible as a mediator of harm, because ongoing terminal pathway activation can contribute to endothelial activation, microvascular dysfunction, tubular stress responses, and inflammatory amplification. The data of course does not prove causation, but they do demonstrate dynamic activation and clinically relevant associations consistent with a mechanistically meaningful role.

3.5.8 Tissue Proteins: Separating Donor Priming & Reperfusion Biology

The paired multiplex IF data shows the graft transitioning between a pre-NMP baseline following SCS to an early post-reperfusion state, after prolonged NMP. The readouts markers localise complement biology to the graft and provide mechanistic plausibility for why early perfusate phenotypes relate to recovery.

First, pre-NMP C4d positivity correlated with UKDRI, supporting the inference that a component of the early complement profile reflects ante-mortem donor biology and donor management injury, rather than being generated de novo on the circuit. This aligns with emerging donor literature showing that systemic complement activation is already present during deceased donor management, with elevated circulating activation products including C4d and C5b-9 compared with living donors, and substantial inter-donor variability at the earliest donor timepoints[58].

In this framework, higher UKDRI kidneys plausibly arrive to NMP with a higher baseline burden of endothelial stress/innate immune priming, which is consistent with greater baseline C4d deposition detected on the pre-NMP biopsy. While specific drivers within UKDRI such as donor hypertension causing endothelial stress or prolonged ICU stay reflected ante-mortem illness are biologically plausible contributors to this priming, there isn't a clear reason based on this small cohort for the associated especially given the effect was not more pronounced in the DBD cohort.

Second, the fall in CD41 and fibrin between pre-NMP and early post-reperfusion biopsies supports the concept of debris clearance and microvascular patency within NMP itself. Residual platelet/fibrin signal on the pre-NMP biopsy, while limited compared to other studies is consistent with retrieval factors like incomplete cold flush, microvascular stasis, and micro-thrombotic material formed during agonal physiology and procurement. The reduction after NMP and early reperfusion suggests that a proportion of this intravascular material is washed out or resolved during prolonged normothermic circulation and early in vivo reperfusion, rather than progressing to sustained platelet-rich adhesion within the transplanted microvasculature. This is in contrast to findings by DiRito et al, who describe a accumulation of fibrin(ogen) in renal tubules following cold storage which is then released on rewarming causing

fibrin(ogen)/RBC based obstruction, which they therapeutically lysed during NMP[152]. In contrast, in the NKP1 cohort reduced platelet (CD41) and fibrin positivity between the pre-NMP biopsy and an early post-reperfusion biopsy taken after prolonged NMP, consistent with net clearance rather than progressive platelet-rich microvascular adhesion. The difference in findings could be resolved by consideration of timing and kidney selection. The phenomenon then witness is early in NMP, and as such during prolonged and/or early in vivo reperfusion evidence for this fibrin has dissipated without the use of thrombolysis. This is also done in a cohort of declined kidneys which may have inherently a different baseline level of injury.

Third, the paired tissue data strongly support a reperfusion-linked effector phase, with C5b-9 increasing ~10-fold and ICAM-1 increasing in the post-reperfusion biopsy. The rise in C5b-9 provides evidence that terminal complement deposition is accentuated across the implantation/reperfusion transition, consistent with IRI exposing damaged endothelial and epithelial surfaces to recipient plasma and triggering terminal pathway assembly. This is in keeping with previous studies on human kidneys early post reperfusion, a study of 75 deceased donors contained renal vein blood sampling in the 5 minutes following anastomosis assessing C3a, C5a and C5b-9, finding the C5b-9 levels in the renal venous blood to correlate significantly with DGF[153]. A subsequent study on 24 recipients, this time form a mix of living and deceased donor with the same methodology of renal vein sampling, but out to 30 minutes finding that deceased donor had the early transient release of C5b-9, but the living donor kidneys did not. Interestingly the release of soluble C5b-9 was not matched by evidence of significant tissue deposition[74]. The association with DGF has been found in systemic blood samples 7 days following implantation, in a cohort of 115 recipients the systemic C5b-9 levels were significantly raised in the DGF group, but were stable in the immediate function group, and those with DGF who went onto have a biopsy found Kocak deposition of C5b-9 and C3d[154]. All this to say the findings here are consistent and mechanistically congruent with experimental renal IRI literature in C5b-9 has a major pathogenic role[73]. The accompanying increase in ICAM-1 is similarly consistent with endothelial activation in response to IRI and early inflammatory signalling, although the

precise kinetics of ICAM-1 induction can vary and likely evolve further beyond the first hour.

Finally, C4d did not show a consistent paired change across the two biopsies, which is interpretable in several non-exclusive ways. Biologically, the first-hour post-reperfusion window may be too early for a robust incremental C4d tissue footprint to emerge across all grafts, particularly if much early classical/lectin activation remains intravascular or transient. In addition, perioperative biopsy literature suggests that C4d positivity is not a generic feature of IRI alone, and may be more strongly informative in antibody-mediated contexts[155], and therefore, absence of a uniform early rise in C4d is not unexpected.

The tissue multiplex supports the conclusions donor risk is reflected by baseline intrarenal complement footprint, consistent with donor priming, while recipient reperfusion is associated with a rapid shift toward effector injury biology with C5b-9 deposition, occurring in parallel with clearance of peri-retrieval intravascular debris (CD41/fibrin). This helps reconcile why early perfusate signatures can be prognostic, while later accumulation of terminal products is biologically plausible as a mediator of ongoing injury.

3.5.9 Limitations, Implications & Next Steps

The are several limitations to be discussed, firstly the trial only contained 36 patients, which is a limited number especially when looking at multiple potential biomarkers. Secondly, the patients all received a different ‘dose’ on NMP, which is an important consideration generally for the trial, while the median was 5.8 hours, some receiving only 2 hours and others over 12. This means that the end of perfusion timepoint is variable, which could have implications on biomarker levels, though assessment was made relative to perfusion duration. Thirdly, the nature of early and end sampling does not capture the pattern of release/production, which again could be relevant for longer perfusion which may have had a different pattern than shorter perfusions.

Overall, the results suggest that complement profiling during NMP could be a promising biomarker platform and justify consideration of complement as a potential ex-situ therapeutic target. Early complement profiles, particularly features consistent with AP

amplification and terminal pathway activity are associated with slower functional recovery and adds prognostic information beyond UKDRI.

Future work should attempt to validate these signatures in a larger cohort with a predetermined complement assessment from an established ARC program, for example. The next immediate key step, as described later in the thesis, is to test targeted ex-situ interventions that modulate complement activation during NMP to determine whether attenuation of specific pathway components improves functional readouts initially in an ex-situ setting, and, thereafter in clinical transplantation.

4

Assessing C2 Inhibition in NMP and Normothermic Reperfusion

Contents

4.1 Introduction

4.1.1 Argx-117 Mechanism of Binding & Safety

4.1.2 C2-Inhibition in a Rat Transplant Model

4.1.3 Current Phase II Trial Design for DGF in Renal Transplantation

4.1.4 Modelling with Human Kidneys Ex-Vivo

4.2 Aims & Objectives

4.3 Methods

4.3.1 Model Development

4.3.2 Blood Only Perfusions

4.3.3 Single Kidney Perfusions

4.3.4 Paired Perfusions

4.3.5 Sample Analysis & Data Handling

4.3.5.1 Perfusate Biochemistry

4.3.5.2 Perfusate Injury Biomarkers

4.3.5.3 Perfusate Complement Proteins & Activity

4.3.5.4 Wieslab Functional Complement Assay

4.3.5.5 Tissue Complement: Western Blotting & Native Gel Electrophoresis

4.3.5.6 Tissue Multiplex Immunofluorescence (CellDIVE)

4.3.5.7 Tissue Complement Immunohistochemistry (QuPath)

4.4 Results

4.4.1 Model Development Perfusions

4.4.2 Blood Only Perfusions

4.4.3 Single Kidney Perfusions

4.4.3.1 Flow and Blood Gas Parameters

4.4.3.2 Perfusate Injury Biomarkers

4.4.3.3 C2 Blockade and Complement Activation Products

4.4.3.4 Tissue C5b-9 Immunohistochemistry

4.4.4 Paired Kidney Perfusions

4.4.4.1 Perfusion Parameters

4.4.4.2 Perfusate Biochemistry

4.4.4.3 Perfusate Injury Biomarkers

4.4.4.4 Perfusate Complement Proteins & Activity

4.4.4.5 Wieslab Assay

4.4.4.6 Tissue Complement on Western Blotting & Native Gel Electrophoresis

4.4.4.7 Tissue Multiplex IF

4.5 Discussion

4.5.1 Model Development and Blood Only Perfusions

4.5.2 Single Kidney Perfusions and Dose Assessment

4.5.3 Paired Kidney Perfusions

4.5.4 Model Limitations and Observations

4.5.5 Concluding Remarks

4.5.6 Further Work

4.1 Introduction

4.1.1 Argx-117 Mechanism of Binding & Safety

Argx-117, commercially known as empasiprubart is an investigational, humanised IgG1 monoclonal antibody targeting C2, developed to inhibit complement activation selectively at the convergence point of the classical (CP) and lectin (LP) pathways[156]. The conceptual appeal of C2 as a target is that it is essential for CP/LP C3 convertase (C4bC2a) formation, such that C2 blockade can prevent CP/LP-driven C3 activation. This inhibits downstream anaphylatoxin generation and amplification to terminal pathway effector formation, while not directly inhibiting the alternative pathway (AP). Argx-117 represents a pathway specific strategy, distinct from terminal pathway blockade seen in C5 inhibition and pan-C3 inhibition. It aims to block the antibody and lectin-triggered arms of the complement cascade that are implicated in multiple antibody-mediated inflammatory pathologies while preserving AP activity that contributes to antimicrobial defence. Research in multifocal motor neuropathy has used anti-C2 blockade to interrogate complement-dependent injury on neural structures, which has been found to be pathway specific, reinforcing that selective CP/LP inhibition can attenuate antibody-triggered tissue injury while not directly suppressing AP[157].

Argx-117 has been engineered as a recycling and sweeping antibody intended to cause durable suppression of free C2 (Fig 4.1). It is described as exhibiting pH- and Ca^{2+}-dependent target binding and incorporating Fc mutations H433K and N434F that enhance affinity for the neonatal Fc receptor (FcRn) at acidic endosomal pH, thereby enabling antibody recycling. The proposed mechanistic consequence is that, following nonspecific pinocytosis by endothelial cells, argx-117 is preferentially rescued via FcRn and recycled back to the plasma, while bound C2 is released and directed towards degradation, supporting sustained target depletion from finite exposure[156].

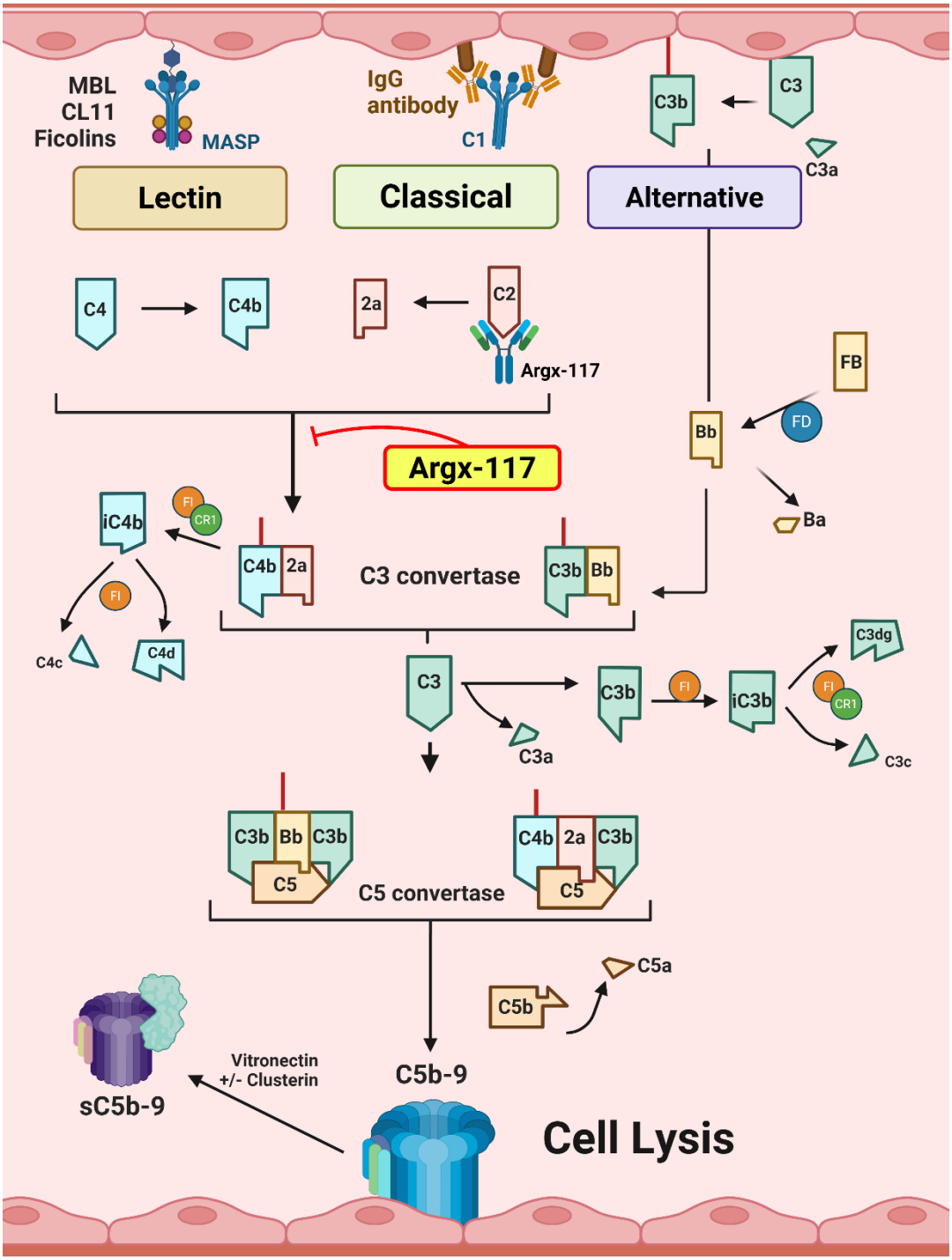


Figure 4.1 ***Schematic overview of the complement cascade showing the site and mechanism of action of Argx-117****. Complement activation is initiated through the lectin, classical, and alternative pathways. The lectin pathway is triggered by pattern-recognition molecules including MBL, collectin-11 (CL11), and ficolins in association with MASPs, while the classical pathway is initiated by C1 binding to IgG-containing immune complexes. Both pathways converge at cleavage of C4 and recruitment of C2 to form the classical/lectin pathway C3 convertase, C4b2a. The alternative pathway proceeds through spontaneous C3 activation and formation of the C3bBb convertase, with factor D and factor B contributing to amplification. Argx-117 is shown as a monoclonal antibody directed against C2, preventing formation of classical and lectin pathway C3 convertase and limiting production of C3a, C3b, C3 breakdown products, and terminal pathway activation to C5b-9, while leaving the alternative pathway relatively preserved upstream of its own convertase. Downstream consequences of complement activation illustrated include generation of C3 fragments, formation of C5 convertases, release of C5a, assembly of C5b-9, and terminal membrane attack complex-mediated cell injury or lysis; fluid-phase terminal pathway activation gives rise to soluble C5b-9. Regulatory processing of C4b and C3b by factor I and CR1 is also depicted.*

Scientists who work for the manufacture, Argenx, published a phase 1 safety trial which also contains a significant level of molecular detail on how it binds C2 and its calcium dependant nature[109]. While functional assays can show that argx-117 reduces free C2 and suppresses CP/LP activity, these do not explain why binding depends on calcium or how specificity is achieved. The authors undertook a structural strategy to visualise the argx-117–C2 interface directly and link macroscopic pharmacology to a concrete binding mechanism, which in practice required an experimental workaround. Crystallisation attempts with full recombinant C2 initially failed, which is not unusual for large, multi-domain complement proteins that can be flexible and heterogeneous in solution, limiting their ability to form the highly ordered crystal lattices required for X-ray diffraction. To overcome this, they generated an N-terminal fragment of C2 containing the first three complement control protein modules (CCP1–3), reasoning that this region retained the relevant binding surface while removing domains that might impair crystallisation. They then added an anti-κ nanobody chaperone that binds the antibody's κ light chain and effectively stiffens and enlarges the complex, improving packing interactions and making crystal formation more likely. Using this approach, they obtained crystals that diffracted to better than 1.9 Å resolution, enabling high-confidence placement of amino-acid side chains and structured waters, and thus permitting a detailed description of the binding interface.

The resulting structure demonstrated that argx-117 binds predominantly to the CCP2 domain of C2. The Fragment antigen-binding arm makes extensive contact with CCP2 using five of its six Complementarity-Determining Region (CDR) loops, with only minimal interaction with CCP3, indicating a focused epitope rather than a broad multi-domain binding mode. This is mechanistically informative, because it implies that inhibition can selectivity derive from recognition of a specific modular surface on C2, rather than a diffuse interaction that might be more likely to cross-react with related complement proteins, such as Factor B.

The Argenx investigators found that the binding was organised around a centrally positioned Ca^{2+} ion, rather than calcium simply stabilising C2 globally. The Ca^{2+} ion acts as a structural component within the antibody–antigen interface itself, sitting between the heavy and light chains. The authors argue that this Ca^{2+} coordination is relatively

buried and shielded from solvent, which would strengthen the interaction and explains why chelating calcium disrupts binding. In other words, the Ca^{2+} dependence is an integral part of how the antibody achieves tight target engagement. They also interrogate the basis of the antibody's reported pH-dependent binding behaviour, relevant to the broader recycling and sweeping concept. The investigators solved a second structure under low-pH conditions and report that it is practically indistinguishable from the neutral-pH structure. This suggests that pH dependence is not driven by a large, easily visualised conformational rearrangement of either the antibody or the epitope. The authors further note that classic engineered histidine switch explanations, often invoked for pH-dependent recycling antibodies are not clearly supported by the static structural snapshots at the interface, but do not elaborate any further. A reasonable interpretation is that pH dependence may reflect subtler shifts in protonation, electrostatics, and hydrogen-bonds or trafficking-related effects that are difficult to infer from crystallography alone.

The Phase 1 clinical component of the study provides granular human PK data for the complement inhibition. The study evaluated single ascending doses and multiple ascending doses in healthy participants, the single dose cohorts received a single IV infusions up to 80 mg/kg, and multiple dose cohorts received repeated IV doses up to 60 mg/kg. Argx-117 induced a rapid, dose-dependent reduction in circulating free C2 of up to 99% and dose-dependent inhibition of both CP and LP, while sparing AP activity as intended. Notably, reductions in free C2 following multiple doses persisted to the endpoint of observation at 41 weeks, consistent with a reported elimination half-life of 70–88 days. The paper also highlights that a subset of participants developed low-titre treatment-induced anti-drug antibodies without clear impact on PK or safety by inspection of individual curves. Safety reporting in the Phase 1 suggests that single and multiple ascending doses were generally safe and well tolerated. They explicitly contextualise risk by noting that genetic C2 deficiency is relatively common and may go unnoticed. However, C2 deficiency is associated with increased risk of infections by encapsulated bacteria and autoimmunity. Within the trial, no such characteristic severe infections were observed, though infections were numerically more frequent in argx-117 treated participants, largely comprising COVID-19, folliculitis and nasopharyngitis. In

terms of hypersensitivity, no anaphylaxis or severe reactions were reported, but one participant developed a mild urticarial rash on day 4 after first exposure, interpreted as a possible delayed type-I hypersensitivity reaction though not definitive given timing and a history of allergies. The authors also report no induction of ANA or anti-DNA antibodies during follow-up. Collectively providing early human safety data for sustained CP/LP inhibition at the level of C2, but appreciating that rarer infectious and autoimmune risks require larger exposed populations and longer observation.

4.1.2 C2-Inhibition in a Rat Transplant Model

Argenx scientists then went on to extend the translational rationale into transplantation by building a rat analogue informed by argx-117's structural principles and testing C2 blockade in a stringent DGF and IRI kidney transplant model[108]. Because argx-117 has low affinity for rat C2, the investigators used CDR randomisation and bacteriophage display to generate a high-affinity anti-rat C2 antibody, selecting a clone that inhibited both CP (half maximal inhibitory concentration (IC50) 7.45 µg/mL) and LP (IC50 16.10 µg/mL) without interfering with AP activity. The analogue preserved Ca^{2+}-dependent binding like argx-117, but lacked pH-dependent target release once bound at neutral pH, meaning it does not fully reproduce the recycling and sweeping behaviour central to argx-117's prolonged human durability. To mitigate unintended effector stimulation, the antibody Fc region was altered to be human IgG1 LALA (L234A/L235A) to reduce Fcγ receptor and C1q interactions.

In the rat model single-dose PK was dose-proportional (2–50 mg/kg) with an estimated apparent terminal half-life of 12.5 days. Pharmacodynamically, free C2 fell dose-dependently, with ≥95% reductions persisting up to 21 days at 50 mg/kg. The transplant model was intentionally severe with donor kidneys exposed to 32 hours of cold ischemia, recipients underwent contralateral nephrectomy, and antibody was administered IV just prior to reperfusion and again 72 hours later. Under these conditions, isotype-treated animals developed severe renal failure, whereas anti-C2-treated animals maintained deep free-C2 suppression and exhibited significantly improved biochemical outcomes. Specifically, creatinine was 40% lower at day 3 (95% CI 14–59%), with similar reductions in BUN (33% lower at day 3), alongside lower serum

NGAL as supportive evidence of less severe AKI. At day 14, histology suggested improved tubular regeneration and reduced inflammation in treated animals compared with controls. This provides preclinical evidence that CP/LP blockade at C2 can attenuate functional injury and modify repair dynamics following profound cold ischemia and reperfusion, supporting biological plausibility for C2 inhibition as a potential DGF preventive strategy.

However, the translational interpretation of this rat transplant model requires acknowledgement of species differences in complement biology, these influence both the mechanisms of injury and the apparent efficacy of complement inhibitors. A central limitation concerns tissue-level complement regulation. In humans, CD46 (membrane cofactor protein; MCP) is widely expressed on nucleated cells and acts as a cofactor for factor I–mediated cleavage of C3b and C4b, providing broad protection against autologous complement attack. In rodents, by contrast, CD46 expression is very limited meaning it does not play the same ubiquitous systemic tissue protective role as in humans[158]. Instead, rodents rely heavily on the rodent specific complement regulator Crry, which combines functional properties analogous to human DAF/CD55 and CD46 and is prominent in protecting host tissues, including renal tubules. Notably, renal IRI in rodents is associated with altered tubular localisation of Crry that can precede and increase susceptibility to complement activation[159], a feature that may shape both injury pathways and responsiveness to upstream inhibition. Therefore, complement-mediated tissue vulnerability and the balance between opsonisation, inflammation, and lytic injury can differ substantially between rat and human kidneys, potentially exaggerating or altering the apparent protective effect of complement blockade in rodent models relative to human transplantation.

A second limitation relates to complement receptor genetics and immune handling, which differ between rodents and humans and can influence inflammatory responses and immune complexes downstream of complement activation. For example, rodents encode CR1/CR2 isoforms from a single Cr2 gene via alternative splicing, whereas humans require distinct CR1 and CR2 genes, contributing to meaningful differences in receptor structure, expression patterns, signalling function[160]. This matters mechanistically because these complement receptors are the interface that converts

complement deposition such as C3b, iC3b and C3d into immune-complex clearance, phagocyte activation, and B-cell signalling[161]. Because CR1/CR2 genetics and expression differ between rodents and humans, the downstream handling of complement-opsonised debris and immune complexes and the cellular signalling triggered by C3 fragments may not scale directly across species. As a result, upstream complement inhibition can modify not only acute effector injury, C3a, C5a and C5b-9, but also immune-complex trafficking and adaptive immune priming in ways that are model and species dependent.

A third limitation is that the relative dominance of complement pathways in renal IRI is model and species dependent, with rodent studies often identifying strong roles for the alternative pathway in some IRI contexts[162], whereas human and non-human primate data and clinical signals with CP/LP-targeted interventions support a role for CP/LP in transplant IRI[83,163]. Consequently, benefit in a rat cold-ischemia model supports plausibility for CP/LP contribution but does not prove CP/LP predominance in heterogeneous human DGF, where donor injury phenotypes, recipient immune status, perioperative inflammation, and medications interact.

Finally, there is a drug specific translational limitation, the anti-rat C2 antibody was designed to reproduce argx-117's target and pathway selectivity but does not replicate argx-117's pH-dependent target release once bound, and therefore cannot be assumed to mirror the recycling kinetics and exposure response relationships that underpin argx-117's long human half-life and sustained PD effect. The rat study is therefore best interpreted as mechanistic support for C2 blockade in IRI and DGF, rather than a quantitative predictor of human dosing requirements or effect size.

4.1.3 Current Phase II Trial Design for DGF in Renal Transplantation

This preliminary work led to the design and commencement of a human phase 2 trial funded by the manufacturer. A multicentre, randomised, double-blind, placebo-controlled trial evaluating whether argx-117 improves early allograft function in deceased-donor kidney transplant recipients at risk of DGF[164].

The study is designed as a proof-of-concept efficacy and safety study in a setting of renal IRI and subsequent development of DGF. The therapeutic hypothesis is that

transient, peri-transplant suppression of CP and LP from C2 inhibition will reduce early IRI driven injury and accelerate recovery of GFR, while leaving the alternative pathway relatively intact.

The inclusion criteria are for dialysis dependant prospective adult kidney recipients, receiving a first or second single kidney transplant from a deceased donor (DBD or DCD), with ABO compatibility and a negative crossmatch. Because complement inhibition increasing susceptibility to certain encapsulated organisms, the protocol incorporates vaccination requirements for meningococcal, pneumococcal, and H. influenzae.

Participants are to be randomised 1:1 to receive two IV doses of argx-117 or placebo, one dose during transplantation and a second dose 1 week later, on top of standardised background induction and maintenance immunosuppression.

The primary endpoint is eGFR at 24 weeks post-transplant. The key secondary outcomes are proportion with DGF, functional DGF (fDGF), duration of dialysis in the first 30 days, dialysis dependence at day 31, creatinine reduction ratio at 72 hours and day 8, primary non-function (PNF), eGFR at 52 weeks, (death-censored) allograft survival, and dialysis-free survival. Also assessed alongside will be pharmacology and safety data: serum drug concentrations (PK), changes in free C2, total C2 and CH50, and anti-drug antibodies. The required recruitment is 102 participants, with a 1-year follow-up, followed by an additional safety follow-up to 18 months, and an optional longer-term observational component.

4.1.4 Modelling with Human Kidneys Ex-Vivo

While the rat transplant model was very effective, the inherent species differences make adding a human kidney model a useful next step. As perfusion platforms have become more stable their uses have diversified: the precedent of using a perfusion phase in this way with whole-blood or a whole-blood like perfusate has been established previously.

Even in porcine organs, where experimental transplantation can be performed and is still the gold standard for porcine organ studies and the outcomes are much more

powerful, but there are some benefits to an ex vivo model. Using a whole blood perfusion model is reliable, with experimental conditions being controlled, compared with the recovery and follow-up of a pig following transplant. With an organ on an isolated circuit a greater degree of scrutiny can occur on the organ, due to ease of increased sampling of both perfusate and tissue. There is also the consideration of animal welfare and the 3Rs, in which for some biological questions an ex vivo model may be of equal use. For declined human organ a reperfusion model is the only option, and we must be cognisant of its limitations. This sort of model is only suitable for the early post reperfusion phase given that stable physiological ex vivo kidney perfusion is currently limited to 24-48hours reliably. The organ is in isolation and is without the interplay of the whole organism on its physiology and is in a circuit made of non-biological surfaces which may have important effects depending on what aspect of the early transplant period is trying to be modelled. For early IRI and complement biology the model holds promise, having been used successfully to model ABOi & HLA AMR[42]. In this model, the authors adapted a standard NMP circuit specifically to allow early complement activation to occur in a transplant-like setting by restoring key plasma proteins. The circuit was primed with packed red cells and clinically unutilised FFP was added as the source of complement and coagulation factors. Of note, the investigators were able to lower the heparin dose down to 400 units without having the circuit thrombose, which was desirable in order to investigate the thrombo-inflammatory endpoints of ABOi/HLA AMR.

Using this plasma perfusate, they induced a reproducible early rejection-like phenotype by adding antibody triggers after a stabilisation phase. In the HLA-incompatible model, addition of the complement-fixing anti–HLA class I monoclonal antibody (W6/32) in the presence of low-titre FFP caused rapid haemodynamic collapse and was accompanied by multifocal linear glomerular capillary C4d deposition, with microvascular and macroscopic thrombosis observed in some experiments, consistent with early classical-pathway activation downstream of antibody–endothelial interaction. In the ABO-incompatible model, high-titre anti-A/anti-B FFP produced a marked fall in flow and peritubular microthrombi, demonstrating that a plasma-containing perfusate can also reproduce early thrombotic injury patterns in blood-group antibody settings, even

where C4d was not detected, which demonstrates that the complement activity in this setting depending on the stimulus, such as the monoclonal antibody type. This provides a good basis that a similar model could be utilised to look at complement activation and inhibition.

4.2 Aims & Objectives

This chapter aimed to establish and optimise a human ex vivo kidney perfusion model of NMP followed by plasma-based NR, designed to reproduce the complement activation associated with early transplant reperfusion injury. Having established the model, the principal aim was to test the effect of the investigational anti-C2 monoclonal antibody argx-117 within this setting. Specifically, the study sought to determine whether C2 inhibition produced effective blockade of the classical and lectin pathways, whether this translated into reduced downstream complement activation, and whether any such inhibition was associated with improvement in perfusion characteristics, reduction in injury biomarkers, and attenuation of tissue complement deposition.

Objectives:

- To optimise and validate a stable ex vivo model of NMP followed by plasma NR.
- To characterise background complement activation generated by the circuit using blood-only perfusions.
- To confirm rapid and sustained C2 depletion by argx-117 within the perfusion system.
- To explore dose-related pharmacodynamic effects of argx-117 in single-kidney perfusions.
- To define the pattern of complement activation during NMP and during subsequent plasma reperfusion.
- To assess the effect of argx-117 on classical and lectin pathway functional activity.
- To determine whether C2 blockade reduced downstream complement activation products and terminal pathway formation.
- To examine whether argx-117 improved physiological and biochemical measures of kidney perfusion and function.
- To assess the effect of treatment on perfusate injury biomarkers.

- To evaluate tissue complement deposition and related injury signals across perfusion phases.
- To test, in a paired human kidney design, whether C2 inhibition modified complement-mediated injury in this ex vivo reperfusion model.

4.3 Methods

For these experiments the investigational predecessor of empasiprubart was used, argx-117, which is functionally the same drug, but is not manufactured to clinical grade specificity and as such will be referred to as argx-117 throughout.

4.3.1 Model Development

Two pilot perfusions were performed for model development, firstly to assess the layout of the circuit and the method of simultaneously flushing the kidney and the circuit, followed by repriming and reperfusion of the kidney in a timely manner, akin to the out-of-ice time between cold storage and recipient reperfusion. The final circuit design was that as described in the common methods. The first pilot perfusion was performed with 2.5mg fondaparinux used as anti-coagulant in both phases which resulted in thrombosis after 30 minutes of reperfusion. This was changed to 5000 units of unfractionated heparin during NMP and 10000 units during plasma reperfusion, which resulted in a stable 12-hour perfusion, and was taken forward for the model.

4.3.2 Blood Only Perfusions

Four blood only perfusions experiments were performed in a paired design with pooled pRBCs and a shared unit of FFP divided between each circuit with no kidney on board. Three experiments consisted of complete 12-hour perfusion with 6 hours of NMP and 6 hours of NR. The fourth experiment was a minute-by-minute assessment of early NR to assess the rate of clearance of C2 from the circuit.

For the 12-hour perfusions the circuit was identical with a closed loop design and a ¼ inch connector between arterial inflow and venous outflow. O negative blood was used for both NMP and NR, and A positive plasma was used for the NR. Samples were taken as per the schedule for the kidney perfusion. For the C2 clearance kinetics experiment, the first 30 minutes of NR were performed with O negative blood and A positive plasma with samples taken every minute.

4.3.3 Single Kidney Perfusions

With the circuit and perfusate optimised such that stable NMP and NR reperfusion could be performed 4 single kidney perfusions were undertaken as an exploratory start for an early assessment of complement activation in the context of the model and for argx-117 dosing effects. Two kidneys were perfused with an isotype control of argx-117, then perfusions with a high and low dose of argx-117. The low dose perfusion was done based on kidney weight as per the phase 1 healthy volunteer trial at 80mg/kg and then one at a higher dose based on the volume of plasma in the circuit with 1200µg/ml of plasma, 144mg of argx-117 in the circuit, a near 10-fold increase. The perfusions were performed on the XVIVO Kidney Assist device with the optimised circuit as per the description in the common methods.

4.3.4 Paired Perfusions

6 pairs of human kidneys accepted through the NHS Blood and Transplant (NHSBT) research organ offering scheme were accepted and transported to the lab in the NHSBT building at the John Radcliffe Hospital in Oxford. The left and right kidneys were randomised in each pair using a predetermined sequence, which was generated using random number sequencer (random.org) and detailed which kidney from the pair received argx-117. Perfusions were done using the circuit optimised on the XVIVO kidney assist and conducted as detailed in the common methods.

Perfusate samples were taken as per common methods, into both SST and EDTA tubes, centrifuged and the immediately placed in liquid nitrogen. 5mm punch biopsies were halved and one half was placed in formalin, and the other half was immediately frozen in liquid nitrogen and then stored at -80.

4.3.5 Sample Analysis & Data Handling

Perfusate analysis was again done as per common methods, as per manufacture instructions for commercial kits and antibodies, or as per optimised in-house protocols for those analyses not commercially available.

All data processing, statistical analyses, and figure generation for this chapter were performed in R using RStudio. Raw data exports from the perfusion platform, blood gas and biochemical analyser outputs, and assay readouts were imported as CSV files. Data was cleaned with variables standardised for naming, units were retained as reported by the originating assay platform, and each observation was mapped to a unique perfusion identifier with treatment allocation (control vs argx-117) and, where applicable, a shared pair identifier to preserve the matched design of paired kidney experiments.

For paired analyses, inclusion required non-missing values in both the control and argx-117 at that timepoint. Given the modest sample sizes and the non-normal distributions of perfusate biomarkers, results are presented primarily as medians with interquartile ranges (IQR), and where paired contrasts were central to interpretation, paired differences (argx-117 minus control) were additionally summarised using median (IQR). In single kidney perfusions values were reported explicitly or as medians with individual values in brackets, as these experiments are purely descriptive.

For biomarkers with repeated sampling over each phase, phase-specific area under the curve (AUC) was calculated separately for NMP and NR using the trapezoidal rule across observed timepoints, providing an integrated summary of the biomarker over time. AUC was calculated only when at least two observations were available within the phase. Where C2 pharmacodynamics were reported as blockade, free C2 concentrations were used to derive the degree of depletion relative to the contemporaneous control reference, expressed as percent reduction, and summarised across timepoints and by dose where relevant.

Inferential comparisons were performed using non-parametric tests. For paired, two-sided Wilcoxon signed-rank tests. Within-kidney longitudinal comparisons across timepoints also used paired Wilcoxon signed-rank tests. All p values were interpreted with a nominal significance threshold of $p<0.05$.

All figures were generated directly in R from the analysis-ready dataset to ensure reproducibility. Time-course figures were produced to visualise trajectories across NMP and NR. Distributions at prespecified timepoints were displayed using summary plots

and boxplots with individual kidney values overlaid, and paired designs were visualised by connecting matched control and argx-117 observations within each pair where appropriate. Reported p values shown on figures correspond to the statistical tests described above.

4.4 Results

4.4.1 Model Development Perfusions

Two pilot perfusions were performed early during NR for the first perfusion the kidney flow began to reduce and eventually dropped to 0 mL/min at 32 minutes. The kidney had thrombosed during plasma reperfusion due to insufficient anticoagulation in the presence of plasma based perfusate, along with slower flows in an injured declined kidney. The clotting profile was assessed from the samples taken early in NR, within 15 minutes we see a sharp rise in d-dimers, with rapid consumption of fibrinogen, vWF and AT, with prolonging of PT and APTT in keeping with widespread thrombus formation (Fig 4.2). The clotting profile was tested in units of plasma thawed and then refrigerated at different intervals from testing which demonstrated retention of normal clotting profiles and proteins up to 10 days after thawing.



B

Clotting Profiles

Time/ Samples	PT (secs)	APTT (secs)	FIB (g/L)	DD (ug/L)	vWF (U/dL)	AT (U/dL)
NR Baseline	12.3	32.3	2.3	<190	146	81
15 mins	>170	>180	<0.3	5132	9	15
30 mins	>170	32.3	<0.3	508	26	<1.0
Thawed Day 1	11.6	31.9	2.5	<190	135	88
Thawed Day 2	12.4	26.6	1.8	<190	76	95
Thawed day 5	11.4	26.4	2.5	<190	89	95
Thawed Day 7	13.5	44.8	2	<190	152	84
Thawed Day 10	14	32.6	2	<190	182	77
Normal Range	9.5-12.0	20-30	1.5-4.0	<500	50-200	>80

Figure 4.2 ***Macroscopic clot formation and coagulation profile in NMP pilot perfusions. (A)*** *Representative photograph demonstrating extensive clot burden within the main renal artery after a thrombosis during NMP.* ***(B)*** *Serial coagulation parameters measured in normothermic reperfusion perfusate during the thrombosis event and compared with thawed fresh frozen plasma controls after different durations of sotrage. At NR baseline, coagulation indices were near expected ranges, but by 15 minutes there was profound coagulopathy with marked prolongation of PT and APTT, severe fibrinogen consumption, a striking rise in D-dimer, and substantial depletion of vWF and antithrombin. By 30 minutes, PT remained markedly prolonged, fibrinogen remained severely reduced, D-dimer remained elevated, and antithrombin was almost completely depleted, despite partial normalisation of APTT. In contrast, thawed plasma assessed over storage days 1, 2, 5, 7, and 10 showed relative stability of coagulation parameters within or near expected ranges, indicating that the abnormalities observed during reperfusion were not attributable to plasma thawing alone.*

For the second perfusion the use of 10000 units of heparin as anticoagulant was effective, and a stable NR was achieved. This along with further circuit refinements could be taken forward into the experimental series as per the circuit description in the common method.

4.4.2 Blood Only Perfusions

Four blood-only perfusion experiments were performed, and selected complement markers were measured to determine the impact on levels of complement resulting directly from the circuit (Fig 4.3). Firstly, considering C2, the target protein of argx-117, in the control, C2 remained low during NMP (Basline 0.196 µg/mL, 6 hours 0.156 µg/mL), but during NR was elevated to 4.849 µg/mL from the start and remained at a similar level till hour 12, 4.854 µg/mL. In the paired argx-117 perfusion, C2 was again low during NMP, 0.568 µg/mL at baseline and 0.691 µg/mL at the end of NMP. At the start of NR there was an attenuated rise to 1.833 µg/mL, but then rapidly fell to near-zero levels (0.052 µg/mL) by the 15 minutes and remained low thereafter (hour 7: 0.112 µg/mL, hour 10: 0.272 µg/mL, hour 12: 0.317 µg/mL), demonstrating argx-117 rapidly binding all available C2. Consistent with this, the dedicated clearance experiment (panel B) demonstrated very rapid C2 removal: C2 fell from 3.828 µg/mL at 0 min to 0.470 µg/mL at 0.5 min and 0.023 µg/mL at 1 min, plateauing at ~0.020 µg/mL , ending at 0.314 µg/mL by 20 min, again demonstrating the efficacy of the monoclonal in the context of this model. Normal circulating serum levels of C2 range from 5-30 µg/mL.

Downstream activation markers follow an activation curve pattern in the NR phase, but all of which are significantly attenuated when compared to the NR phase with the kidney in the circuit and with normal circulating serum levels. For soluble C5b-9, concentrations were low and stable during NMP (Control median 25.8 (15.7–36.0) ng/mL; argx-117 22.9 (13.4–32.4) ng/mL), after NR starts, there is progressive rise to hour 12, controls 176.6 (159.4–193.7) ng/mL and lower in argx-117 137.9 (120.7–155.2) ng/mL. Normal serum levels of sC5b-9 are 50-250ng/mL, and with this antibody with a kidney in circuit end NR levels can climb to 20000 ng/mL. In the third perfusion, C5b-9 quantified by the TM assay with alternative antibody (panel D), again during NMP levels start low (baseline: Control 0.020 vs argx-117 0.025 CAU/mL) with no rise over the 6 hours. During NR there is the same shape of activation to hour 12 (Control 0.320 vs

argx-117 0.370 CAU/mL). Using this antibody with the kidney in circuit in the same assay levels can reach as high as 40 CAU/mL.

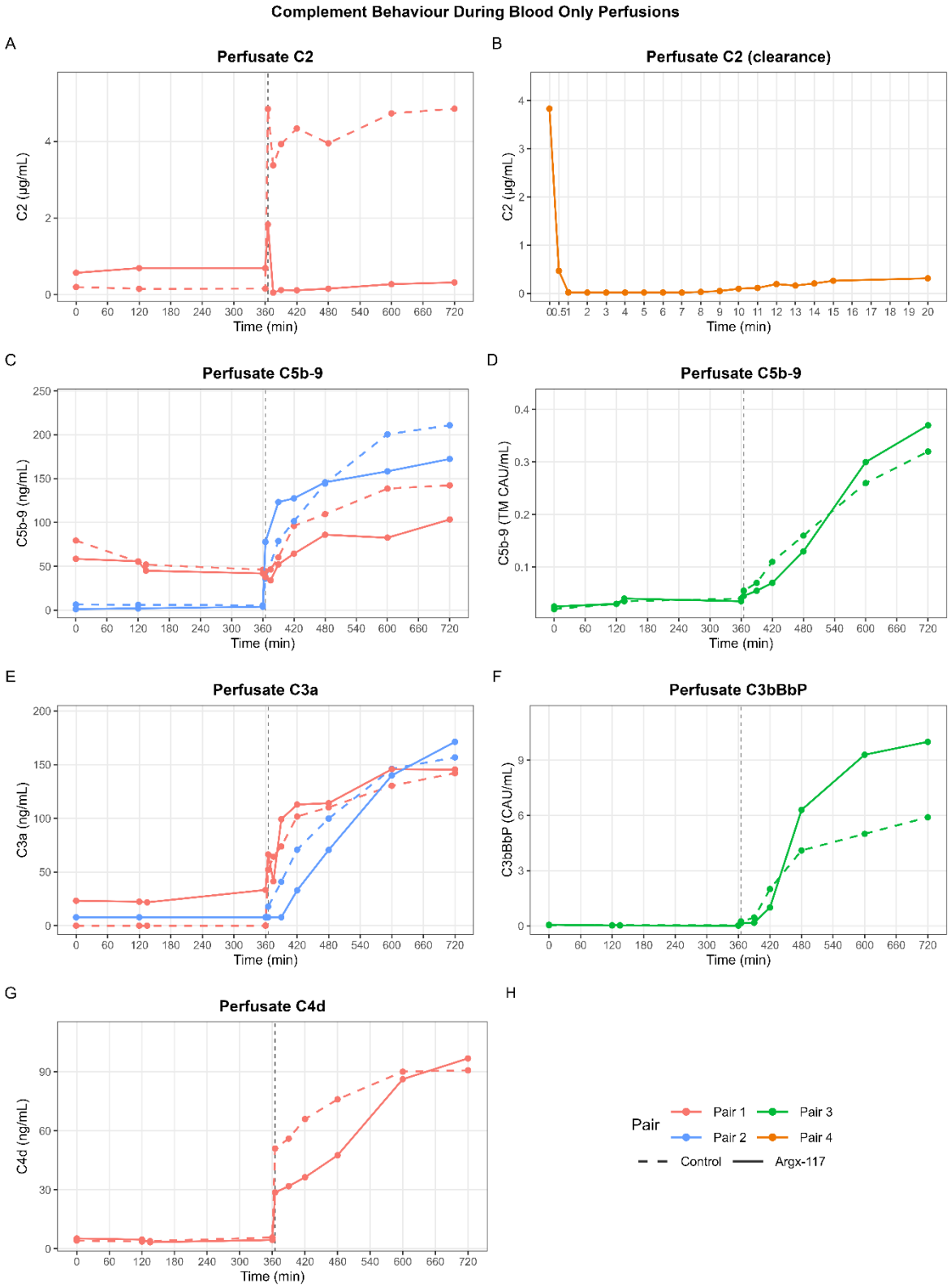


Figure 4.3 ***Complement behaviour during blood-only perfusions.*** *Serial perfusate measurements are shown from paired blood-only perfusions performed in the absence of a kidney to determine the extent of complement activation*

*generated by the circuit itself. Panels show concentrations or assay readouts for **(A, B)** C2, **(C, D)** C5b-9, **(E)** C3a, **(F)** C3bBbP, and **(G)** C4d. Each colour represents an experimental pair, with dashed lines indicating control circuits and solid lines indicating Argx-117-treated circuits. The vertical dashed line marks the change from NMP to NR. Across blood-only circuits, measurable complement activation occurred over time, confirming that the extracorporeal circuit alone is capable of triggering complement. However, the magnitude of activation was modest compared with kidney perfusions, with terminal and upstream activation products generally rising to levels approximately one order of magnitude lower than those observed when a kidney was present on the circuit. Argx-117-treated circuits showed attenuation of classical/lectin pathway-associated activation in keeping with C2 blockade, while residual complement activity remained detectable, consistent with persistent circuit-related and alternative pathway-associated activation.*

Considering other fragments, C3a (panel E) similarly was negligible and static in NMP, but had a characteristic rise from the start of NR, reaching similar concentrations in both groups, control 149.5 (145.8–153.1) ng/mL and in argx-117 158.4 (152.0–164.9) ng/mL by the end of NR. Specific alternative pathway convertase signal was assessed with an antibody to C3bBbP (panel F), during NMP, again a consistently negligible amount. During NR there was an activation curve, for the control 0.029 to 5.900 CAU/mL and to a higher level in argx-117 0.010 to 10.000 CAU/mL. With a kidney in the circuit levels reach up to 400 CAU/mL.

Finally, C4d (panel G) remained low during NMP, Control 4.13–5.73 ng/mL and argx-117 3.32–5.21 ng/mL. During NR, again an activation curve starting from control 50.97 ng/mL and argx-117 28.64 ng/mL in the baseline plasma, and by the end of NR reaching 90.73 ng/mL in the control and 96.77 ng/mL in argx-117. Normal circulating levels of C4d are 30-150ng/mL, and in this model with the kidney in circuit over 400 ng/mL by the end of NR.

Overall, the blood only circuit provides a physiological activation curve, but to a significantly attenuated level when compared to having the kidney in the circuit and when compared to normal circulating levels.

4.4.3 Single Kidney Perfusions

Four isolated single kidneys were perfused for initial testing of dose response and complement behaviour in the novel model. A selection of kidneys deemed unsuitable for transplant were acquired from donors aged 53 to 76, 3 DCD and 1 DBD, perfused with longer CITs from 20hrs 37 minutes to 29hrs 8 minutes (Table 4.1)

Characteristic	Kidney 1	Kidney 2	Kidney 3	Kidney 4
ARGX-117 dose	80 mg/kg	n/a	1200 mg	n/a
Donor type	DCD	DBD	DCD	DCD
Cause of death	ICH	ICH	ACLF	OOHCA
Downtime (mins)	0	0	0	47
Age (years)	76	66	53	57
Sex	M	F	F	M
Reason for decline	Donor age	Anatomy	Anatomy	AKI
CIT (hrs:mins)	22:15	20:37	24:35	29:08
WIT (flush NMP-NR, mins)	16	14	15	16
BMI (kg/m²)	26	21	25	33
Blood type	A+	O+	A+	A+
Creatinine (µmol/L)	80	43	125	440
T2DM	N	N	N	N
HTN	N	N	Y	N
Smoker	N	Y	Y	N
Kidney weight (g)	161	168	187	225

Table 4.1 ***Donor and graft characteristics for kidneys included in the argx-117 single kidney perfusion.*** *The table summarises treatment allocation, donor demographics, donor type, cause of death, reasons for organ decline, ischaemic times, relevant clinical characteristics, and graft weight for the four kidneys studied. One kidney received argx-117 at 80 mg/kg (total dose 20 mg), while the remaining kidneys were untreated comparators. Variables shown include donor age, sex, donor type, blood group, body mass index (BMI), admission creatinine, comorbidity and risk factor history, cold ischaemia time (CIT), interval warm ischaemia time between NMP and normothermic reperfusion (NR), and kidney weight.*

4.4.3.1 Flow and Blood Gas Parameters

Given the small number of perfusions values are expressed explicitly or as the median with the two specific values in brackets (Fig 4.4).

Weight adjusted renal artery flow was acceptable in all kidneys and similar during NMP in both control and argx-117, stable from hour 2 to end of NMP, flows between 166 and 249 mL/min/100 g. After NR flows recovered well in 3 of the 4 kidneys, with both controls with good flows till the end of NR, 265 (257 & 273). The two argx-117 kidneys performed differently with one behaving similar to controls ending at 221 and the other falling gradually to around 120, which is still adequate flow, but notably lower than the others.

Lactate was high in all perfusions at baseline, as a result of variable quality unwashed blood, with varying trajectory over the course of NMP, baseline was a median of 14.3 (7.6 & 21) mmol/L in controls and 13.7 (10.4 & 17) mmol/L with argx-117. At the end of NMP lactate had climbed in control 19.3 (12.6 & 26) but had fallen slightly in argx-117

11.0 (9.8 & 12.2). Over NR, both groups experience rises in lactate, control from 11.9 (6.8 & 17) up to 23 (15 & 31) and to a lesser extent argx-117 from 11.9 (11.4–12.8) to 12.9 (8.8 & 17).

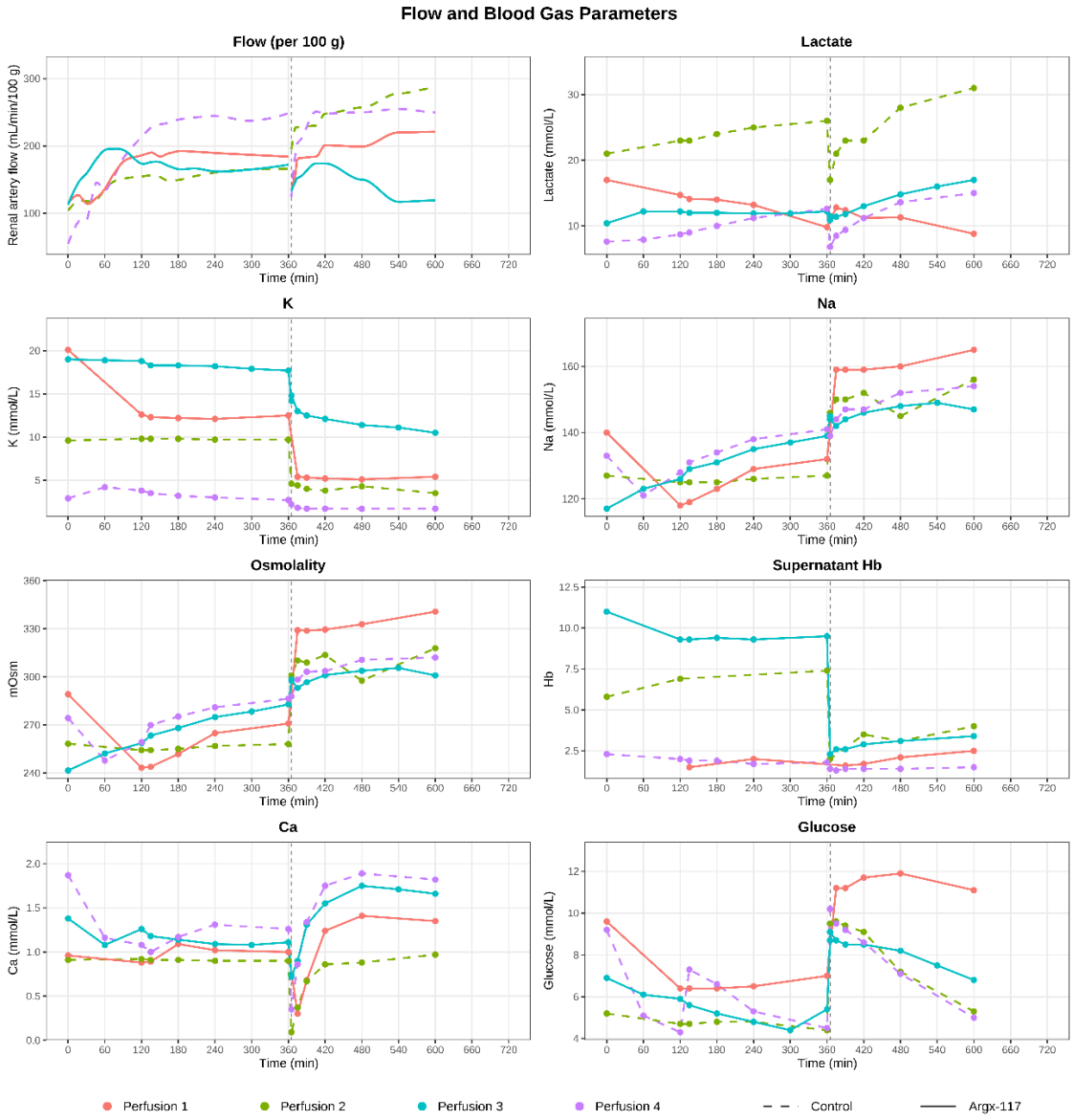


Figure 4.4 ***Physiological and blood gas parameters during isolated kidney perfusions performed for Argx-117 dose refinement****. Serial measurements are shown for renal artery flow (normalised to 100 g kidney weight), lactate, potassium, sodium, osmolality, supernatant haemoglobin, ionised calcium, and glucose across four perfusions. Each colour represents an individual perfusion, with dashed lines denoting control perfusions and solid lines Argx-117 treated perfusions. The vertical dashed line indicates the transition point between NMP and NR. Across the perfusions, renal blood flow was adequate throughout the perfusions, although inter-perfusion variability was evident. Biochemical changes reflected the altered perfusate composition and ongoing metabolic activity, with abrupt shifts when transitioning to NR in potassium, sodium, osmolality, calcium, supernatant haemoglobin, and glucose. Lactate remained elevated throughout and generally increased over time, particularly in one control perfusion, consistent with variable metabolic stress and clearance capacity between kidneys. Supernatant haemoglobin decreased sharply at the transition point and then remained relatively low, while calcium also showed an acute dip followed by recovery. Glucose rose transiently after transition in some perfusions before falling with consumption.*

Potassium was generally stable through the phases continuing at the level determined early in the perfusion phases, with the level during NMP being determined by completeness of UW flush out and the quality of the blood, and for NR the quality of the blood. Both argx-117 kidneys had high levels through NMP ending at 15.1 (12.5 & 17.1) mmol/L. For NMP controls were closer to physiology ending at 6.2 (2.7 & 9.7). During NR overall levels were lower in controls ending at 2.6 (1.7 & 3.5) and argx-117 7.95 (5.4 & 10.5).

Sodium was also stable, with a slight gradual climb throughout both phases. In NMP from a baseline in controls of 130 (127 & 133) vs argx-117 with 128.5 (117 & 140) to 134 (127 & 141) in controls vs 135.5 (132 & 139). For NR, 149.5 (147 & 152) in controls vs 152.5 (146 & 159), ending at 155 (154 & 156) in controls and 156 (147 & 165) in argx-117. Calcium and glucose were maintained at physiological levels, calcium 1-1.4mmol/L and 4.5-9 mmol/L. Calcium of particular importance to facilitate both complement activation and argx-117 binding.

Osmolality was maintained at close to physiological values during NMP, controls 266.3 (258.3 & 274.3) to 272.25 (258.1 & 286.4) and in argx-117 265.4 (241.6 & 289.2) to 276.85 (270.9 & 282.8). During NR osmolality was slightly raised, controls going from 308.65 (303.6 & 313.7) to 315.0 (312.1 & 317.9) and argx-117 from 315.3 (301.1 & 329.5) to 320.8 (300.9 & 340.7).

Free haemoglobin (Hb) was raised at baseline, most likely due to blood quality, and increased over the course of perfusion. During NMP controls increased from 4.0 (2.3 & 5.8) g/L to 4.6 (1.8 & 7.4) and in argx-117 went from 5.4 (1.5 & 9.4) to 5.6 (2 & 9.5). During NR levels started lower, and again rise, in controls from 1.7 (1.4 & 2.0) to 2.8 (1.5–4.0), and in argx-117 from 2.1 (1.6 & 2.6) to 2.9 (2.5 & 3.4).

4.4.3.2 Perfusate Injury Biomarkers

At the end of NMP and NR NGAL was similar in both groups, with the argx-117 group being slightly higher in both cases. In controls, at the end of NMP, it was 29.6 (23.7 & 35.5) ng/mL and 36.4 (26.7 & 46.0) in argx-117, and at the end of NR, 26.6 (20.3 & 32.9) in controls and 32.4 (29.0 & 35.9) in argx-117. For IL-18, it was slightly higher in controls at the end of NMP with 1399.9 (867.5 & 1932.2) pg/mL compared with argx-117 at

1174.4 (857.9 & 1491.0), but more similar by the end of NR, 1214.4 (657.2 & 1771.7) in controls and 1482.1 (1225.4 & 1738.8) in argx-117 (Fig 4.5).

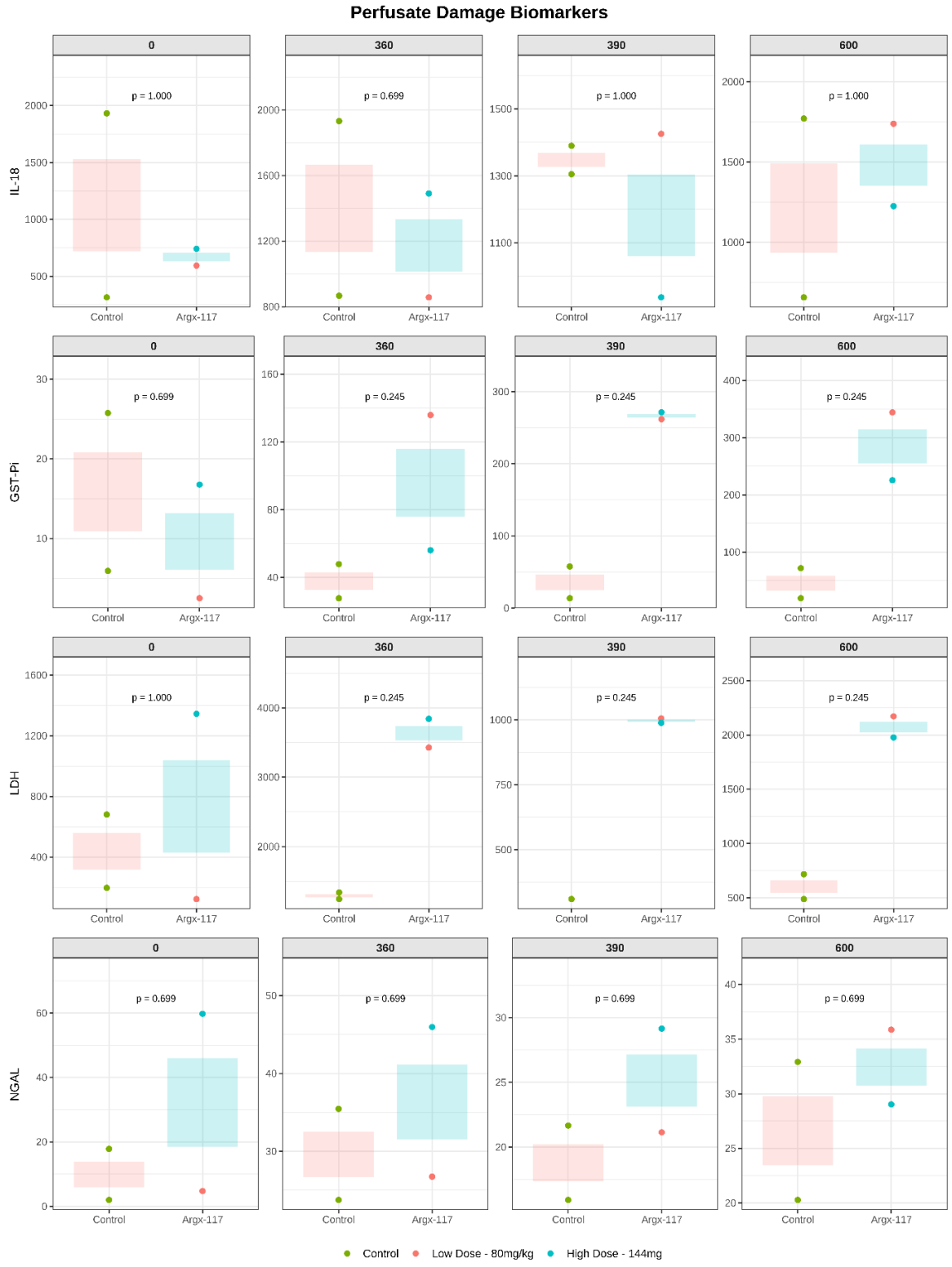


Figure 4.5 ***Perfusate injury biomarker concentrations during isolated kidney perfusions performed for Argx-117 dose refinement.*** *Boxplots compare control and Argx-117-treated perfusions at baseline (0 min), end-NMP (360 min), early reperfusion (390 min), and late reperfusion (600 min). Biomarkers shown are IL-18, GST-Pi, LDH, and NGAL.*

Overlaid points represent individual perfusions, including the low-dose (80 mg/kg) and high-dose (144 mg/kg) Argx-117 cases. Across timepoints, no statistically significant differences were detected between control and Argx-117-treated perfusions for IL-18, GST-Pi, LDH, or NGAL, reflecting the small number of dose-refinement experiments. Nonetheless, descriptively, IL-18 was broadly similar between groups throughout. GST-Pi and LDH were higher in Argx-117-treated perfusions during and after reperfusion, particularly at 390 and 600 minutes, while NGAL also tended to be numerically higher in treated perfusions across most sampled timepoints.

GST-Pi levels were lower at the end of NMP and NR in the controls. At the end of NMP, in controls levels were 37.8 (27.8 & 47.9) ng/mL compared with 96.0 (56.1 & 135.9) in argx-117. At the end of NR, GST-Pi remained lower, in controls 45.4 (19.2 & 71.7), but much higher in argx-117 at 284.9 (225.6 & 344.3). LDH was similar and was lower in controls at the end of both NMP and NR. At the end of NMP, controls were 1290.7 (1242.6 & 1338.8) U/L and 3634.5 (3427.1 & 3841.8) in argx-117. By the end of NR levels were 601.95 (487.4 & 716.5) in controls compared to 2074.2 (1976.9 & 2171.4) in argx-117.

This preliminary look at biomarkers in these early perfusions was intended to find any early signal, either from treatment or dose. Across the perfusion, injury biomarkers rose over time in both groups, but the largest late elevations were seen in the argx-117 perfusions, particularly for GST-Pi, LDH and IL-18, with overall levels being higher compared to controls. This could be reflective of greater injury in those treated kidneys but given the heterogeneity of the perfusions and kidneys it is hard to interpret, and overall, there was no clear pattern.

4.4.3.3 C2 Blockade and C5b-9 Formation

Free C2 levels demonstrate good antibody binding and clearance with sustained elimination, as well as a dose dependant effect. During NMP, introduction of argx-117 clears C2 rapidly to undetectable levels for the duration of NMP (median 0.00001 µg/mL, for hours 2 to 6), which contrasts with the control perfusions having measurable levels throughout NMP (0.579 µg/mL (0.477 & 0.681) by hour 6). During NR as expected C2 levels are much higher, for the controls C2 increased sharply, 5.670 µg/mL (4.758 & 6.582) from the start of NR. and remained elevated, with a gradual decline in keeping with consumption from the cascade, by the end of NR to 3.762 µg/mL (3.497 & 4.026). For argx-117 the immediate C2 rise is attenuated as a result of rapid and significant antibody binding and remains low throughout NR ending at 0.748 µg/mL for the lower dose of argx-117, and 0.296 µg/mL for the higher dose. Consistent with this, the calculated C2 blockade is 100% for both doses during NMP and remained for NR but

was dose dependent. With the lower dose blockade was 82.9–85.6% across the duration of NR, compared with the increases dose yielding 94.1–96.6% blockade throughout NR (Fig 4.6).

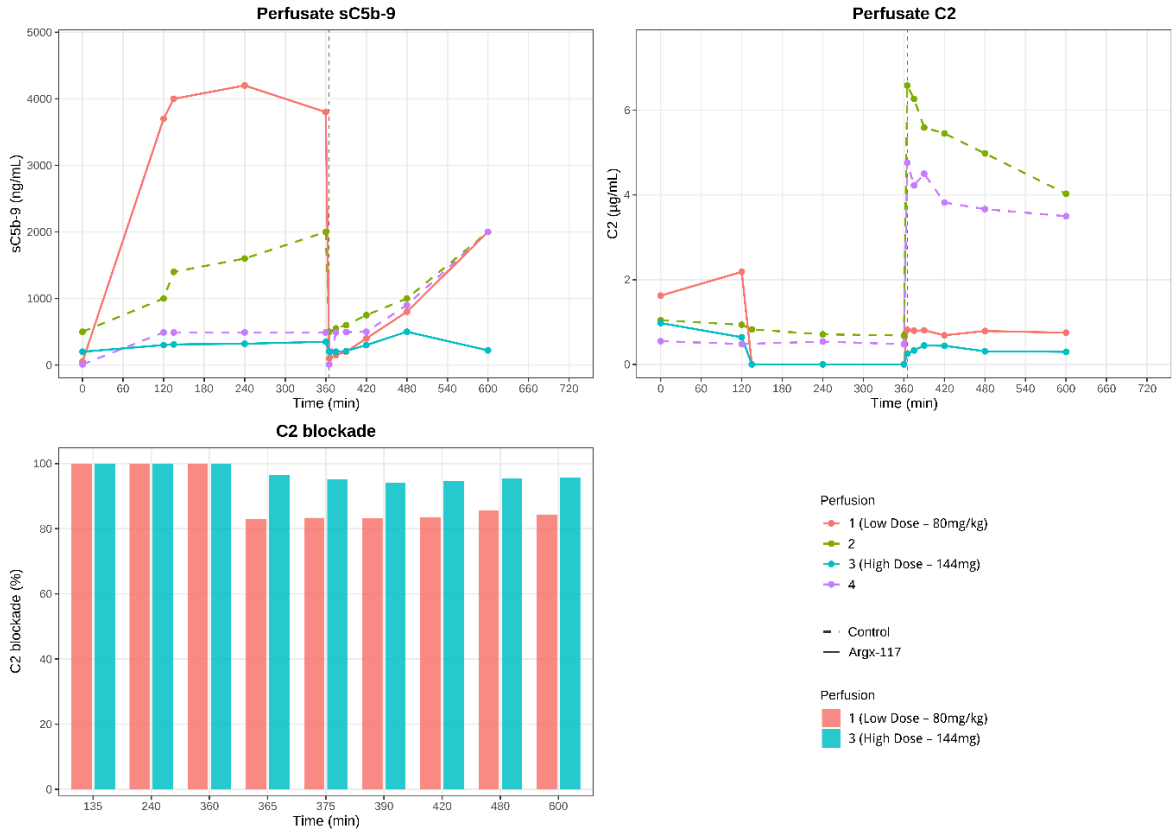


Figure 4.6 ***Perfusate C2 and sC5b-9 profiles during isolated kidney perfusions performed for Argx-117 dose refinement.*** *Serial perfusate concentrations of soluble C5b-9 and C2 are shown across the four perfusions, together with estimated percentage C2 blockade in the two Argx-117-treated cases. Each line represents an individual perfusion; dashed lines denote control perfusions and solid lines Argx-117-treated perfusions. The vertical dashed line indicates the transition point between NMP and NR. The lower panel shows calculated C2 blockade over time for the low-dose (80 mg/kg) and high-dose (144 mg/kg) Argx-117 perfusions. Control perfusions demonstrated higher circulating C2 concentrations and greater terminal pathway activation overall, with sC5b-9 rising substantially over time, particularly in one control case. In contrast, Argx-117-treated perfusions showed marked suppression of measurable free C2, consistent with effective target engagement. Following transition to reperfusion, sC5b-9 increased in all perfusions, but remained lower in the high-dose treated case than in the low-dose treated case and in the highest-activating control circuit. Estimated C2 blockade was sustained throughout the treated experiments and was consistently greater with the 144 mg/kg dose than with the 80 mg/kg dose, supporting a dose-response relationship in target inhibition. Demonstrating effective pharmacodynamic C2 engagement by Argx-117 during NMP and NR, with higher-dose treatment achieving more complete and sustained C2 blockade and associated attenuation of downstream terminal complement activation.*

Perfusate C5b-9 was inconsistent across the kidneys in both phases. During NMP C5b-9 increased substantially in one kidney in both control and argx-117. For argx-117, kidney 1 rose from a low baseline to 4,200 ng/mL at hour 2 and was 3,800 ng/mL at end of NMP, while kidney 3 remained comparatively low, with a 200 ng/mL at baseline, getting no higher than 350 ng/mL during NMP. The controls had a less extreme, but

similar disparity, with kidney 2 reaching 2000 ng/mL, but kidney 4 only going as high as 490 ng/mL. For NR kidney 1, 2 and 4 all followed the same trajectory of formation and to a similar magnitude ending at 2000 ng/mL, whereas the high dose kidney had a shallower rise over the first 3 hours to 500 ng/mL and then a fall to 220 ng/mL at the end of perfusion.

4.4.3.4 C5b-9 Immunohistochemistry

C5b-9 deposition was quantified by IHC as the percentage of C5b-9 positive cells at baseline, end of NMP, and end of NR using the manually trained QuPath pipeline. Overall, within the early perfusions there was no statistically significant separation between control kidneys and those treated with argx-117 at any timepoint. At baseline, C5b-9 positivity was similar between groups, with 3.33% (1.95–8.32) in controls vs 2.15% (2.01–2.76) in argx-117, p = 1.000. At the end of NMP, values remained low and variable, 1.40% (0.91–6.55) in controls vs 2.51% (2.40–3.88) in argx-117, p = 0.663. By the end of NR, C5b-9 positivity was numerically higher in controls, 7.10% (5.65–10.16), compared with argx-117 4.26% (3.17–6.96), although this did not reach statistical significance, p = 0.331.

Within-group paired analyses over time also showed no statistically significant changes within either arm, although controls demonstrated a numerically higher C5b-9 at the end of NR. In controls, baseline to the end of NMP showed no change (p = 0.423), baseline to the end of NR was not significant (p = 0.211), and the increase from the end of NMP to the end of NR approached significance (p = 0.091). In argx-117 kidneys, there was no significant change from baseline to the end of NMP (p = 0.181), baseline to the end of NR (p = 0.211), or the end of NMP to end-NR (p = 0.211). When both groups were pooled, there was numerically increased C5b-9 positivity from baseline to the end of NR, but it was not statistically significant (p = 0.071), and a statistically significant increase from the end of NMP to the end of NR (p = 0.030), consistent with greater terminal complement deposition during the NR (Fig 4.7).

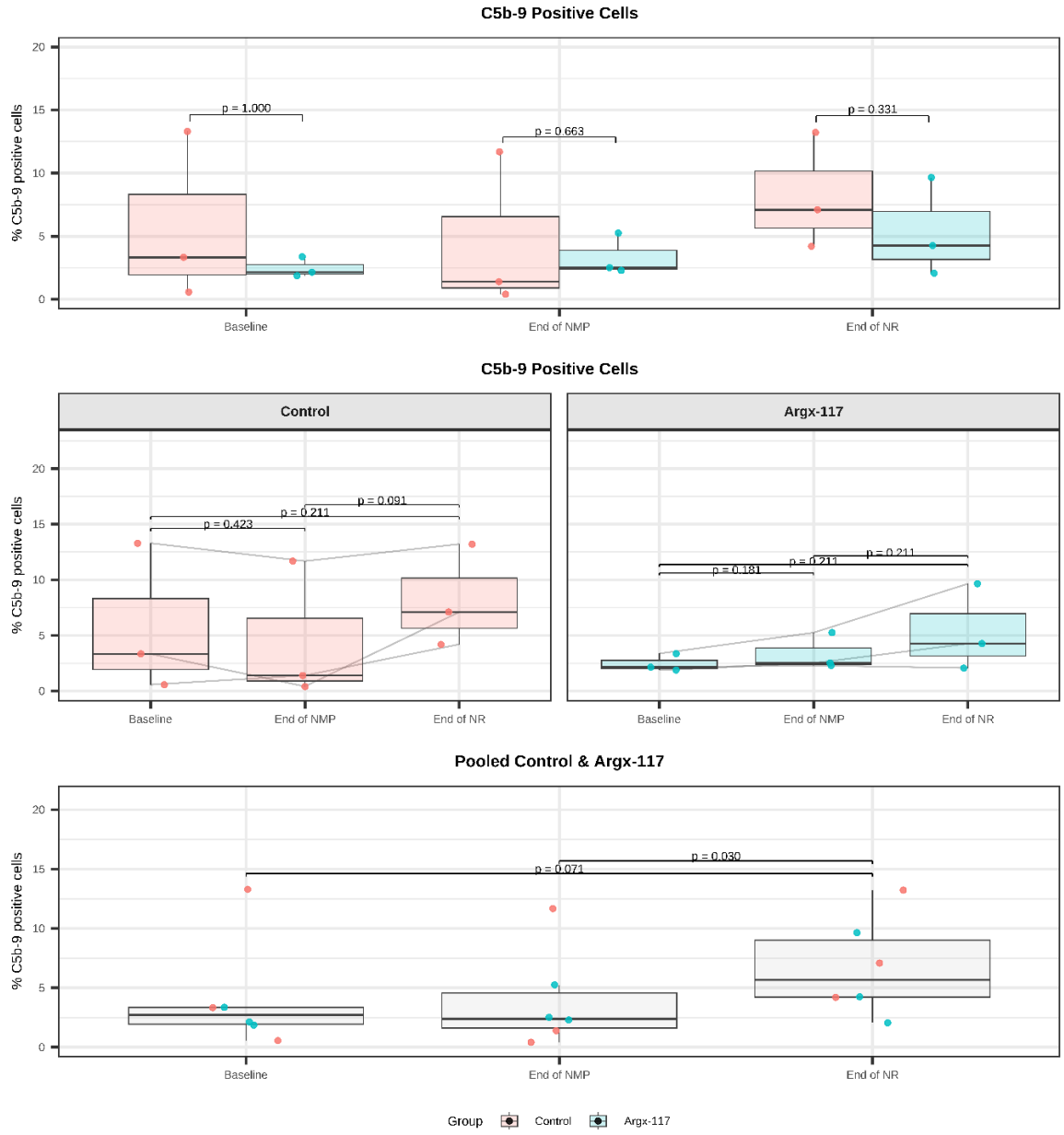


Figure 4.7 ***Tissue C5b-9 immunohistochemistry in biopsies from isolated kidney perfusions performed for Argx-117 dose refinement.*** *Quantification of C5b-9-positive cells is shown at baseline, end of NMP, and end of NR for control and Argx-117-treated kidneys. In the upper panel, boxplots compare treatment groups at each timepoint. In the middle panel, data are shown longitudinally within each treatment group with paired lines linking samples from the same kidney. In the lower panel, all cases are pooled by timepoint to illustrate overall change across the experiment. There was no statistically significant difference in C5b-9-positive cell burden between control and Argx-117-treated kidneys at baseline, end of NMP, or end of NR. Within-group analysis showed no statistically significant paired temporal change in either the control or treated kidneys across the three biopsy timepoints, although control kidneys showed a numerical rise in C5b-9 positivity by the end of reperfusion. When all kidneys were considered together, C5b-9-positive cell burden increased over time, with the strongest increase seen between end of NMP and end of NR and a similar trend from baseline to end of NR. These findings suggest that tissue terminal complement deposition increased during the experimental course, particularly after reperfusion, but that a clear treatment effect could not be demonstrated in this small dose-refinement series.*

4.4.4 Paired Perfusion

Six pairs of kidneys deemed unsuitable for transplant were acquired under the ethics for the project (REC 21/PR/1546) and 6 paired perfusions were completed and analysed. Data is presented as median (IQR) with paired two-sided Wilcoxon p values where applicable. The donor and kidney characteristics are displayed in Table 4.2.

Pair	1	2	3	4	5	6
ARGX-117 dose	1200 µg/mL FFP	2400 µg/mL FFP	2400 µg/mL FFP	2400 µg/mL FFP	2400 µg/mL FFP	2400 µg/mL FFP
Donor type	DBD	DCD	DBD	DBD	DBD	DBD
Cause of death	ICH	ICH	ICH	Hypoxic brain injury	ICH	ICH
Downtime (mins)	45	0	0	0	0	0
Age (years)	34	75	67	68	76	70
Sex	F	M	M	M	F	M
Reason for decline	Poor perfusion	Renal mass	Adrenal mass	Small bowel tumour	Hepatic tumour	Colonic tumour
CIT (hrs:mins)	31:15 / 31:24	15:35 / 16:01	16:39 / 16:56	20:20 / 20:53	21:41 / 22:15	26:08 / 26:23
WIT (flush NMP-NR, mins)	16	14	15	16	14	12
BMI (kg/m²)	32	27	28	27	33	25
Blood type	A+	O+	A+	B+	O+	O+
Creatinine (µmol/L)	104	68	102	90	49	63
T2DM	N	Y	N	Y	N	N
HTN	N	Y	N	Y	Y	Y
Smoker	N	Y	N	N	N	Y
Kidney weight (g) R/L	198 / 175	247 / 279	321 / 294	301 / 314	175 / 165	211 / 208

Table 4.2 ***Donor and kidney characteristics for the paired perfusions with Argx-117.*** *The table summarises the characteristics of each donor pair, variables shown include donor sex, body mass index (BMI), blood group, admission creatinine, history of type 2 diabetes mellitus (T2DM), hypertension (HTN), and smoking status, together with cold ischaemia time (CIT), interval warm ischaemia time between flush, NMP and normothermic reperfusion (NR), and kidney weights. Kidney weight is reported separately for right and left kidneys within each donor pair. The cohort included both DBD and DCD donors with a broad age range and variable donor risk profiles, reflecting the heterogeneity typical of declined research kidneys.*

4.4.4.1 Perfusion Parameters

Weight-adjusted renal artery flow was comparable between groups throughout NMP and NR, with no evidence of a treatment effect across time points. At 120 min, flow was 180 (142–209) mL/min/100g in controls versus 159 (134–193) mL/min/100g with argx-

117 (p = 0.500). At end-NMP (360 min) flows remained similar (Control 204 (154–235) vs argx-117 195 (165–210) mL/min/100 g; p = 0.600). During NR, flows at 420 min were 179 (159–222) vs 190 (152–206) mL/min/100g (p = 0.752), and at end-NR (720 min) 186 (165–221) vs 187 (151–202) mL/min/100g (p = 0.500).

Urine output was variable across pairs, with a tendency toward higher urine production in the argx-117 arm during NMP, but this did not reach significance. At 120 min, urine production was 17 (14.2–22.8) mL/h in controls versus 24 (14.5–42.5) mL/h with argx-117 (p = 0.172). At end-NMP (360 min), this difference was more marked (18.5 (11.8–23) vs 31 (16.5–35) mL/h; p = 0.080). Following the plasma switch, urine output increased substantially in both groups; at 420 min it was 132 (81–167) vs 159 (148–241) mL/h (p = 0.249), and by end-NR (720 min) was 168 (60–187) vs 132 (114–186) mL/h (p = 0.345) (Fig 4.8).

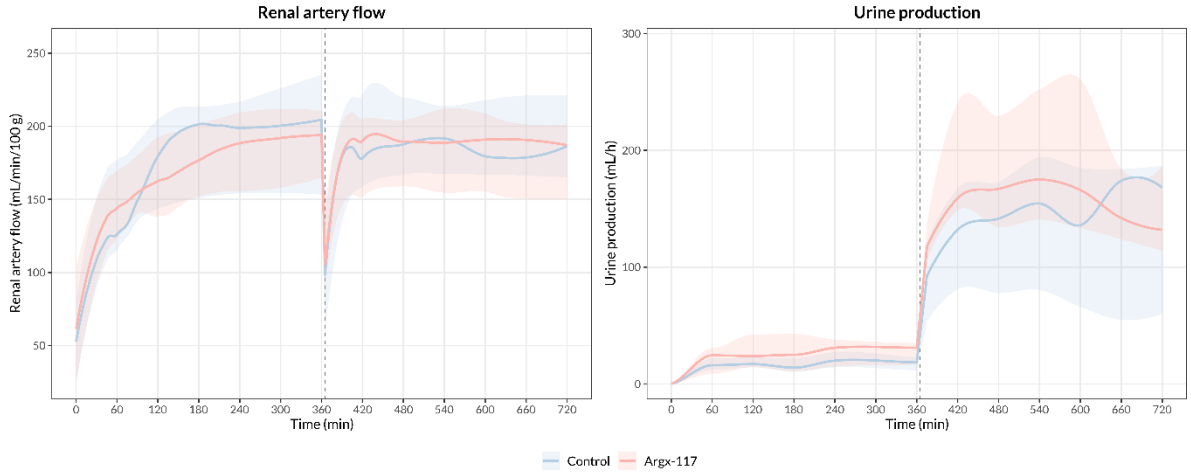


Figure 4.7 ***Renal artery flow and urine production during paired perfusions with Argx-117****. Time-course plots show mean renal artery flow normalised to 100 g kidney weight and mean urine production over the course of perfusion for paired experiments. Shaded ribbons indicate variability around the group mean. The vertical dashed line marks the transition from NMP to NR. Renal artery flow increased rapidly during early NMP in both groups and was then maintained at similar levels throughout the remainder of the experiment, with no clear sustained separation between Argx-117-treated and control kidneys. At the onset of reperfusion there was an abrupt transient fall, followed by recovery to near pre-reperfusion values. Urine production was low during NMP but increased sharply after transition to reperfusion in both groups. Argx-117-treated kidneys showed numerically higher urine output than controls through much of the reperfusion phase, although substantial overlap in variability was present.*

4.4.4.2 Perfusate Biochemistry

Across perfusions initials samples showed some early differences, consistent with variable washout, blood quality and perfusate adjustments for pH, calcium and

glucose. As the perfusion phases progressed electrolytes stabilised and were consistent within the pairs. For all blood gas measures there were no significant differences between the groups, with consistent controlled perfusions.

Arterial pH increased during NMP in both groups, from hour 2 in controls at 7.33 (7.32–7.36) vs argx-117 7.31 (7.28–7.35), p = 0.345, to hour 6, 7.36 (7.35–7.41) vs 7.38 (7.33–7.38), p = 0.463. Again, in NR, pH begins lower and as bicarbonate correction is done, then is physiological, with a gradual increase as perfusion duration progresses (controls 6.96 (6.92–6.98) vs argx-117 6.80 (6.63–6.94), p = 0.046), and is normal at the end of NR (7.33 (7.32–7.37) vs 7.33 (7.33–7.37), p = 0.893).

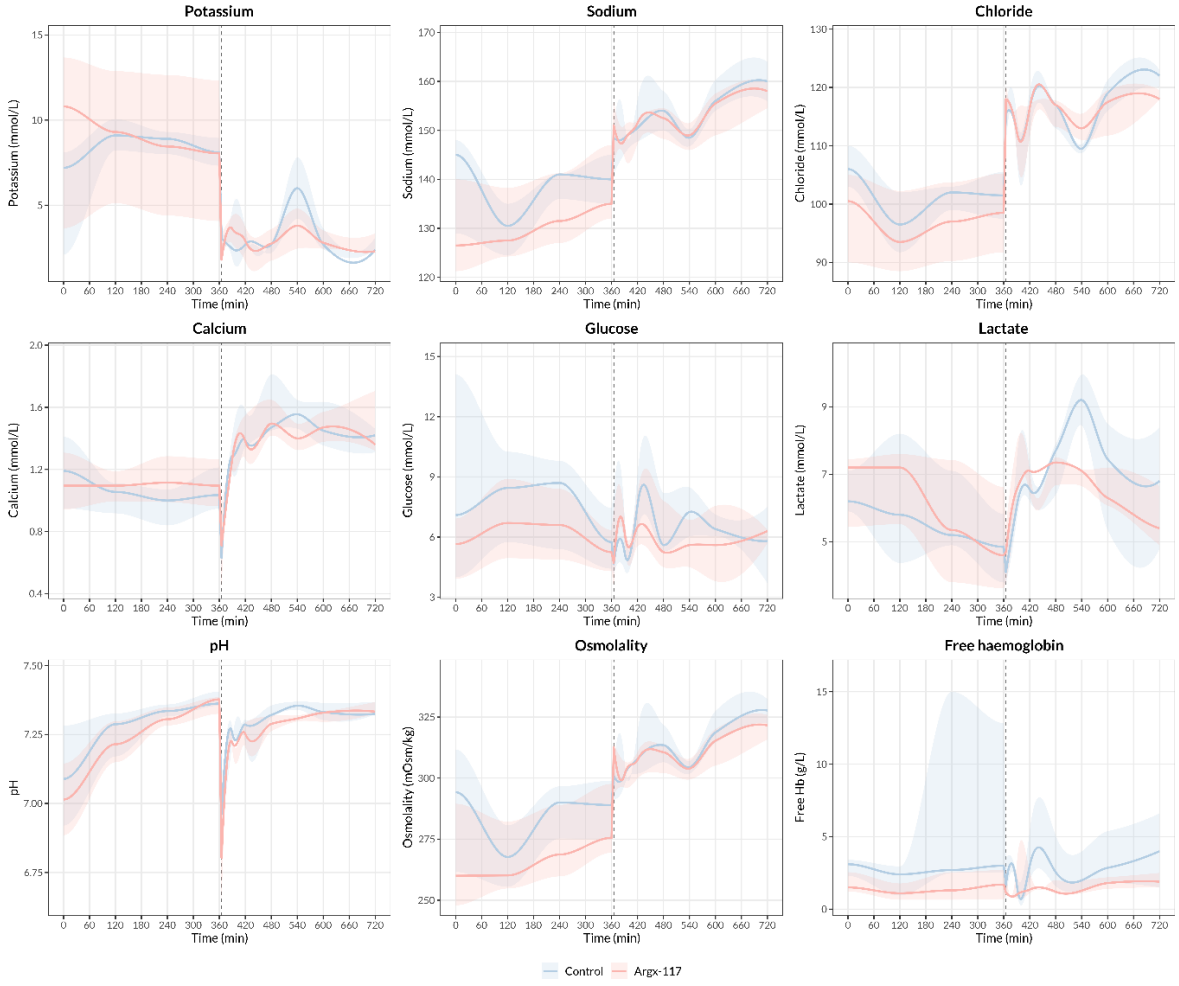


Figure 4.9 ***Perfusate biochemical and blood gas parameters during paired perfusions with Argx-117.*** *Time-course plots show group mean values for potassium, sodium, chloride, calcium, glucose, lactate, pH, osmolality, and free haemoglobin across the experiment. Blue lines represent control kidneys and red lines Argx-117-treated kidneys; shaded ribbons indicate variability around the group mean. The vertical dashed line marks the transition from NMP to NR. Electrolyte and metabolic profiles followed similar overall trajectories in both groups, with abrupt shifts at the onset of reperfusion reflecting the change in perfusate conditions. Potassium fell sharply after reperfusion and then remained relatively low in both groups, while sodium, chloride, calcium, and osmolality increased after transition and subsequently stabilised. pH dropped briefly at the point of transition before recovering towards physiological values.*

Lactate rose after reperfusion in both groups, with a more pronounced peak in controls, but then trended down in both groups. Free haemoglobin remained low overall. Overall, these data indicate broadly comparable biochemical stability between groups.

Potassium was elevated and variable early, then stabilised during NMP and returned to near-physiological levels during NR. At hour 2 potassium was 9.1 (8.22–10.1) mmol/L in controls and 9.3 (5.12–12.9) mmol/L with argx-117 (p = 0.917), remaining similar at end-NMP (8.1 (7.32–8.95) vs 8.05 (4.08–12.3) mmol/L, p = 0.753). Following the plasma switch, potassium was lower in both groups (3.05 (2.15–3.27) vs 1.8 (1.75–3.3) mmol/L, p = 0.345) and remained low at end-NR (2.4 (2.4–3.1) vs 2.3 (2.25–3.35) mmol/L, p = 0.465).

Sodium drifts as with pH over perfusion duration. Beginning slightly sub-physiological in NMP, at hour 2 was 130 (124–135) mmol/L in controls and 128 (124–138) mmol/L with argx-117 (p = 0.528), rising modestly to normal range by end of NMP (140 (135–145) vs 135 (132–147) mmol/L, p = 0.463). For NR, it began higher (148 (141–150) vs 151 (144–156) mmol/L, p = 0.463), and reaching slightly above normal by the end of NR, 160 (156–164) vs 158 (154–160) mmol/L at end-NR (p = 0.279). Chloride was lower at baseline in the argx-117 arm (106 (103–110) vs 100 (90–105) mmol/L, p = 0.043), but thereafter was similar to the end of NMP (102 (97.5–106) vs 98.5 (91.8–105) mmol/L, p = 0.279) with a similar stable levels during NR (116 (110–117) vs 118 (114–120) mmol/L, p = 0.596).

Calcium was controlled within the physiological range during NMP and NR, with a small difference at hour 2 (control 1.00 (0.84–1.07) vs argx-117 1.11 (0.99–1.28) mmol/L; p = 0.043) but no consistent separation at end of NMP (1.03 (0.948–1.21) vs 1.09 (0.963–1.26) mmol/L, p = 0.345) or the end of NR (1.42 (1.31–1.46) vs 1.36 (1.32–1.71) mmol/L; p = 0.686). Glucose was maintained at clinically acceptable levels with no meaningful differences (end of NMP: 5.75 (4.42–7.45) vs 5.25 (4.3–6.35) mmol/L, p = 0.528; and end of NR: 5.8 (3.7–7.5) vs 6.3 (5.7–6.35) mmol/L, p = 0.500).

Lactate fell slightly through NMP in both groups, an encouraging sign of perfusion quality, and rose slightly during NR. At hour 2 lactate was 5.8 (4.38–8.2) mmol/L in controls versus 7.2 (5.53–7.6) mmol/L with argx-117 (p=0.600), decreasing by the end of NMP (4.85 (3.8–5.83) vs 4.6 (3.62–6.62) mmol/L, p = 0.917). After NR commences lactate remained similar in both groups (4.1 (3.75–4.75) vs 4.7 (3.8–5.45) mmol/L,

p=0.075), increasing slightly by end of NR (6.8 (4.8–8.4) vs 5.4 (4.9–6.65) mmol/L, p=0.686).

Osmolality increased during NR, with no statistically clear group separation. Early in NMP osmolality was below physiological range, 268 (256–281) mOsm/kg in controls versus 260 (255–282) mOsm/kg with argx-117 (p=0.345), but normalised by the end of NMP, 289 (275–299) vs 276 (269–298) mOsm/kg (p = 0.463). During NR, it begins higher, reflecting the higher baseline sodium, (301 (292–304) vs 312 (294–314) mOsm/kg; p=0.463) and increases further during NR, ending at 328 (322–332) vs 322 (316–326) mOsm/kg (p=0.138).

Free haemoglobin was elevated and variable, consistent with blood quality and haemolysis over time, especially in NR. At baseline Hb was 3.1 (2.3–3.4) g/L in controls and 1.5 (1.23–2.55) g/L with argx-117 (p=0.66). By the end of NMP it was 3.0 (2.55–12.8) vs 1.7 (0.7–2.7) g/L (p = 0.138), and at the end of NR 4.0 (1.5–6.6) vs 1.9 (1.5–2.5) g/L (p=0.50) (Fig 4.9).

Creatinine clearance (CrCl) showed a modest numerical shift towards higher values with argx-117, but it was not significant. At the end of NMP, CrCl was 1.02 (0.72–1.74) in controls versus 1.33 (0.87–1.66) with argx-117 (p=0.337), and at early NR it was 6.86 (5.53–9.72) versus 7.39 (6.07–8.89) (p=0.708). By the end of NR, CrCl remained numerically higher in the argx-117 group, 7.05 (5.94–7.67) versus 4.99 (2.86–8.56) in controls (p=0.417).

Fractional excretion of sodium (FENa) did not differ with argx-117 treatment and had values which were not physiological due to tubular injury. At the end of NMP, FENa was 12.47 (8.34–25.22) in controls vs 16.24 (8.31–40.19) with argx-117 (p=0.417), and at early NR 19.83 (15.37–27.87) vs 26.38 (22.75–29.14) (p=0.708). At the end of NR, FENa remained higher in the argx-117 kidneys, 31.98 (23.71–36.71) compared with 24.53 (18.08–30.97) in controls (p=0.896) (Fig 4.10).

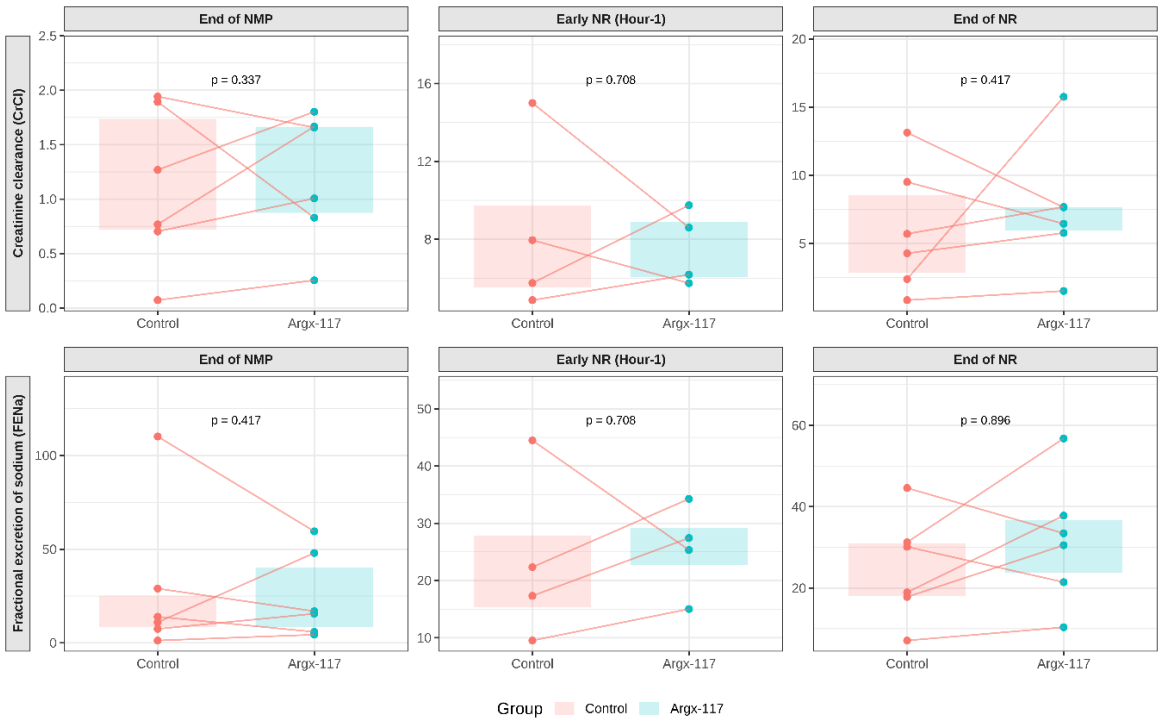


Figure 4.10 ***Paired comparison of renal function during paired perfusions with Argx-117.*** *Boxplots with paired connecting lines show creatinine clearance (CrCl) and fractional excretion of sodium (FENa) at the end of NMP, early normothermic reperfusion (NR; Hour 1), and end of NR. Each point represents an individual kidney, with paired lines linking contralateral kidneys from the same donor pair. Creatinine clearance and FENa were broadly similar between control and Argx-117-treated kidneys across all sampled timepoints, with no statistically significant differences detected. CrCl increased from end-NMP to reperfusion in both groups, reflecting improved filtration following transition to reperfusion, while FENa also rose over time, consistent with evolving tubular dysfunction.*

4.4.4.3 Perfusate Injury Biomarkers

Perfusate injury biomarkers, IL-18, GST-Pi, KIM-1 and NGAL were assessed in the paired kidney perfusions at baseline, end of NMP, start of NR and end of NR. Group comparisons used a paired, Wilcoxon signed-rank test, with values reported as median (IQR) and paired differences reported as argx-117 to controls.

IL-18 showed no consistent reduction with argx-117. At Baseline, IL-18 was similar between groups (Control 9.855 (9.399–24.44) pg/mL vs argx-117 13.69 (6.423–14.74); paired difference 0.3937 (−12.85–4.291), p=0.394). At the end of NMP, IL-18 was numerically lower with argx-117 (Control 88.81 (51.34–146.2) vs argx-117 63.36 (54.60–92.86)), but without statistical significance (paired difference −4.536 (−40.61–50.29), p=0.500). Early in NR, IL-18 was again comparable (Control 51.57 (40.88–60.72) vs argx-117 36.36 (30.24–55.53); paired difference −6.628 (−15.27–1.914), p=0.201). By End NR, IL-18 was numerically higher in the argx-117 arm (Control 126.1 (118.3–127.1) vs argx-

117 148.3 (103.4–202.9)), with a paired difference of 26.45 (−24.21–76.25), but again not statistically significant (p=0.663).

NGAL demonstrated the clearest evidence of lower values with argx-117 during reperfusion. At Baseline, NGAL was similar (Control 38.85 (27.07–57.28) ng/mL vs argx-117 38.71 (18.16–60.74); paired difference 1.918 (−12.85–4.291), p=0.201). At the end of NMP, NGAL was lower with argx-117 (Control 23.68 (15.82–29.25) vs argx-117 17.80 (12.03–27.18)), showing a trend without statistical significance (paired difference −4.507 (−11.30–2.902), p=0.071). At Early NR, NGAL was significantly reduced with argx-117 (Control 29.38 (25.97–33.82) vs argx-117 17.85 (13.90–26.94); paired difference −10.53 (−13.84–−4.267), p=0.018). This reduction persisted to End NR (Control 17.36 (9.249–21.01) vs argx-117 13.77 (6.848–16.00); paired difference −3.334 (−4.353–−2.401), p=0.030).

KIM-1 did not show evidence of reduction with argx-117 and displayed marked variability. At Baseline, KIM-1 was broadly similar (Control 997 (595–1,072) ng/mL vs argx-117 1,502 (929–1,824); paired difference 104 (−817–820), p=0.971). At End NMP, KIM-1 was lower in argx-117 on the median (Control 75.89 (57.72–114.2) vs argx-117 27.16 (24.99–166.6)), but variability was substantial and the paired comparison was not significant (paired difference −38.09 (−60.86–136.4), p=0.583). Early in NR, KIM-1 remained similar (Control 778.0 (646.8–1,426) vs argx-117 1,053 (668.8–1,405), paired difference 22.26 (−383–370), p=0.265). By End NR, KIM-1 was again numerically higher with argx-117 (Control 121.6 (39.21–221.3) vs argx-117 143.9 (47.21–164.9), paired difference 3.244 (0.000–11.05), p=0.708).

GST-Pi showed a mixed pattern with differences during NMP, but a significant reduction by the end of NR. At Baseline, GST-Pi was comparable (Control 16.78 (8.232–37.35) ng/mL vs argx-117 29.34 (5.689–87.66); paired difference 1.698 (−6.078–7.106), p=0.853). At the end of NMP, GST-Pi was numerically higher with argx-117 (Control 24.10 (11.11–43.38) vs argx-117 52.32 (17.29–67.02), paired difference 2.637 (−2.864–17.89), p=0.663). Early in NR, values were similar (Control 26.71 (20.23–34.19) vs argx-117 23.59 (16.62–31.55), paired difference −11.32 (−15.51–4.170), p=0.201). At the end of NR, GST-Pi was significantly lower with argx-117 (Control 8.546 (6.825–10.23) vs argx-117 4.853 (2.094–5.611), paired difference −3.886 (−6.313–−1.551), p = 0.018).

For delta GST-Pi, change over NMP and NR did not show a reduction with argx-117. Change of the course of NMP was similar between groups (Control −2.744 (−6.078–7.106) vs argx-117 0.4460 (−0.1672–2.887), paired difference 3.010 (1.698–6.612), p=0.853). Over NR, GST-Pi decreased in both arms to a similar extent (Control −21.46 (−25.27–−11.92) vs argx-117 −20.94 (−26.07–−11.96); paired difference 7.505 (−8.985–10.83), p=0.663) but again was not significant (Fig 4.11).

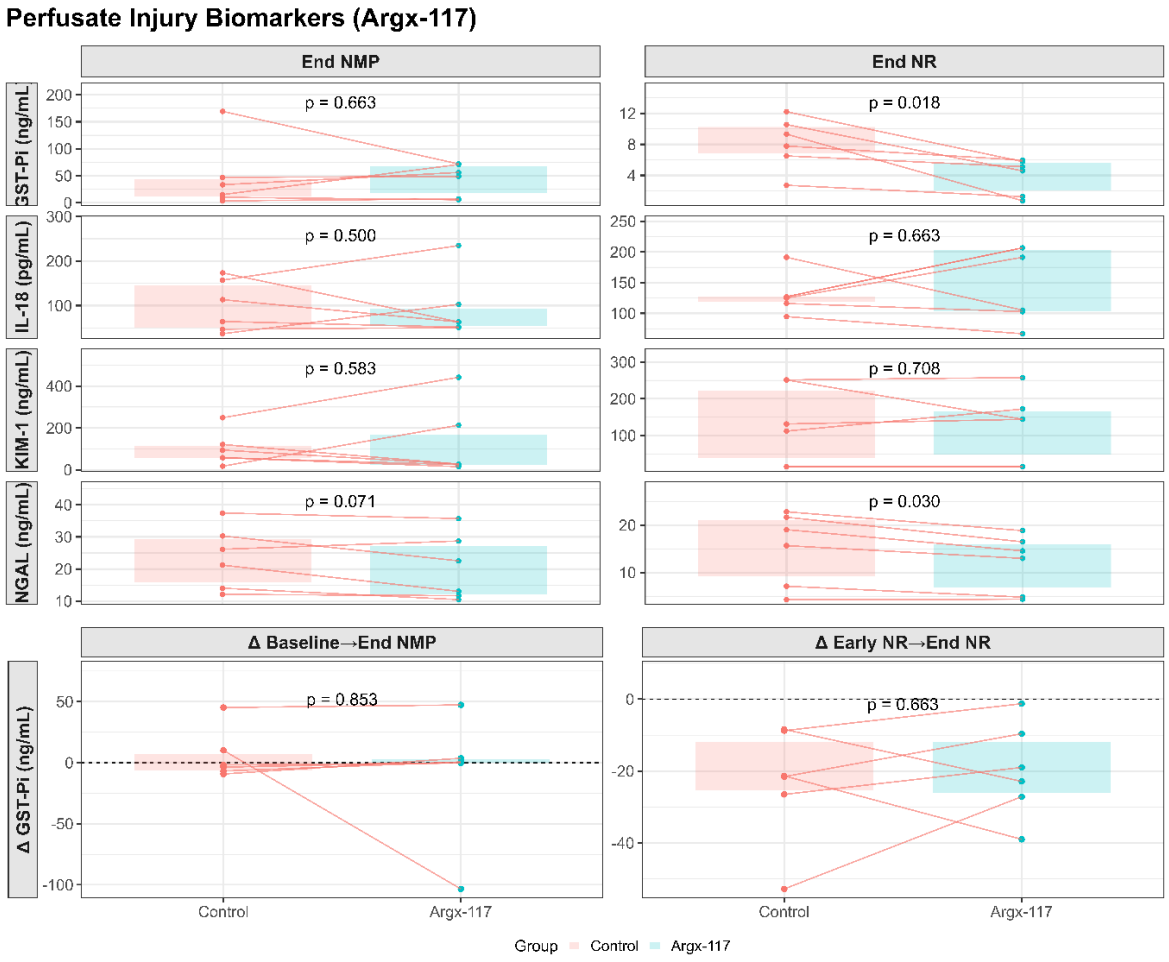


Figure 4.11 ***Perfusate injury biomarkers in paired perfusions with Argx-117.*** *Boxplots with paired connecting lines show GST-Pi, delta GST=Pi, IL-18, KIM-1, and NGAL concentrations at end of NMP and end of NR. Each point represents an individual kidney, with paired lines linking contralateral kidneys from the same donor pair. At the end of NMP, no significant between-group differences were identified for GST-Pi, IL-18, KIM-1, or NGAL, although NGAL showed numerically lower concentrations in Argx-117-treated kidneys. By end NR, GST-Pi and NGAL were significantly lower in Argx-117-treated kidneys than in paired controls, consistent with reduced tubular injury following reperfusion, whereas IL-18 and KIM-1 remained similar between groups.*

4.4.4.4 Perfusate Complement Proteins & Activity

The perfusate complement proteins assessed were C2, C3a, C4d, C3bBbP and C5b-9, with C5b-9 quantified using two antibodies (sC5b-9 and sC5b-9 TM). Overall, the clearest pharmacodynamic effect of argx-117, as to be expected, was on C2, consistent

with target binding and clearance, with additional evidence of attenuation of alternative pathway activation (C3bBbP) during NR.

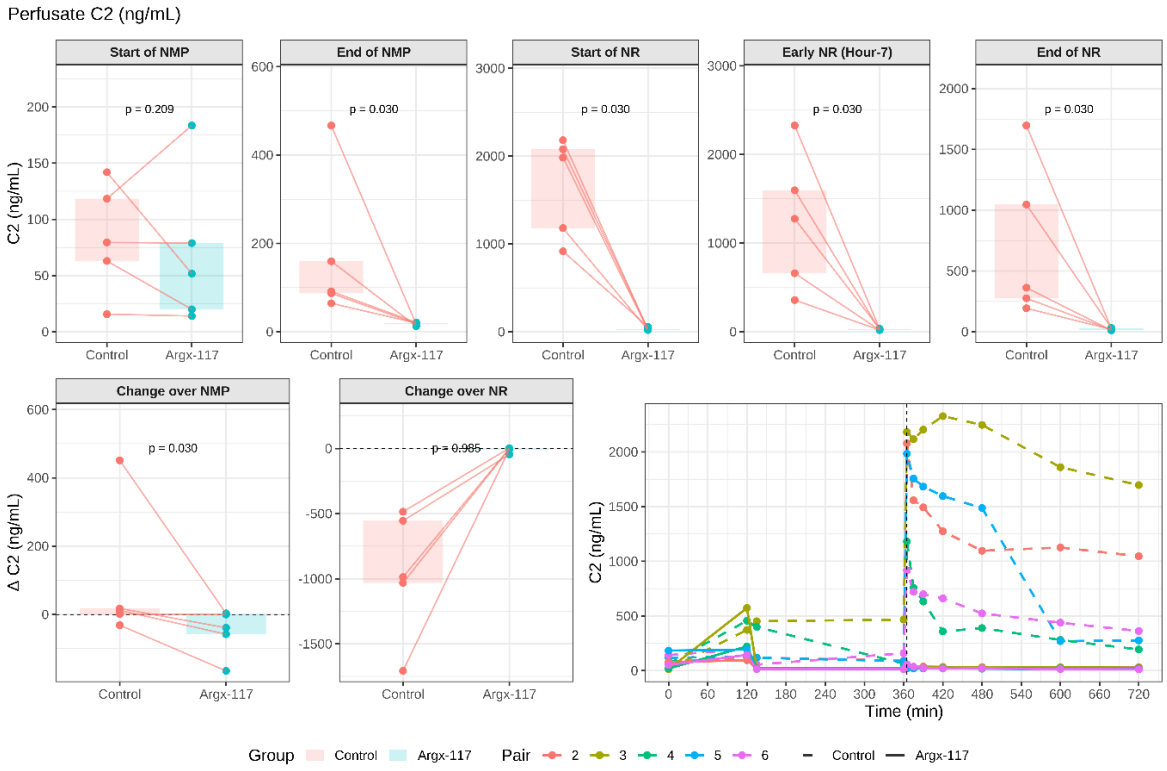


Figure 4.12 ***Perfusate C2 concentrations during paired perfusions with Argx-117.*** *Boxplots with paired connecting lines show C2 concentrations at the start of NMP, end of NMP, start of NR, early NR (Hour 1), and end of NR, together with interval change in C2 over NMP and over NR. Each point represents an individual kidney, with paired lines linking contralateral kidneys from the same donor pair. The lower right panel shows the full time-course of perfusate C2 for each donor pair, with dashed lines indicating control kidneys and solid lines Argx-117-treated kidneys. At the start of NMP, perfusate C2 concentrations were similar between groups. By the end of NMP, and throughout reperfusion, C2 concentrations were markedly lower in Argx-117-treated kidneys than in paired controls, consistent with sustained target engagement and depletion of measurable free C2 following treatment. This separation is persistent throughout NR, with all corresponding paired comparisons reaching statistical significance. Change-score analysis likewise demonstrated a significant between-group difference over NMP, reflecting a fall in C2 in treated kidneys compared with relative stability or increase in controls. Demonstrating effective and sustained pharmacodynamic blockade of C2 by Argx-117 across the paired perfusion experiments.*

Perfusate C2 was low at the start of NMP for both groups (control 79.5 (63–118.4) vs argx-117 51.74 (20–78.9), *p*=0.209). By end of NMP, C2 was significantly lower with argx-117 (18.38 (17.25–20.0)) compared with controls (91.5 (87.09–159.6)), *p*=0.030. Following the switch into NR, control circuits demonstrated a marked rise in C2 at the start of NR (1,983.7 (1,181–2,078.5)), while levels remained near-assay floor with argx-117 (23.30 (21.48–32.6)), *p*=0.030. This separation persisted at early NR (Hour-7) (control 1,274.6 (660.9–1,596.1) vs argx-117 20.69 (20.0–30.44), *p*=0.030, and at the end of NR (control 362.7 (276.2–1,046.6) vs argx-117 20.0 (15.35–26.72), *p*=0.030. Reflected

in the significant AUC differences in both phases, for NMP the controls were 46,511 (39,726–89,806) vs 20,808 (16,061–27,856), p=0.0295 and for NR 324,412 (180,582–417,439) vs 7,100 (6,552–10,646), p=0.0295 (Fig 4.12).

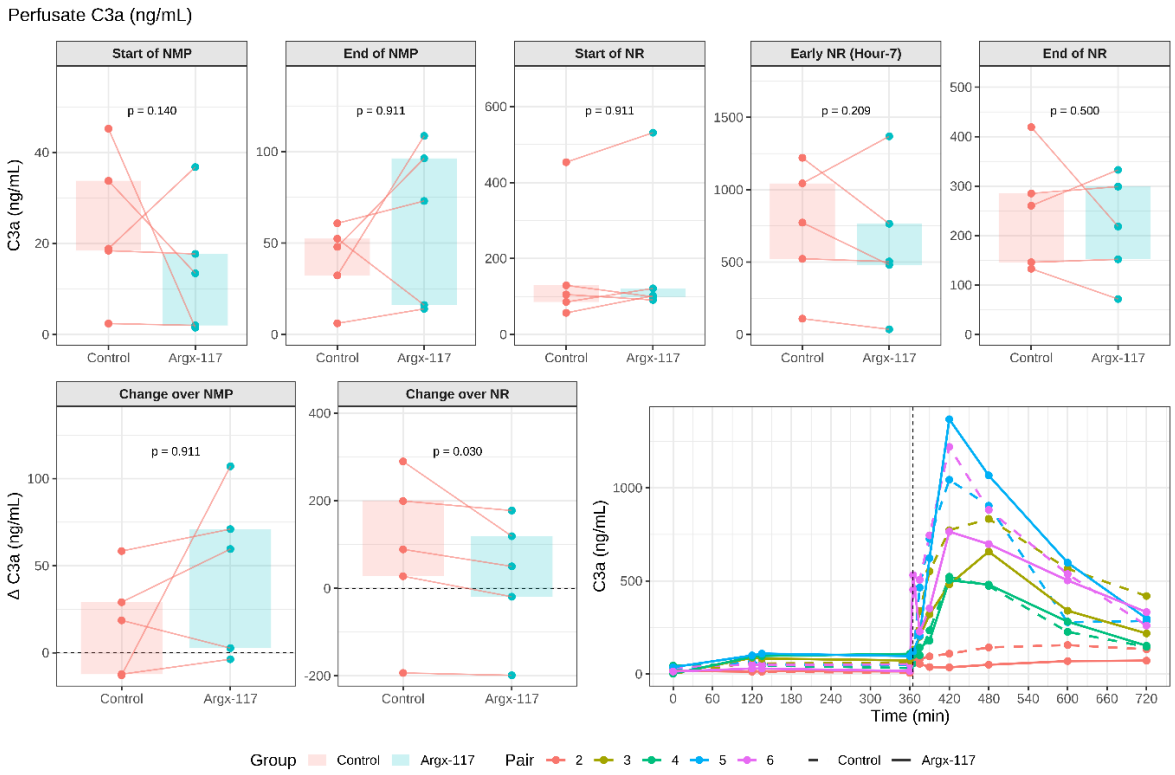


Figure 4.13 ***Perfusate C3a concentrations during paired perfusions with Argx-117****. Boxplots with paired connecting lines show C3a concentrations at the start of NMP, end of NMP, start of NR, early NR (Hour 1), and end of NR, together with interval change in C3a over NMP and over NR. Each point represents an individual kidney, with paired lines linking contralateral kidneys from the same donor pair. The lower right panel shows the full time-course of perfusate C3a for each donor pair, with dashed lines indicating control kidneys and solid lines Argx-117-treated kidneys. At the start and end of NMP, perfusate C3a concentrations were similar between groups, and no clear separation was seen at the start of NR or at the end of NR. During reperfusion, C3a increased markedly in both control and Argx-117-treated kidneys, consistent with substantial downstream complement activation despite proximal C2 blockade. The clearest between-group difference was seen in the change over NR, where the rise in C3a was significantly attenuated in Argx-117-treated kidneys compared with paired controls. The time-course plots similarly show a prominent early reperfusion surge in C3a in both groups, but with lower overall accumulation in treated kidneys in several pairs. Argx-117 treatment may have reduced the magnitude of C3a increase during reperfusion.*

C3a levels reflected some subtle effects, with argx-117 causing a modest but statistically significant attenuation in C3a formation over the course of NR. The levels at baseline were comparable (control 18.85 (18.4–33.76) vs argx-117 13.43 (2–17.7), *p*=0.14). At end of NMP, C3a remained similar, though numerically higher in argx-117 (control 47.90 (32.3–52.40) vs argx-117 73.0 (16.12–96.33), *p*=0.91), and immediately post-switch values were comparable (control 105.2 (85.71–129.4) vs argx-117 101.8 (99.2–121.24), *p*=0.91). During NR, C3a rose substantially in both groups as expected,

with a numerically lower median at early NR (Hour-7) in argx-117 (control 772.9 (522.5–1,043.7) vs argx-117 504.2 (480.8–764.9), *p*=0.209) and at end of NR (Control 260.3 (146.0–285.1) vs argx-117 218.3 (152.0–298.9), *p*=0.500). The change over NMP did not differ (Control 18.64 (−12.3–29.05) vs argx-117 59.57 (2.69–71.0), *p*=0.91), whereas during NR the change was significantly attenuated with argx-117 (Control 89.1 (27.7–199.4) vs argx-117 50.2 (−19.2–119.1), *p*=0.03). This difference, however, is not also present in AUC analysis, for NMP p=0.91 and NR p=0.30 (Fig 4.13).

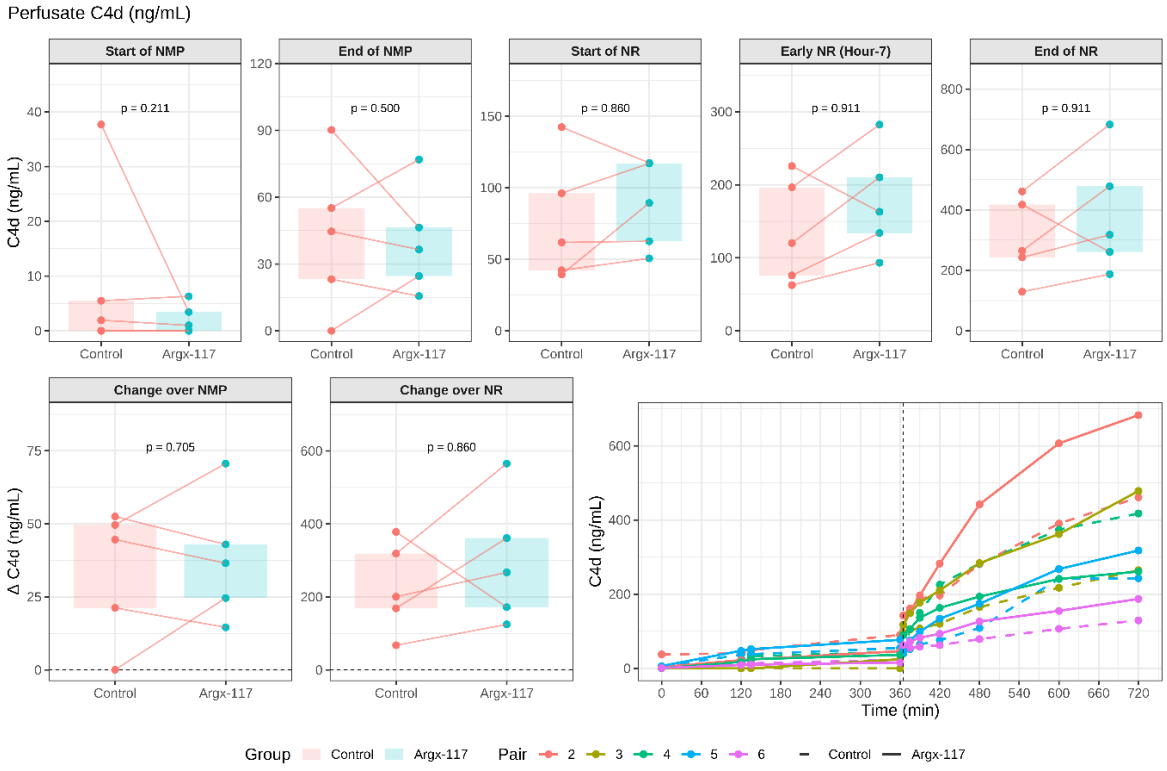


Figure 4.14 ***Perfusate C4d concentrations during paired perfusions with Argx-117.*** *Boxplots with paired connecting lines show C4d concentrations at the start of NMP, end of NMP, start of NR, early NR (Hour 1), and end of NR, together with interval change in C4d over NMP and over NR. Each point represents an individual kidney, with paired lines linking contralateral kidneys from the same donor pair. The lower right panel shows the full time-course of perfusate C4d for each donor pair, with dashed lines indicating control kidneys and solid lines Argx-117-treated kidneys. At the start of NMP, perfusate C4d concentrations were low and similar between groups. C4d increased over time in both control and Argx-117-treated kidneys, with the most marked rise occurring after transition to reperfusion, consistent with ongoing activation. However, no clear between-group separation was identified at the end of NMP, start of NR, early NR, or end of NR, and change-score analysis likewise showed no significant difference in C4d accumulation over either NMP or NR. The time-course plots similarly demonstrate progressive C4d generation in both groups across the experiment, without consistent attenuation by treatment. Argx-117 did not produce a clear measurable reduction in perfusate C4d in the paired perfusion experiments.*

There was no effect on C4d concentrations, which again were low at baseline with no between-group difference (control 1.94 (0–5.5) vs argx-117 1.0 (0–3.45), *p*=0.21). No significant differences were seen at the end of NMP (control 44.6 (23.16–55.11) vs argx-117 36.5 (24.6–46.4), p=0.500), at the start of NR (control 61.82 (42.31–96.2) vs argx-117

89.4 (62.6–117.0), p=0.860), in early NR (Hour-7) (control 120.2 (75.87–196.5) vs argx-117 163.1 (133.95–210.2), *p*=0.911), or the end of NR (control 264.7 (242.88–417.6) vs argx-117 317.87 (261.1–478.4), p=0.911). Similarly, neither changed over NMP (Control 44.6 (21.22–49.61) vs argx-117 36.5 (24.6–42.95), p=0.705) nor changed over NR (Control 200.6 (168.5–318.8) vs argx-117 267.2 (171.7–361.4), p=*0*.860) differed between groups (Fig 4.14).

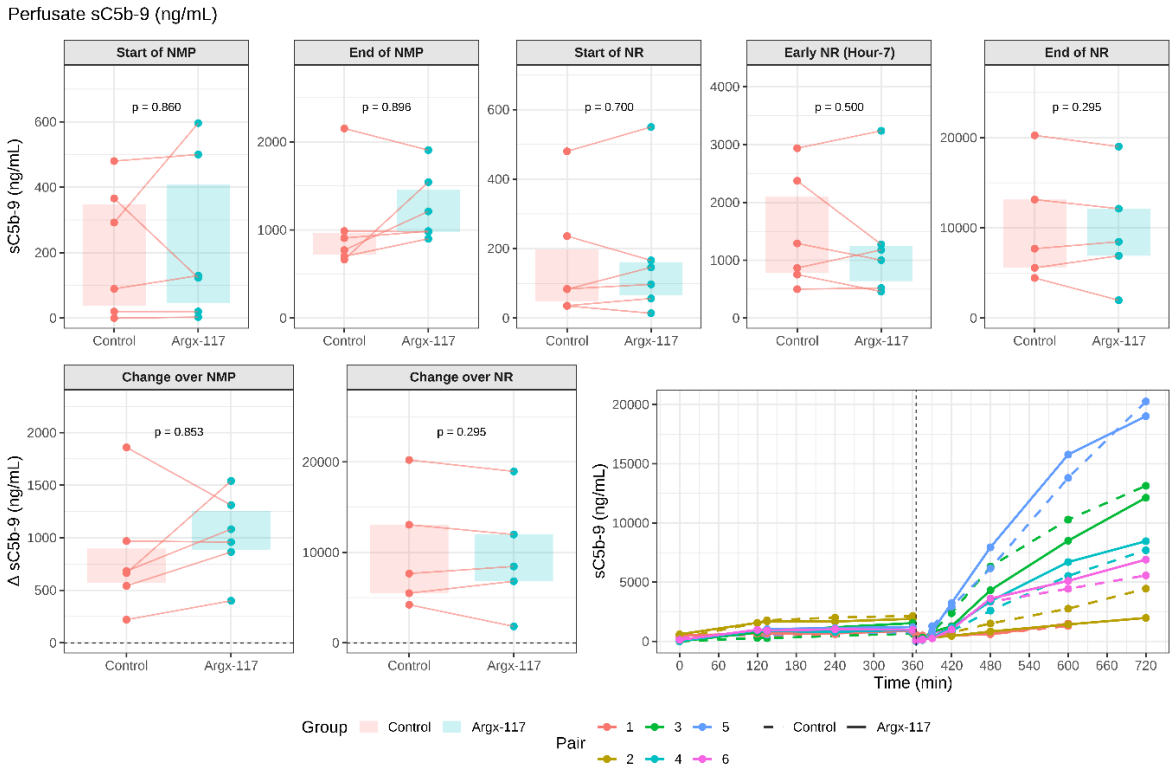


Figure 4.15 ***Perfusate sC5b-9 concentrations during paired perfusions with Argx-117.*** *Boxplots with paired connecting lines show sC5b-9 concentrations at the start of NMP, end of NMP, start of NR, early NR (Hour 1), and end of NR, together with interval change in sC5b-9 over NMP and over NR. Each point represents an individual kidney, with paired lines linking contralateral kidneys from the same donor pair. The lower right panel shows the full time-course of perfusate sC5b-9 for each donor pair, with dashed lines indicating control kidneys and solid lines Argx-117-treated kidneys. At the start of NMP, and at subsequent sampled timepoints, perfusate sC5b-9 concentrations were broadly similar between groups, with no statistically significant between-group differences identified. sC5b-9 increased progressively during the experiments, with the most marked rise occurring after transition to reperfusion, consistent with substantial terminal pathway activation in this model. Change-score analysis likewise showed no significant difference in sC5b-9 accumulation over either NMP or NR. The time-course plots demonstrate considerable inter-pair variability, but in most pairs sC5b-9 rose sharply during reperfusion in both control and Argx-117-treated kidneys. Despite effective proximal C2 blockade, Argx-117 did not produce a clear measurable reduction in terminal complement activation as assessed by perfusate sC5b-9 in the paired perfusion experiments.*

C5b-9 was produced effectively in the model, again, with no difference with argx-117 treatment. At the start of NMP, sC5b-9 was similar between groups (control 190.7 (37.35–347.4) vs argx-117 126.5 (45.78–407.5), *p*=0.86). During NMP levels increased but were also comparable (control 839.5 (717.8–967.9) vs argx-117 1,099.0 (980.2–

1,460.0), p=0.90). For NR, again baseline levels were low and comparable (control 83.45 (47.53–197.98) vs argx-117 121.55 (66.58–161.0), *p*=0.700). During NR, sC5b-9 increased markedly in both groups without evidence of reduction with argx-117, by early NR (Hour-7) levels were comparable with the end of NMP, and were not different between groups (control 1,078.8 (780.5–2,103.4) vs argx-117 1,090.1 (640.3–1,250.2), p=0.50). By the end of NR levels had risen dramatically, but again with no difference between groups (control 7,694.0 (5,568.3–13,137.0) vs argx-117 8,458.0 (6,903.3–12,125.0), p=0.30). (Fig 4.15).

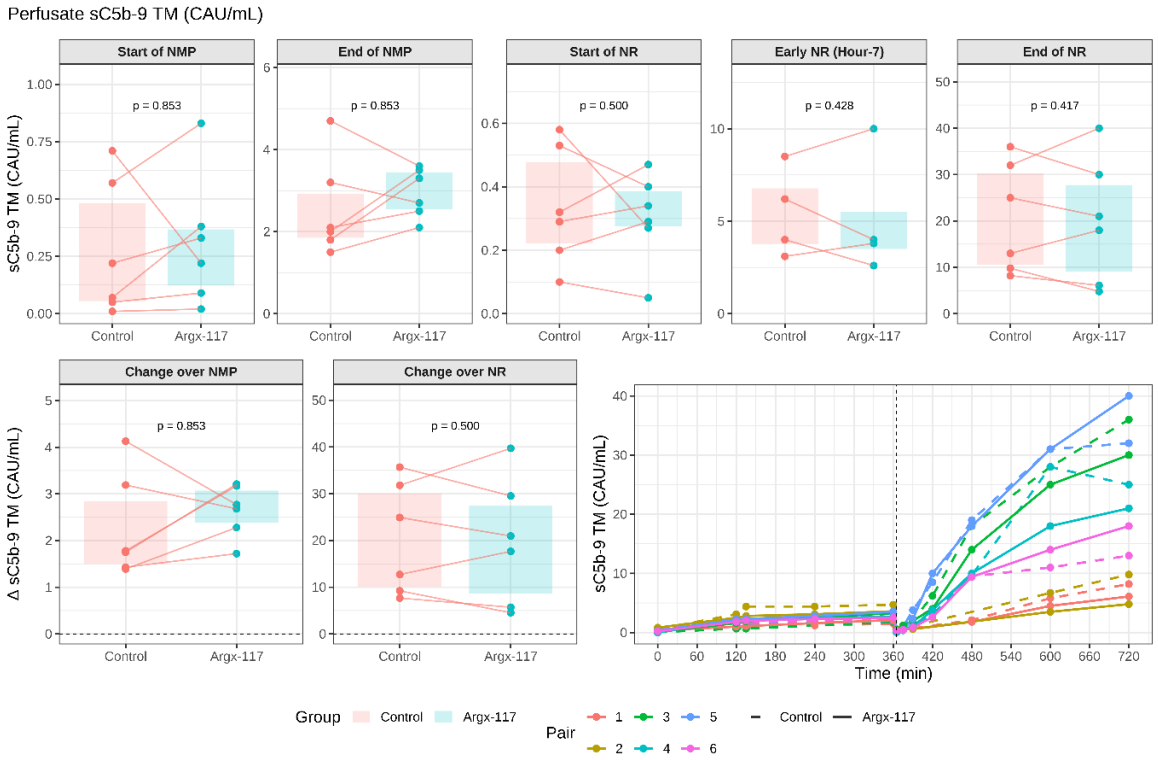


Figure 4.16 ***Perfusate sC5b-9 terminal complex concentrations during paired perfusions with Argx-117, measured using an alternative antibody and assay.*** *Boxplots with paired connecting lines show sC5b-9 terminal complex concentrations at the start of NMP, end of NMP, start of NR, early NR (Hour 1), and end of NR, together with interval change in sC5b-9 terminal complex over NMP and over NR. Each point represents an individual kidney, with paired lines linking contralateral kidneys from the same donor pair. The lower right panel shows the full time-course of perfusate sC5b-9 terminal complex for each donor pair, with dashed lines indicating control kidneys and solid lines Argx-117-treated kidneys. At the start of NMP, and at subsequent sampled timepoints, perfusate sC5b-9 terminal complex concentrations were broadly similar between groups, with no statistically significant between-group differences identified. Concentrations increased progressively over the course of the experiments, with the most marked rise occurring after transition to reperfusion, again indicating substantial terminal pathway activation in this model. The time-course plots demonstrate considerable inter-pair variability, but in most pairs there was a clear reperfusion-associated increase in both control and Argx-117-treated kidneys. The data confirm the findings seen with the other sC5b-9 assay, showing no clear measurable reduction in terminal complement activation despite proximal C2 blockade by Argx-117.*

Assessment with alternative assay and antibody for sC5b-9 demonstrated the same pattern of activation with no differences between groups. Again, values were low and

similar at baseline (control 0.145 (0.055–0.482) vs argx-117 0.275 (0.123–0.368), *p*=0.853). No reduction was observed at end of NMP (control 2.05 (1.85–2.92) vs argx-117 3.0 (2.55–3.45), p=0.853), and values remained low at the start of NR (control 0.305 (0.223–0.478) vs argx-117 0.315 (0.275–0.385), p=0.500). During NR, values increased in both groups with no significant differences at early NR (Hour-7) (control 5.1 (3.78–6.78) vs argx-117 3.9 (3.5–5.5), p=0.428) or end of NR (control 19.0 (10.6–30.25) vs argx-117 19.5 (9.08–27.75), p=0.417) (Fig 4.16).

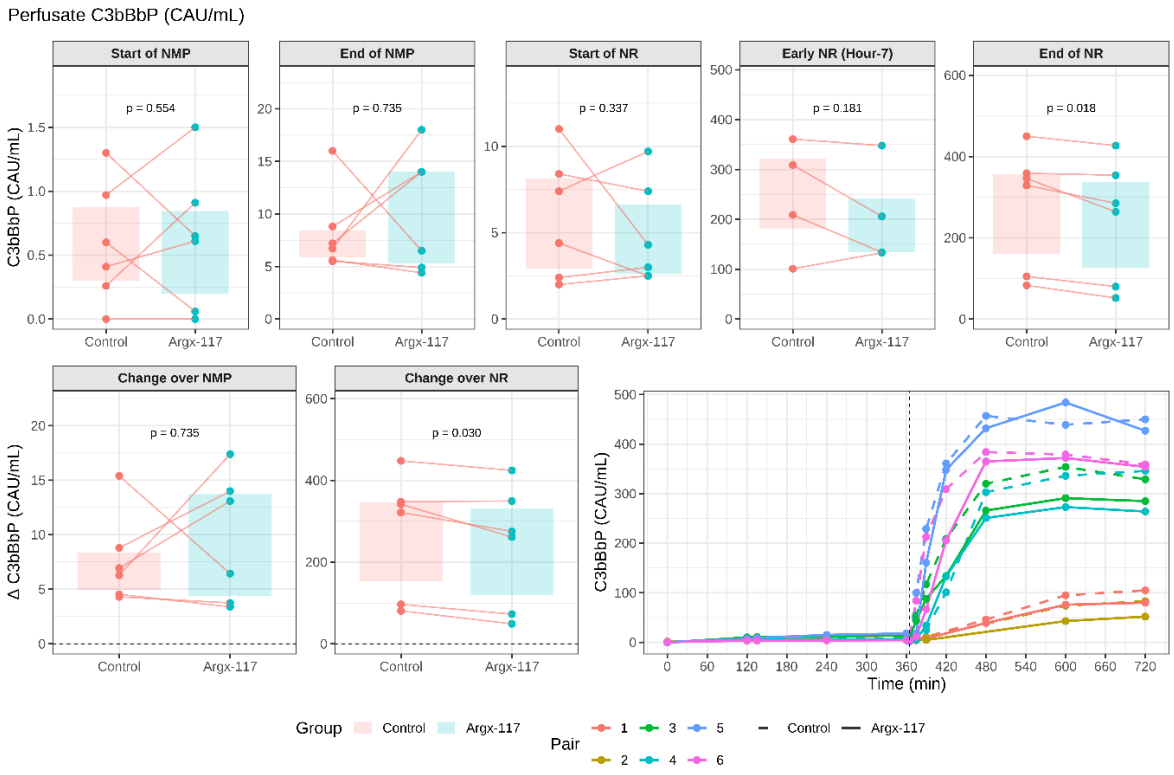


Figure 4.17 ***Perfusate C3bBbP concentrations during paired perfusions with Argx-117.*** *Boxplots with paired connecting lines show C3bBbP concentrations at the start of NMP, end of NMP, start of NR, early NR (Hour 1), and end of NR, together with interval change in C3bBbP over NMP and over NR. Each point represents an individual kidney, with paired lines linking contralateral kidneys from the same donor pair. The lower right panel shows the full time-course of perfusate C3bBbP for each donor pair, with dashed lines indicating control kidneys and solid lines Argx-117-treated kidneys. At the start and end of NMP, perfusate C3bBbP concentrations were similar between groups, with no clear separation during the NMP phase. Following transition to reperfusion, C3bBbP increased markedly in both control and Argx-117-treated kidneys, consistent with strong alternative pathway amplification during NR. Although between-group differences were not evident at the start of NR or early NR, by the end of NR C3bBbP concentrations were significantly lower in Argx-117-treated kidneys than in paired controls. Change-score analysis similarly demonstrated a significant between-group difference over NR, reflecting a smaller rise in C3bBbP in treated kidneys during reperfusion. The time-course plots support this pattern, showing substantial reperfusion-associated increases in all pairs, but with attenuation in several Argx-117-treated kidneys relative to their matched controls.*

For specific alternative pathway behaviour, the stabilised AP convertase was measured, C3bBbP. As with all markers, levels at baseline were low and not different between groups (control 0.505 (0.297–0.878) vs argx-117 0.63 (0.198–0.845), *p*=0.554). By the

end of NMP, values were numerically higher with argx-117 (control 6.95 (5.88–8.4) vs argx-117 10.25 (5.3–14.0), p=0.735). Baseline in NR values remained comparable (control 5.9 (2.9–8.15) vs argx-117 3.65 (2.62–6.62), p=0.337). During NR, C3bBbP increased substantially, at early NR (Hour-7) there was no significant difference (Control 259.0 (182.0–322.0) vs argx-117 170.0 (133.8–241.5), p=0.181). By the end of NR, however, C3bBbP was significantly lower in argx-117 kidneys (control 337.5 (161.0–355.8) vs argx-117 274.5 (126.0–336.8), p=0.018). Consistent with this, the change during NR was significantly attenuated with argx-117 (control 331.6 (152.9–346.4) vs argx-117 268.4 (119.8–331.1), p=0.03) and significantly lower AUC during NR, with control 98,678 (40,834–116,979) vs argx-117 81,295 (33,405–103,392), p=0.018. While the change during NMP did not differ (Control 6.62 (4.97–8.34) vs argx-117 9.77 (4.42–13.77), *p*=0.735), nor the AUC (Fig 4.17).

4.4.4.5 Wieslab Assay

Complement functional activity using the Wieslab assay showed evidence of reduced classical pathway activity with argx-117 by the end of NR, with less clear separation earlier. At end-NMP, CP activity was 1.080 (1.080–2.664) in controls versus 0.870 (0.799–0.938) with argx-117, p=0.09. At the start of NR, CP activity was similar between groups (control 4.775 (4.171–5.378) vs argx-117 6.962 (3.886–7.340), p=0.833). By the end of NR, CP activity was lower in the argx-117, 3.328 (3.007–3.748) vs 7.095 (5.709–8.262) in controls, p=0.036, consistent with greater suppression of classical pathway function, principally due to C2 depletion.

Lectin pathway activity was markedly reduced with argx-117 at the end of NMP, with a persisting trend toward lower activity thereafter. At the end of NMP, LP activity was 0.533 (0.489–0.550) in controls versus 0.069 (0.067–0.078) with argx-117, p=0.036. At the start of NR, values remained lower in the argx-117 group but without statistical separation (control 0.094 (0.091–0.096) vs argx-117 0.058 (0.047–0.140), p=0.675). By the end of NR, LP activity remained numerically reduced (control 0.421 (0.211–0.672) vs argx-117 0.094 (0.000–0.193), p = 0.09). This provides evidence for the reduction of C2 present in the perfusate as a result of argx-117 (Fig 4.18).

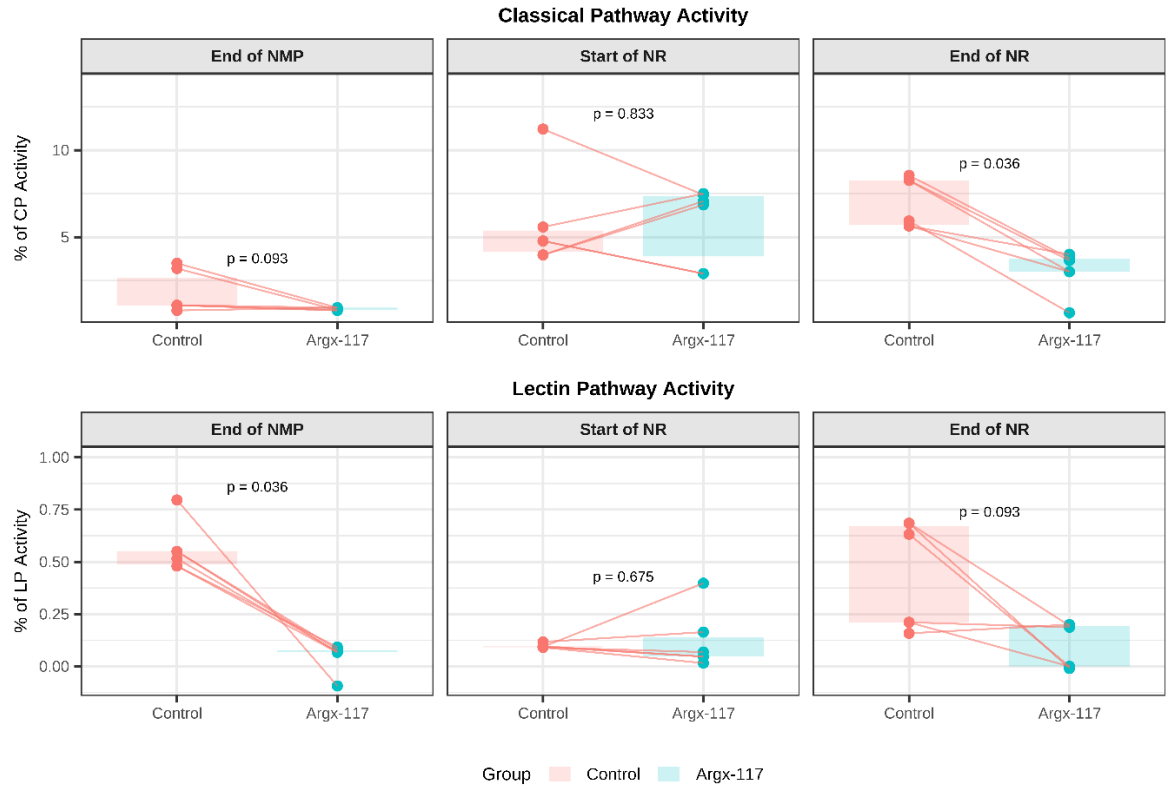


Figure 4.18 ***Functional classical and lectin pathway activity measured by Wieslab assay during paired perfusions with Argx-117.*** *Boxplots with paired connecting lines show percentage classical pathway (CP) and lectin pathway (LP) activity at the end of NMP, start of NR, and end of NR in matched control and Argx-117-treated kidneys. Each point represents an individual kidney, with paired lines linking contralateral kidneys from the same donor pair. At the end of NMP, classical pathway activity showed a numerically lower residual activity in Argx-117-treated kidneys though not statistically significant, while lectin pathway activity was significantly reduced, consistent with effective C2 blockade at this stage. At the start of NR, no clear between-group difference was evident for either pathway, with activity remaining low overall. By the end of NR, classical pathway activity was significantly lower in Argx-117-treated kidneys than in paired controls, while lectin pathway activity again trended lower without reaching statistical significance. Overall, these data demonstrate suppression of residual functional classical and lectin pathway activity by Argx-117 in the paired perfusion model, with Argx-117 suppression of C2 having a measurable mechanistic effect on those pathways in the perfusate.*

4.4.4.6 Tissue Complement Levels on Western Blotting & Native Gel Electrophoresis

Fresh frozen tissue from baseline, the end of NMP and the end of NR were used to assess C3 and its fragments by western blotting and C5b-9 by native gel electrophoresis. Quantitative analysis was normalised to β-actin on the same gels and statistical tests were done using a paired Wilcoxon.

Normalised intact C3 did not show any differences. At baseline, intact C3 was 769.58 (638.96–2,747.92) in controls vs 541.30 (438.67–1,859.69) with argx-117, p=0.90. At the end of NMP, values were 355.17 (203.69–541.49) vs 207.66 (175.72–217.66), p=0.71,

and at the end of NR 1,710.68 (844.66–2,492.32) vs 1,228.21 (724.45–2,029.02), p=0.90. Consistent with this, changes over time were also similar between groups, over NMP was −621.79 (−687.20 to −280.70) in controls versus −293.65 (−2,050.73 to −200.48) with argx-117, p=0.50, and over NR was 1,461.66 (1,063.03–2,513.79) versus 1,349.83 (681.27–1,495.35), p=0.86.

For C3 fragments, there was no convincing evidence of suppression with argx-117. Normalised C3dg was 137.89 (120.26–160.23) in controls vs 177.44 (96.68–262.12) with argx-117 at baseline, (p=0.80), 56.59 (33.39–118.68) vs 50.93 (37.76–54.41) at the end of NMP (p=0.50), and 383.94 (178.65–464.76) vs 245.41 (191.32–440.97) at the end of NR (p=0.34). The C3dg change over NMP showed a tendency toward a larger fall with argx-117 (controls −93.57 (−104.26 to 30.40) vs argx-117 −168.62 (−186.53 to −100.95)), but this did not reach significance (p=0.14). Over NR, changes were 289.76 (−14.04 to 408.44) vs 176.07 (−22.67 to 242.63) (p=0.50). Similarly, combined normalised C3d & C3dg showed no consistent separation, at the end of NR, C3d & C3dg was 1,004.50 (619.64–2,064.84) versus 1,125.45 (786.50–2,048.71), p=0.34.

Normalised C5b-9 was numerically lower with argx-117 at baseline and the end of NR, but differences were not statistically significant. At baseline, C5b-9 was 1,520.84 (939.32–1,774.40) in controls vs 521.74 (471.95–1,406.54) with argx-117, p=0.27. At the end of NMP, values were 1,833.20 (1,542.21–2,152.11) vs 2,084.49 (1,223.67–2,584.87), p=0.50. At the end of NR, C5b-9 was 1,981.04 (838.63–2,493.93) in controls vs 1,349.70 (1,055.61–1,825.28) with argx-117, with a non-significant trend in the expected direction, p = 0.15. Delta analyses were likewise non-significant, over NMP, the delta was 726.23 (44.78–1,741.91) in controls vs 893.48 (671.67–1,593.00) with argx-117 (p = 0.50), and during NR, the dela was −274.53 (−943.58 to 251.30) vs 64.18 (−1,564.65 to 697.50), p=0.61 (Fig 4.19).

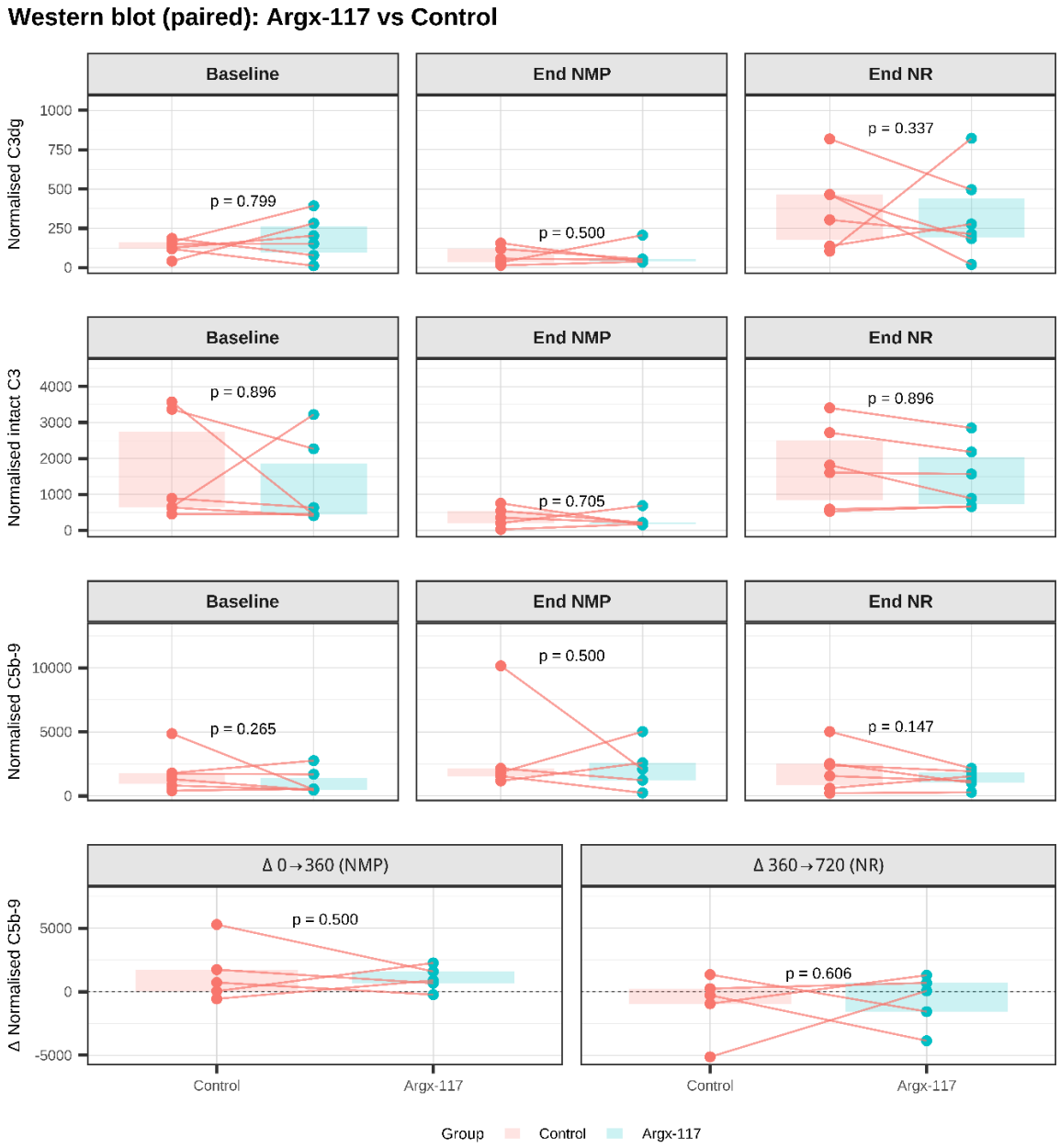


Figure 4.19 ***Western blot analysis of complement proteins in paired perfusions with Argx-117.*** *Boxplots with paired connecting lines show normalised band intensity for C3dg, intact C3, and C5b-9 at baseline, end of NMP, and end of NR, together with interval change in C5b-9 over NMP (0–360 min) and NR (360–720 min). Each point represents an individual kidney, with paired lines linking contralateral kidneys from the same donor pair. At baseline, end of NMP, and end of NR, there were no significant between-group differences in normalised C3dg, intact C3, or C5b-9 signal. Across the experiment, intact C3 was reduced at end NMP relative to baseline in both groups, with some increase by end NR, while C3dg and C5b-9 showed substantial inter-kidney variability. Analysis of interval change in C5b-9 demonstrated no significant difference between Argx-117-treated and control kidneys over either the NMP or NR phases. No clear treatment-associated reduction in complement deposition or breakdown products by western blot in the paired perfusion series.*

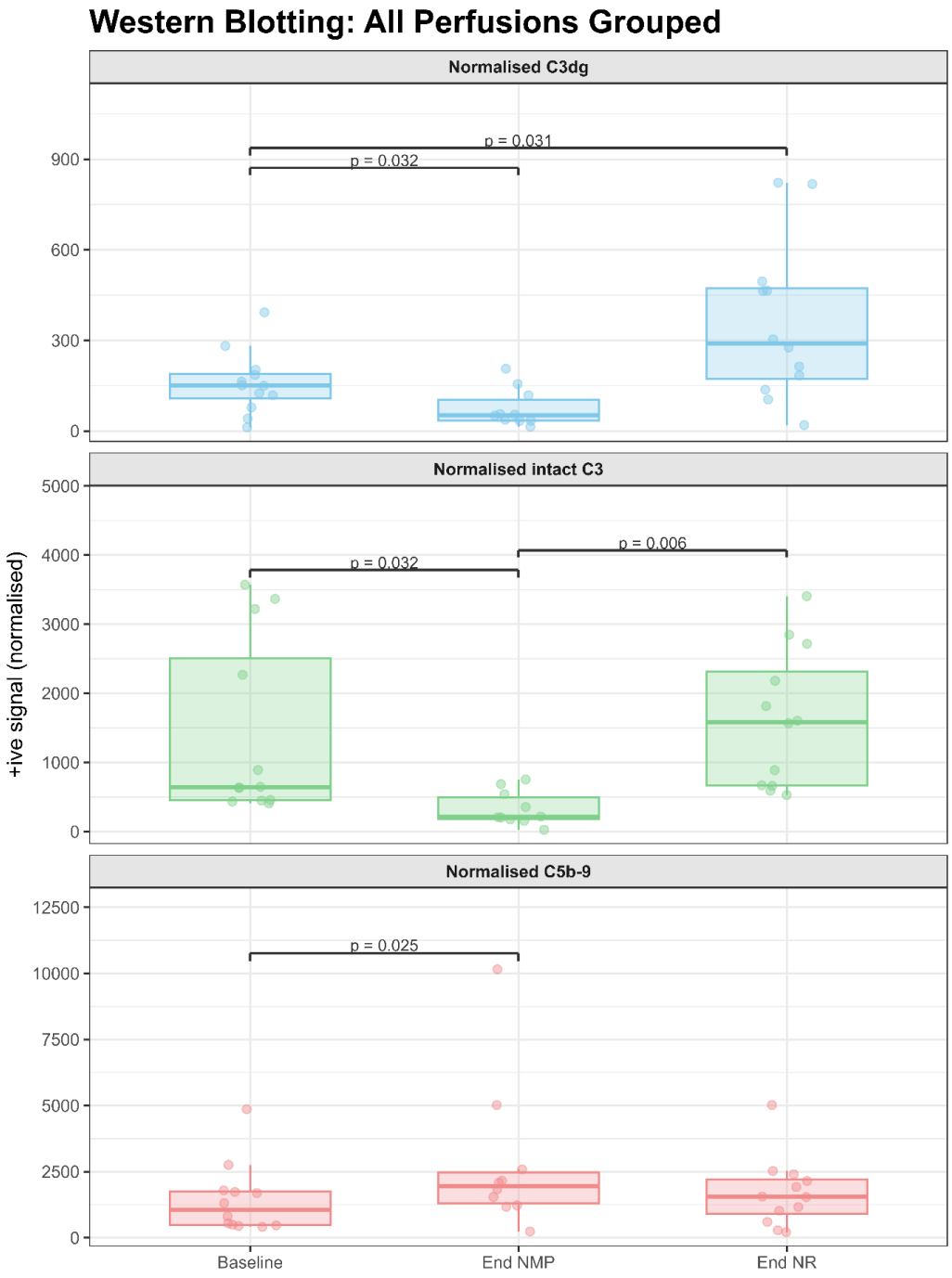


Figure 4.20 ***Western blot analysis of tissue complement across all perfused kidneys grouped by experimental timepoint.*** *Boxplots show normalised positive signal for C3dg, intact C3, and C5b-9 in biopsies taken at baseline, end of NMP, and end of NR, with all kidneys analysed together to increase overall sample size and characterise complement behaviour within the model. Overlaid points represent individual kidneys, and p values indicate significant pairwise comparisons shown on the figure. When all kidneys were considered together, C3dg was lower at end NMP than at baseline, but increased again by end NR, with significantly higher levels at end NR than at end NMP. Intact C3 showed a similar pattern, falling significantly during NMP and then increasing significantly after reperfusion, consistent with dynamic depletion and re-accumulation of tissue-associated C3 signal across the experimental course. By contrast, C5b-9 increased during NMP relative to baseline, indicating progressive terminal complement deposition during perfusion, but did not change significantly further by end NR.*

Taking all the perfusions as a single group (irrespective of treatment allocation) and assessing within-perfusion change, there was evidence of dynamic effects on C3 and its fragments across the perfusion–reperfusion sequence (Fig 4.20). Normalised C3dg fell significantly from baseline to the end of NMP (median delta of −102.60, IQR −159.01 to −4.12, p=0.032), but then increased by the end of NR relative to baseline (+193.63, IQR 50.45–340.49, p=0.031), with the end-NMP to end-NR rise not meeting conventional significance (+209.35, IQR −17.87 to 378.77, p=0.083). Critically, there was a significant baseline to end of NR increase in C3 fragment deposition (+193.63, IQR 50.45–340.49; p = 0.031). In parallel, intact C3 showed a significant decline during NMP (−457.72, IQR −1709.85 to −220.53, p=0.032) followed by a marked increase during NR (+1405.75, IQR 776.71–2259.18, p=0.006). For C5b-9, there was an increase during NMP (+809.85, IQR 201.51–1704.68, p=0.025), but did not differ materially between baseline and end NR (−2.13, IQR −340.10 to 1146.42, p=0.610) nor between end NMP and end NR (−105.17, IQR −1409.39 to 585.95, p=0.476).

4.4.4.7 Tissue Multiplex IF

Quantitative CellDIVE analysis expressed as positive pixels per nucleus demonstrated a rise in C4d tissue deposition across the perfusion time-course when considering all perfusions together (Fig 4.21). Median C4d had a significant 4-fold change from 0.287 (0.023–1.071) at baseline to 1.107 (0.022–1.938) at the end of NR, p=0.021. The end of NMP was not significantly different from baseline (p=0.108) or end of NR (p=0.272).

Fibrin signal showed no consistent time-dependent accumulation, with positivity highest and most variable at baseline (0.406 (0.254–1.759)), falling to near-zero by the end of NMP (0.000 (0.000–0.358)) and remaining low at the end of NR (0.114 (0.000–0.736)), pairwise time comparisons did not meet conventional significance. ICAM-1 tissue levels were broadly stable over time (baseline: 10.975 (1.689–14.671); end of NMP: 11.110 (9.360–13.752), end of NR: 11.098 (10.029–13.395)) and no evidence of significant difference between time points (all pairwise p≥0.423).

When stratified by intervention, no convincing effect was observed for any marker at any timepoint with argx-117 treatment (Fig 4.21). For C4d, values were numerically higher, but not significant with argx-117 at the end of NR, 0.543 (0.016–1.131) vs 1.531 (0.578–

2.638), p=0.471. Fibrin did not differ between groups at any time point (all p≥0.435), despite low median signal at later timepoints. ICAM-1 also showed no group separation at any time point (all p≥0.676). Paired analyses within matched kidneys were concordant, with no evidence of a reproducible treatment-associated shift for C4d, fibrin, or ICAM-1 at any timepoint (all paired p≥0.371), indicating that argx-117 did not measurably alter these tissue proteins in this cohort.

C5b-9 staining was attempted on the CellDIVE platform, but the antibody performance on this cohort of tissue was very poor, with only artefactual uptake, such that unfortunately no quantitative analysis could be performed from the slides.

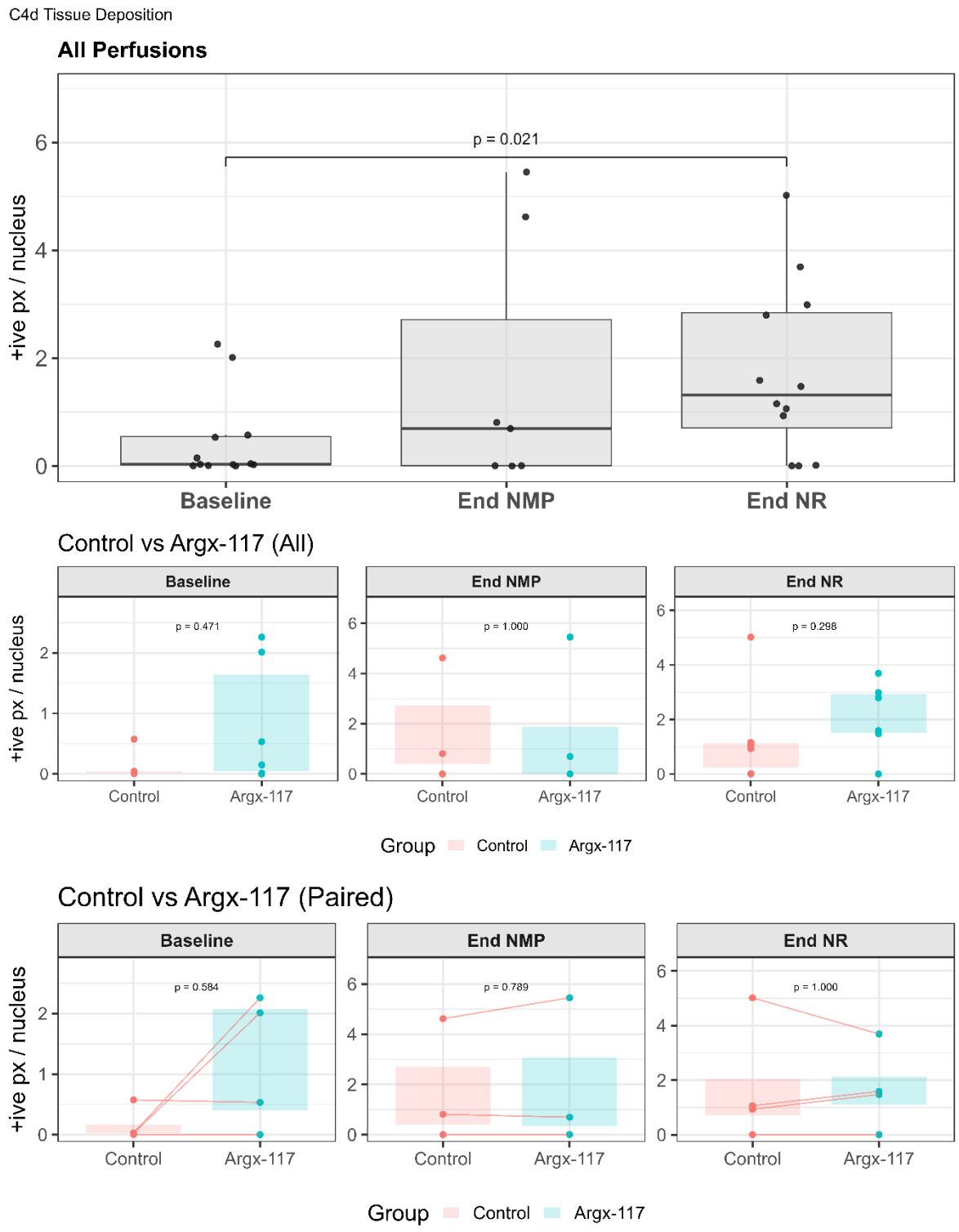


Figure 4.21 ***Tissue C4d deposition on multiplex IF across the perfusion model.*** *C4d positivity is expressed as positive pixels per nucleus and shown at baseline, end of NMP, and end of NR. The upper panel presents all perfusions grouped by timepoint to assess overall temporal behaviour within the model. The middle panel compares control and Argx-117-treated kidneys at each timepoint using all available samples. The lower panel shows paired comparisons between matched control and Argx-117-treated kidneys from the paired perfusion experiments. When all perfusions were analysed together, tissue C4d deposition increased over the course of the experiment, with significantly higher levels at end NR than at baseline. However, when kidneys were stratified by treatment group, no significant differences were identified between control and Argx-117-treated kidneys at baseline, end NMP, or end NR, either in the overall grouped comparison or in the paired analysis.*

4.5 Discussion

4.5.1 Model Development and Blood Only Perfusions

Perfusion experiments are relatively complex and dynamic with the potential for a lot of variability, and thus potentially difficult models to scrutinise subtle biological effects which can be influenced by a multitude of factors. Complement biology is challenging to characterise given it is a highly dynamic process on both cell surfaces and in soluble proteins, many of which are unstable with short half-lives and require carful sample handling. As such if using an NMP model, the basics of the circuit, perfusion, perfusate and control during perfusion must be as consistent as possible. The perfusions in the NKP1 clinical trial were hugely informative, both in the theory of stable kidney perfusion, but also in a practical sense from the cannulation to management of the kidney. Translating this back to a laboratory benchtop set up required optimisation, especially when adding a flush and reperfusion phase, and not using the OrganOx prototype.

After preliminary practice on abattoir porcine kidneys, the early human kidney perfusions using NHS blood products demonstrated that the model is technically feasible, but with an initial early thrombosis event that, as one might expect, the circuit with a plasma based perfusate is highly thrombogenic. Within NKP1 anticoagulation was used on the basis that packed red cells are likely to contain trace amounts of plasma, with NHSBT stating up to as much as 30ml. The red cells contain citrate, which is an effective anticoagulated in the storage, but as calcium replacement is required for normal homeostasis during NMP, not just for normal renal function, but also in the context of these experiments, for complement activation and argx-117 binding, extra anticoagulation is needed. For NKP1 fondaparinux was used, selected because it is a synthetically pure LMWH, it has almost exclusively renal clearance, meaning it has a longer half-life of 14-16 hours in a circuit in which the urine is recirculated. In the context of clinical NMP fondaparinux is a good choice, though for plasma reperfusion may not be optimal because it is a synthetic analogue of LMWH. This means it is exclusively short chains and as such produces a very predictable effect, with anticoagulation via conformational activation of antithrombin (AT), making it a more potent inhibitor of factor Xa. Unfractionated heparin also has longer chains, HMWH,

which are of sufficient length to bind both AT and thrombin, causing direct inhibition on thrombin. In a plasma rich perfusate in a highly thrombotic state, like that of cardiopulmonary bypass circuitry, this dual targeting produces an increased anticoagulant state. The reperfusion phase is only for 6 hours, rather than 24 hours of renal NMP, so the focus on half-life and endothelium saturation is less of a concern in the context of a model of this duration, making a switch to unfractionated heparin a good option. Switching from fondaparinux to heparin and an increased dose produced a stable NR phase and was take forward for the model.

Given the circuit is pro-thrombotic, a key baseline to establish is how activating the circuit is for the complement cascade. The previously mentioned evidence from cardiopulmonary bypass, ECMO and haemodialysis, with rises in C3a, C5a, and sC5b-9, led us to decide that the ex vivo kidney circuit should be assessed in the context of plasma NR. The three blood-only perfusions performed in a paired design with three different units of plasma were highly encouraging with regards the model. Firstly, with regards argx-117 performance in this context, C2 clearance was rapid, within the first minute of mixing with the circuit and suppresses perfusate C2 levels. There is a slight upward drift of C2 from a trough of inhibition in NR, but marginal from 0.052 µg/mL to 0.317 µg/mL. There are no cells present to internalise the bound C2 as per it's in-vivo mechanism of clearance so in this context is reliant on binding all available C2, which is does effectively compared with the untreated circuit at around 5 µg/mL, comparable to the quoted normal serum levels of 5-30µg/mL.

For products of activation, C3a, C4d, C3bBbP and C5b-9 all produce activation curves, but these are all much lower in magnitude compared with perfusions with the kidney in circuit and none of which exceed the quoted normal serum values. This is in keeping with the constant balance of complement activation and regulation seen in normal mammalian systems which can produce strong innate immune response rapidly. These blood only perfusions strongly support that the kidney, with its IRI, damaged endothelium and exposed activators are the driving force for activation in the model rather than the artificial surface activation in the circuit.

4.5.2 Single Kidney perfusions and Dose Assessment

Overall, these four pilot single-kidney perfusions demonstrated that the model delivered stable haemodynamics and blood gas control across NMP and NR, despite clear variability driven by blood quality and individual kidney performance. Argx-117 achieved rapid, sustained and dose-dependent C2 suppression, which was complete during NMP, with 100% at both doses, and to a high level of 84% to 95% and maintained throughout NR, confirming effective target engagement in this model. However, downstream readouts were heterogeneous: injury biomarkers generally rose over time with higher late elevations in the argx-117 kidneys, while C5b-9 formation was inconsistent between kidneys and only suggested possible attenuation in the high-dose NR perfusion. The tissue assessment of C5b-9 on IHC was limited by the small sample number and the quality of some of the slides; this limits robust conclusions, but taken as a pooled cohort they do seem to support that there is progressive C5b-9 deposition over the course of NR, in keeping with an activation process occurring at a cellular level rather than associated with the artificial surfaces within the circuit, which along with the evidence from the blood only perfusions is supporting evidence for the model.

Taken together, the data supported feasibility and pharmacodynamic activity of C2 blockade from argx-117, but that baseline complement levels and injury levels are highly heterogenous making elucidating differences in single kidney perfusions difficult or misleading. The findings support the development and switching to a paired kidney perfusion design, such that even subtle differences could be evaluated and trusted in a tightly controlled experimental design.

4.5.3 Paired Kidney Perfusions

The six paired kidney perfusion experiments were performed, and they were completed in a consistent manner with tight electrolyte control, with drifts in pH and osmolality consistent between the isotype controls and the argx-117 treated kidneys. Osmolality is one of the key factors in relation to free haemoglobin level, this is important in prolonged clinical renal NMP. The experimental cohort described here is not an ideal cohort in which to scrutinise this for a few reasons: (i) the blood are units not used for transfusion; (ii) the success of washing was variable, even if washed effectively, the

fragility of the cell membranes in unused and improperly stored blood is variable and after washing there could be an ongoing propensity for lysis which younger healthier red cells may not have; (iii) the circuit was modified specifically for this perfusion and is not the clinical specification OrganOx disposable set with large diameter pump as used in the clinical trial. However, when analysing all the perfusions as a group, accumulation was low, during NMP, as per NKP1 there was an accumulation of 0.05g/L/hr and during NR slightly more at 0.12h/L/hr, with no significant difference between start and end of either phase. This is supporting evidence that despite the model limitations, the perfusions are stable and consistent for red cell health.

Both groups had closely aligned arterial flows with the kidneys in each pair performing similarly with regards weight adjusted flow, as was the case with urine production. Urine production between pairs was quite variable as is normal, but within pairs there was no significant difference. The NR phase on average saw a greater urine production, though this is possibly simply an oncotic effect. In the NMP phase, especially at the start plasma protein levels are dictated by the added albumin, producing a perfusate protein (albumin) level of 35-40g/L, which is physiological level of albumin, though slightly low for total protein, in which a normal level is 60-80g/L. For NR, due to the need to have the same plasma across the perfusion a unit is split, with the minimum volume of NHSBT supplied FFP being 240mL, the design is such that each circuit receives 120mL, this produces a perfusate albumin level 10-15g/L, and a total protein level of 18-25 g/L. This reduced level of oncotic pressure may account for the urine differences, rather than a biological effect on the tubules because of the use of plasma rather than albumin in isolated perfusion.

For surrogate markers of potential attenuated complement damage, various perfusate markers were assessed, based on those of particular interest in NKP1. Despite the paired design and tightly controlled perfusions, overall, there was no clear pattern across the injury markers. NGAL during NR was the only marker to have a small but consistent and statistically significant reduction. This would possibly suggest subtle signs of reduced tubular injury.

As with the single kidney perfusions there was effective suppression and clearance of C2 in both phases, which was rapid and sustained, meaning the model achieved

effective antibody delivery with a clear, measurable pharmacodynamic effect on the target molecule. Using the Wieslab assay it was demonstrated that clearance of C2 causes a significant reduction in the capability of the classical pathway to be activated, which is supportive of the fact that the C2 depletion is biologically meaningful. However, despite this strong blockade this did not ultimately translate to any meaningful limitation in the formation of C5b-9 tested across two antibodies and assays. This suggests that in the context of this model and the IRI present in the untransplantable kidneys that terminal complement formation is not tightly or uniquely linked to the availability of C2 for CP and LP activity, such that C2 depletion alone was insufficient to suppress C5b-9 formation.

There was however some evidence of attenuation in markers upstream of C5b-9, during NR the amount of C3a formed and the amount of C3bBbP was significantly lower with C2 inhibition. This suggests the possibility that as a result of C2 clearance there is less CP and LP convertase (C4b2a) and as such there is less C3 hydrolyzation and release of C3a, and as a result attenuation in the formation of AP convertase (C3bBb) and its stabilised form C3bBbP. This may not then have a downstream effect on terminal formation, because the attenuation is only mild and there is sufficient buffering capacity in the system such that enough C5 convertase can be produced for a profound terminal complement formation regardless, meaning that it's possible that not vast amounts of C5 convertase are required to produce large amounts of C5b-9.

Across the tissue readouts, the plasma reperfusion phase provided clear evidence that this ex vivo model can drive measurable complement activation not only in the circulating compartment but also within the renal parenchyma itself. When perfusions were analysed as a pooled cohort, both western blotting and multiplex immunofluorescence demonstrated time-dependent accumulation of complement products in tissue, with significant increases in C3d/C3dg and C4d by the end of NR. These findings are important because they indicate that the model is not simply generating soluble activation products, but complement activation is occurring on, and being deposited within, biologically relevant renal structures exposed to ischaemia–reperfusion injury. In that sense, the combined perfusate and tissue data supports the

central premise that using plasma during NR recreates a transplant-like environment in which injured renal surfaces can initiate and sustain complement activation.

The pattern across the perfusion phases also provides mechanistic insight. During the NMP phase there was evidence of reduced intact C3 and activated fragments in tissue, alongside an increase in C5b-9, suggesting a modest level of ongoing complement turnover even before plasma re-exposure. This pattern is consistent with the kidney contributing endogenous complement substrates and driving limited activation on damaged cellular surfaces during NMP, reflected in parallel by rises in soluble markers. However, the most pronounced and consistent signals of complement activation are unsurprisingly in NR, aligning with the concept that the abrupt restoration of plasma proteins to an injured endothelium is a key driver of early post-transplant complement biology.

Despite the strong pharmacodynamic effect of argx-117 on its target (over 94% blockade in NR), there was no reproducible reduction in tissue complement deposition across the markers successfully quantified. In pooled analyses and matched-pair comparisons, tissue C3 fragments and C4d did not show a consistent treatment-associated shift, and the attempted CellDIVE C5b-9 staining was not interpretable due to poor antibody performance on the tissue. Taken together with the perfusate findings, the most likely interpretation is that C2 depletion achieved some degree of CP/LP functional suppression but was insufficient, on its own, to materially blunt the overall burden of complement deposition in the setting of severe IRI in declined kidneys in this model, because residual convertase activity remained adequate to sustain downstream activation, because alternative-pathway amplification and terminal pathway assembly were only modestly impacted, or because complement activation was already strongly primed by the extent of surface injury and thus relatively insensitive to upstream CP/LP restriction within the perfusion window of the experiment.

The strongest complement signal in this model lies in the perfusate, and that tissue sampling at the end of NR may underestimate the true magnitude and kinetics of terminal pathway accumulation. Once complement activation is initiated on injured renal surfaces, much of the terminal complex detected in the circuit may appear predominantly as soluble C5b-9 in the fluid phase rather than persisting as stable

membrane-inserted deposits. This is biologically plausible because nucleated cells can limit sustained membrane attack by shedding the C5b-9 complex in microvesicles and/or internalising it, meaning that tissue deposition can peak earlier and then diminish despite ongoing accumulation of sC5b-9 in the circulating compartment[165]. Hence the biopsies at the end of NR may provide only a late snapshot of the C5b-9 that may miss earlier peaks, whereas serial perfusate sampling integrates ongoing activation throughout reperfusion.

Finally, the divergence between high perfusate sC5b-9 and relatively modest residual tissue signal at the end of NR could also be explained by injury-linked export of C5b-9 positive material out of the tissue compartment. In a whole kidney undergoing reperfusion injury, vulnerable tubular and microvascular cells may detach, undergo necrosis, or lyse, and C5b-9-bearing membrane fragments or vesicles can then be washed into the perfusate[166]. This process would increase circulating sC5b-9 while leaving less residual staining in the remaining attached tissue that is subsequently sampled, supporting the interpretation that perfusate sC5b-9 is not merely a marker of static deposition, but measuring dynamic injury during reperfusion. In this context, correlating perfusate kinetics with tissue endpoints is essential, together they indicate that the model successfully induces complement activation during NR.

4.5.4 Model Limitations and Observations

This is of course a model: all models are wrong, but some are useful. The principal aim of the experiment is to attempt to effectively model complement activation in the context of renal IRI in the immediate post-transplant period in order to assess the possible effects of C2 inhibition. As discussed above there is evidence that this was achieved to some degree, however there are some important limitations to consider.

Firstly, to consider the perfusate composition for NR, FFP and pRBCs are not complete blood. The principal reason for this was practical, it being difficult to source whole blood, as it is not a readily used blood product clinically, and almost always it is still leukodepleted; FFP, however, is available in abundance and can be stored for long durations. While the FFP provides a ready source of complement proteins, which are stable during frozen storage[167], to facilitate cascade activation in its pure form, it does not contain white cells or platelets. This is important, white cells and platelets have

receptors for various fragments which play pivotal role in the response to the cascade and mediate the injury which is induced.

Neutrophils, dendritic cells (DCs), monocytes and macrophages all express the anaphylatoxin receptors C3aR and C5aR1/R2, as well as opsonin receptors. For Neutrophils C5a is a major driver of recruitment and activation, promoting chemotaxis[168], integrin upregulation, degranulation and oxidative burst[169], while CR3–iC3b interactions stabilise firm adhesion to activated endothelium and support phagocytosis and inflammatory effector functions[170]. Functionally, this can promote thrombo-inflammatory crosstalk by facilitating neutrophil–platelet aggregate formation (via platelet P-selectin/PSGL-1[171]) and, in some contexts, NETosis, which can further amplify complement activation on extracellular DNA/protein scaffolds[172].

For monocytes and macrophages C5a promotes recruitment and primes inflammatory activation programs, but it is their opsonin receptors which also have a prominent effect. They express CR1 (CD35), CR3 (CD11b/CD18) and CR4 (CD11c/CD18), which are important in surface bound C3 fragment interactions. Fragments such as iC3b bound to targets engage CR3/CR4 to drive adhesion, uptake and phagocytosis. The complement signalling in IRI type inflammatory settings, C5a-driven activation can support a more procoagulant monocyte phenotype with enhanced tissue-factor–linked activity[173].

DCs important activity is also through CR3/CR4, allowing complement to influence antigen capture, maturation and the quality of downstream T-cell priming[174]. Opsonised material carrying C3 fragments, again such as iC3b, can be taken up and leads to immune complex formations, while their C3a/C5a signalling affecting migration and cytokine signalling, thereby shaping the balance of T-helper differentiation and the intensity of adaptive responses[175].

For B cells, they are affected via CR2 (CD21), which binds C3d and C3dg (often carried on antigen or immune complexes), and can associate with co-receptors CD19 and CD81 to amplify signalling. When antigen is tagged with C3d/C3dg, co-ligation of BCR and CR2–CD19–CD81 lowers the threshold for activation[176], enhancing proliferation, germinal centre responses, antibody production and memory formation[177]. T-cells, in a

complement sense are governed by anaphylatoxins as they can express C3aR and C5aR1/C5aR2 and are influenced by locally generated complement signals. C3a/C5a signalling can modulate T-cell activation strength, survival, trafficking and differentiation, often by shaping APC cytokine output as well as through direct receptor engagement on T-cells[178]. These mechanisms are the central route by which complement fragments expand from innate to humoral immunity.

The perfusate is also missing platelets, which sit at the centre of complement-driven immune-thrombosis, integrating inflammatory complement signals with coagulation and leukocyte recruitment. Platelets can be activated by C5b-9 on their surface, which promotes platelet activation, granule release and a procoagulant shift, and platelet activation can be further supported, directly or via crosstalk by anaphylatoxins C3a and C5a. Once activated, platelets upregulate P-selectin (CD62P), enabling binding to leukocyte PSGL-1 and formation of platelet–neutrophil and platelet–monocyte aggregates that intensify leukocyte activation, promote endothelial adhesion and can facilitate NET formation[179]. Platelets also shed microparticles that are highly procoagulant and can carry complement fragments themselves, while platelet and leukocyte-rich aggregates create local surfaces that support further complement activation, forming a perpetuating cycle. This overall thrombo-inflammatory effect is a source of organ disfunction in the context of IRI endothelial injury with microvascular inflammation and clot propagation.

All that to say, the lack of platelets and white cells causes limitations on the biological interpretation, given clinically relevant downstream consequences of complement, particularly those mediated by anaphylatoxins and opsonins via leukocyte and platelet receptors. Consequently, the injury profile here is focused directly on the effects of complement on renal endothelium and epithelium, which will be under-representing the thrombo-inflammatory and leukocyte-driven components of IRI that would occur in a recipient. These constraints have important implications for interpreting inhibitor efficacy and for comparing different complement targets. For proximal blockade at the CP/LP convergence point, such as the C2 inhibition tested here, this model offers a clean test of mechanism, by removing cellular confounders, changes in pathway activity assays and downstream biomarkers can be attributed more directly to inhibition

of CP/LP convertase formation, with expected reductions in CP/LP-driven C3 activation and terminal pathway activity (reflected in suppressed C3a/C3 fragment generation and reduced sC5b-9). Nevertheless, because the model lacks leukocytes, it will not capture the full extent to which CP/LP blockade may mitigate cell-recruited injury in vivo through downstream reductions in C5a-mediated neutrophil/monocyte activation and endothelial–leukocyte interactions, meaning we may be underestimating the beneficial effects of C2 blockade.

For common pathway blockade, such as C5 inhibitors, the limitation could be even more pronounced. While the model can demonstrate suppression of C5 cleavage and C5b-9 formation and thus isolate direct C5b-9 related tissue effects, it inherently cannot demonstrate a major in vivo benefit mediated through prevention of C5a-driven leukocyte recruitment, activation and inhibition of platelet activation and immune-thrombotic propagation. Conversely, a strong protective effect of C5 blockade within this model would argue for a substantial role of direct C5b-9 related renal cell injury independent of circulating cells. For upstream C3 blockade, the model similarly allows rigorous demonstration of reduced opsonisation and downstream terminal activation but cannot address the full in vivo consequences of interrupting C3-fragment engagement with leukocyte complement receptors or altering immune-complex handling in the systemic circulation.

There is a further consideration to the absence of platelets and leukocytes, this may alter the apparent kinetics and compartmentalisation of complement activation products. In vivo, circulating cells act as both targets and sinks for complement fragments, provide additional activating surfaces, and generate complement-bearing microparticles; their absence may shift the balance towards fluid-phase accumulation of soluble activation products and may reduce secondary amplification loops that depend on cellular scaffolds. Therefore, discordance between high perfusate sC5b-9 and modest residual end-point tissue staining in this system should be interpreted in light of timing, shedding, solubilisation, and the known capacity of nucleated renal cells to limit stable membrane C5b-9 by internalisation or vesiculation[180,181], rather than taken to imply minimal tissue engagement. Overall, this model should be framed as a mechanistic platform to establish whether human plasma complement activates on

injured renal tissue under controlled reperfusion conditions, and whether a candidate inhibitor achieves biochemical pathway blockade and reduces direct complement-associated renal stress. Its translational limitation is that it cannot reproduce the full immuno-thrombo-inflammatory effector phase of transplantation and thus may underestimate the apparent clinical impact of inhibitors which have benefit in vivo via mediated through prevention of leukocyte recruitment and platelet-dependent microvascular injury.

Secondly, the model may provide a difficult test for an inhibitor in the context of an NMP organ with IRI. As mentioned, cellular components of blood can act as sinks for complement, so in this model all complement and potential activation is directed against the injured renal endothelium, which may yield artificially high levels of activation. This along with the kidney is in isolation on the circuit with no other healthy organ or vascular endothelium on which inhibitory regulation can occur. That being said, the circuit contains 120ml of plasma, approximately 4% of the normal volume of plasma in a human, which is not disproportionately high for a single organ.

Finally, the circuit itself has a role in activation, albeit it has been demonstrated that is relatively minimal, but none the less this could play a role in surface kinetics and amplification in the context of a very activated system with an injured kidney. Overall, the limitations of the model are important to consider, but it is a clean system in which to test the fundamental activation and inhibition of components within the cascade.

4.5.5 Concluding Remarks

A technically robust human ex vivo kidney reperfusion model has been established, combining NMP with plasma-based NR, generating complement activation in both perfusate and tissue. Blood-only experiments showed that the circuit itself caused only modest activation, whereas the presence of an injured kidney drove a much stronger complement response. In both single-kidney and paired experiments, argx-117 produced significant rapid depletion of free C2, confirming effective target engagement. In the paired design, this produced reduced residual classical pathway activity at the end of reperfusion, marked lectin pathway suppression at the end of NMP, and attenuation of C3a and C3bBbP during reperfusion.

Despite this clear biochemical effect on C2, argx-117 did not produce a consistent reduction in terminal complement activation or a broad physiological benefit in these declined kidneys with severe IRI. Perfusate sC5b-9 remained high and similar between groups, and tissue complement deposition on western blotting, multiplex IF, and IHC showed no reproducible treatment-associated reduction. Functional and biochemical perfusion parameters were comparable between groups, although paired kidneys treated with argx-117 showed modest evidence of reduced tubular injury, with significantly lower NGAL during and at the end of reperfusion. Overall, the findings suggest that C2 inhibition in this model achieved strong mechanistic blockade of CP/LP activity, but this alone was insufficient to meaningfully suppress downstream terminal complement formation or substantially alter the overall burden of reperfusion injury.

4.5.6 Further Work

Given this is not a membrane bound molecule and its target, C2 is a in circulation prior to cascade activation, argx-117 is a therapy that could be delivered to the donor or recipient but is likely of limited benefit in a preservation capacity. There is good evidence for spikes of complement activation in brain death, particularly in the early phase, and based on evidence discussion in chapter 3 this early priming in the donor is a marker of injury, and possibly an ongoing mediator in IRI during storage and possibly implantation. An exploratory study into donor delivered complement inhibition would be of interest and possibly yield organ protection during brain death and organ retrieval. C2 is a reasonable target to consider because its relatively low levels compared to other more abundant complement proteins, given the amount of antibody required is a manageable amount compared to for example C3 blockade.

For donor treatment its limitation, is possibly what we have observed here with incomplete cascade inhibition, the residual CP/LP and unblocked AP can continue and cause complement injury. Given there is less consequence to complete innate immunity blockade in donor a complete strategy may be more advantageous. This short coming as a donor therapy is what may make it attractive as a recipient therapy, as in the immunosuppressed patient there isn't complete blockade of the innate immune system. The possible utilisation as a supplementary induction agent to mediate IRI with

an aim to improve early function as well as possible ABMR is an interesting possibility, hence the design of their phase 2 study. The model is established and produces a good complement response such that it is an appropriate platform to test alternative inhibitor strategies, such as mirococept.

5

Assessing C3b Inhibition in NMP and Normothermic Reperfusion

Contents

5.1 Introduction

5.1.1 Mirococept, Mechanism & Pre-clinical Development

5.1.2 EMPIRIKAL, Porcine Dose Finding & EMPIRIKAL-2

5.1.3 Mirococept and NMP Delivery

5.2 Aims & Objectives

5.3 Methods

5.3.1 Kidney allocation and Perfusions

5.3.2 Perfusate Analysis

5.3.3 Tissue Analysis

5.3.3.1 Western Blotting and Native Gel Electrophoresis

5.3.3.2 C5b-9 IHC and Quantification

5.4 Results

5.4.1 Dose Assessment Perfusions

5.4.1.1 Perfusion Parameters and Blood Gas Analysis

5.4.1.2 Perfusate C5b-9 Formation

5.4.1.3 Tissue Complement on Western Blotting & Native Gel Electrophoresis

5.4.2 Paired Perfusions

5.4.2.1 Perfusion Parameters and Blood Gas Analysis

5.4.2.2 Perfusate Injury Biomarkers

5.4.2.3 Perfusate Complement Proteins

5.4.2.4 Tissue Complement on Western Blotting & Native Gel Electrophoresis

5.4.2.5 C5b-9 IHC

5.5 Discussion

5.5.1 Dose Finding Perfusions

5.5.2 Paired Perfusions

5.5.3 The Model & Its Limitations

5.5.4 Overall Conclusion & Translational Implications

5.1 Introduction

5.1.1 Mirococept, Mechanism & Pre-clinical Development

The complement activation that takes place upon recipient reperfusion is key in IRI. The amplification of sterile inflammation via anaphylatoxins (C3a, & C5a), leukocyte recruitment, endothelial activation and ultimately direct tissue injury from C5b-9 formation causes organ damage and immune priming[72,73,182]. Within transplant complement therapeutics, the optimal treatment is something which can modulate complement behaviour within the transplanted organ, without disrupting systemic complement activity vital in the immunosuppressed patient.

Mirococept (also known originally as APT070) is a membrane-localising inhibitor derived from human complement receptor 1 (CR1/CD35), a regulator causing inhibitory activity via binding of C3b and C4b[183]. The binding of C3b and C4b causes both decay-accelerating activity, disrupting C3 and C5 convertases and increased Factor I activity, promoting proteolysis of C3b and C4b[184]. Together this causes inhibition of classical, lectin and alternative pathways upstream of the level of C3 activation and amplification, thus reducing formation of C3a, C5a and C5b-9 (Fig 5.1). The membrane localising element comes from a membrane-targeting amphiphilic peptide and a membrane-inserting myristoyl group so it can insert into lipid bilayers allowing it to be anchored to endothelial surfaces, making it an excellent candidate for ex-vivo delivery.

In reality, mirococept only contains the first three SCR domains of the LHR-A of CR1, which is fused to its myristoylated peptide tail, to create the inhibitor in its current form: the programme of work which resulted in this, was initiated by Professor Richard Smith and colleagues in the late 1990s & early 2000s. The development of mirococept was iterative and began with the generation of the SCR1-3 fragment years before with the successful expression and purification of these domains from *E.Coli* with yields of 6-15mg/L, it was then subsequently demonstrated the fragment had cofactor affinity to C3b and C4b and similar decay accelerating activity as the complete domain[185]. It was however less potent than complete CR1 at pathway inhibition, to overcome this a cysteine residue was added at the C-terminus of SCR1-3 (creating APT898), this could then have a membrane localising peptide (APT542) chemically coupled to it via

disulphide bonds forming the finalised molecule, mirococept (ATP070)[186]. Comparing the modified molecule, mirococept to the unmodified APT898 (SCR1-3), in human and rat assays, mirococept had a >100-fold increase in affinity[187,188].

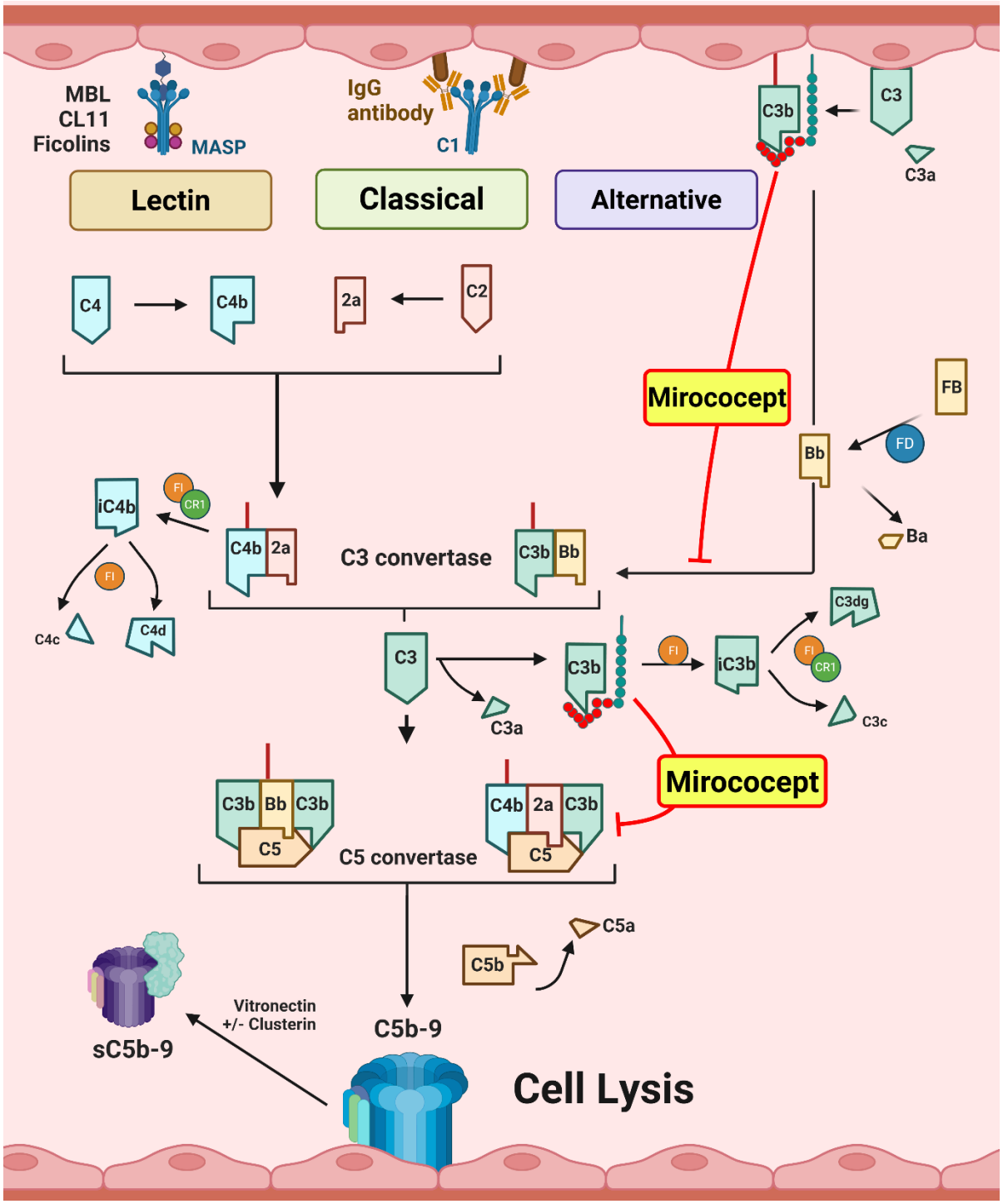


Figure 5.1 ***Schematic overview of the complement cascade and mechanism of action of mirococept****. Complement activation is initiated through the lectin, classical, and alternative pathways. The lectin pathway is triggered by pattern-recognition molecules including MBL, collectin-11 (CL11), and ficolins in association with MASPs, while the classical pathway is initiated by C1 binding to IgG-containing immune complexes. These pathways converge at cleavage of C4 and C2 to generate the classical/lectin pathway C3 convertase, C4b2a. The alternative pathway proceeds through spontaneous C3 activation and formation of the C3bBb convertase, with factor B and factor D*

driving amplification. Mirococept is shown acting at the level of C3/C5 convertase activity on tissue-bound complement activation products through its CR1-derived inhibitory domains and membrane-localising tail. By targeting sites of complement activation on cell membranes, mirococept is intended to inhibit C3 activation and amplification, thereby limiting downstream generation of C3 breakdown products, C5 cleavage, and terminal pathway activation to C5b-9. This schematic illustrates the rationale for assessing mirococept in NMP delivery as a strategy to reduce complement-mediated injury.

Mirococept was investigated in various rat, mouse, and pig models for a spectrum of disease states, Miller-Fisher syndrome, Intra-vascular shock, antigen-induced arthritis, acute MI, intestinal IRI and to this study, rat renal transplant models[186,188-192] (Table 5.1). In the context of renal IRI and transplantation, the addition of mirococept to the cold perfusion fluid, resulted in binding to the glomerular endothelium and tubular epithelial cells. This was done prior to syngeneic renal transplant in a rat model. The mirococept perfused organs had improved graft function for up to 20 weeks. In the early post-transplant period, 24-hours post-op there was reduced acute tubular necrosis, neutrophil activation, lower blood urea nitrogen levels, and lower levels of complement deposition[184]. Its potential for reducing complement activity within an implanted renal graft without systemic complement disruption was an attractive prospect and led to investigation in a human clinical setting.

Species	Experiment / model	Route of administration	Dose(s)	Design	Outcome Measures	Effect	References
Rat	Antigen-induced Arthritis	intra-articular	90 & 250 µg/joint	Prophylactic local treatment given intra-articular at arthritis induction	Arthritis severity (joint swelling/clinical score), histology (synovitis/cartilage/bone injury) and some local complement/inflammation markers	Protective	Linton *et al* (2000)[186]
Rat	Intravascular shock	intravenous	up to 5 mg/kg	Prophylactic / early treatment in systemic inflammatory shock model	Survival and haemodynamics, plus organ injury/inflammation readouts (vascular leak, neutrophil infiltration, cytokines/complement activation markers)	Protective	Smith and Smith (2001)[191] Smith (2002)[192]
Rat	Kidney Allograft	Perfusion	40 µg/mL	Prophylactic ex vivo grafts during donor kidney perfusion before implantation	Early graft injury and function (serum creatinine/urea, urine output), histologic injury, and complement deposition in the graft (C3 and C5b-9)	Protective	Smith (2001)[191] Smith (2002)[192] Pratt *et al* (2003)[190]
Mouse	Miller-Fisher Syndrome	intravenous	580 µg/mouse	Prophylactic treatment given before complement-mediated neuromuscular injury	Neuromuscular junction (NMJ) protection, typically assessed by C5b-9 deposition and structural integrity of motor nerve terminals/perisynaptic Schwann cells	Protective	Halstead *et al* (2005)[189]
Mouse	Miller-Fisher Syndrome	intravenous	580 µg/mouse	Therapeutic treatment given after injury trigger/antibody exposure	NMJ injury reversal/prevention progression: reduced C5b-9 deposition and preserved NMJ morphology/function	Protective	Halstead *et al* (2005)[189]
Rat	Intestinal IRI	intravenous	1, 3, 10 mg/kg	Prophylactic treatment administered before reperfusion/IRI	Intestinal and remote lung injury: vascular permeability, neutrophil influx, haemorrhage, tissue/serum cytokines, and mortality	Protective	Souza *et al* (2005)[188]
Rat	Kidney Allograft	Perfusion	40 µg/mL	Prophylactic ex vivo perfusion delivery pre-implantation	Graft function + injury (biochemistry/urine output), histology, and tissue complement activation/deposition	Protective	Patel *et al* (2006)[184]
Pig	Acute Myocardial Infarction	intra-coronary	0.5 mg/kg	Peri-ischaemia/reperfusion treatment delivered locally into coronary circulation at/around reperfusion	Infarct size and myocardial injury, LV function and complement deposition/inflammation within myocardium	Protective	Banz *et al* (2007)[193]

Pig to Baboon	Heart Xenograft	Perfusion & Intravenous	0.1 mg/mL (perfusion) & 3 mg/kg (2 doses i.v.)	Prophylactic with ex vivo perfusion and plus peri-transplant systemic dosing	Xenograft survival and function, haemodynamics, and complement-mediated rejection/injury markers (C3/C4d/C5b-9 deposition on histology)	No effect	Wu *et al* (2007)[194]
Rat	Hind Limb IRI	intravenous	9 mg/kg	Prophylactic / peri-reperfusion systemic dosing	Skeletal muscle IRI outcomes: oedema, microvascular perfusion, muscle necrosis/enzymes, histology and inflammation/complement deposition	No effect	Duehrkop *et al* (2013)[195]
Human to Mouse	human islet Xenograft	*in vitro*	0.4 µM	Prophylactic treatment of islets before transplant	Complement deposition on graft (quantified C4d and C5b-9), and islet graft function/survival (glycaemic control, graft histology)	Protective	Xiao *et al* (2016)[196]
Human	healthy volunteers - Phase I	intravenous	2, 5, 10, 20, 40, 70, 100 mg	Dose-escalation safety/PK study	Safety/tolerability (AEs, labs), pharmacokinetics, and systemic complement activity markers	safe and well tolerated	Smith *et al* (2007)[183] Kassimatis *et al* (2017)[187]
Human	Kidney transplant - Phase IIa	Perfusion	10 mg	Randomised, double-blind, placebo-controlled; ex vivo donor kidney perfusion treatment pre-implantation	Delayed graft function plus early graft function and safety endpoints	No effect	Kassimatis *et al* (2017)[187]
Human	Kidney transplant - Phase IIb	Perfusion	10 mg	Randomised, double-blind (expanded/confirmatory cohort at same low dose)	DGF incidence and early graft outcomes (function, safety, mechanistic biomarkers)	No effect	Kassimatis *et al* (2021)[88]
Pig	Kidney transplant - Dose finding	Perfusion	20, 40, 80, 160 mg	Ex vivo dose-finding perfusion study assessing binding/retention and biological effect	Graft binding/retention of inhibitor, tissue histology for injury and perfusion parameters	80mg dose suitable (120mg human equivalent)	Kassimatis *et al* (2021)[88]

Table 5.1 ***Table summarising the published use of Mirococept (APT070) across animal models, xenotransplant settings, human islet studies, healthy volunteer trials, and kidney transplantation****. Studies are organised by species and model, with details of route of administration, dose, study design, principal outcome measures, and overall reported effect. Across most pre-clinical inflammatory and ischaemia–reperfusion models, Mirococept demonstrated protective effects in many studies, with reductions in complement*

deposition, tissue injury, and functional impairment. In kidney transplantation, experimental perfusion studies supported graft binding and biological activity, which informed subsequent clinical evaluation; however, phase II trials in human kidney transplantation did not demonstrate a reduction in delayed graft function at the doses tested.

5.1.2 EMPIRIKAL, Porcine Dose Finding & EMPIRIKAL-2

Mirococept was initially tested in healthy volunteers with intravenous administration of incremental doses from 2-100mg was safe and well tolerated. This led to the design of a phase 2 trial (EMPIRIKAL), in which in which mirococept was added to the static cold storage solution (Soltran) and flushed into the kidney, then the inflow and outflow clamped to retain the drug loaded perfusion solution in the organ for 1 hour, with the primary endpoint being DGF rate. Within the phase 2a study 16 patients received a renal transplant that had been treated with 10mg of mirococept, which was reported to be well tolerated and with around 80% of the drug retained within the tissue, assessed using a specially manufactured mirococept labelled with pegylated fluorescein. There was no effect on systemic complement activity, and with a 'trend' to a lower serum creatinine in those treated kidneys. This was taken forward into the 2b EMPIRIKAL trial, originally designed to test 5-25mg in cohorts of 80 patients. After completing cohort 1 with 10mg there was no efficacy signal and the funding body recommended terminating the study, prompting the investigators to conduct a dose finding study in pigs before continuing with human investigation[88].

To assess tissue binding with increased doses a series of porcine experiments were conducted. The same pegylated fluorescein labelled mirococept was delivered in 4 escalating doses of 20, 40, 80, and 160mg to 4 kidneys per dose and 4 kidneys used as controls, flushed only with Soltran. The kidneys received cold flush containing mirococept and following 1-hour of storage, biopsies were taken to assess tissue uptake, which showed that the porcine glomeruli were saturated at 80mg. They determined that 80mg (by weight equivalent to 120mg in human kidney) was the optimal dose, then performed a washout study using a higher dose of 120mg, determining around 12.5% of the mirococept was flushed out of the kidneys upon reperfusion, which was well within the safe systemic dose range determined from the administration to healthy volunteers. A surrogate safety assessment was also conducted on 3 porcine kidneys in which the optimal dose of 80mg was delivered in SCS and then the kidneys underwent 3 hours of NMP with autologous whole blood to mimic transplantation. The safety assessment was focused on histology, acute tubular injury and rudimentary perfusion data (blood flow, intrarenal resistance, and

temperature), there were no differences between the 3 mirococept kidneys and the 2 control kidneys across the parameters. There was no assessment on complement behaviour during the whole blood NMP to assess for any mechanistic effects on activation during reperfusion and early post-transplant.

Following the dose finding study, the funding body (MRC) refinanced the clinical trial to continue with 3 cohorts of higher doses, 60, 120 and 180mg with a total of 144 patients randomised. Recruitment for the study is currently underway.

5.1.3 Mirococept and NMP Delivery

There three key questions to consider about the use of mirococept around NMP, (i) does it work in reducing complement activation and injury during NMP and/or upon recipient reperfusion, (ii) is NMP a more effective way to deliver it, and (iii) are there any safety issues with its use in NMP. The porcine dose study demonstrated that the equivalent of 120mg provided good glomerular uptake in SCS with around 12.5% washout on whole blood reperfusion[88].

The biophysics of the membrane anchoring involved in mirococept are relevant to is mode and temperature of delivery when considering SCS compared with NMP. The membrane localisation is not a receptor-ligand interaction, but a physiochemical one with the lipid bilayer as a result of its two engineered elements. First, the membrane-targeting amphiphilic peptide containing both hydrophobic residues (interact with lipid tails) and polar/charged residues (interact with headgroups)[188]. Second, the covalently attached myristoyl group a long hydrophobic alkyl chain structurally similar to endogenous lipid modifications (e.g. N-myristoylation of Src kinases). The effect of these together cause mirococept to behave like a peripheral, lipid-anchored membrane protein rather than a soluble protein[197]. As such the membrane insertion is determined by a combination of forces, the dominant being a hydrophobic interaction. The myristoyl chain inserts into the hydrophobic core of the phospholipid bilayer. This is entropically favourable because it removes hydrophobic surface from contact with water, similar to how fatty acids, detergents, and lipidated proteins associate with membranes. This interaction is reversible, but the strength increases with lipid fluidity within the membrane, lipid fluidity would be greater at physiological temperatures. Once inserted

there are stabilising Van der Waals interactions, the myristoyl chain packs against acyl chains of phospholipids. These weak, cumulative interactions stabilise residence time within the membrane, which is sensitive to lipid packing density[198]. The subsequent electrostatic interactions are secondary, but important for positioning and orientation[199]. The amphiphilic peptide contains positively charged residues (e.g. Lys, Arg) which interact electrostatically with negatively charged phospholipid headgroups, phosphatidylserine and phosphatidylinositol phosphates. This keeps the mirococept molecule oriented correctly at the membrane surface, reducing dissociation once the lipid tail is inserted. There is also a degree of hydrogen bonding at the membrane interface, with polar residues forming transient hydrogen bonds with lipid headgroups and interfacial water stabilising the resting position of mirococept.

Given that temperature has a profound effect on lipid bilayers, it therefore theoretically would also have a marked effect on mirococept binding. At 4°C the membrane is in a solid-ordered state with the lipids tightly packed and rigid, whereas at 37°C the membrane is a liquid-crystaline state with far more fluid and dynamic lipids. At 4°C the lipid acyl chains are tightly packed with low lateral diffusion and reduced membrane defects[200,201]. This means that for mirococept the myristoyl insertion is energetically less favourable with fewer transient gaps in the bilayer for insertion. The effect on its anchoring could be that it is slower, more superficial, and more reversible. Meaning at 4°C mirococept can associate with membranes, but at lower insertion depth, possibly with shorter residence time and that some binding likely relies more on electrostatic peptide–headgroup interactions than deep lipid insertion. Conversely at 37 °C the membrane will have high lipid fluidity and increased lateral diffusion, with frequent transient packing defects allowing for more insertion. The overall effect for mirococept could be hydrophobic insertion becomes strongly favourable, the myristoyl chain inserts more deeply and stably and the amphiphilic peptide embeds at the lipid–water interface[197]. Potentially resulting in more effective coating of endothelium with higher local surface density which could in turn lead to greater functional complement inhibition.

The combined pre-clinical animal work, safety in humans with SCS and the theoretical benefit of normothermia on membrane integration make investigating mirococept with NMP delivery a logical next step.

5.2 Aims & Objectives

This chapter aimed to assess whether mirococept, a membrane-localising CR1-derived complement inhibitor, could be effectively delivered during NMP and whether this altered complement activation during NMP itself and during subsequent plasma-based NR. A further aim was to determine whether any effect on complement behaviour was accompanied by measurable differences in renal perfusion, biochemical function, injury biomarkers, and tissue complement deposition. To address this, an initial dose-assessment series was performed to compare NMP delivery with static cold storage delivery and to identify a suitable NMP dose for subsequent paired kidney perfusions.

Objectives:

- To assess the feasibility of delivering mirococept during normothermic machine perfusion.
- To explore whether different NMP doses of mirococept produced measurable differences in complement behaviour in perfusate and tissue.
- To identify an appropriate NMP-delivered dose of mirococept to take forward into paired kidney perfusions.
- To characterise complement activation during NMP and subsequent plasma-based NR in kidneys treated with mirococept.
- To determine whether mirococept reduced perfusate complement activation products, particularly C3d and C5b-9.
- To assess whether mirococept reduced tissue complement deposition, including C3 fragments and C5b-9.
- To examine whether mirococept treatment was associated with changes in renal perfusion parameters, urine production, and biochemical measures of function.
- To assess whether mirococept altered perfusate injury biomarker profiles during NMP and reperfusion.

- To evaluate, in a paired human kidney perfusion design, whether NMP-delivered mirococept attenuated early complement-mediated renal injury in this ex vivo reperfusion model.

5.3 Methods

5.3.1 Kidney allocation and Perfusions

Initially five human kidneys deemed unsuitable for transplantation were acquired through NHS BT research organ offering scheme under ethics for this series of perfusions. A random allocation order determined by random number generator was used to assign the kidneys to their intervention. One kidney received 120mg of mirococept in SCS as per the EMPIRIKAL clinical trial protocol, two kidneys received 120mg delivered during NMP (the optimal dose for SCS determined by the porcine dosing study) and two kidneys received 60mg during NMP. For the kidneys that underwent NMP, this was done over 6 hours as per the NKP1 trial protocol discussed previously using the OrganOx Kidney prototype. Following NMP, kidneys were flushed with 500ml of cold UW at 30 mmHg and the circuit flushed and replaced with plasma based perfusate.

After SCS or NMP all kidneys underwent a 6-hour NR using a plasma based perfusate containing physiological levels of complement proteins from assessment of baseline perfusate. During NMP and NR standard perfusion parameters are continually measured as well as blood gas analysis throughout the phases. The perfusions are optimised throughout to ensure as far as possible the kidneys are in consistent conditions as close to normal physiology as possible.

After the series of single perfusions, 4 pairs of human kidneys deemed unsuitable for transplant were acquired in the same way. Again, there was a random sequence generated in which one of the kidneys in the pair would be allocated 60mg or 120mg of mirococept delivered during NMP. Whether the right or left kidney was allocated to treatment was also randomised. As previously, both kidneys underwent 6 hours of NMP, then a flush followed by 6 hours of plasma-based NR (Fig 5.2).

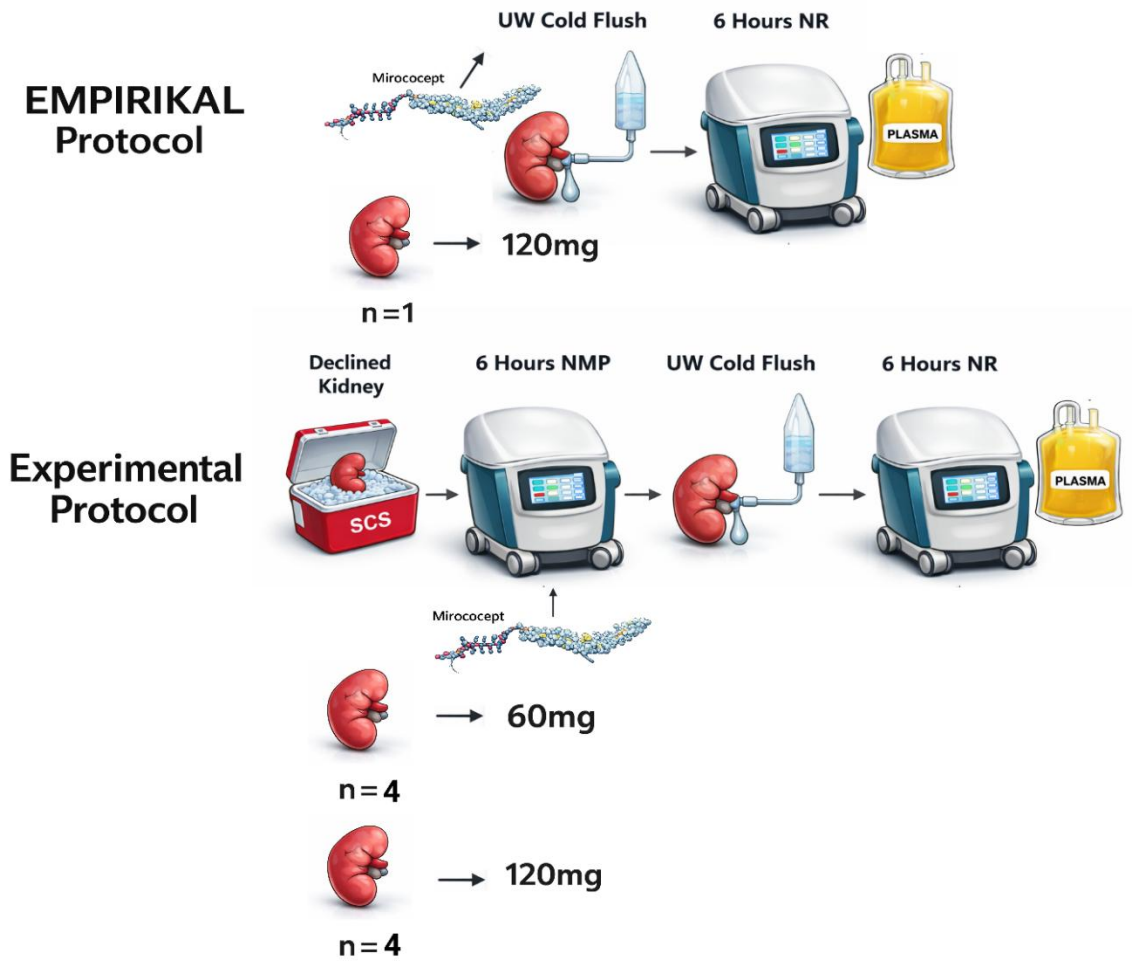


Figure 5.2 ***Schematic overview of the Mirococept dosing for the protocols across all the perfused kidneys.*** *In the initial single-kidney series, human kidneys declined for transplantation were randomly allocated to receive 120 mg Mirococept SCS, n=1 according to the EMPIRIKAL protocol, or 60 mg or 120 mg delivered during 6 hours of NMP, n=2. In the subsequent paired-kidney experiments, one kidney from each donor pair was randomly allocated to receive 60 mg (n=2) or 120 mg (n=2) Mirococept during NMP, while the contralateral kidney served as control. Following SCS or NMP, kidneys were flushed with cold UW solution and underwent 6 hours of plasma-based NR.*

5.3.2 Perfusate Analysis

The perfusate underwent laboratory biochemical assessment and ELISAs for injury biomarkers and complement proteins as done in previous chapters and described in the common methods.

5.3.3 Tissue Analysis

5.3.3.1 Western Blotting and Native Gel Electrophoresis

Using fresh frozen tissue from baseline, end of NMP and end of NR traditional western blotting or native gel techniques were used to assess tissue levels of C3d and C5b-9 as per the technique described in detail in the common methods.

5.3.3.2 C5b-9 IHC and Quantification

Immunohistochemistry (IHC) for terminal complement complex (C5b-9) was performed on FFPE sections using a Leica Bond RXm autostainer (Bond™ protocol F30). Slides were baked (30 min, 60°C), dewaxed using Bond Dewax Solution (72°C), and rehydrated through alcohols. Heat-induced epitope retrieval was carried out with Historeveal (Abcam, #ab103720) for 5 min, followed by Bond Wash steps and endogenous peroxidase blocking with 3–4% (v/v) hydrogen peroxide for 5 min. Sections were incubated with the primary antibody (TCC/C5b-9, 1:200) for 30 min at room temperature, then processed using the Bond Polymer Refine Detection Kit (Leica, #DS9800) with a rabbit anti-mouse post-primary reagent and an anti-rabbit poly-HRP polymer (8 min each). Signal was developed with DAB for 10 min, counterstained with haematoxylin for 5 min, rinsed in water, and mounted with Aquatex. Whole slide brightfield imaging was performed on a PhenoImager HT (Akoya Biosciences; software v2.1.0) at 40× magnification (0.25 µm/pixel).

For quantitative analysis of C5b-9 whole-slide images (QuPath pyramidal. qptiff) from this single experimental batch were quantified using a tissue-first, stain-separation workflow implemented in Python (NumPy/pandas/scikit-image; tifffile, with optional OpenSlide support). For each slide, a downsampled pyramid level was selected to balance speed and stability (targeting a maximum image dimension of ~2.2k pixels while preventing excessive downsampling by forcing a higher-resolution level when the chosen level's minimum dimension was <900 px). Images were converted to RGB and a tissue mask was generated against a white background using combined colour-space thresholds (HSV value and CIE-Lab lightness) with Otsu thresholding, followed by morphological clean-up to remove small objects, close gaps and fill holes; the largest connected tissue components were retained as the working tissue mask. These were

manually quality control (QC) checked to ensure all tissue was included, with no artifact or inappropriate tissue islands. Edge effect removed by automated exclusion of 25 pixels around margin of working mask.

C5b-9 (DAB) signal was quantified after colour deconvolution (HED) to extract the DAB channel. To minimise slide-to-slide differences in illumination and background, each slide's DAB channel was background-referenced by subtracting the median DAB value from non-tissue pixels (glass), with negative values clipped to zero. A single global DAB positivity threshold for the batch was then derived from pooled background pixels across all slides (high-percentile of background DAB multiplied by a small safety factor). DAB-positive area was reported as the fraction of tissue pixels exceeding this global threshold, measured within the working tissue mask, minus the excluded edge.

Quality control was embedded at each stage. Per-slide QC panels were exported showing RGB overview, tissue mask, and DAB-positive overlay, along with a tissue contour overlay and a histogram of DAB values in tissue with the global threshold indicated. In addition, the pipeline recorded the pyramid level used, whether higher-resolution reading was forced, tissue coverage, the tissue-mask mode used (default vs rescue), and background DAB statistics to support reproducibility.

5.4 Results

5.4.1 Dose Assessment Perfusions

Five single kidney perfusions were performed, kidney 1 received 120mg of mirococept in SCS, kidneys 3 & 5 received 60mg during NMP, and kidneys 2 & 4 received 120mg during NMP. The kidneys were a mix of DBD/DCD from donors aged 40–73 years old, with CIT 14:52-31:06 and the NMP to NR WIT was 14-19 minutes (Table 5.2).

Characteristic	Kidney 1	Kidney 2	Kidney 3	Kidney 4	Kidney 5
Mirococept dose	120mg SCS	120mg NMP	60mg NMP	120mg NMP	60mg NMP
Donor Type	DBD	DCD	DCD	DCD	DBD
Cause of death	ICH	Hypoxic brain injury	Hypoxic brain injury	ICH	ICH
Downtime (mins)	0	35	38	30	0
Age	66	64	40	65	73
Gender	M	F	M	M	F
Reason for Decline	Poor perfusion	Organ damage	Organ damage	Poor function	Anatomy – atherosclerotic patch
CIT (hrs:mins)	16:07	31:06	19:28	22:37	14:52
WIT (flush NMP-NR - mins)	n/a	17	19	16	14
BMI	33	35	29	29	39
Blood Type	O-	A+	O-	B+	A-
Creatinine	117	53	83	100	88
T2DM	N	N	N	N	N
HTN	N	Y	N	N	Y
Smoker	N	N	Y	Y	Y
Kidney weight (g)	184	172	230	290	210

Table 5.2 ***Donor and kidney characteristics for mirococept dose refinement perfusions.*** *The table summarises treatment allocation, donor age, sex, donor type, blood group, body mass index (BMI), admission creatinine, comorbidity and risk factor history, cold ischaemia time (CIT), interval warm ischaemia time between NMP and normothermic reperfusion (NR), and kidney weight for the five kidneys studied. Kidneys received either 120 mg mirococept during SCS as per the empirkal trial protocol, 120 mg mirococept during NMP, or 60 mg mirococept during NMP. These perfusions comprised the initial dose refinement series and were used to assess technical feasibility, physiological behaviour, and preliminary complement biomarker responses across differing doses and delivery strategies.*

5.4.1.1 Perfusion Parameters and Blood Gas Analysis

The perfusions were stable with globally well perfused kidneys for complement assessment. Weight adjusted renal artery blood flow during NMP, median flow was 175.8 (166.7–185.0) mL/min/100g for 120mg NMP (n=2) and 144.6 (101.4–187.8) mL/min/100g for 60mg NMP (n=2). During NR, median flow was 141.8 (140.3–143.4) mL/min/100g for 120mg NMP, 150.2 (107.2–193.2) mL/min/100g for 60mg NMP, and 131.9 mL/min/100g for SCS (n=1) (Fig 5.3).

Urine output was variable across kidneys, during NMP, median urine output was 2.3 (1.1–3.4) mL/hr for 120mg NMP, with one of the kidneys being anuric and 25.5 (22.5–28.5) mL/hr for 60mg NMP. During NR, median urine output was 6.0 (3.0–9.0) mL/hr for 120mg NMP, the same kidney continued to be anuric, 45.8 (32.6–58.9) mL/hr for 60mg NMP , and 148.5 mL/hr for SCS (Fig 5.3).

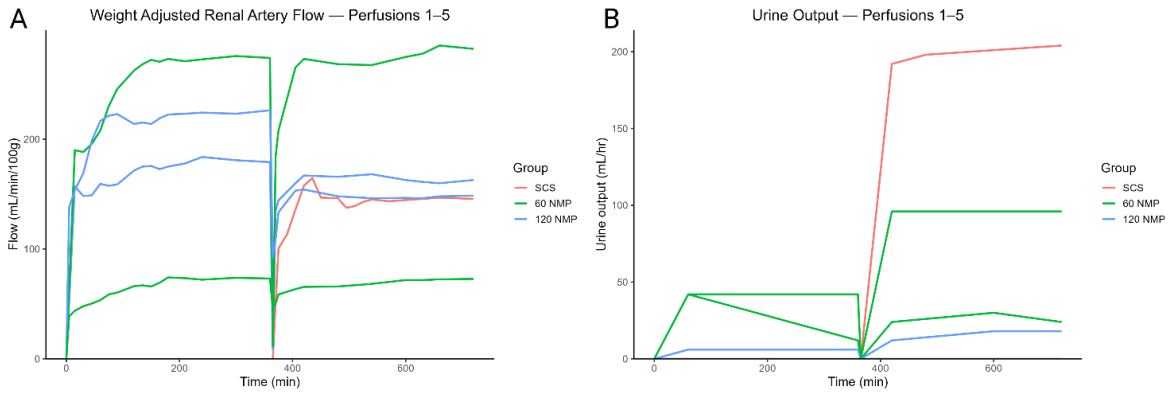


Figure 5.3 ***Renal artery flow and urine output during mirococept dose refinement perfusions.*** *Serial measurements are shown for weight-adjusted renal artery flow and urine output across perfusions 1–5. Each line represents an individual kidney, grouped according to treatment strategy: 120 mg administered during SCS, 120 mg during NMP, or 60 mg during NMP. Across the perfusions, renal blood flow was established in all kidneys, although substantial inter-perfusion variability was evident. The 120 mg NMP kidneys generally demonstrated the highest and most sustained renal artery flows, while the 60 mg NMP kidneys showed lower flows overall. Urine production also varied between kidneys and treatment groups, with one SCS-treated kidney demonstrating the greatest urine output during reperfusion.*

Perfusions were biochemically stable, during NMP from hour 2 to hour 6, median arterial pH was 7.25 (7.18–7.30) to 7.37 (7.22–7.42), potassium 12.8 mmol/L (11.9–16.9) to 12.7 mmol/L (11.9–16.9), sodium 134 mmol/L (132.5–135.0) to 142 mmol/L (141.5–142.0), ionised calcium 0.97 mmol/L (0.97–0.98) to 0.97 mmol/L (0.91–1.01), and lactate 10.0 mmol/L (9.8–12.1) to 10.9 mmol/L (10.2–14.0). Potassium was raised in the cohort more than expected, once due to suboptimal blood washing and once due to incomplete flushing of UW solution prior to connection to NMP.

During NR from hour 7 to hour 12, arterial pH was 7.22 (7.12–7.23) to 7.45 (7.40–7.46), potassium 5.6 mmol/L (5.6–5.7) to 5.3 mmol/L (5.15–6.50), sodium 150 mmol/L (148.0–153.0) to 157 mmol/L (157.0–161.5), calcium 1.12 mmol/L (0.93–1.23) to 1.33 mmol/L (1.27–1.42), and lactate 10.3 mmol/L (9.7–10.8) to 9.6 mmol/L (9.0–15.8).

5.4.1.2 Perfusate C5b-9 Formation

Perfusate C5b-9 levels (ng/mL) were assessed pre-connection, hour 2 and hour 6 of NMP, then pre-reperfusion, hours 7, 10 and 12 of NR. For 120mg delivered during NMP baseline levels were low (141.9 and 7.9 ng/mL) and rose over the course of NMP, by the end of NMP, concentrations reached 1,617.5 ± 373.6 ng/mL. Baseline levels were again low at the start of NR but increased dramatically to 6,228.4 ± 1,431.5 ng/mL at hour 10 and peaking at 14,575.8 ± 2,238.6 ng/mL at the end of NR. The divergence in end NR values (12,337.2 and 16,814.3 ng/mL) highlight the inter-perfusion variability despite identical dose and delivery modality.

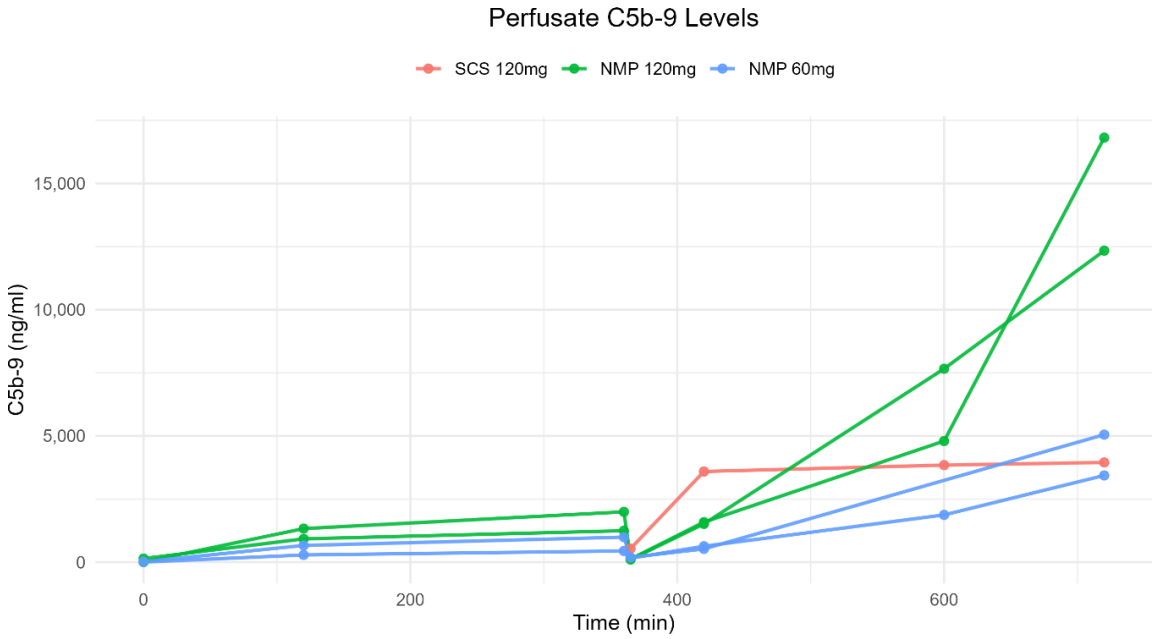


Figure 5.4 ***Perfusate C5b-9 concentrations during mirococept dose refinement perfusions.*** *Serial perfusate concentrations of soluble C5b-9 are shown across the five dose refinement perfusions. Each line represents an individual kidney, grouped according to delivery strategy and dose: 120 mg administered during SCS, 120 mg during NMP, or 60 mg during NMP. C5b-9 concentrations were low at the start of perfusion and increased over time, particularly following transition from NMP to NR, consistent with progressive terminal complement activation during reperfusion. The greatest rises were observed in some kidneys receiving NMP delivery, particularly at the 120 mg dose, indicating marked inter-kidney variability in terminal pathway activation.*

In contrast, 60mg NMP perfusions exhibited a more attenuated rise in perfusate C5b-9. Baseline concentrations again were minimal (1.3 and 18.7 ng/mL), increasing to 715.9 ± 274.0 ng/mL by the end of NMP. Again, baseline NR levels were low but rose, in a less dramatic fashion during NR reaching 4,241.8 ± 808.0 ng/mL at the end of NR. Although both 60mg NMP perfusions showed a consistent upward trajectory, absolute C5b-9

concentrations remained substantially lower than those observed in the 120mg NMP group throughout perfusion.

The EMPIRIKAL protocol kidney had a sharper rise within the first hour of NR to 3,590.2 ng/mL at hour 7, but unlike the other perfusions, the gradient then plateaued and only rose slightly over the remaining 5 hours to reach 3,948.4 ng/mL at the end of NR (Fig 5.4). Statistically there was no significant differences in 120mg in SCS, 120mg NMP, and 60mg NMP, across the time points there were no significant p-values, notably at end of NR p=0.22.

Comparing the isolated mirococept perfusions to earlier performed unpaired control perfusion for C2 inhibition, at 2 hours levels were similar, 798.9 ± 219.6 vs 750.9 ± 78.2 , p=0.93 and at the end of NMP, 1166.7 ± 321.7 vs 1006.2 ± 95.8, p=0.44. During NR there were no significant differences across the time points, at hour 7, 1568.2 ± 550.7 vs 1770.2 ± 330.5, p=0.82; hour 10, 4542.7 ± 1204.5 vs 8766.8 ± 1486.2, p=0.07 and at the end of NR, 8316.7 ± 2664.3 vs 11644.0 ± 1964.1, p=0.21. There was numerical separation at hour 10 and end of NR, but without reaching statistical significance, though close at hour 10 (Fig 5.5)

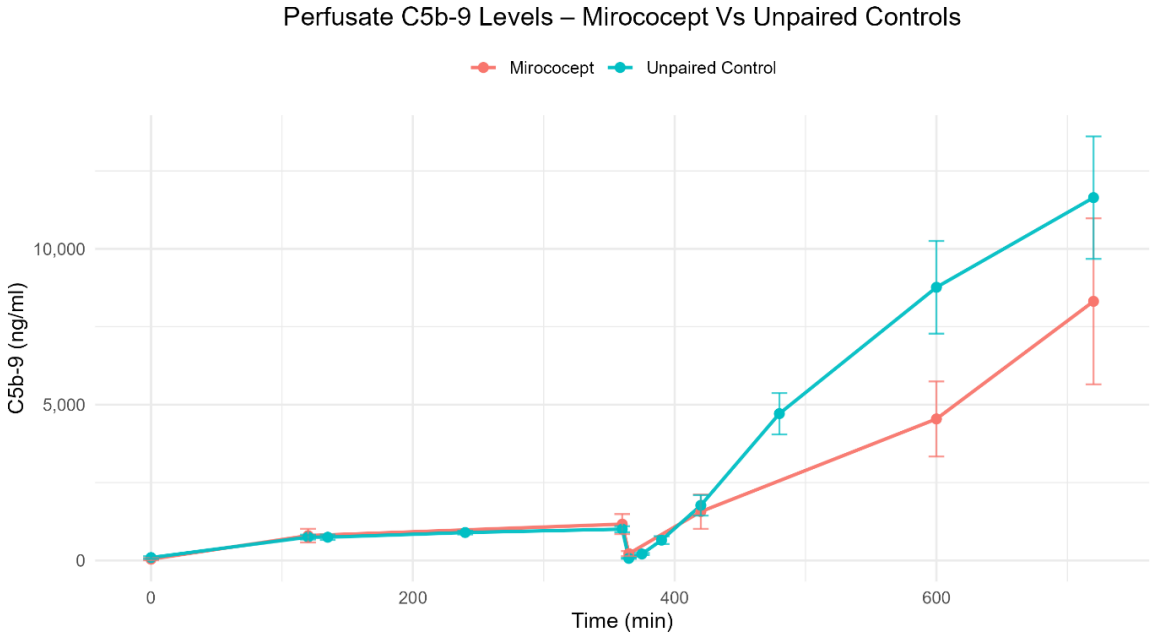


Figure 5.5 ***Perfusate C5b-9 concentrations during mirococept dose refinement perfusions compared with unpaired controls.*** *Mean perfusate concentrations of soluble C5b-9 are shown over time for mirococept-treated kidneys and unpaired control kidneys. C5b-9 concentrations were similar at baseline and during early NMP, but diverged during NR, with both groups showing rising terminal pathway activation over time. Descriptively, the mirococept-treated group showed lower mean C5b-9 concentrations than unpaired controls at later reperfusion timepoints, although there was overlap between groups and appreciable variability. These findings suggest that mirococept may have attenuated downstream terminal complement activation during early reperfusion.*

5.4.1.3 Tissue Complement on Western Blotting & Native Gel Electrophoresis

Central and alternative pathway fragment C3d, and its slightly larger and more stable precursor C3dg were assessed and normalised to β-actin on the same gel. Pre-NR, levels were lowest for the EMPIRIKAL protocol kidney 46.0 AU, compared with post-NMP levels which was higher, 60mg NMP at 471.3 AU (403.1–539.6), and 120mg NMP at 260.4 AU (222.2–298.6). By the end of NR there was a divergence, the SCS delivered kidney demonstrated a very high signal (23277.2 AU), whereas both NMP interventions remained within the low range: 60mg NMP median 757.8 AU (729.7–785.9) and 120mg NMP 1175.4 AU (1123.2–1227.6), with no statistically significant differences. Looking at the changes over NMP and NR, for normalised delta C3d and C3dg during NMP, both 60mg and 120mg showed a net decrease, −567.402 (−784.304, −350.500) and −434.118 (−650.362, −217.874) respectively, p=0.70. During NR, deltas were positive, with a non-significant smaller increase in 60 mg NMP, 286.511 (190.188, 382.835) vs 914.998(824.596, 1005.401) with 120mg, p=0.25. The 120 mg SCS delivery showed a markedly larger increase with a delta of 23231.228. (Fig 5.6).

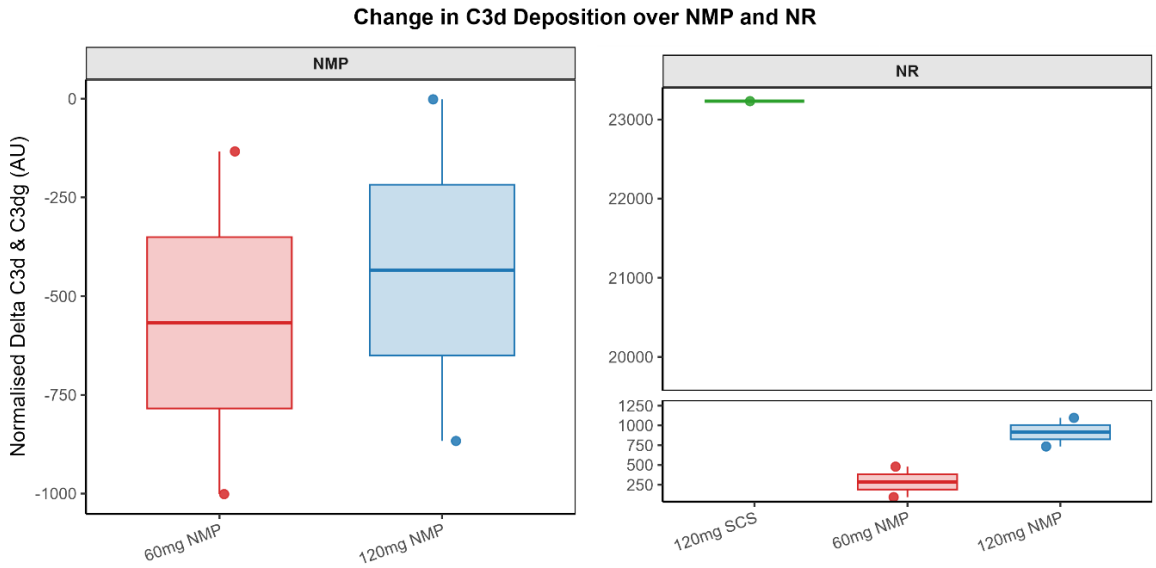


Figure 5.6 ***Change in tissue C3d/C3dg deposition over NMP and NRduring mirococept dose refinement.*** *Western blot-derived change in normalised tissue C3d/C3dg signal is shown over the NMP phase and over the NR phase according to mirococept delivery strategy and dose. The left panel shows change in C3d/C3dg over NMP, while the right panel shows change over NR. During NMP, both the 60 mg and 120 mg NMP groups showed negative delta values, indicating a reduction in tissue C3d/C3dg signal across the NMP phase, although there was variability between kidneys. In contrast, during NR all groups showed positive delta values, indicating accumulation of tissue C3d/C3dg during reperfusion. The greatest increase was observed in the kidney treated with 120 mg during SCS, while the increase appeared smaller in the 60 mg NMP group and intermediate in the 120 mg NMP group.*

Considering the level of terminal C5b-9 formation in the tissue at the end of NR, 120mg delivered during SCS produced the lowest level of tissue signal 2604.4 AU, intermediate signal for 120mg in NMP at 9828.5 AU (9685.3–9971.7), and highest in 60mg in NMP with 11020.1 AU (10259.7–11780.5), none of which reach statistical significance given the number of experiments (Fig 5.7).

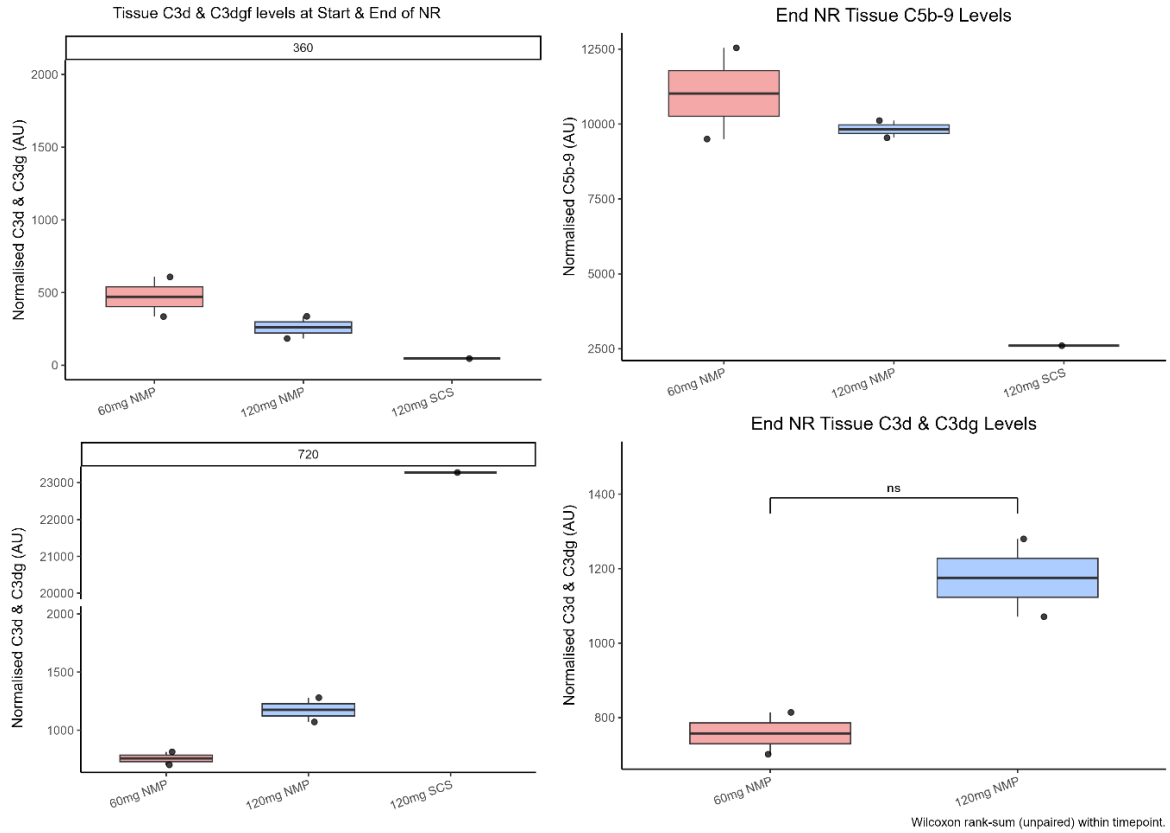


Figure 5.7 ***Tissue C3d/C3dg and C5b-9 levels in biopsies from mirococept dose refinement perfusions.*** *Western blot quantification of tissue C3d/C3dg and C5b-9 is shown for biopsies obtained during the dose refinement perfusions. The upper left panel shows tissue C3d/C3dg levels at the end of NMP, while the lower left panel shows tissue C3d/C3dg levels at the end of NR. The upper right panel shows tissue C5b-9 levels at end NR. The lower right panel compares end-NR tissue C3d/C3dg levels between the 60 mg NMP and 120 mg NMP groups. At the start of reperfusion, tissue C3d/C3dg levels were highest in the 60 mg NMP group, lower in the 120 mg NMP group, and lowest in the single kidney treated during static cold storage. By the end of reperfusion, tissue C3d/C3dg levels had increased in all groups, with the highest level seen in the kidney treated during SCS and intermediate levels in the 120 mg NMP group. End-NR tissue C5b-9 levels were highest in the 60 mg NMP group, intermediate in the 120 mg NMP group, and lowest in the SCS-treated kidney. The comparison between 60 mg and 120 mg NMP at end NR did not demonstrate a significant difference in tissue C3d/C3dg.*

Looking at these levels compared to a selection of unpaired controls from baseline, end NMP and end NR. At Baseline, C5b-9 levels were similar between groups: mirococept median 15434.7 AU (11036.3–19976.7) vs unpaired Control 16001.3 AU (13622.1–23656.9), with no significant difference (p=0.89). At End NMP, C5b-9 levels remained

similar 12675.4 AU (8610.1–14293.2) vs 14131.6 AU 12444.4–15818.7, p=0.82. At End NR, C5b-9 remained numerically lower in the mirococept group, 9828.5 AU (9531.4–10721.4) vs 19828.7 AU (13433.7–25099.9), although this was not statistically significant (p=0.31) (Fig 5.8).

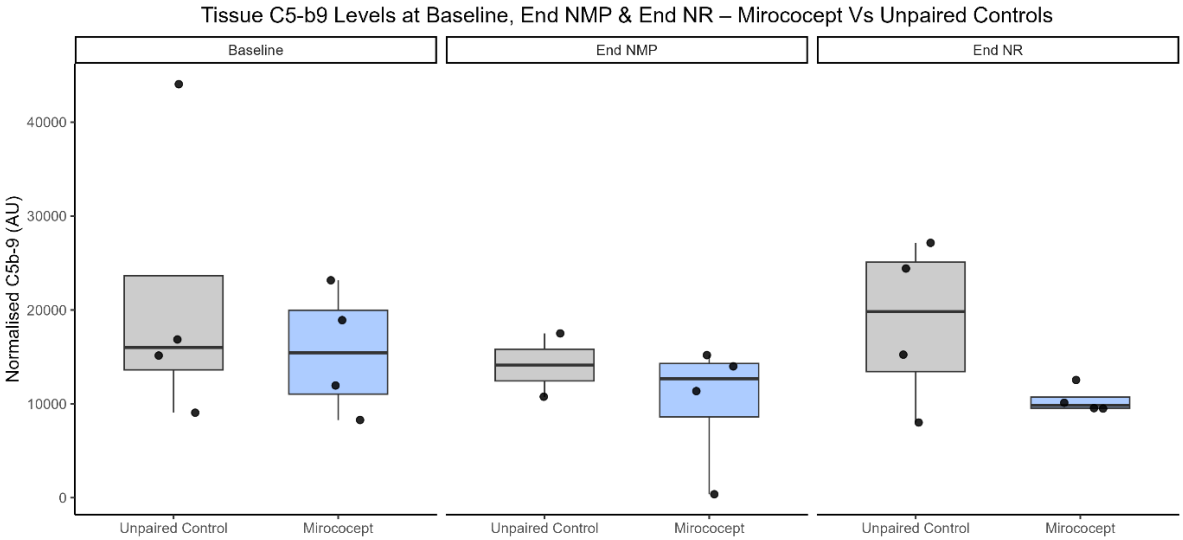


Figure 5.8 ***Tissue C5b-9 levels at baseline, end of NMP, and end of NR in mirococept-treated kidneys compared with unpaired controls.*** *Western blot quantification of tissue C5b-9 is shown for biopsies taken at baseline, end of NMP, and end of NR in kidneys treated with mirococept and in unpaired control kidneys. Tissue C5b-9 was present at baseline in both groups, indicating pre-existing terminal complement deposition in these declined donor kidneys prior to perfusion. By the end of NMP, tissue C5b-9 levels remained broadly similar between groups, although variability was evident within the mirococept-treated kidneys. At the end of NR, tissue C5b-9 levels are possibly lower in the mirococept-treated group than in unpaired controls, consistent with attenuation of terminal complement deposition during reperfusion.*

5.4.2 Paired Perfusions

Four paired perfusions were conducted in which one kidney was randomly allocated as a control and the other treated with either 120mg (n=2) or 60mg (n=2) of mirococept during NMP. Three of the four pairs were DCDs, one of which underwent NRP, from donors aged 54-74 years. The CITs ranged from 15-22 hours and the NMP to NR WIT was 11-15 minutes (Table 5.3).

Characteristic	6&7	8&9	10&11	12&13
Mirococept Dose	120mg	120mg	60mg	60mg
Donor Type	DCD (NRP)	DCD	DCD	DBD
Cause of Death	ICH	ICH	ICH	Hypoxic brain injury
Downtime	32	0	0	37
Age	74	71	72	53
Gender	M	F	M	M
Reason for Decline	Poor Perfusion	Organ Damage	? Malignancy	Aortic dissection
CIT	17:15/17:25	15:00/15:07	22:29/22:39	16:12/16:19
WIT (flush NMP-NR - mins)	11/12	12/12	14/15	11/11
BMI	26	21	28	26
Blood Type	O+	O-	A+	O+
Creatinine	65	70	65	78
T2DM	N	N	N	N
HTN	Y	N	Y	N
Smoker	Y	Y	Y	N
Kidney Weight (g)	248/225	163/128	210/191	261/302

Table 5.3 ***Donor and graft characteristics for kidneys included in the paired mirococept perfusions.*** *The table summarises treatment allocation, donor type, cause of death, reasons for organ decline, donor age, sex, donor type, blood group, BMI, admission creatinine, comorbidity and risk factor history, CIT, interval warm ischaemia time between NMP and NR, and kidney weight, ischaemic times,, and graft weight for the four paired kidney perfusions studied. In each donor pair, one kidney underwent control perfusion and the contralateral kidney received mirococept, with paired experiments performed at either 120 mg or 60 mg.*

5.4.2.1 Perfusion Parameters and Blood Gas Analysis

All perfusions had good weight adjusted renal artery flow, which all rose sharply from the start of NMP over the first 60 minutes, plateauing by hour 2, control kidney flows reaching 193.1 mL/min/100g (175.5–202.5), compared with 164.7 (148.1–195.8) in mirococept, and at the end of NMP pooled controls maintained a slightly higher median flow, 199.8 (175.8–214.1) compared with mirococept treated kidneys 170.2 (155.0–194.7). The same was true for NR, which stabilised at hour 7, with controls at 166.9 (157.5–169.7) and mirococept at 146.8 (115.2–177.9). At the end of NR, flow remained higher in controls, 165.9 (147.7–175.3) than mirococept at 137.3 (119.3–163.1). Looking

at overall flow with AUC, no statistically significant differences are present between pooled controls and mirococept, or when subset by dose. In total pooled controls had a total AUC of 128,864.2 (115,252.7–133,322.80) vs 114,828.5 (93,220.8–134,437.9) in mirococept (p=1.00), with no difference in NMP or NR.

For 120mg total AUC 104354.6 (93456.5–115252.7) in controls vs 89622.3 (86023.8–93220.8) in 120 NMP (p=0.37). NMP AUC was similar (p=1), whereas AUC in NR non-significantly favoured controls 48,931.4 (44236.8–53626.0) vs 39176.0 (37045.9–41306.0), p=0.37. For 60mg total AUC was 135068.0 (133322.8–136813.1) in controls vs 136038.0 (134437.9–137638.1), p=0.37. With no differences in AUC during NMP (p=1.00) or during NR (p=1.00) (Fig 5.9).

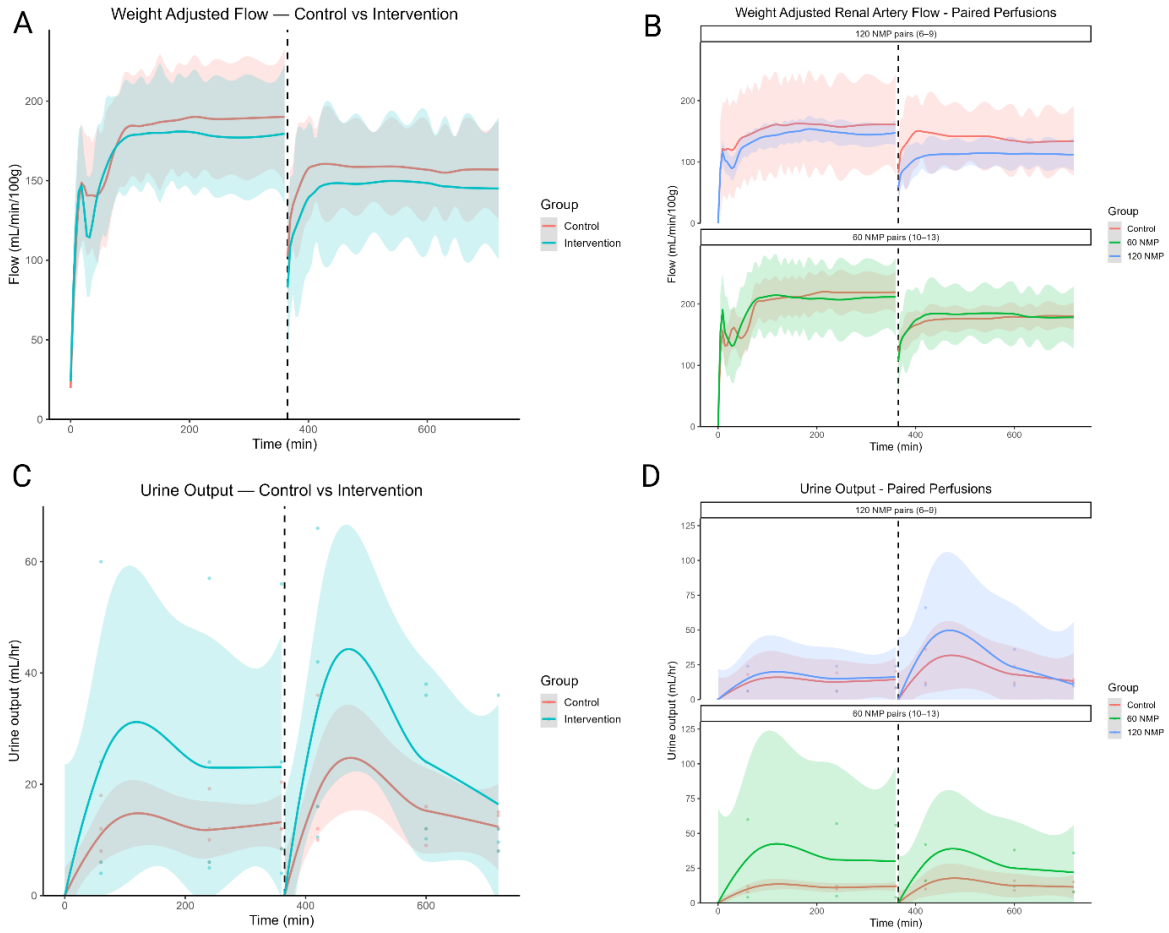


Figure 5.9 ***Renal artery flow and urine output during paired mirococept perfusuions****. Serial measurements are shown for weight-adjusted renal artery flow and urine output during the paired perfusions. Panel A shows mean weight-adjusted renal artery flow comparing all control and intervention kidneys, while panel B shows the same data stratified by dose group, with separate panels for the 120 mg NMP pairs and the 60 mg NMP pairs. Panel C shows mean urine output comparing all control and intervention kidneys, and panel D shows urine output stratified by dose group.*

Urine production was not statistically different with the addition of mirococept compared with control, or altered based on dose, but there towards higher urine flow in the mirococept kidneys. For the pairs pooled together, total AUC, Control was 7690 (6220-12000) vs mirococept 13700 (5560-26900), p=0.58. NMP AUC, Control 3570 (2650-5110) vs mirococept 5020 (1800-13500), p=0.79. NR AUC, Control 4630 (3540-6860) vs mirococept 8480 (3750-13300), p=0.58 (Fig 5.9).

Perfusate biochemistry was consistent throughout the pairs, and was stable throughout perfusion, sodium, potassium, calcium, glucose, and pH had no statistically significance between groups or across time points. With regards lactate trends, during NMP the control kidneys demonstrated a small rise 1.35 (0.85-1.40) mmol/L and the mirococept kidneys a small fall −0.25 (−1.00-0.40), though not significant (p=0.13). During NR, both groups had a rise from hour 7 to 12, Control was 4.05 (3.05-5.53), and mirococept was 4.00 (2.98-5.35), p=0.63 (Fig 5.10).

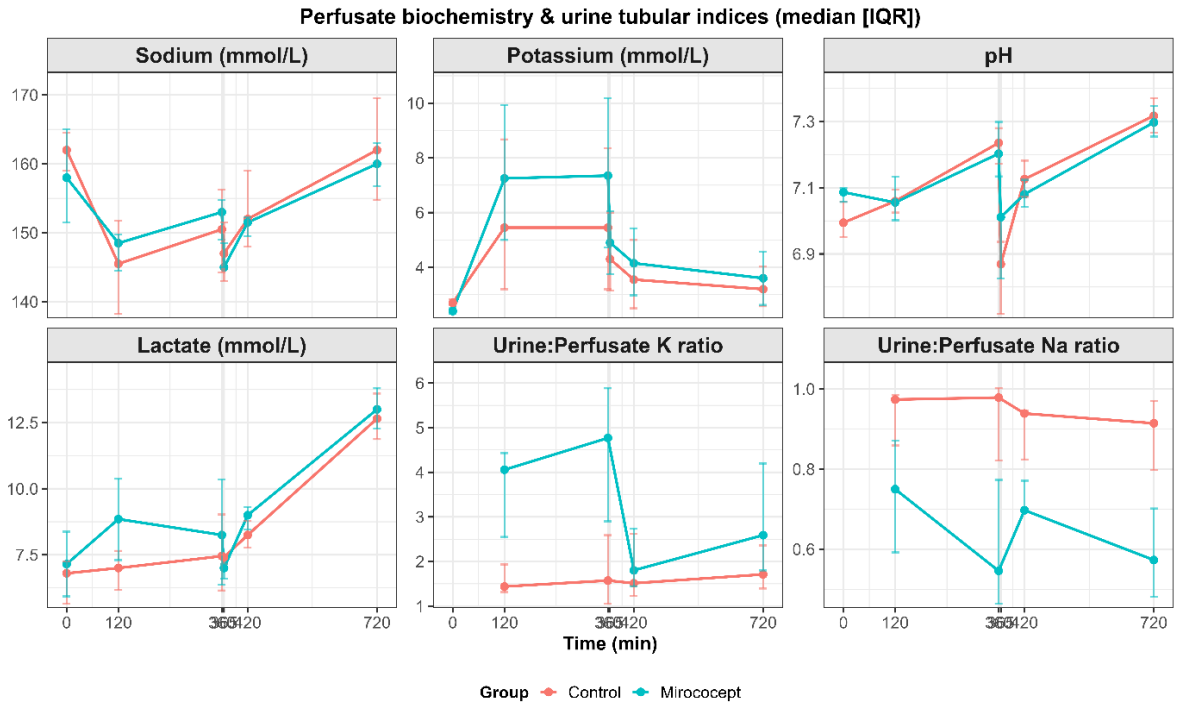


Figure 5.10 ***Perfusate and urine biochemistry during paired mirococept perfusions.*** *Median values with interquartile ranges are shown for perfusate sodium, potassium, pH, and lactate, together with urine:perfusate potassium and sodium ratios, across the experimental time-course. Electrolyte and acid-base profiles were broadly similar between groups throughout the perfusions, with expected shifts occurring at the transition from NMP to NR. Urine:perfusate potassium ratios were consistently higher in the mirococept-treated group, whereas urine:perfusate sodium ratios were lower, suggesting relatively greater tubular handling of sodium and potassium in treated kidneys.*

Urine biochemistry showed tubular function in those kidneys treated with mirococept compared with controls, but there were no statistically significant differences between groups. At the end of NMP, urinary potassium was 4.8 (4.2-6.2) in controls vs 23.1 (16.4-24.0) mmol/L in mirococept, p=0.18, as a ratio with perfusate that is 1.41 (1.18-1.44) vs 3.44 (2.72-3.95), p=0.42. Similarly urinary sodium was 154 (146-155) in controls vs 83 (72-112) mmol/L in mirococept, p=0.423, and as a ratio with perfusate that is 0.99 (0.96-1.00) vs 0.58 (0.47-0.74), p=0.181. This pattern continued in NR, and by the end of NR, the urine perfusate potassium ratio was 1.71 (1.39-2.36) vs 2.59 (1.80-4.20), p=0.201, and the sodium ratio 0.91 (0.80-0.97) vs mirococept at 0.57 (0.48-0.70), p=0.100.

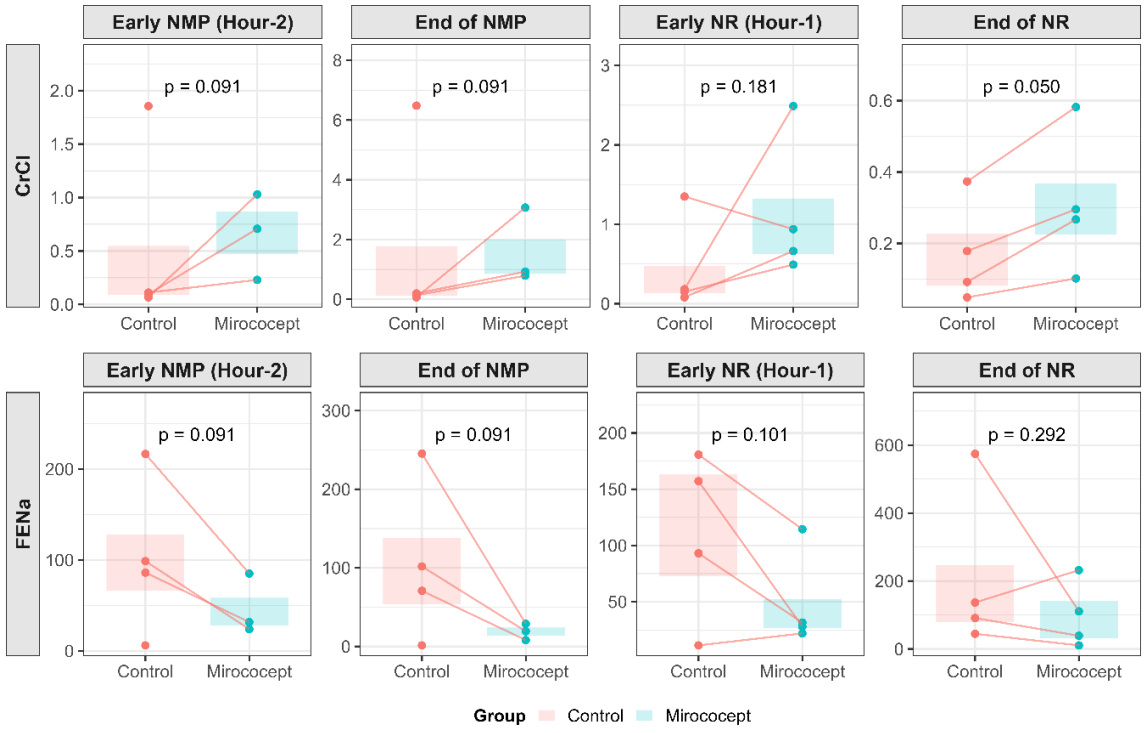


Figure 5.11 ***Creatinine clearance and fractional excretion of sodium during paired mirococept perfusions****. Boxplots with paired connecting lines CrCl and FENa between control and mirococept-treated kidneys at Early NMP (Hour-2), end of NMP, Early NR (Hour-1), and end of NR. Each point represents an individual kidney, with paired lines linking contralateral kidneys from the same donor pair. Across timepoints, creatinine clearance tended to be higher in mirococept-treated kidneys than in paired controls, with the largest apparent separation seen by the end of NR, where the comparison approached nominal significance. In contrast, FENa tended to be lower in the mirococept-treated kidneys, particularly during NMP and early reperfusion, consistent with relatively better tubular sodium handling.*

Across the pairs, creatinine clearance (CrCl) was consistently higher in the mirococept-treated kidneys, reaching significance by the end of NR. At Early NMP, CrCl was 0.096 (0.081–0.104) in controls vs 0.708 (0.469–0.869) with mirococept, p=0.091, and at the End of NMP 0.138 (0.102–0.168) vs 0.924 (0.857–1.998), p=0.091. During Early NR CrCl

remained higher with mirococept, 0.167 (0.134–0.475) vs 0.801 (0.621–1.326), p=0.181, and by the End of NR this separation persisted, 0.135 (0.081–0.227) vs 0.281 (0.226–0.367), p=0.050.

Fractional excretion of sodium (FENa) showed the reciprocal pattern, with markedly lower values in treated kidneys during NMP, albeit still far off from physiological values. Early NMP 98.7 (92.4–157.6) in controls vs 31.7 (27.8–58.4) with mirococept, p=0.091, and End of NMP 101.8 (86.3–173.6) vs 19.4 (13.7–24.1), p=0.091. This trend continued into Early NR (125.1 (72.6–163.1) vs 29.7 (26.5–52.3), p=0.101, but was less clear by the End of NR (113.8 (79.4–246.1) vs 74.8 (31.8–141.1), p=0.292 (Fig 5.11).

5.4.2.2 Perfusate Injury Biomarkers

The perfusate damage biomarkers assessed were IL-18, GST-Pi, KIM-1, LDH, and NGAL, at start and end of NMP, and start of NR, hour 7 and hour 12.

At the end of NMP IL-18 was significantly lower in mirococept treated kidneys, 109.0 (79.65–152.4) pg/mL in controls vs 89.89 (53.78–120.2) in the treated kidneys, p=0.05. At the end of NR, IL-18 remained numerically lower with mirococept but without statistical support 249.2 (169.2–528.4) in controls vs 200.7 (175.7–409.1), paired difference −56.02 (−119.2–−1.048), p=0.18.

NGAL was also significantly lower at the end of NMP with mirococept, 2180.8 (1593.0–3047.3) ng/mL in controls vs 1797.7 (1075.7–2404.9), p= 0.05. Again, at the end of NR NGAL remained numerically lower but without significance, 4984.3 (3383.9–10568) in controls vs 4014.2 (3513.1–8182.6), p=0.18 in the mirococept group.

For KIM-1 there were no significant differences, and the directional changes were not consistent between NMP and NR. KIM-1 increased in the mirococept group at the end of NMP 600.7 (557.7–753.8) pg/mL in controls vs 781.2 (532.2–1,021.3), p=0.82. At the end of NR 444.1 (365.0–671.8) in controls vs 554.2 (464.3–584.1), p= 0.43.

Similarly, GST-Pi had no significant differences, end of NMP, 24.13 (20.16–36.41) ng/mL in controls vs 41.72 (35.91–47.81), p=0.9498. At the end of NR, GSTPi was similar between groups 31.12 (23.75–51.43) in controls vs 28.04 (19.51–55.41), p=0.57.

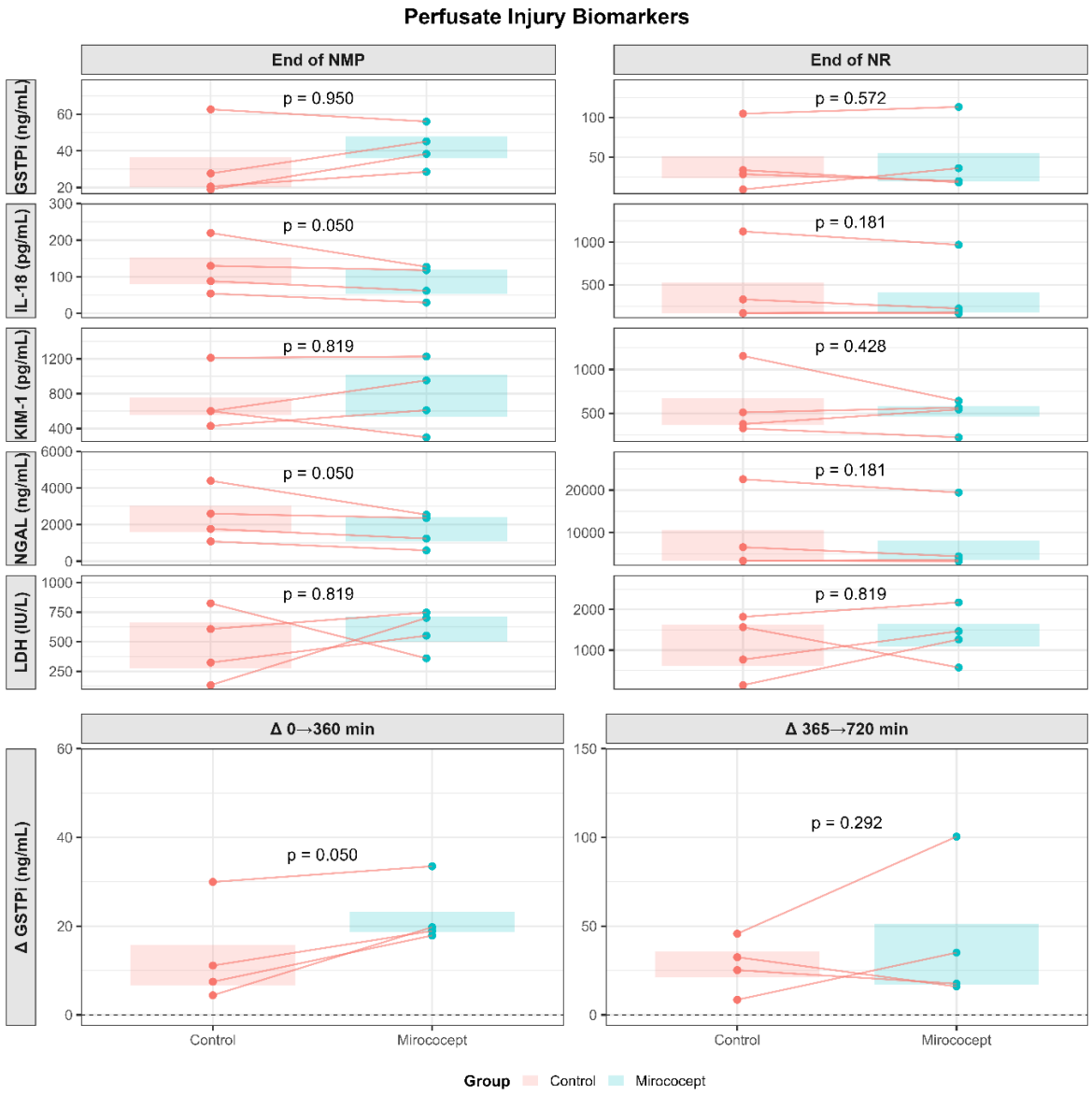


Figure 5.12 ***Perfusate injury biomarker concentrations during paired mirococept perfusions.*** *Paired comparisons of GSTPi, IL-18, KIM-1, NGAL, and plasma LDH are shown at the end of NMP (T6, 360 min) and end of normothermic reperfusion (T12, 720 min), together with interval change over NMP (Δ 0–360 min) and over reperfusion (Δ 365–720 min) for GSTPi. At the end of NMP, IL-18 and NGAL were lower in the mirococept-treated kidneys than in paired controls, with both comparisons reaching nominal significance, while GSTPi, KIM-1, and LDH were similar between groups. By the end of reperfusion, biomarker concentrations remained broadly comparable between groups, although IL-18, NGAL, and KIM-1 remained numerically lower in the mirococept-treated kidneys. The increase in GSTPi over the NMP phase was greater in the mirococept-treated kidneys than in paired controls, whereas the change over reperfusion was variable and did not differ clearly between groups.*

Looking at delta GST-Pi, mirococept has a significantly higher delta-GST-Pi over NMP, 9.289 (6.707–15.82) in controls vs 19.34 (18.66–23.21), p=0.05. This is not the case during NR in with delta GST-Pi is similar between groups, with 28.85 (21.04–35.80) in controls vs 26.33 (17.17–51.42), p=0.29 (Fig 5.12).

For LDH, there was no evidence of a treatment effect at either timepoint. At the end of NMP, plasma LDH was 465.7 (276.2–661.8) IU/L in controls vs 626.2 (503.4–712.6) IU/L with mirococept, a paired difference of 183.7 (−11.3–312.5), p=0.584. At the end of NR, 1165.8 (609.3–1,628.5) IU/L in controls vs 1364.9 (1090.5–1643.2) IU/L with mirococept, a paired difference of 527.4 (18.0–806.2), p=0.584.

5.4.2.3 Perfusate Complement Proteins

Perfusate levels of C3d and C5b-9 were measured at start and end of NMP, and start of NR, hour 7 and hour 12. Baseline concentrations were low and similar between groups, the largest between-group separation occurred in the first hour of NR, where both markers were significantly lower in mirococept treated kidneys.

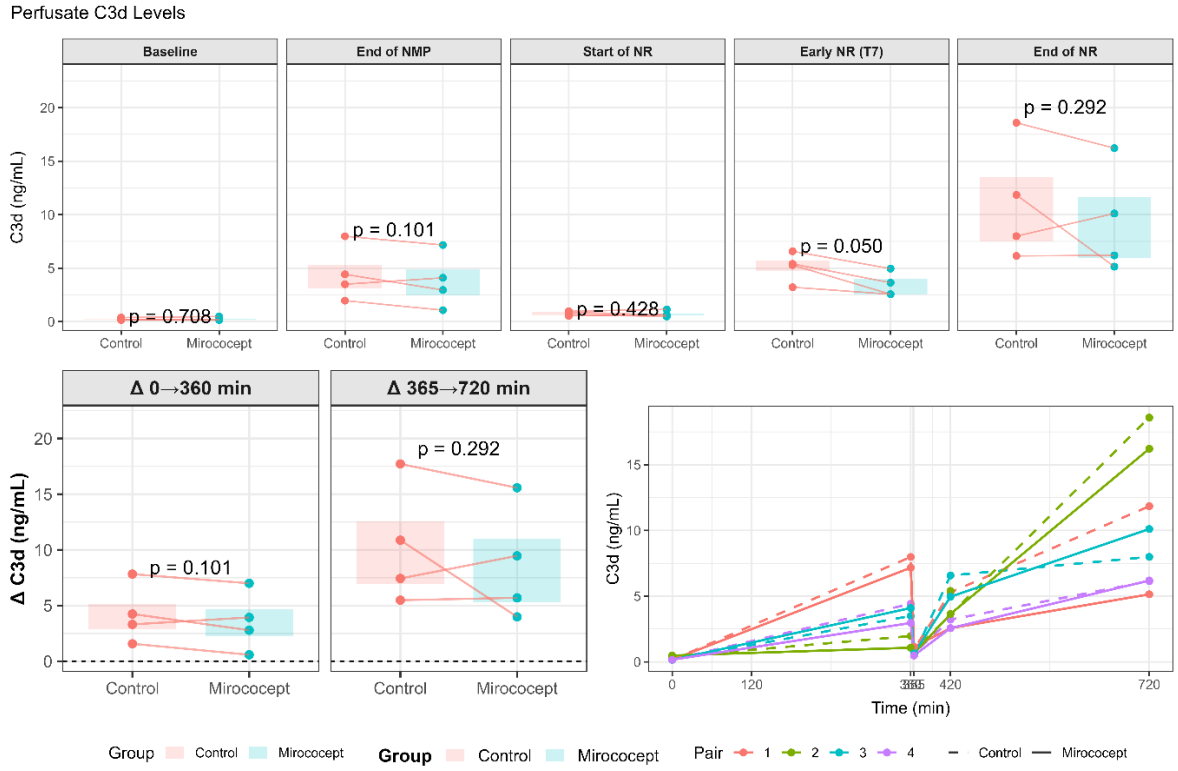


Figure 5.13 ***Perfusate C3d concentrations during paired mirococept perfusions.*** *Panelled plots show perfusate C3d concentrations at baseline (T0), end of NMP (T6, 360 min), immediately after transition to reperfusion (T6+, 365 min), early reperfusion (T7, 420 min), and end of reperfusion (T12, 720 min), together with interval changes over NMP and over NR. The lower right panel shows the full time-course for each paired experiment, with dashed lines denoting control kidneys and solid lines mirococept-treated kidneys. Perfusate C3d concentrations rose during the course of the experiments in both groups, with the largest increases occurring during reperfusion. Concentrations tended to be lower in the mirococept-treated kidneys than in paired controls with significance at T7. These findings are consistent with reduced downstream C3 activation early in reperfusion in kidneys receiving mirococept.*

For C3d at the end of NMP, levels were not different, 3.959 (3.113–5.311) ng/mL in controls vs 3.528 (2.488–4.863), p=0.10. After the first hour of NR more C3d had

accumulated in the control perfusion 5.344 (4.770–5.694) vs 3.104 (2.566–3.972), p=0.05. This significant difference was not maintained by the end of NR 9.917 (7.526–13.53) vs 8.151 (5.929–11.64), p=0.29 (Fig 5.13).

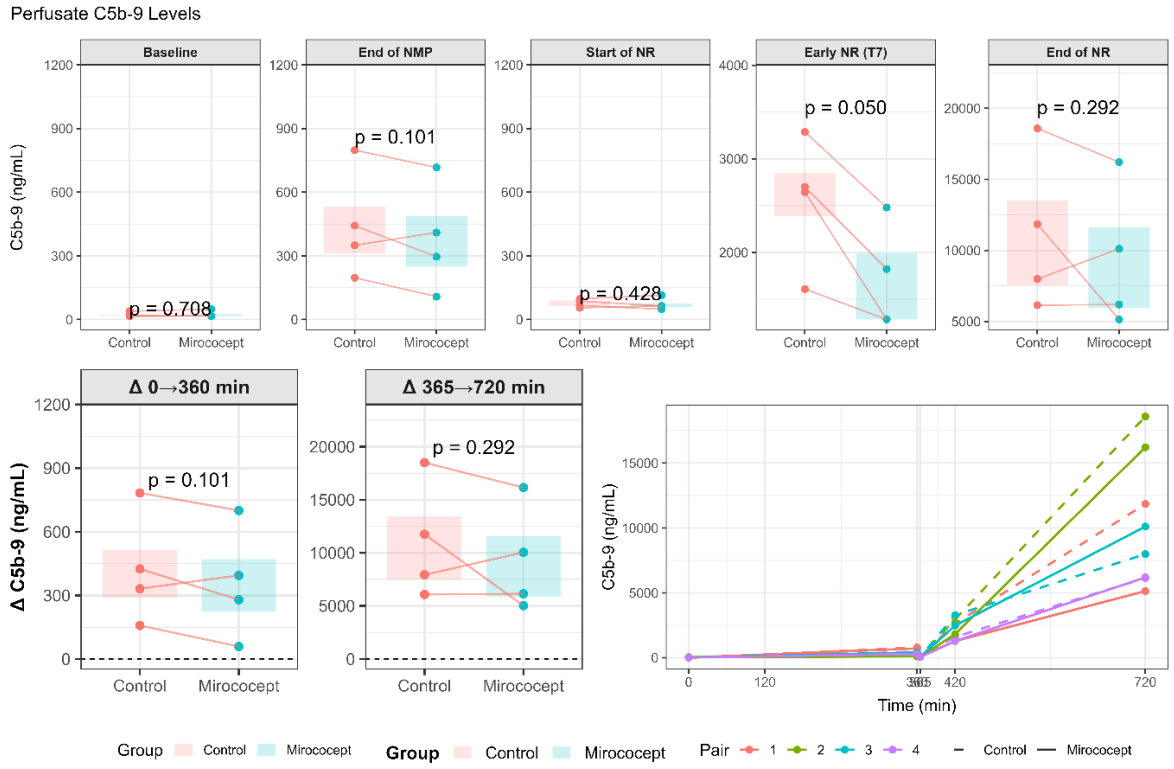


Figure 5.14 ***Perfusate C5b-9 concentrations during paired mirococept perfusions****. Panelled plots show perfusate soluble C5b-9 concentrations at baseline (T0), end of NMP (T6, 360 min), immediately after transition to reperfusion (T6+, 365 min), early reperfusion (T7, 420 min), and end of reperfusion (T12, 720 min), together with interval changes over NMP and over NR. The lower right panel shows the full time-course for each donor pair, with dashed lines denoting control kidneys and solid lines mirococept-treated kidneys. Soluble C5b-9 increased in all experiments over time, with the most marked rise occurring during reperfusion. At early reperfusion and end NR, the mirococept-treated kidneys generally showed lower C5b-9 concentrations than their paired controls, with significance at T7. Demonstrating that mirococept reduced terminal pathway activation early during reperfusion in the paired model.*

For C5b-9, by the end of NMP there was no difference between the groups 395.9 (311.3–531.1) ng/mL vs 352.8 (248.8–486.3), p=0.10. However, within the first hour mirococept had attenuated the accumulation of C5b-9 and levels at hour 7 were 2672.0 (2385.0–2846.8) in controls vs 1552.2 (1282.8–1986.2), p=0.05 in the treatment group. However, as with C3d, this significant difference was not maintained to the end of NR, with 9916.5 (7526.4–13530) in controls vs 8150.6 (5928.9–11635), p=0.29). The delta over the course of NR was numerically lower, but not significant, 9840.6 (7468.9–13435.6) in controls vs 8094.2 (5863.8–11571.5), p=0.29 (Fig 5.14).

5.4.2.4 Tissue Complement on Western Blotting & Native Gel Electrophoresis

Fresh frozen tissue taken pre-NMP, end of NMP and at the end of NR was used to assess C3 and its fragments on western blotting and C5b-9 on native gel electrophoresis.

Normalised intact C3 band intensity was numerically higher in mirococept kidneys, particularly at the end of perfusion phases, but as directional changes weren't uniform it was not statistically significant. At the end of NMP band intensity was 9851.52 (3934.77–16652.78) in controls vs 15939.23 (10356.00–20168.01), p=0.10. At the end of NR, C3 levels were numerically much higher in the mirococept kidneys, with 24568.01 (21835.02–42079.29) in controls vs 75617.96 (64463.64–87057.24), p=0.18 in treated kidneys, but this did not reach statistical significance.

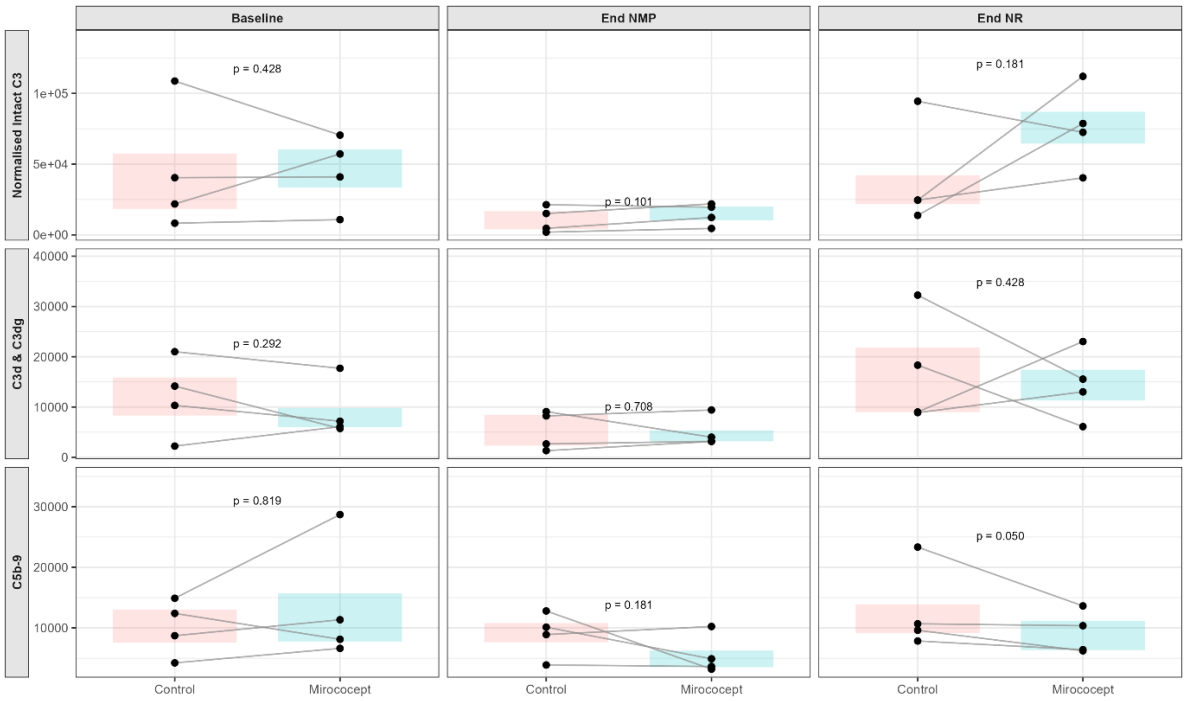


Figure 5 .15 ***Tissue complement deposition in biopsies from paired mirococept perfusions****. Western blot quantification of normalised intact C3, C3d/C3dg, and C5b-9 is shown for biopsies taken at baseline, end of NMP, and end of NR in paired control and mirococept-treated kidneys. Intact C3 signal was similar between groups at baseline and end NMP, but appeared higher in mirococept-treated kidneys at end NR. Tissue C3d/C3dg levels were broadly comparable between groups across the time-course, with no clear evidence of a marked treatment effect. In contrast, tissue C5b-9 levels appeared lower in the mirococept-treated kidneys by end NR, with the comparison reaching nominal significance. These findings suggest that while upstream C3-related tissue signals were not clearly altered, mirococept may have attenuated terminal complement deposition within the kidney tissue during reperfusion.*

C3d/C3dg showed no consistent separation across phases, at the end of NMP 5442.68 (2322.01–8444.30) in controls vs 3588.23 (3168.06–5352.43), p=0.71. at the end NR 13670.26 (8986.28–21804.90) in controls vs 14280.68 (11285.61–17415.29), p=0.43.

C5b-9 was numerically lower at the end of NMP and significantly so at the end of NR. At the end of NMP, 9513.51 (7650.62–10792.31) in controls vs 4278.04 (3533.18–6244.10), p=0.181. At the end NR, 10147.83 (9171.89–13845.81) in controls vs mirococept 8387.73 (6365.92–11180.20), p=0.05 (Fig 5.15).

5.4.2.5 C5b-9 Immunohistochemistry

C5b-9 IHC was quantified by whole-slide DAB analysis as detailed above, in a paired experimental design, using the percentage of tissue area classified as C5b-9-positive as the primary readout. The inbuilt QC was done across 27 slides (24 experimental plus 3 positive control slides) and demonstrated stable performance, with median tissue coverage of 21.352% (16.867–23.925%), a constant global DAB threshold (0.01134573), and with limited use of the rescue logic in built into the pipeline for handling slide to slide variation (pale-rescue in 7/27 slides, pale & morphological rescue in 1/27 and higher-resolution fall back in 2/27).

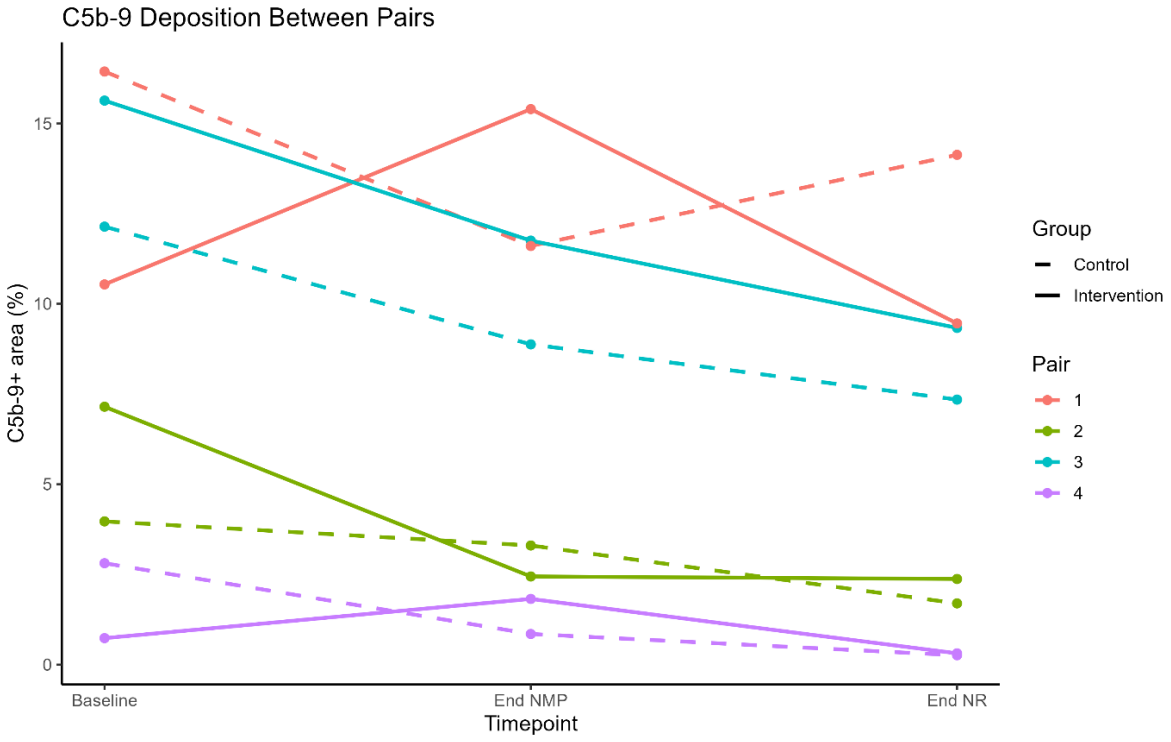


Figure 5.16 ***Tissue C5b-9 deposition in paired kidneys over the course of perfusion and reperfusion in parier mirococept perfusions****. Line plots show the percentage C5b-9-positive tissue area at baseline, end of NMP, and end of NR for each donor pair. Dashed lines denote control kidneys and solid lines the corresponding mirococept-treated contralateral kidneys, with colours identifying each donor pair. Considerable heterogeneity was evident between pairs at baseline, reflecting variable pre-existing terminal complement deposition in declined donor kidneys. This IHC tissue data was inconsistent with the western blot results.*

In the experimental cohort, median C5b-9+ area at baseline was, as to be expected, similar 8.054% (3.969–12.139) in controls versus 8.843% (3.544–13.306) with mirococept, p=1.00. At the end of NMP, levels were no different with, 6.089% (2.689–9.558) in controls versus 7.097% (1.970–12.345), p=0.20 in mirococept treated kidneys. At the end of NR, levels were also no different with 4.521% (0.945–8.648) in controls versus 5.853% (1.459–8.965), p=0.86 (Fig 5.16) in the treatment group. There was no evidence of significant difference at any other time point.

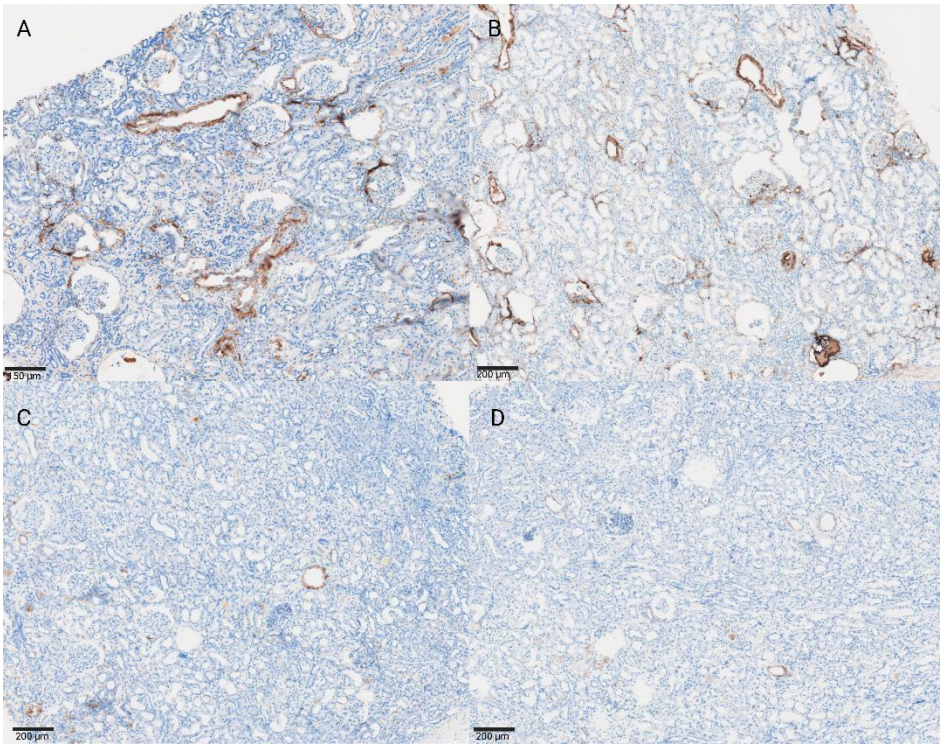


Figure 5.17 ***Basline tissue biopsies demonstrating consistency between pairs.*** *Panel A and B basline biopsises from the right and left kidenys of pair 1 demonstrating similarly high levbels of C5b-9 staining and a comparable significant baseline level of injury, in keeping with the greater level of basline C5b-9. Compared with panel C and D, the right and left kidney of pair 4, showing similarly low levels of C5b-9 staining at baseline, and less baseline injury.*

Pairs tended to follow the same patterns, with some small differences at each stage. Delta C5b-9 for the different pairs (mirococept − Control) ranged from −5.901% to +3.494% at Baseline, −0.859% to +3.794% at the end of NMP, and −4.672% to +1.988% at the end of NR. As expected, the difference between pairs was more marked than the differences within the pairs, with each pair falling within its own range, with some kidneys such as pair 1 having a higher baseline consistent in control and mirococept, which contrasted with others such as pair 4 with a consistent low baseline (Fig 5.17) and this same pattern continuing through to end of NR (Fig 5.18).

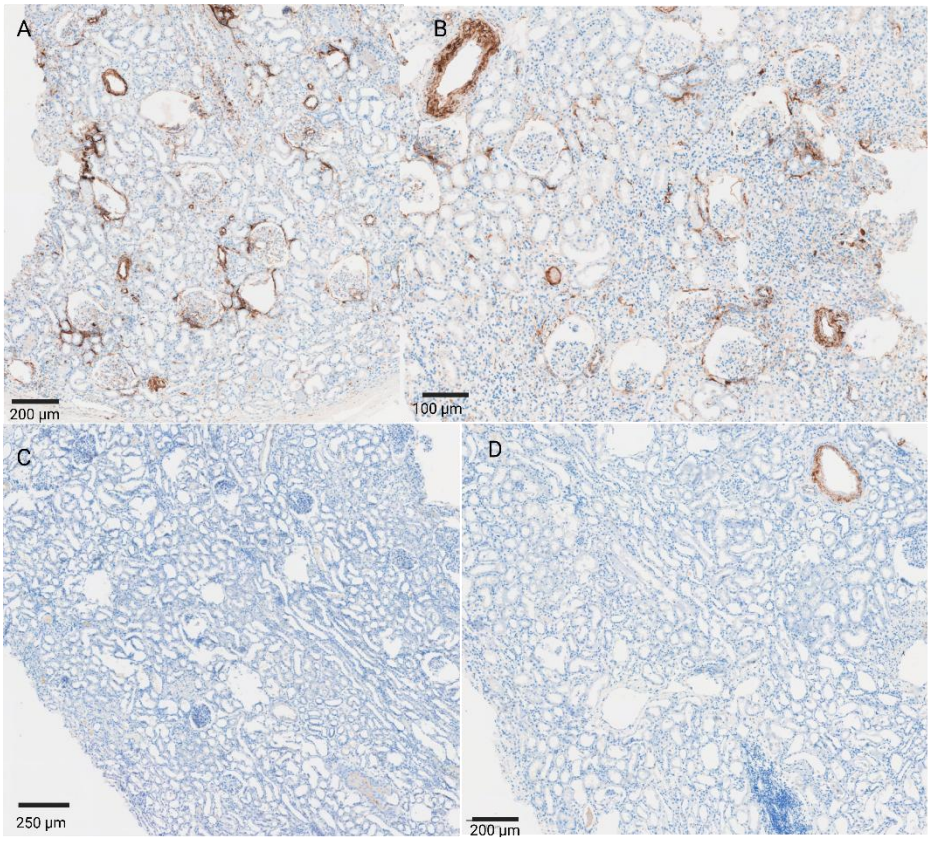


Figure 5.18 ***End of NR tissue biopsies demonstrating consistency between pairs.*** *Panel A and B end of NR biopsises from the right and left kidenys of pair 1 demonstrating similarly high levbels of C5b-9 staining post reperfusion with significant tissue injury. Compared with panel C and D, the right and left kidney of pair 4, showing similarly lower levels of C5b-9 staining at the ned of NR along with tissue damage from IRI.*

The positive control slides, which is from a staged active thrombosis during NMP designed to produced diffuse thrombosis and strong complement activation, with a large luminal thrombus noted in the main renal artery with endothelial activation and dramatic deposition within the cortex across, tubules, glomeruli, and vasculature (Fig 5.19).

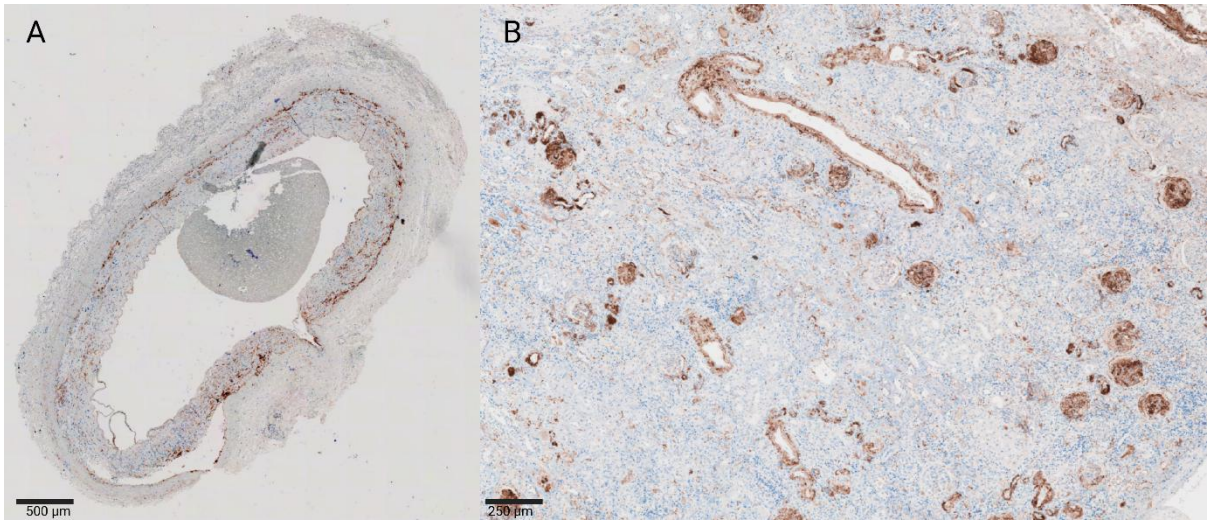


Figure 5.19 ***C5b-9 Staining in thrombosed positive control kidney.*** *Positive control perufion with intentionally thrombosed kidney during NR to induce diffusecomplement and coagulation cascade activity. Panel A mainrenal artery with thrombus in situ. Panel B punch biopsy showing significant and diffuse glomerular, tubular and vascular C5b-9 staining.*

5.5 Discussion

5.5.1 Dose Finding Perfusions

The investigation of mirococept in the context is novel, and there is no pre-clinical animal work on which to base a hypothesis about NMP behaviour or delivery. The basic biophysics of cell membranes at different temperature make NMP a good candidate for membrane inserted drug delivery in general and given the evidence from the porcine study that uptake that there is measurable uptake even in the cold, it seemed likely that the drug would perform well in NMP. However, little was known about this, and in view of the high the cost of the drug, a small series of single kidney perfusions was performed for dose assessment. Unfortunately, the specially made mirococept labelled with pegylated fluorescein was not available to us: the remainder of this extremely expensive production run carried out to support the first phase of the clinical trial has been used in the porcine dosing study, therefore was unfortunately not available for these perfusions: standard (i.e. non-pegylated) clinical grade mirococept was used. The 5 perfusions were done in a series of broadly similar declined kidneys, kidney 2 had a notably longer CIT (31:06), which likely accounts its becoming anuric: apart from this, baseline creatinine and injury across the kidneys were comparable. The perfusions were tightly controlled biochemically and produced stable homogeneously perfused kidneys, a model in which we chose to assess dose-based differences in complement behaviour.

Looking at the formation of terminal complement in the perfusate over the course of the perfusion the trajectories were not as expected, the higher dose of 120mg followed the pattern seen previously in C2 inhibited kidneys and their controls, with a small but physiologically significant amount produced and/or released during NMP, the bulk of which was in the first 2 hours. Then over the course of NR a significant rise over the 6 hours with a steeper gradient in the final hour, in keeping with increasing amplification via the alternative pathway. In contrast the kidneys with the lower dose of 60mg and the EMPIRIKAL protocol kidney with SCS delivered mirococept showed a more attenuated response during NR. During NMP, the 60mg kidneys reach lower levels of C5b-9, however this effect was somewhat limited and the baseline variability between kidneys

is such that one cannot interpret this effect as meaningful. With NR, the EMPIRIKAL kidney had early activation and then plateaued over the later hours of the perfusion, which was not something that had been noted in the model up to this point. The 60mg dosed kidneys did have progressive activation as we would expect, but at a shallower gradient, reaching a lower final level. Within the groups there were consistent patterns with both the 60mg following a consistent trajectory, as with the 120mg dosed kidneys.

When taking all the NMP delivered mirococept kidneys together with the two NMP doses as a single group and comparing them with unpaired controls from the C2 inhibition series to provide further insight. There appears to be an attenuated production early on, but the difference did not reach significance in this unpaired analysis, however by the end of NR, the divergence had narrowed, though numerically there is less C5b-9 with mirococept.

To quantify the tissue compartment, which must be considered alongside the soluble phase proteins, western blotting and native gel electrophoresis were performed to assess C3d and C5b-9, respectively. For C3d the EMPIRIKAL protocol kidney had a very low baseline level and over the course of NR, large amounts of C3d were deposited in the tissue >20-fold compared to the NMP mirococept kidneys. By the end of NR, the 60mg kidneys have only a slightly increased in tissue C3d level, 471 to 757, and the 120mg had a greater increase 260 to 1175, but both markedly lower than SCS, and the difference between the doses is not significant, given the unpaired sample size. In terms of C5b-9 tissue deposition, there was relatively little in the EMPIRIKAL protocol kidney, with deposition in both 60 and 120mg, with a numerically slightly lower amount in 120mg delivered kidneys.

When comparing the C5b-9 levels to a set of unpaired controls run on the same gel, there is no significant difference between mirococept and control, though at the end of NR, numerically mirococept is lower and more tightly packed, which could point towards an efficacy signal.

Though hard to draw solid conclusions from such a small unpaired series, there are some biological considerations that could explain the differences between the doses and modes of delivery. For the SCS delivery, we know from the porcine dosing study that

there is good uptake into the kidney, and for this NR phase there will be mirococept present. For this perfusion there was a significant generation of C3d & C3dg over NR, but relatively low levels of C5b-9 accumulation in the tissue, albeit starting from a lower baseline, and in the perfusate when compared with both the C2 inhibition perfusions and the 120mg NMP kidneys in this series. This could represent the drug being in situ and exerting biological effect, attenuating C5b-9 formation, but it should also attenuate C3d formation as it binds both forms of C3 convertase C2aC4b and C3bBb, its contradictory nature and isolated perfusion make it difficult to interpret. 60mg and 120mg seemed to behave consistently, and possibly in a slight activation attenuation relative to the unpaired controls, without a clear difference from the dose effect with mirococept.

Overall, the series of single kidney perfusions did not give a clear picture on dose effect or even on NMP delivered mirococept relative to SCS or unpaired controls. There was subtle trend for lower perfusate C5b-9 with mirococept and the markedly lower tissue C3d levels, and possibly tissue C5b-9 levels, so it was reasonable to proceed and conduct a more tightly controlled paired series. There are inherent limitations to the use of single kidneys, especially in the case of a donor-influenced biological processes such as complement deposition and activation, and paired perfusions are preferable. There was also an unclear does effect, for this reason, 2 pairs with 60mg and 2 pairs with 120mg delivered in NMP were selected for the subsequent study using kidney pairs.

5.5.2 Paired Perfusions

Four pairs of human kidneys declined for transplant were perfused, and they were more homogeneous in terms of donor demographics and baseline injury, and retrieval creatinine than the individual kidney group. The cold ischaemic times were shorter and closer between pairs, within transplantable times, and the NMP to NR WIT was tightly controlled and near equivalent between groups. The pattern of flow and the weight adjusted renal artery flows were consistent between pairs and across the series, all kidneys demonstrated global macroscopic perfusion.

Electrolyte biochemistry control across the series and between the pairs was tight and there were no statistical differences. A good platform was delivered for stable paired

perfusion, such that interpretation of the complement behaviour and associated biomarkers was reliable.

None of the kidneys were anuric, some producing measurable volumes of filtrate with biochemical evidence of good tubular function. There was a trend for the mirococept-treatedkidneys to produce more urine, especially during NR, but the differences in AUC were not statistically significant. There was some evidence of greater tubular function, with respect to sodium conservation and potassium excretion. By the end of NR CrCl was significantly higher in treated kidneys, possibly due to the tubular protective effects of complement inhibition.

At the end of NMP levels of IL-18 and NGAL were significantly lower in mirococept treated kidneys. These have been shown to be significant biomarkers in early post-transplant function in the NKP1 cohort. Also some previous studies in HMP correlate these to early outcomes, although the mechanism in this context of HMP is presumably different. There was no significant baseline difference, implying a dynamic process in the formation of the injury markers during NMP, and which in the series of mirococept delivered kidneys is attenuated. Another key marker from the NKP1 clinical trial was delta-GST-Pi, the ability to generate GST-Pi over the course of NMP, representing tubular recovery and improved early and longer-term function in the cohort of patients in NKP1. Delta GSTP-pi levels were significantly higher in the mirococept cohort at 19 compared with 9, magnitudes similar to those seen in NKP1 cases which went on to show an improved 3-month GFR.

Despite these biomarker effects during NMP, the was no evidence of altered complement formation or deposition in the NMP phase. Similarly in the NR phase where there was evidence of an attenuated complement response, there was no corresponding injury biomarker evidence. That doesn't necessarily negate the significance of the findings in NMP when correlating to the NKP1 cohort, as this is the only available series to compare with equivalent NMP durations.

Both C3d and C5b-9 formation was attenuated in the early NR phase, within the first hour both were significantly lower compared with paired controls, this is in keeping with membrane anchored common pathway complement inhibition. As NR progresses the

difference reduces, and while slightly numerically lower, there is not a significant difference in either by the end of the NR. However, when you look at frozen tissue, there is significantly lower level of C5b-9 deposited in the tissue, though this difference is not found in the quantitative analysis for the C5b-9 IHC. It is plausible that there is an effect seen with both benefit in the NMP phase with regard injury biomarkers and subtle evidence of effect on complement formation in NR. One must consider whether this small reduction, would be biologically meaningful in the early post-transplant period.

5.5.3 The Model & Its Limitations

As with all models, this model's effect on interpretation is an important consideration. At a basic level, plasma reperfusion clearly generates a complement response and provides a physiological spectrum of complement proteins capable of initiating the cascade and driving progressive amplification. This makes the model a useful surrogate for the earliest phase of reperfusion, when complement activity is typically most pronounced, and therefore a relevant window in which to interrogate complement inhibition. However, the reperfusion period does not continue for long enough to observe a clear plateau in C5b-9 formation once substrate becomes limiting, so the absolute maximum response in each case is not established.

From the observed kinetics, it is plausible that mirococept binding is at least partially reversible, with the dominant attenuating signal occurring early in NR (when endothelial coating may be highest) and diminishing as the drug redistributes, is washed from key surfaces, or is functionally outcompeted at the membrane interface by abundant plasma proteins. This time-dependent profile would be consistent with the early separation in perfusate complement markers that narrows by end of NR, despite evidence of reduced terminal complex deposition on native gel analysis.

There is also a high degree of variation across pairs, making modest biological effects harder to detect with small numbers of perfusions, even in a paired design. This variability likely reflects donor heterogeneity (DCD/DBD status, NRP exposure, CIT, and pre-existing vascular disease), which influences baseline endothelial injury and the abundance of complement-activating surfaces. In addition, several elements of the experimental platform may shape complement behaviour in ways that differ from

clinical transplantation. First, these declined organs may carry greater baseline injury, including endothelial disruption and exposed basement membrane, which can accentuate complement triggering. Second, the closed-circuit, isolated nature of the system is likely to promote accumulation of circulating DAMPs, free haemoglobin and concentrated debris. There is also the small additional complement activation from circuit contact surfaces, collectively creating a more activating environment than the in vivo setting.

Plasma reperfusion in a closed circuit lacks key in vivo modulators. There is no liver-driven replenishment of complement regulators and no systemic clearance mechanisms, again exacerbating activation. However, there is also no recruitment of recipient leukocytes that would amplify inflammatory injury through C3a/C5a-driven chemotaxis and endothelial–leukocyte interactions. As a result, the model captures an important mechanistic component of early humoral complement activation, but only partially reflects the full biology of clinical reperfusion injury.

Endpoint alignment across compartments remains an additional challenge. Perfusate complement fragments reflect a mixture of intravascular generation, release from tissue-bound pools, and dilutional effects, whereas tissue measures reflect local deposition and retention. Differences between western/native gel readouts and whole-slide IHC quantification may therefore reflect genuine spatial heterogeneity (including focal microvascular deposition), differences in epitope accessibility, and/or thresholding and segmentation constraints inherent to DAB quantification, even with an optimised workflow.

Finally, the small sample size in the dose-finding series and the mixed dosing in the paired series limits firm inference on dose–response, particularly if the true biological effect is confined to a short peri-reperfusion window and is modest in magnitude within this model. Overall, the model is well-suited to detecting early mechanistic signals of complement activation and inhibition during controlled reperfusion, but it cannot fully recapitulate the systemic inflammatory milieu of transplantation or quantify longer-term immunological priming. The most appropriate interpretation is therefore that the findings provide evidence of time-limited, organ-localised complement modulation, which requires further optimisation and validation.

5.5.4 Overall Conclusion & Translational Implications

Across both the dose-finding and paired series, NMP delivery of mirococept was feasible and did not compromise perfusion stability. The most consistent biological signal was a reduction in complement activation during the early phase of NR, with significantly lower perfusate C3d and C5b-9 at one hour, and a concordantly lower tissue levels of C5b-9 on native gel electrophoresis. In contrast, perfusate complement markers across both the dose-finding and paired series, NMP delivery of mirococept was feasible and did not compromise perfusion stability. The most consistent biological signal was attenuation of complement activation during the early phase of NR, with significantly lower perfusate C3d and C5b-9 at one hour and concordantly lower tissue C5b-9 on native gel electrophoresis. In contrast, perfusate complement markers converged by end-NR, suggesting that any inhibitory effect may be transient, potentially reflecting partial wash-off, redistribution, or saturation kinetics at the endothelial surface.

Importantly, during NMP itself, mirococept-treated kidneys demonstrated significantly lower IL-18 and NGAL at end-NMP and a higher delta GST-Pi, a pattern compatible with reduced acute tubular stress and possible improved tubular recovery during perfusion. While these injury-marker effects were not clearly mirrored by perfusate complement readouts during NMP, they suggest either that complement modulation acts predominantly at the tissue level and is incompletely captured in the soluble compartment, or that mirococept may influence injury pathways not fully reflected by bulk perfusate complement fragment concentrations alone.

Taken together, these data support the concept that organ-localised C3b/C4b convertase inhibition can measurably blunt early reperfusion complement activation and may favourably influence injury biomarker trajectories during NMP. The clinical relevance of a time-limited effect could be high, as the earliest post-reperfusion window is when complement-driven endothelial activation and downstream inflammatory amplification are likely greatest. However, the modest effect size and convergence of perfusate markers by end of NR tempers the strength of inference.

The immediate next steps of benefit would be to find a commercially available antibody to the compound to assess NMP binding and retention into NR. Following that there is sufficient early evidence that mirococept has a beneficial effect to warrant usage in a clinical NMP perfusate, especially if the findings of the EMPIRIKAL clinical trial are favourable.

6

Concluding Remarks

Contents

6.1 Thesis Objectives

6.2 Summary of Key Points

6.3 Outstanding Basic Scientific Questions

6.4 Future Clinical and Pre-Clinical Directions

6.1 Thesis Objectives

This thesis set out to characterise complement behaviour during renal NMP and to examine whether complement inhibition delivered in the ex vivo setting could modulate early injury relevant to kidney transplantation. The work was motivated by two linked questions. First, whether complement activation is a meaningful component of the biological response to occur during prolonged clinical NMP and early reperfusion. Second, whether NMP provides a practical therapeutic window in which targeted complement inhibition can be delivered to the graft before implantation.

To address these questions, the thesis first examined complement proteins and activation products in the NKP1 clinical trial cohort, in which kidneys underwent prolonged pre-transplant NMP and were subsequently implanted. This provided an opportunity to assess whether complement activation could be detected in perfusate, whether it correlated with related to donor and graft characteristics, and whether it was associated with clinical outcomes. The second objective was to investigate complement inhibitor intervention by establishing a controlled ex vivo model of NMP followed by plasma-based normothermic reperfusion, designed to reproduce early transplant-like complement activation in declined human kidneys. Within this platform, pathway-specific inhibition at different points in the cascade was assessed using C2 inhibition with argx-117 and C3b/C4b convertase inhibition with mirococept.

The first and overarching objective of the thesis was to determine whether complement activity during renal NMP should be understood principally as a biomarker of donor and retrieval injury, as a mechanistic mediator of early graft injury, or as both. My second objective was to define whether the ex vivo perfusion platform could be used not only to study this biology, but also to support the rational development of graft-directed complement therapeutics for kidney transplantation.

6.2 Summary of Key Points

The first major finding described in this thesis is that complement activation is feature of prolonged clinical renal NMP. In the NKP1 cohort, perfusate analysis demonstrated measurable complement proteins and activation products across the classical, lectin, alternative, and terminal pathways. Over the course of perfusion, C3d, C1s, collectin-11 and sC5b-9 increased, while C2 and factor B fell, supporting a model in which activation, consumption, washout, and release occur simultaneously during NMP.

A second key finding is that early complement profiles during NMP relate to donor biology and to transplant outcome. Early and end-perfusion complement markers associated with donor age, UKDRI, donor type, and functional delayed graft function. In particular, early multi-marker complement profiles stratified against TCr50 and appeared to add prognostic information beyond donor risk alone. These findings support the interpretation that complement activity measured during NMP captures biologically important information about graft quality and innate inflammatory priming. Complement in this setting therefore appears to function, at least in part, as a clinically informative biomarker platform.

The third important observation is that the ex vivo NMP plus plasma reperfusion model successfully recreated a transplant-relevant complement environment. Blood-only perfusions showed that the circuit itself generated only modest activation, whereas the addition of an injured kidney drove a much stronger complement response in both perfusate and tissue. This established the model as a useful platform for testing complement inhibitors under tightly controlled conditions. The data also reinforce the concept that the kidney, rather than the circuit, is the dominant biological driver of activation in this setting.

The interventional chapters demonstrated that ex vivo complement inhibition is pharmacodynamically achievable, but that efficacy depends on where and how the cascade is targeted. Argx-117 produced rapid and sustained depletion of free C2, with corresponding suppression of residual classical and lectin pathway activity and modest attenuation of C3a and C3bBbP during reperfusion. However, this did not translate into consistent suppression of terminal pathway activation, with sC5b-9 remaining high and tissue complement readouts showing no reproducible broad reduction. This suggests that selective C2 blockade, while mechanistically active, may be insufficient on its own to overcome the intensity and redundancy of complement activation present in severely injured kidneys during the reperfusion model.

Mirococept showed a different pattern. NMP delivery was feasible, did not impair perfusion stability, and was associated with reduced IL-18 and NGAL at the end of NMP together with a higher delta GST-Pi, suggesting a possible benefit on tubular stress and recovery during perfusion. During early reperfusion, mirococept-treated kidneys

showed significantly lower perfusate C3d and C5b-9 early in reperfusion, and tissue native gel analysis suggested reduced terminal complex deposition by the end of reperfusion. Although these effects were modest and appeared to attenuate over time, they support the idea that organ-localised inhibition at the level of C3b/C4b convertase activity.

In summary, the thesis supports three broad conclusions. First, complement is active and biologically relevant during renal NMP and reperfusion. Second, complement behaviour during NMP reflects both donor-derived injury signals and ongoing graft-level activation. Third, ex vivo perfusion can be used not only to measure complement behaviour, but also to manipulate it, although the success of intervention is likely to depend on target selection, pharmacokinetics at the graft surface, and the degree of baseline injury within the organ.

6.3 Outstanding Basic Scientific Questions

Despite the findings presented, several important basic scientific questions remain unresolved. One central question is the precise origin of the complement proteins and activation products measured during NMP. The data strongly support that early perfusate complement signals reflect donor and retrieval injury, but the relative contribution of residual donor plasma, passive washout from tissue, endothelial release, and active intrarenal synthesis remains uncertain. This is especially relevant for proteins such as C3, C2, C1s, and collectin-11, for which the kidney may contribute locally, but where the quantitative importance of that contribution during ex vivo perfusion is still unclear.

A second unresolved issue is where complement activation is occurring within the perfused kidney. Perfusate biomarkers integrate the whole organ and provide excellent temporal resolution, but they cannot localise activation to specific compartments. The tissue data supports complement deposition in the graft, particularly during reperfusion, but a full compartment analysis has not been conducted, and it is hard to resolve how much terminal pathway activation is membrane-bound and persistent, versus rapidly shed or internalised and therefore mainly represented in the fluid phase.

Thirdly, it is not clear what the relative importance of classical, lectin, and alternative pathway activation at different phases of NMP and NR. Overall, the data suggests that early injury is likely shaped by a mixture of donor priming, CP/LP triggering, and AP amplification. However, the failure of C2 depletion to meaningfully suppress terminal pathway readouts, despite clear pharmacodynamic target engagement, suggests that AP amplification and pathway redundancy may be sufficient to sustain downstream injury even when proximal CP/LP activity is reduced. Defining when CP/LP initiation matters most, and when AP amplification becomes dominant, remains a mechanistic challenge and difficult in any model.

It is also unclear how well soluble complement biomarkers reflect true biological injury. Here, the perfusate markers often showed stronger and cleaner signals than tissue endpoints, and some of the most clinically informative findings came from soluble profiles. Yet it remains uncertain whether these biomarkers are simply correlates of pre-existing injury, or whether they also capture biologically meaningful ongoing complement-mediated damage. The most likely answer is that they represent both, but the relative weighting of these roles probably changes over time and between organs. The crux is that soluble proteins are far easier to work with, with a wide range of commercial validated antibodies and kits and sample acquisition and handling is much more straightforward.

Finally, the model is complement focused by design, with the use of FFP, so has not fully characterised the role of non-complement cellular effectors. The plasma reperfusion

system recreates complement activation effectively, but lacks leukocytes and platelets, both of which are central to the downstream biology of C3a, C5a, opsonisation, endothelial activation, and immunothrombosis. This means that this model isolates direct graft–complement interactions well but likely underestimates the full downstream effect of complement in transplantation. Understanding how ex vivo complement modulation translates into leukocyte recruitment, platelet activation, microvascular thrombosis, and later adaptive alloimmune consequences remains an important unanswered question.

6.4 Future Clinical and Pre-Clinical Directions

The findings of this thesis support several directions for future work. A straightforward immediate step is for validation of the complement biomarkers. The complement biomarker signals identified during clinical NMP, particularly the early composite profiles associated with functional recovery, this can be tested in an Assessment and Reconditioning Centre (ARC) type setting where a larger volume of kidneys will undergo standardised NMP across several sites. This would help to determine whether the signals observed here are robust enough to support risk stratification as a part of graft assessment.

A useful step would be the refinement of this ex vivo reperfusion model. The present platform is technically robust and biologically informative, but it should now be developed further to address some of its known limitations. Incorporation of more physiologically complete blood components, particularly platelets and selected leukocyte populations, which is possible with good collaboration with NHSBT blood services, this could help bridge the gap between isolated complement activation and the full thromboinflammatory response seen after implantation.

For therapeutic testing, the data suggest that target selection is critical. Selective C2 inhibition clearly altered pathway function, but in this model it was insufficient to produce broad suppression of terminal activation. This does not mean that C2 inhibition lacks clinical relevance; indeed, it may still be highly valuable as a donor- or recipient-directed systemic therapy, where its effects extend beyond the isolated kidney to the wider inflammatory environment, and outside of a model which may have excessively harsh complement activating capacity. However, as an ex vivo graft-directed strategy, the results imply that more proximal or membrane-localised approaches may be more effective. The early signal seen with mirococept supports continued interest in graft-surface complement modulation, particularly if methods can be developed to measure tissue binding and retention more directly during NMP and reperfusion. Showing definitive evidence mirococept is present within the tissue after NMP along with mechanistic effect would strengthen the findings.

Clinically, there three good avenues to pursue. The first is to use complement profiling during NMP as a biomarker tool, validating this in an ARC NMP kidney setting, early complement profile could contribute to graft assessment, identify organs at particularly high risk of slow recovery. The second is to use NMP as a therapeutic delivery platform. In this context, complement inhibitors are attractive because they can be delivered directly to the organ before recipient exposure, potentially reducing systemic toxicity while targeting one of the key mechanisms of early reperfusion injury. The ideal agent may be one that combines strong local retention with sufficient breadth of pathway inhibition to blunt downstream amplification and terminal injury during the first hours after implantation. Given there have been biologically relevant signals with the use of

mirococept a small pilot trial with some high-risk donor kidneys and assess TCr50 relative to matched historic controls.

The third is the important consideration of donor intervention. There is evidence here that complement activation begins before implantation and that donor biology contributes substantially to the graft's inflammatory state. Donor treatment, peri-retrieval treatment are likely to be an important window. A small pilot donor trial of donor delivered complement inhibition, delivered as proximal to brain death as possible, with complement based mechanistic outcomes relating specifically to the donor and organs initially would be of interest. C2 or C5 are attractive targets given their relatively lower abundance compared to C3, needing much less volume of monoclonal. These are not competing strategies as there is evidence of complement having effects across the transplant journey, with potential benefit of intervening at several stages.

In broader terms, this thesis supports the view that renal NMP should not be considered solely a preservation technology. It is also a period of biological observation and a therapeutic platform. By allowing serial sampling, and direct drug delivery to the graft, it provides a unique opportunity to interrogate early transplant injury in human kidneys in a way not possible in standard clinical transplantation. Complement biology is well suited to this platform because it is dynamic, injury-responsive, and may prove to be therapeutically tractable. The challenge now is to translate this mechanistic insight into clinically useful strategies that improve the utilisation and early function of deceased donor kidneys.

7

References

1 Tonelli, M. *et al.* Systematic review: kidney transplantation compared with dialysis in clinically relevant outcomes. *Am J Transplant* **11**, 2093–2109 (2011). https://doi.org/10.1111/j.1600-6143.2011.03686.x

2 Summers, D. M. *et al.* Kidney donation after circulatory death (DCD): state of the art. *Kidney Int* **88**, 241–249 (2015). https://doi.org/10.1038/ki.2015.88

3 Trachsel, C. *et al.* Outcomes of Kidney Transplants from Donors after Circulatory Death with Acute Kidney Injury: A Systematic Review. *Current Transplantation Reports* **12** (2025). https://doi.org/10.1007/s40472-025-00496-2

4 Mohan, S. *et al.* Factors leading to the discard of deceased donor kidneys in the United States. *Kidney Int* **94**, 187–198 (2018). https://doi.org/10.1016/j.kint.2018.02.016

5 Abicht, J. M. *et al.* Complement C3 inhibitor Cp40 attenuates xenoreactions in pig hearts perfused with human blood. *Xenotransplantation* **24** (2017). https://doi.org/10.1111/xen.12262

6 Butala, N. M., Reese, P. P., Doshi, M. D. & Parikh, C. R. Is delayed graft function causally associated with long-term outcomes after kidney transplantation? Instrumental variable analysis. *Transplantation* **95**, 1008–1014 (2013). https://doi.org/10.1097/TP.0b013e3182855544

7 Kim, D. W. *et al.* Financial impact of delayed graft function in kidney transplantation. *Clin Transplant* **34**, e14022 (2020). https://doi.org/10.1111/ctr.14022

8 Zhao, H., Alam, A., Soo, A. P., George, A. J. T. & Ma, D. Ischemia-Reperfusion Injury Reduces Long Term Renal Graft Survival: Mechanism and Beyond. *EBioMedicine* **28**, 31–42 (2018). https://doi.org/10.1016/j.ebiom.2018.01.025

9 Peters-Sengers, H. *et al.* Impact of Cold Ischemia Time on Outcomes of Deceased Donor Kidney Transplantation: An Analysis of a National Registry. *Transplant Direct* **5**, e448 (2019). https://doi.org/10.1097/TXD.0000000000000888

10 Belzer, F. O., Ashby, B. S., Gulyassy, P. F. & Powell, M. Successful seventeen-hour preservation and transplantation of human-cadaver kidney. *N Engl J Med* **278**, 608–610 (1968). https://doi.org/10.1056/NEJM196803142781108

11 O'Callaghan, J. M., Morgan, R. D., Knight, S. R. & Morris, P. J. Systematic review and meta-analysis of hypothermic machine perfusion versus static cold storage of kidney allografts on transplant outcomes. *Br J Surg* **100**, 991–1001 (2013). https://doi.org/10.1002/bjs.9169

12 Peng, P. *et al.* Hypothermic Machine Perfusion Versus Static Cold Storage in Deceased Donor Kidney Transplantation: A Systematic Review and Meta-Analysis of Randomized Controlled Trials. *Artif Organs* **43**, 478–489 (2019). https://doi.org/10.1111/aor.13364

13 Tingle, S. J. *et al.* Machine perfusion preservation versus static cold storage for deceased donor kidney transplantation. *Cochrane Database Syst Rev* **3**, CD011671 (2019). https://doi.org/10.1002/14651858.CD011671.pub2

14 Tingle, S. J. *et al.* Hypothermic machine perfusion is superior to static cold storage in deceased donor kidney transplantation: A meta-analysis. *Clin Transplant* **34**, e13814 (2020). https://doi.org/10.1111/ctr.13814

15 Nicholson, M. L. & Hosgood, S. A. Renal transplantation after ex vivo normothermic perfusion: the first clinical study. *Am J Transplant* **13**, 1246–1252 (2013). https://doi.org/10.1111/ajt.12179

16 Rabelink, T. J. *et al.* Opportunities and challenges with the implementation of normothermic machine perfusion in kidney transplantation. *Nat Commun* **16**, 6883 (2025). https://doi.org/10.1038/s41467-025-60410-3

17 Guzzi, F., Knight, S. R., Ploeg, R. J. & Hunter, J. P. A systematic review to identify whether perfusate biomarkers produced during hypothermic machine perfusion can predict graft outcomes in kidney transplantation. *Transpl Int* **33**, 590–602 (2020). https://doi.org/10.1111/tri.13593

18 van Smaalen, T. C. *et al.* Presence of Cytotoxic Extracellular Histones in Machine Perfusate of Donation After Circulatory Death Kidneys. *Transplantation* **101**, e93–e101 (2017). https://doi.org/10.1097/TP.0000000000001590

19 Franzin, R. *et al.* Renal Delivery of Pharmacologic Agents During Machine Perfusion to Prevent Ischaemia-Reperfusion Injury: From Murine Model to Clinical Trials. *Front Immunol* **12**, 673562 (2021). https://doi.org/10.3389/fimmu.2021.673562

20 Golshayan, D., Schwotzer, N., Fakhouri, F. & Zuber, J. Targeting the Complement Pathway in Kidney Transplantation. *J Am Soc Nephrol* **34**, 1776–1792 (2023). https://doi.org/10.1681/ASN.0000000000000192

21 Zulpaite, R. *et al.* Ex-vivo Kidney Machine Perfusion: Therapeutic Potential. *Front Med (Lausanne)* **8**, 808719 (2021). https://doi.org/10.3389/fmed.2021.808719

22 Hameed, A. M. *et al.* Normothermic Ex Vivo Perfusion Before Transplantation of the Kidney (NEXT-Kidney): A Single-center, Nonrandomized Feasibility Study. *Transplantation* **109**, 881–889 (2025). https://doi.org/10.1097/TP.0000000000005233

23 Zlatev, H., von Horn, C., Kaths, M., Paul, A. & Minor, T. Clinical use of controlled oxygenated rewarming of kidney grafts prior to transplantation by ex vivo machine perfusion. A pilot study. *Eur J Clin Invest* **52**, e13691 (2022). https://doi.org/10.1111/eci.13691

24 Montagud-Marrahi, E. *et al.* Ex vivo normothermic preservation of a kidney graft from uncontrolled donation after circulatory death over 73 hours. *Front Bioeng Biotechnol* **11**, 1330043 (2023). https://doi.org/10.3389/fbioe.2023.1330043

25 Pearson, R. *et al.* Viability assessment and utilization of declined donor kidneys with rhabdomyolysis using ex vivo normothermic perfusion without preimplantation biopsy. *Am J Transplant* **21**, 1317–1321 (2021). https://doi.org/10.1111/ajt.16329

26 Hosgood, S. A. & Nicholson, M. L. First in man renal transplantation after ex vivo normothermic perfusion. *Transplantation* **92**, 735–738 (2011). https://doi.org/10.1097/TP.0b013e31822d4e04

27 Hosgood, S. A. *et al.* Normothermic machine perfusion versus static cold storage in donation after circulatory death kidney transplantation: a randomized controlled trial. *Nat Med* **29**, 1511–1519 (2023). https://doi.org/10.1038/s41591-023-02376-7

28 MacMillan, S. *et al.* Enzymatic conversion of human blood group A kidneys to universal blood group O. *Nat Commun* **15**, 2795 (2024). https://doi.org/10.1038/s41467-024-47131-9

29 Kaths, J. M. *et al.* Continuous Normothermic Ex Vivo Kidney Perfusion Is Superior to Brief Normothermic Perfusion Following Static Cold Storage in Donation After Circulatory Death Pig Kidney Transplantation. *Am J Transplant* **17**, 957–969 (2017). https://doi.org/10.1111/ajt.14059

30 Mazilescu, L. I. *et al.* Normothermic Ex Vivo Kidney Perfusion for Human Kidney Transplantation: First North American Results. *Transplantation* **106**, 1852–1859 (2022). https://doi.org/10.1097/TP.0000000000004098

31 Rijkse, E. *et al.* Safety and feasibility of 2 h of normothermic machine perfusion of donor kidneys in the Eurotransplant Senior Program. *BJS Open* **5** (2021). https://doi.org/10.1093/bjsopen/zraa024

32 Dumbill, R. *et al.* Prolonged normothermic perfusion of the kidney prior to transplantation: a historically controlled, phase 1 cohort study. *Nat Commun* **16**, 4584 (2025). https://doi.org/10.1038/s41467-025-59829-5

33 Capey, S. & van den Berg, C. W. Porcine complement regulators protect aortic smooth muscle cells poorly against human complement-induced lysis and proliferation: consequences for xenotransplantation. *Xenotransplantation* **12**, 217–226 (2005). https://doi.org/10.1111/j.1399-3089.2005.00217.x

34 Heckl-Ostreicher, B., Binder, R. & Kirschfink, M. Functional activity of the membrane-associated complement inhibitor CD59 in a pig-to-human in vitro model for hyperacute xenograft rejection. *Clin Exp Immunol* **102**, 589–595 (1995). https://doi.org/10.1111/j.1365-2249.1995.tb03857.x

35 Schmidt, P., Goto, M., Le Mauff, B., Anegon, I. & Korsgren, O. Adenovirus-mediated expression of human CD55 or CD59 protects adult porcine islets from complement-mediated cell lysis by human serum. *Transplantation* **75**, 697–702 (2003). https://doi.org/10.1097/01.TP.0000053249.39753.D6

36 Kuwaki, K. *et al.* Suppression of natural and elicited antibodies in pig-to-baboon heart transplantation using a human anti-human CD154 mAb-based regimen. *Am J Transplant* **4**, 363–372 (2004). https://doi.org/10.1111/j.1600-6143.2004.00353.x

37 Lin, S. S. *et al.* The role of natural anti-Gal alpha 1-3Gal antibodies in hyperacute rejection of pig-to-baboon cardiac xenotransplants. *Transpl Immunol* **5**, 212–218 (1997). https://doi.org/10.1016/s0966-3274(97)80040-8

38 Sahu, A., Morikis, D. & Lambris, J. D. Compstatin, a peptide inhibitor of complement, exhibits species-specific binding to complement component C3. *Mol Immunol* **39**, 557–566 (2003). https://doi.org/10.1016/s0161-5890(02)00212-2

39 Brachet, G. *et al.* Eculizumab epitope on complement C5: Progress towards a better understanding of the mechanism of action. *Mol Immunol* **77**, 126–131 (2016). https://doi.org/10.1016/j.molimm.2016.07.016

40 Pischke, S. E. *et al.* Complement factor 5 blockade reduces porcine myocardial infarction size and improves immediate cardiac function. *Basic Res Cardiol* **112**, 20 (2017). https://doi.org/10.1007/s00395-017-0610-9

41 Messner, F. *et al.* 48 h Normothermic Machine Perfusion With Urine Recirculation for Discarded Human Kidney Grafts. *Transpl Int* **36**, 11804 (2023). https://doi.org/10.3389/ti.2023.11804

42 Chandak, P. *et al.* Modelling acute antibody-mediated rejection of human kidney transplants using ex-vivo warm machine perfusion. *EBioMedicine* **86**, 104365 (2022). https://doi.org/10.1016/j.ebiom.2022.104365

43 Zhu, Y., Thangamani, S., Ho, B. & Ding, J. L. The ancient origin of the complement system. *EMBO J* **24**, 382–394 (2005). https://doi.org/10.1038/sj.emboj.7600533

44 Matsushita, M. The Complement System of Agnathans. *Front Immunol* **9**, 1405 (2018). https://doi.org/10.3389/fimmu.2018.01405

45 Ghebrehiwet, B. The complement system: an evolution in progress. *F1000Res* **5**, 2840 (2016). https://doi.org/10.12688/f1000research.10065.1

46 Ricklin, D., Hajishengallis, G., Yang, K. & Lambris, J. D. Complement: a key system for immune surveillance and homeostasis. *Nat Immunol* **11**, 785–797 (2010). https://doi.org/10.1038/ni.1923

47 Santos-Lopez, J., de la Paz, K., Fernandez, F. J. & Vega, M. C. Structural biology of complement receptors. *Front Immunol* **14**, 1239146 (2023). https://doi.org/10.3389/fimmu.2023.1239146

48 Zarantonello, A., Revel, M., Grunenwald, A. & Roumenina, L. T. C3-dependent effector functions of complement. *Immunol Rev* **313**, 120–138 (2023). https://doi.org/10.1111/imr.13147

49 Shadid, A. *et al.* Enigmatic Roles of Complement Anaphylatoxin Signaling in Health and Disease. *Immune Netw* **25**, e32 (2025). https://doi.org/10.4110/in.2025.25.e32

50 de Boer, E. C. W., van Mourik, A. G. & Jongerius, I. Therapeutic Lessons to be Learned From the Role of Complement Regulators as Double-Edged Sword in Health and Disease. *Front Immunol* **11**, 578069 (2020). https://doi.org/10.3389/fimmu.2020.578069

51 Pratt, J. R., Basheer, S. A. & Sacks, S. H. Local synthesis of complement component C3 regulates acute renal transplant rejection. *Nat Med* **8**, 582–587 (2002). https://doi.org/10.1038/nm0602-582

52 West, E. E. & Kemper, C. Complosome - the intracellular complement system. *Nat Rev Nephrol* **19**, 426–439 (2023). https://doi.org/10.1038/s41581-023-00704-1

53 Biglarnia, A. R., Huber-Lang, M., Mohlin, C., Ekdahl, K. N. & Nilsson, B. The multifaceted role of complement in kidney transplantation. *Nat Rev Nephrol* **14**, 767–781 (2018). https://doi.org/10.1038/s41581-018-0071-x

54 Bouatou, Y. *et al.* Atypical Hemolytic Uremic Syndrome Recurrence after Renal Transplantation: C3-Glomerulonephritis as an Initial Presentation. *Transplant Direct* **1**, e9 (2015). https://doi.org/10.1097/TXD.0000000000000518

55 Obata, S., Vaz de Castro, P. A. S., Riella, L. V. & Cravedi, P. Recurrent C3 glomerulopathy after kidney transplantation. *Transplant Rev (Orlando)* **38**, 100839 (2024). https://doi.org/10.1016/j.trre.2024.100839

56 Weinstein, A., Alexander, R. V. & Zack, D. J. A Review of Complement Activation in SLE. *Curr Rheumatol Rep* **23**, 16 (2021). https://doi.org/10.1007/s11926-021-00984-1

57 Macedo, A. C. & Isaac, L. Systemic Lupus Erythematosus and Deficiencies of Early Components of the Complement Classical Pathway. *Front Immunol* **7**, 55 (2016). https://doi.org/10.3389/fimmu.2016.00055

58 Knijff, L. W. D. *et al.* Early Activation of the Complement System After Brain Death in Clinical Kidney Donation and Transplantation. *Transplantation* **109**, 1845–1854 (2025). https://doi.org/10.1097/TP.0000000000005520

59 Damman, J. *et al.* Systemic complement activation in deceased donors is associated with acute rejection after renal transplantation in the recipient. *Transplantation* **92**, 163–169 (2011). https://doi.org/10.1097/TP.0b013e318222c9a0

60 Halpern, S. E. *et al.* Systemic Complement Activation in Donation After Brain Death Versus Donation After Circulatory Death Organ Donors. *Exp Clin Transplant* **19**, 635–644 (2021). https://doi.org/10.6002/ect.2020.0425

61 Ponticelli, C. E. The impact of cold ischemia time on renal transplant outcome. *Kidney Int* **87**, 272–275 (2015). https://doi.org/10.1038/ki.2014.359

62 Lo, S., Jiang, L., Stacks, S., Lin, H. & Parajuli, N. Aberrant activation of the complement system in renal grafts is mediated by cold storage. *Am J Physiol Renal Physiol* **320**, F1174–F1190 (2021). https://doi.org/10.1152/ajprenal.00670.2020

63 Kenawy, H. I., Boral, I. & Bevington, A. Complement-Coagulation Cross-Talk: A Potential Mediator of the Physiological Activation of Complement by Low pH. *Front Immunol* **6**, 215 (2015). https://doi.org/10.3389/fimmu.2015.00215

64 Bongoni, A. K. *et al.* Complement-mediated Damage to the Glycocalyx Plays a Role in Renal Ischemia-reperfusion Injury in Mice. *Transplant Direct* **5**, e341 (2019). https://doi.org/10.1097/TXD.0000000000000881

65 Fu, X. *et al.* Target deletion of complement component 9 attenuates antibody-mediated hemolysis and lipopolysaccharide (LPS)-induced acute shock in mice. *Sci Rep* **6**, 30239 (2016). https://doi.org/10.1038/srep30239

66 Farrar, C. A. *et al.* Collectin-11 detects stress-induced L-fucose pattern to trigger renal epithelial injury. *J Clin Invest* **126**, 1911–1925 (2016). https://doi.org/10.1172/JCI83000

67 Zhang, M. *et al.* Activation of the lectin pathway by natural IgM in a model of ischemia/reperfusion injury. *J Immunol* **177**, 4727–4734 (2006). https://doi.org/10.4049/jimmunol.177.7.4727

68 Farrar, C. A., Zhou, W., Lin, T. & Sacks, S. H. Local extravascular pool of C3 is a determinant of postischemic acute renal failure. *FASEB J* **20**, 217–226 (2006). https://doi.org/10.1096/fj.05-4747com

69 Naesens, M. *et al.* Expression of complement components differs between kidney allografts from living and deceased donors. *J Am Soc Nephrol* **20**, 1839–1851 (2009). https://doi.org/10.1681/ASN.2008111145

70 van Leeuwen, L. L. *et al.* Proteomic analysis of machine perfusion solution from brain dead donor kidneys reveals that elevated complement, cytoskeleton and lipid metabolism proteins are associated with 1-year outcome. *Transpl Int* **34**, 1618–1629 (2021). https://doi.org/10.1111/tri.13984

71 Nieuwenhuijs-Moeke, G. J. *et al.* Ischemia and Reperfusion Injury in Kidney Transplantation: Relevant Mechanisms in Injury and Repair. *J Clin Med* **9** (2020). https://doi.org/10.3390/jcm9010253

72 Peng, Q. *et al.* C3a and C5a promote renal ischemia-reperfusion injury. *J Am Soc Nephrol* **23**, 1474–1485 (2012). https://doi.org/10.1681/ASN.2011111072

73 Zhou, W. *et al.* Predominant role for C5b-9 in renal ischemia/reperfusion injury. *J Clin Invest* **105**, 1363–1371 (2000). https://doi.org/10.1172/JCI8621

74 de Vries, D. K. *et al.* Acute but transient release of terminal complement complex after reperfusion in clinical kidney transplantation. *Transplantation* **95**, 816–820 (2013). https://doi.org/10.1097/TP.0b013e31827e31c9

75 Skinner, S. C. *et al.* Hemodialysis-Related Complement and Contact Pathway Activation and Cardiovascular Risk: A Narrative Review. *Kidney Med* **3**, 607–618 (2021). https://doi.org/10.1016/j.xkme.2021.04.006

76 Wagner, S. *et al.* Hemocompatibility of Polysulfone Hemodialyzers - Exploratory Studies on Impact of Treatment Modality and Dialyzer Characteristics. *Kidney360* **1**, 25–35 (2020). https://doi.org/10.34067/KID.0000342019

77 Mares, J., Thongboonkerd, V., Tuma, Z., Moravec, J. & Matejovic, M. Specific adsorption of some complement activation proteins to polysulfone dialysis membranes during hemodialysis. *Kidney Int* **76**, 404–413 (2009). https://doi.org/10.1038/ki.2009.138

78 Mastellos, D. C. *et al.* Taming hemodialysis-induced inflammation: Are complement C3 inhibitors a viable option? *Clin Immunol* **198**, 102–105 (2019). https://doi.org/10.1016/j.clim.2018.11.010

79 Poppelaars, F. *et al.* The Complement System in Dialysis: A Forgotten Story? *Front Immunol* **9**, 71 (2018). https://doi.org/10.3389/fimmu.2018.00071

80 Loupy, A. *et al.* Complement-binding anti-HLA antibodies and kidney-allograft survival. *N Engl J Med* **369**, 1215–1226 (2013). https://doi.org/10.1056/NEJMoa1302506

81 Sicard, A. *et al.* Detection of C3d-binding donor-specific anti-HLA antibodies at diagnosis of humoral rejection predicts renal graft loss. *J Am Soc Nephrol* **26**, 457–467 (2015). https://doi.org/10.1681/ASN.2013101144

82 Huang, E. *et al.* Three-Year Outcomes of a Randomized, Double-Blind, Placebo-Controlled Study Assessing Safety and Efficacy of C1 Esterase Inhibitor for Prevention of Delayed Graft Function in Deceased Donor Kidney Transplant Recipients. *Clin J Am Soc Nephrol* **15**, 109–116 (2020). https://doi.org/10.2215/CJN.04840419

83 Jordan, S. C. *et al.* A phase I/II, double-blind, placebo-controlled study assessing safety and efficacy of C1 esterase inhibitor for prevention of delayed graft function in deceased donor kidney transplant recipients. *Am J Transplant* **18**, 2955–2964 (2018). https://doi.org/10.1111/ajt.14767

84 Huang, E. *et al.* Back-table intra-arterial administration of C1 esterase inhibitor to deceased donor kidney allografts improves posttransplant allograft function: Results of a randomized double-blind placebo-controlled clinical trial. *Am J Transplant* **25**, 1926–1939 (2025). https://doi.org/10.1016/j.ajt.2025.05.003

85 Vo, A. A. *et al.* A phase I/II placebo-controlled trial of C1-inhibitor for prevention of antibody-mediated rejection in HLA sensitized patients. *Transplantation* **99**, 299–308 (2015). https://doi.org/10.1097/TP.0000000000000592

86 Montgomery, R. A. *et al.* Plasma-Derived C1 Esterase Inhibitor for Acute Antibody-Mediated Rejection Following Kidney Transplantation: Results of a Randomized Double-Blind Placebo-Controlled Pilot Study. *Am J Transplant* **16**, 3468–3478 (2016). https://doi.org/10.1111/ajt.13871

87 Keshavjee, S., Davis, R. D., Zamora, M. R., de Perrot, M. & Patterson, G. A. A randomized, placebo-controlled trial of complement inhibition in ischemia-reperfusion injury after lung transplantation in human beings. *J Thorac Cardiovasc Surg* **129**, 423–428 (2005). https://doi.org/10.1016/j.jtcvs.2004.06.048

88 Kassimatis, T. *et al.* Ex vivo delivery of Mirococept: A dose-finding study in pig kidney after showing a low dose is insufficient to reduce delayed graft function in human kidney. *Am J Transplant* **21**, 1012–1026 (2021). https://doi.org/10.1111/ajt.16265

89 Kassimatis, T. *et al.* Multicentre, multi-arm, double-blind randomised placebo-controlled dose-finding trial investigating the safety and Efficacy of MirococePt (APT070) In Reducing delayed graft function In the Kidney ALlograft (EMPIRIKAL-2): study protocol for a randomised controlled trial. *BMJ Open* **15**, e097029 (2025). https://doi.org/10.1136/bmjopen-2024-097029

90 Marks, W. H. *et al.* Safety and efficacy of eculizumab in the prevention of antibody-mediated rejection in living-donor kidney transplant recipients requiring desensitization therapy: A randomized trial. *Am J Transplant* **19**, 2876–2888 (2019). https://doi.org/10.1111/ajt.15364

91 Glotz, D. *et al.* Safety and efficacy of eculizumab for the prevention of antibody-mediated rejection after deceased-donor kidney transplantation in patients with preformed donor-specific antibodies. *Am J Transplant* **19**, 2865–2875 (2019). https://doi.org/10.1111/ajt.15397

92 Schroppel, B. *et al.* Peritransplant eculizumab does not prevent delayed graft function in deceased donor kidney transplant recipients: Results of two randomized controlled pilot trials. *Am J Transplant* **20**, 564–572 (2020). https://doi.org/10.1111/ajt.15580

93 Kaabak, M. *et al.* A prospective randomized, controlled trial of eculizumab to prevent ischemia-reperfusion injury in pediatric kidney transplantation. *Pediatr Transplant* **22** (2018). https://doi.org/10.1111/petr.13129

94 de Boer, E. *et al.* Normothermic Machine Perfusion Reconstitutes Porcine Kidney Tissue Metabolism But Induces an Inflammatory Response, Which Is Reduced

by Complement C5 Inhibition. *Transpl Int* **37**, 13348 (2024). https://doi.org/10.3389/ti.2024.13348

95 Adams, A. B. *et al.* Anti-C5 Antibody Tesidolumab Reduces Early Antibody-mediated Rejection and Prolongs Survival in Renal Xenotransplantation. *Ann Surg* **274**, 473–480 (2021). https://doi.org/10.1097/SLA.0000000000004996

96 Jayne, D. R. W., Merkel, P. A., Schall, T. J., Bekker, P. & Group, A. S. Avacopan for the Treatment of ANCA-Associated Vasculitis. *N Engl J Med* **384**, 599–609 (2021). https://doi.org/10.1056/NEJMoa2023386

97 Bauer, M. *et al.* Efficacy and Safety of Vilobelimab (IFX-1), a Novel Monoclonal Anti-C5a Antibody, in Patients With Early Severe Sepsis or Septic Shock-A Randomized, Placebo-Controlled, Double-Blind, Multicenter, Phase IIa Trial (SCIENS Study). *Crit Care Explor* **3**, e0577 (2021). https://doi.org/10.1097/CCE.0000000000000577

98 Gueler, F. *et al.* Complement 5a receptor inhibition improves renal allograft survival. *J Am Soc Nephrol* **19**, 2302–2312 (2008). https://doi.org/10.1681/ASN.2007111267

99 Lewis, A. G., Kohl, G., Ma, Q., Devarajan, P. & Kohl, J. Pharmacological targeting of C5a receptors during organ preservation improves kidney graft survival. *Clin Exp Immunol* **153**, 117–126 (2008). https://doi.org/10.1111/j.1365-2249.2008.03678.x

100 Arumugam, T. V. *et al.* A small molecule C5a receptor antagonist protects kidneys from ischemia/reperfusion injury in rats. *Kidney Int* **63**, 134–142 (2003). https://doi.org/10.1046/j.1523-1755.2003.00737.x

101 Heo, Y. A. Pegcetacoplan: A Review in Paroxysmal Nocturnal Haemoglobinuria. *Drugs* **82**, 1727–1735 (2022). https://doi.org/10.1007/s40265-022-01809-w

102 Schmitz, R. *et al.* C3 complement inhibition prevents antibody-mediated rejection and prolongs renal allograft survival in sensitized non-human primates. *Nat Commun* **12**, 5456 (2021). https://doi.org/10.1038/s41467-021-25745-7

103 Bomback, A. S. *et al.* Efficacy and Safety of Pegcetacoplan in Kidney Transplant Recipients With Recurrent Complement 3 Glomerulopathy or Primary Immune Complex Membranoproliferative Glomerulonephritis. *Kidney Int Rep* **10**, 87–98 (2025). https://doi.org/10.1016/j.ekir.2024.09.030

104 Jodele, S. Targeting the lectin pathway in TA-TMA. *Blood Adv* **10**, 181–182 (2026). https://doi.org/10.1182/bloodadvances.2025018551

105 Khaled, S. K. *et al.* Narsoplimab, a Mannan-Binding Lectin-Associated Serine Protease-2 Inhibitor, for the Treatment of Adult Hematopoietic Stem-Cell Transplantation-Associated Thrombotic Microangiopathy. *J Clin Oncol* **40**, 2447–2457 (2022). https://doi.org/10.1200/JCO.21.02389

106 Schoettler, M. L. *et al.* Narsoplimab Results in Excellent Survival in Adults and Children With Hematopoietic Cell Transplant Associated Thrombotic Microangiopathy (TA-TMA). *Am J Hematol* **100**, 2040–2051 (2025). https://doi.org/10.1002/ajh.70044

107 Bongoni, A. K. *et al.* Targeting the complement lectin pathway with a highly specific MASP-2 inhibitor protects against renal ischemia-reperfusion injury. *Proc Natl Acad Sci U S A* **122**, e2424754122 (2025). https://doi.org/10.1073/pnas.2424754122

108 Bracke, L. *et al.* Development of an anti-rat complement C2 antibody that improves renal outcome in a rat kidney transplant model. *Frontiers in Immunology* **16** (2026). https://doi.org/10.3389/fimmu.2025.1668376

109 Van de Walle, I. *et al.* Randomized phase I trial outcomes show safe and sustainable inhibition of classical and lectin complement pathways by empasiprubart. *Nat Commun* **16**, 7639 (2025). https://doi.org/10.1038/s41467-025-62925-1

110 Wu, W. *et al.* Collectin-11 Promotes the Development of Renal Tubulointerstitial Fibrosis. *J Am Soc Nephrol* **29**, 168–181 (2018). https://doi.org/10.1681/ASN.2017050544

111 Nester, C. M. *et al.* Iptacopan Reduces Proteinuria and Stabilizes Kidney Function in C3 Glomerulopathy. *Kidney Int Rep* **10**, 432–446 (2025). https://doi.org/10.1016/j.ekir.2024.10.023

112 AlKhatib, L., Omaish, R., Gokden, N. & Bhusal, S. Iptacopan treatment for recurrent dense deposit disease after kidney transplant: A case report. *SAGE Open Med Case Rep* **13**, 2050313X251380533 (2025). https://doi.org/10.1177/2050313X251380533

113 Escudero-Saiz, V. J. *et al.* Factor B Inhibition with Iptacopan in Recurrent C3 Glomerulopathy Following Kidney Transplant: A Report of Two Cases. *Kidney Med* **6**, 100823 (2024). https://doi.org/10.1016/j.xkme.2024.100823

114 Casiraghi, F. *et al.* Complement Alternative Pathway Deficiency in Recipients Protects Kidney Allograft From Ischemia/Reperfusion Injury and Alloreactive T Cell Response. *Am J Transplant* **17**, 2312–2325 (2017). https://doi.org/10.1111/ajt.14262

115 Thurman, J. M. *et al.* Treatment with an inhibitory monoclonal antibody to mouse factor B protects mice from induction of apoptosis and renal ischemia/reperfusion injury. *J Am Soc Nephrol* **17**, 707–715 (2006). https://doi.org/10.1681/ASN.2005070698

116 Jager, N. M. *et al.* Blocking Complement Factor B Activation Reduces Renal Injury and Inflammation in a Rat Brain Death Model. *Front Immunol* **10**, 2528 (2019). https://doi.org/10.3389/fimmu.2019.02528

117 Nester, C. *et al.* Mo126clinical and Biomarker Characteristics of Patients with C3g or Ic-Mpgn Enrolled in Two Phase Ii Studies Investigating the Factor D Inhibitor Danicopan*. *Nephrology Dialysis Transplantation* **36** (2021). https://doi.org/10.1093/ndt/gfab092.004

118 Hess, J. R. *et al.* Red blood cell hemolysis during blood bank storage: using national quality management data to answer basic scientific questions. *Transfusion* **49**, 2599–2603 (2009). https://doi.org/10.1111/j.1537-2995.2009.02275.x

119 Sawant, R. B., Jathar, S. K., Rajadhyaksha, S. B. & Kadam, P. T. Red cell hemolysis during processing and storage. *Asian J Transfus Sci* **1**, 47–51 (2007). https://doi.org/10.4103/0973-6247.33446

120 Jager, N. M. *et al.* Complement Is Activated During Normothermic Machine Perfusion of Porcine and Human Discarded Kidneys. *Front Immunol* **13**, 831371 (2022). https://doi.org/10.3389/fimmu.2022.831371

121 Tang, S., Sheerin, N. S., Zhou, W., Brown, Z. & Sacks, S. H. Apical proteins stimulate complement synthesis by cultured human proximal tubular epithelial cells. *J Am Soc Nephrol* **10**, 69–76 (1999). https://doi.org/10.1681/ASN.V10169

122 Muhlig, A. K. *et al.* Podocytes Produce and Secrete Functional Complement C3 and Complement Factor H. *Front Immunol* **11**, 1833 (2020). https://doi.org/10.3389/fimmu.2020.01833

123 Wan, J. X. *et al.* Complement 3 is involved in changing the phenotype of human glomerular mesangial cells. *J Cell Physiol* **213**, 495–501 (2007). https://doi.org/10.1002/jcp.21129

124 Miyazaki, M. *et al.* Intraglomerular C3 synthesis in human kidney detected by in situ hybridization. *J Am Soc Nephrol* **7**, 2428–2433 (1996). https://doi.org/10.1681/ASN.V7112428

125 Andrews, P. A. *et al.* Expression and tissue localization of donor-specific complement C3 synthesized in human renal allografts. *Eur J Immunol* **25**, 1087–1093 (1995). https://doi.org/10.1002/eji.1830250434

126 Brown, K. M. *et al.* Influence of donor C3 allotype on late renal-transplantation outcome. *N Engl J Med* **354**, 2014–2023 (2006). https://doi.org/10.1056/NEJMoa052825

127 Varagunam, M., Yaqoob, M. M., Dohler, B. & Opelz, G. C3 polymorphisms and allograft outcome in renal transplantation. *N Engl J Med* **360**, 874–880 (2009). https://doi.org/10.1056/NEJMoa0801861

128 Gerritsma, J. S., Gerritsen, A. F., De Ley, M., van Es, L. A. & Daha, M. R. Interferon-gamma induces biosynthesis of complement components C2, C4 and factor H by human proximal tubular epithelial cells. *Cytokine* **9**, 276–283 (1997). https://doi.org/10.1006/cyto.1996.0164

129 Song, D., Zhou, W., Sheerin, S. H. & Sacks, S. H. Compartmental localization of complement component transcripts in the normal human kidney. *Nephron* **78**, 15–22 (1998). https://doi.org/10.1159/000044876

130 Parikh, S. V. *et al.* Characterising the immune profile of the kidney biopsy at lupus nephritis flare differentiates early treatment responders from non-responders. *Lupus Sci Med* **2**, e000112 (2015). https://doi.org/10.1136/lupus-2015-000112

131 Korsten, P. & Tampe, B. A Transcriptome Array-Based Approach to Link SGLT-2 and Intrarenal Complement C5 Synthesis in Diabetic Nephropathy. *Int J Mol Sci* **24** (2023). https://doi.org/10.3390/ijms242317066

132 Trailin, A. *et al.* Chronic Active Antibody-Mediated Rejection Is Associated With the Upregulation of Interstitial But Not Glomerular Transcripts. *Front Immunol* **12**, 729558 (2021). https://doi.org/10.3389/fimmu.2021.729558

133 Kellnerova, S. *et al.* Shiga Toxin 2a Binds to Complement Components C3b and C5 and Upregulates Their Gene Expression in Human Cell Lines. *Toxins (Basel)* **13** (2020). https://doi.org/10.3390/toxins13010008

134 McEvoy, C. M. *et al.* Single-cell profiling of healthy human kidney reveals features of sex-based transcriptional programs and tissue-specific immunity. *Nat Commun* **13**, 7634 (2022). https://doi.org/10.1038/s41467-022-35297-z

135 Lamarthee, B. *et al.* Transcriptional and spatial profiling of the kidney allograft unravels a central role for FcyRIII+ innate immune cells in rejection. *Nat Commun* **14**, 4359 (2023). https://doi.org/10.1038/s41467-023-39859-7

136 Parikh, S. V. *et al.* Molecular profiling of kidney compartments from serial biopsies differentiate treatment responders from non-responders in lupus nephritis. *Kidney Int* **102**, 845–865 (2022). https://doi.org/10.1016/j.kint.2022.05.033

137 Xavier, S. *et al.* Complement C1r serine protease contributes to kidney fibrosis. *Am J Physiol Renal Physiol* **317**, F1293–F1304 (2019). https://doi.org/10.1152/ajprenal.00357.2019

138 Hansen, S. W. K. *et al.* CL-L1 and CL-K1 Exhibit Widespread Tissue Distribution With High and Co-Localized Expression in Secretory Epithelia and Mucosa. *Front Immunol* **9**, 1757 (2018). https://doi.org/10.3389/fimmu.2018.01757

139 Gerritsma, J. S., Gerritsen, A. F., Van Kooten, C., Van Es, L. A. & Daha, M. R. Interleukin-1 alpha enhances the biosynthesis of complement C3 and factor B by human kidney proximal tubular epithelial cells in vitro. *Mol Immunol* **33**, 847–854 (1996). https://doi.org/10.1016/0161-5890(96)84610-4

140 Li, D. *et al.* Complement Factor B Production in Renal Tubular Cells and Its Role in Sodium Transporter Expression During Polymicrobial Sepsis. *Crit Care Med* **44**, e289–299 (2016). https://doi.org/10.1097/CCM.0000000000001566

141 Mahajan, S. *et al.* Local complement factor H protects kidney endothelial cell structure and function. *Kidney Int* **100**, 824–836 (2021). https://doi.org/10.1016/j.kint.2021.05.033

142 Welch, T. R., Beischel, L. S., Frenzke, M. & Witte, D. Regulated expression of complement factor B in the human kidney. *Kidney Int* **50**, 521–525 (1996). https://doi.org/10.1038/ki.1996.344

143 Wang, Z. *et al.* Endothelial-derived complement factor D contributes to endothelial dysfunction in malignant nephrosclerosis via local complement activation. *Hypertens Res* **46**, 1759–1770 (2023). https://doi.org/10.1038/s41440-023-01300-3

144 Thul, P. J. *et al.* A subcellular map of the human proteome. *Science* **356** (2017). https://doi.org/10.1126/science.aal3321

145 Uhlen, M. *et al.* Proteomics. Tissue-based map of the human proteome. *Science* **347**, 1260419 (2015). https://doi.org/10.1126/science.1260419

146 Java, A., Liszewski, M. K., Hourcade, D. E., Zhang, F. & Atkinson, J. P. Role of complement receptor 1 (CR1; CD35) on epithelial cells: A model for understanding complement-mediated damage in the kidney. *Mol Immunol* **67**, 584–595 (2015). https://doi.org/10.1016/j.molimm.2015.07.016

147 Krogstrup, N. V., Bibby, B. M., Aulbjerg, C., Jespersen, B. & Birn, H. A new method of modelling early plasma creatinine changes predicts 1-year graft function after kidney transplantation. *Scand J Clin Lab Invest* **76**, 319–323 (2016). https://doi.org/10.3109/00365513.2016.1161233

148 Krogstrup, N. V. *et al.* Remote Ischemic Conditioning on Recipients of Deceased Renal Transplants Does Not Improve Early Graft Function: A Multicenter Randomized, Controlled Clinical Trial. *Am J Transplant* **17**, 1042–1049 (2017). https://doi.org/10.1111/ajt.14075

149 Nielsen, M. B. *et al.* Remote ischaemic conditioning and early changes in plasma creatinine as markers of one year kidney graft function-A follow-up of the CONTEXT study. *PLoS One* **14**, e0226882 (2019). https://doi.org/10.1371/journal.pone.0226882

150 Nielsen, M. B. *et al.* Elevated plasma free thiols are associated with early and one-year graft function in renal transplant recipients. *PLoS One* **16**, e0255930 (2021). https://doi.org/10.1371/journal.pone.0255930

151 Sparding, N. *et al.* Endotrophin Levels Are Associated with Allograft Outcomes in Kidney Transplant Recipients. *Biomolecules* **13** (2023). https://doi.org/10.3390/biom13050792

152 DiRito, J. R. *et al.* Lysis of cold-storage-induced microvascular obstructions for ex vivo revitalization of marginal human kidneys. *Am J Transplant* **21**, 161–173 (2021). https://doi.org/10.1111/ajt.16148

153 Blogowski, W. *et al.* Clinical analysis of perioperative complement activity during ischemia/reperfusion injury following renal transplantation. *Clin J Am Soc Nephrol* **7**, 1843–1851 (2012). https://doi.org/10.2215/CJN.02200312

154 Arias-Cabrales, C. E. *et al.* Activation of final complement components after kidney transplantation as a marker of delayed graft function severity. *Clin Kidney J* **14**, 1190–1196 (2021). https://doi.org/10.1093/ckj/sfaa147

155 Haas, M., Ratner, L. E. & Montgomery, R. A. C4d staining of perioperative renal transplant biopsies. *Transplantation* **74**, 711–717 (2002). https://doi.org/10.1097/00007890-200209150-00021

156 Van de Walle, I. *et al.* ARGX-117, a therapeutic complement inhibiting antibody targeting C2. *J Allergy Clin Immunol* **147**, 1420–1429 e1427 (2021). https://doi.org/10.1016/j.jaci.2020.08.028

157 Budding, K. *et al.* Anti-C2 Antibody ARGX-117 Inhibits Complement in a Disease Model for Multifocal Motor Neuropathy. *Neurol Neuroimmunol Neuroinflamm* **9** (2022). https://doi.org/10.1212/NXI.0000000000001107

158 Liszewski, M. K. & Atkinson, J. P. Membrane cofactor protein (MCP; CD46): deficiency states and pathogen connections. *Curr Opin Immunol* **72**, 126–134 (2021). https://doi.org/10.1016/j.coi.2021.04.005

159 Thurman, J. M. *et al.* Altered renal tubular expression of the complement inhibitor Crry permits complement activation after ischemia/reperfusion. *J Clin Invest* **116**, 357–368 (2006). https://doi.org/10.1172/JCI24521

160 Jacobson, A. C. & Weis, J. H. Comparative functional evolution of human and mouse CR1 and CR2. *J Immunol* **181**, 2953–2959 (2008). https://doi.org/10.4049/jimmunol.181.5.2953

161 Ghiran, I., Glodek, A. M., Weaver, G., Klickstein, L. B. & Nicholson-Weller, A. Ligation of erythrocyte CR1 induces its clustering in complex with scaffolding protein FAP-1. *Blood* **112**, 3465–3473 (2008). https://doi.org/10.1182/blood-2008-04-151845

162 Farrar, C. A., Asgari, E., Schwaeble, W. J. & Sacks, S. H. Which pathways trigger the role of complement in ischaemia/reperfusion injury? *Front Immunol* **3**, 341 (2012). https://doi.org/10.3389/fimmu.2012.00341

163 Castellano, G. *et al.* Therapeutic targeting of classical and lectin pathways of complement protects from ischemia-reperfusion-induced renal damage. *Am J Pathol* **176**, 1648–1659 (2010). https://doi.org/10.2353/ajpath.2010.090276

164 Jordan, S. C. *et al.* Empasiprubart in Improving Allograft Function in Recipients of a Deceased Donor Renal Allograft at Risk for Delayed Graft Function: A Phase 2 Trial in Progress. *American Journal of Transplantation* **25** (2025). https://doi.org/10.1016/j.ajt.2025.07.1496

165 Xie, C. B., Jane-Wit, D. & Pober, J. S. Complement Membrane Attack Complex: New Roles, Mechanisms of Action, and Therapeutic Targets. *Am J Pathol* **190**, 1138–1150 (2020). https://doi.org/10.1016/j.ajpath.2020.02.006

166 Moskovich, O., Herzog, L. O., Ehrlich, M. & Fishelson, Z. Caveolin-1 and dynamin-2 are essential for removal of the complement C5b-9 complex via endocytosis. *J Biol Chem* **287**, 19904–19915 (2012). https://doi.org/10.1074/jbc.M111.333039

167 Liu, X. *et al.* Changes in Complement Levels and Activity of Red Blood Cells, Fresh Frozen Plasma, and Platelet Concentrates During Storage. *Indian J Hematol Blood Transfus* **37**, 140–146 (2021). https://doi.org/10.1007/s12288-020-01338-0

168 Metzemaekers, M., Gouwy, M. & Proost, P. Neutrophil chemoattractant receptors in health and disease: double-edged swords. *Cell Mol Immunol* **17**, 433–450 (2020). https://doi.org/10.1038/s41423-020-0412-0

169 Poppelaars, F. *et al.* Critical role for complement receptor C5aR2 in the pathogenesis of renal ischemia-reperfusion injury. *FASEB J* **31**, 3193–3204 (2017). https://doi.org/10.1096/fj.201601218R

170 Lamers, C., Pluss, C. J. & Ricklin, D. The Promiscuous Profile of Complement Receptor 3 in Ligand Binding, Immune Modulation, and Pathophysiology. *Front Immunol* **12**, 662164 (2021). https://doi.org/10.3389/fimmu.2021.662164

171 Wang, W. *et al.* Beyond hemostasis, the immunomodulatory nature of platelets. *Res Pract Thromb Haemost* **9**, 103182 (2025). https://doi.org/10.1016/j.rpth.2025.103182

172 Rayes, J. & Brill, A. Hot under the clot: venous thrombogenesis is an inflammatory process. *Blood* **144**, 477–489 (2024). https://doi.org/10.1182/blood.2023022522

173 Pryzdial, E. L. G., Leatherdale, A. & Conway, E. M. Coagulation and complement: Key innate defense participants in a seamless web. *Front Immunol* **13**, 918775 (2022). https://doi.org/10.3389/fimmu.2022.918775

174 Li, K. *et al.* Expression of complement components, receptors and regulators by human dendritic cells. *Mol Immunol* **48**, 1121–1127 (2011). https://doi.org/10.1016/j.molimm.2011.02.003

175 Posch, W., Bermejo-Jambrina, M., Lass-Florl, C. & Wilflingseder, D. Role of Complement Receptors (CRs) on DCs in Anti-HIV-1 Immunity. *Front Immunol* **11**, 572114 (2020). https://doi.org/10.3389/fimmu.2020.572114

176 Barrington, R. A. *et al.* Uncoupling CD21 and CD19 of the B-cell coreceptor. *Proc Natl Acad Sci U S A* **106**, 14490–14495 (2009). https://doi.org/10.1073/pnas.0903477106

177 Hess, M. W. *et al.* Tracing uptake of C3dg-conjugated antigen into B cells via complement receptor type 2 (CR2, CD21). *Blood* **95**, 2617–2623 (2000). https://doi.org/10.1182/blood.V95.8.2617

178 West, E. E., Kolev, M. & Kemper, C. Complement and the Regulation of T Cell Responses. *Annu Rev Immunol* **36**, 309–338 (2018). https://doi.org/10.1146/annurev-immunol-042617-053245

179 Rinder, C. S. *et al.* Blockade of C5a and C5b-9 generation inhibits leukocyte and platelet activation during extracorporeal circulation. *J Clin Invest* **96**, 1564–1572 (1995). https://doi.org/10.1172/JCI118195

180 Kolka, C. M. *et al.* C5b-9 Membrane Attack Complex Formation and Extracellular Vesicle Shedding in Barrett's Esophagus and Esophageal Adenocarcinoma. *Front Immunol* **13**, 842023 (2022). https://doi.org/10.3389/fimmu.2022.842023

181 Moskovich, O. & Fishelson, Z. Live cell imaging of outward and inward vesiculation induced by the complement c5b-9 complex. *J Biol Chem* **282**, 29977–29986 (2007). https://doi.org/10.1074/jbc.M703742200

182 Cravedi, P. & Heeger, P. S. Complement as a multifaceted modulator of kidney transplant injury. *J Clin Invest* **124**, 2348–2354 (2014). https://doi.org/10.1172/JCI72273

183 Smith, R. A. G. *et al.* Membrane-localising complement inhibitors—clinical progress. *Molecular Immunology* **44** (2007). https://doi.org/10.1016/j.molimm.2007.06.021

184 Patel, H., Smith, R. A., Sacks, S. H. & Zhou, W. Therapeutic strategy with a membrane-localizing complement regulator to increase the number of usable donor organs after prolonged cold storage. *J Am Soc Nephrol* **17**, 1102–1111 (2006). https://doi.org/10.1681/ASN.2005101116

185 Dodd, I. *et al.* Overexpression in Escherichia coli, folding, purification, and characterization of the first three short consensus repeat modules of human complement receptor type 1. *Protein Expr Purif* **6**, 727–736 (1995). https://doi.org/10.1006/prep.1995.0003

186 Linton, S. M. *et al.* Therapeutic efficacy of a novel membrane-targeted complement regulator in antigen-induced arthritis in the rat. *Arthritis Rheum* **43**, 2590–2597 (2000). https://doi.org/10.1002/1529-0131(200011)43:11<2590::AID-ANR29>3.0.CO;2-R

187 Kassimatis, T. *et al.* A double-blind randomised controlled investigation into the efficacy of Mirococept (APT070) for preventing ischaemia reperfusion injury in the kidney allograft (EMPIRIKAL): study protocol for a randomised controlled trial. *Trials* **18**, 255 (2017). https://doi.org/10.1186/s13063-017-1972-x

188 Souza, D. G., Esser, D., Bradford, R., Vieira, A. T. & Teixeira, M. M. APT070 (Mirococept), a membrane-localised complement inhibitor, inhibits inflammatory responses that follow intestinal ischaemia and reperfusion injury. *Br J Pharmacol* **145**, 1027–1034 (2005). https://doi.org/10.1038/sj.bjp.0706286

189 Halstead, S. K. *et al.* Complement inhibition abrogates nerve terminal injury in Miller Fisher syndrome. *Ann Neurol* **58**, 203–210 (2005). https://doi.org/10.1002/ana.20546

190 Pratt, J. R. *et al.* Nontransgenic hyperexpression of a complement regulator in donor kidney modulates transplant ischemia/reperfusion damage, acute rejection, and chronic nephropathy. *Am J Pathol* **163**, 1457–1465 (2003). https://doi.org/10.1016/S0002-9440(10)63503-1

191 Smith, G. P. & Smith, R. A. Membrane-targeted complement inhibitors. *Mol Immunol* **38**, 249–255 (2001). https://doi.org/10.1016/s0161-5890(01)00047-5

192 Smith, R. A. Targeting anticomplement agents. *Biochem Soc Trans* **30**, 1037–1041 (2002). https://doi.org/10.1042/bst0301037

193 Banz, Y. *et al.* Attenuation of myocardial reperfusion injury in pigs by Mirococept, a membrane-targeted complement inhibitor derived from human CR1. *Cardiovasc Res* **76**, 482–493 (2007). https://doi.org/10.1016/j.cardiores.2007.07.016

194 Wu, G. *et al*. Coagulation cascade activation triggers early failure of pig hearts expressing human complement regulatory genes. *Xenotransplantation* **14**, 34–47 (2007). https://doi.org/10.1111/j.1399-3089.2006.00362.x

195 Duehrkop, C. *et al*. C1 esterase inhibitor reduces lower extremity ischemia/reperfusion injury and associated lung damage. *PLoS One* **8**, e72059 (2013). https://doi.org/10.1371/journal.pone.0072059

196 Xiao, F. *et al*. APT070 (mirococept), a membrane-localizing C3 convertase inhibitor, attenuates early human islet allograft damage in vitro and in vivo in a humanized mouse model. *Br J Pharmacol* **173**, 575–587 (2016). https://doi.org/10.1111/bph.13388

197 McLaughlin, S. & Aderem, A. The myristoyl-electrostatic switch: a modulator of reversible protein-membrane interactions. *Trends Biochem Sci* **20**, 272–276 (1995). https://doi.org/10.1016/s0968-0004(00)89042-8

198 Murray, D., Ben-Tal, N., Honig, B. & McLaughlin, S. Electrostatic interaction of myristoylated proteins with membranes: simple physics, complicated biology. *Structure* **5**, 985–989 (1997). https://doi.org/10.1016/s0969-2126(97)00251-7

199 Kim, J., Blackshear, P. J., Johnson, J. D. & McLaughlin, S. Phosphorylation reverses the membrane association of peptides that correspond to the basic domains of MARCKS and neuromodulin. *Biophys J* **67**, 227–237 (1994). https://doi.org/10.1016/S0006-3495(94)80473-4

200 Leekumjorn, S. & Sum, A. K. Molecular studies of the gel to liquid-crystalline phase transition for fully hydrated DPPC and DPPE bilayers. *Biochim Biophys Acta* **1768**, 354–365 (2007). https://doi.org/10.1016/j.bbamem.2006.11.003

201 Leonenko, Z. V., Finot, E., Ma, H., Dahms, T. E. & Cramb, D. T. Investigation of temperature-induced phase transitions in DOPC and DPPC phospholipid bilayers using temperature-controlled scanning force microscopy. *Biophys J* **86**, 3783–3793 (2004). https://doi.org/10.1529/biophysj.103.036681